HEAT TRANSFER FROM A FLAT SURFACE TO AIR FLOWING IN RADIAL DIRECTION.

A thesis
presented for the degree of
Doctor of Philosophy
in the Faculty of Engineering of the
UNIVERSITY OF LONDON

by
Mahmoud Sobhi Mohamed ABDEL-SALAM, B.Sc. (Eng.)

May, 1956.

ProQuest LLC.
789 East Eisenhower Parkway
P.O. Box 1346
Ann Arbor, MI 48106 – 1346

HEAT TRANSFER FROM A FLAT SURFACE
TO AIR FLOWING IN RADIAL DIRECTION.

ABSTRACT.

Some approximate theoretical expressions have been derived to show the effect of flow conditions on heat transfer between flat surfaces and fluids flowing parallel to them. Special comparison was made between the case of uniform parallel flow and that of radial flow parallel to the surface. It was predicted that the heat transfer in uniform parallel flow would be higher than in outward radial flow, other conditions being the same.

Two groups of experiments were carried out. In the first group air was flowing between two parallel plates in an outward radial direction. One of the plates was electrically heated. No such heating was supplied to the second plate, but it was insulated against external radiation. Eight different gaps between the plates were tested, and the average coefficients of heat transfer were obtained.

The effect of the gap on the heat transfer was obtained for both laminar and turbulent flows. All the data of the different gaps were brought together by introducing equations containing the Nusselt and Reynolds numbers and the gap-to-length ratio.

Comparison was also made between the present results and the theoretical and experimental results of other workers on

heat transfer from flat surfaces to air in uniform parallel flow, little or no other information on radial flow being available. The effect of flow conditions was discussed.

In the second group of experiments the unheated plate was rotated. Four different speeds of rotation and four different gaps were tested. The effect of this rotation on both the flow pattern and heat transfer was studied. The experimental results were compared with analytical ones and agreement was generally fair. Finally, from the calculated length of path of the air particles, an expression was found for the effect of the disc rotation on heat transfer.

ACKNOWLEDGEMENTS.

The idea for this research was suggested by Mr. V.C.Davies, B.Sc.(Eng.), M.I.Mech.E., who supervised the work throughout. The writer wishes to express his deep gratitude to Mr. Davies for his guidance and for the frequent advice and encouragement he gave.

The writer is also grateful to Mr. W.J.Peck, M.Eng., M.I.Mech.E. for his interest in the progress of the work and for help readily given on many occasions.

Sincere thanks also go to the stewards and workshop staff of the Engineering Department of Battersea Polytechnic for the assistance they gave in the construction of the apparatus.

NOMENCLATURE.

Except where it is stated otherwise, the symbols used in this thesis have the meanings given below :

A	area of cross-section, square feet.
B	width of plate, feet
b	gap between the plates
c	specific heat at constant pressure, Btu/(lb)(deg.F)
G	dimensionless angular speed
H	amount of heat transferred per unit time, Btu.per hour
H_o	amount of heat given to the main heater, Btu.per hour
H_r	amount of heat lost by radiation, Btu.per hour
H_c	amount of heat lost by conduction, Btu.per hour
h	coefficient of heat transfer, Btu.per (sq.ft)(hr.)(deg.F
K	constant
k	thermal conductivity of fluid, Btu.per(Foot)X(hr.)(Deg.F
L	length of plate, difference between the radii of the heating surface
l	length of path of air particles when given tangential component of velocity
N	speed of rotation of the unheated disc, r.p.m.
n	constant
Q	amount of air discharge from the air blower, pounds per hr.
r	radius
r_1	inner radius of the heating surface
r_2	outer radius of the heating surface
r_m	arithmetic mean radius of the heating surface

S	surface area of the heat transfer surface, square foot
t	temperature, $^{o}F.$
t_w	temperature of the heating surface, $^{o}F.$
t_d	temperature of the unheated disc, $^{o}F.$
t_o	temperature of the fluid, $^{o}F.$
T	absolute temperature, $^{o}F.abs.$
U	velocity of flow of the main stream in the x-direction (U_1 at radius r_1, U_2 at r_2, U_m at r_m)
U_m	effective mean velocity of the main stream
u	velocity in the boundary layer in the direction of x
V	velocity perpendicular to the heating surface, (y-direction)
v	velocity in the boundary layer in the direction of y
x	coordinate in the direction of flow
y	distance from the heat transfer surface
z	distance from the rotating disc

Dimensionless groups:

N_u	Nusselt number
R_e	Reynolds number
P_r	Prandtl number

Greek letters

ρ	density of fluid, pounds per cubic foot
μ	viscosity of fluid, pounds per (foot)(hour)
ν	kinematic viscosity ($= \frac{\mu}{\rho}$), square foot/hour
θ	temperature difference between the surface and fluid, $^{o}F.$

α thermal diffusivity ($= \frac{k}{c\rho}$), square foot/hour

δ thickness of the boundary layer

ω angular velocity

ζ dimensionless distance from the rotating disc ($= z\sqrt{\frac{\omega}{\nu}}$)

LIST OF TABLES.

CONTENTS

INTRODUCTION.

The heat transfer from a surface to a fluid flowing past it depends to a great extent on the boundary conditions. Different cases have been studied by different observers. For the heat transfer between flat surfaces and fluids flowing parallel to them many attempts have been carried out from the simple flat plate to rectangular passages of different aspect ratios.

As far as the writer is aware there is no published data for heat transfer to a fluid flowing in radial direction between two parallel flat plates. Moreover, the available data for the effect of the gap between two parallel plates on heat transfer is not sufficient.

The flow conditions, for the case of radial flow, are somewhat complicated because of the variation of the main stream velocity. The flow conditions have a considerable effect on the heat transfer characteristics. Changing the gap between the plates effects the growth of the boundary layer and the critical flow conditions. Further, if one of the plates is rotated a new factor comes into account. Due to surface friction the fluid near that plate is dragged round tangentially and the plate acts as a kind of compressor. This problem arises in connection with the cooling of rotary compressor runners and similar cases.

In the present case air flows between two parallel flat plates in radial direction. It is the aim of this research

work to study this condition and the effect of the gap between the plates on heat transfer. The effect of the superimposed vortex motion caused by the rotation of one of the plates has also been studied.

CHAPTER I.

HEAT TRANSFER BY FORCED CONVECTION

In the process of heat transfer by convection, new particles of the fluid are continually coming into contact with the heat transfer surface, where they take or give up heat. Since the heat is transferred by the motion of the fluid, then the greater the rate of the fluid flow past the solid surface the more the rate of heat transmission will be. When the motion of the fluid is maintained mechanically, it is referred to as 'forced convection'.

Actually, heat is transferred firstly by conduction through a thin layer of the fluid immediately adjacent to the solid surface. This process can be represented by the equation

$$H = - k S \left(\frac{\delta t}{\delta y}\right)_{y=0} \qquad \text{I-1}$$

where H = amount of heat transferred per unit time

k = thermal conductivity of the fluid

S = area of heat transfer surface

δt = fluid temperature difference across the fluid film immediately adjacent to the surface

δy = thickness of the film.

The heat is then diffused through the rest of the fluid by the contact of its particles and by eddies.

To determine the heat transfer by conduction in the film is very complicated, since it is difficult to determine the

thickness of the film and the temperature gradient across it. An alternative to that is to assume an overall coefficient of heat transfer (h) which is valid for the whole process through the bulk of the fluid., thus

$$H = h S (t_w - t_o) \qquad \text{I-2}$$

where t_w = temperature of the heat transfer surface

t_o = temperature of the fluid.

This equation was first recommended by Newton in 1701, and since that time it has been adopted by all investigators.

Different theories have been made for different cases of heat transfer problems. The following is a summary of some theories of forced convection heat transfer between flat surfaces and fluids flowing parallel to them.

FORCED HEAT CONVECTION IN LAMINAR FLOW PARALLEL TO A PLANE PLATE AT UNIFORM TEMPERATURE:

An exact solution for this case was given by Pohlhausen in 1921 (See reference 25, page 468). It is assumed that velocities are small compared to sound velocity, and that no pressure drop occurs in this sort of unbounded flow.

If the heat generated by dissipation is neglected then the equations of motion, continuity and heat conduction simplify to :

$$u \frac{\partial u}{\partial x} + v \frac{\partial u}{\partial y} = \nu \frac{\partial^2 u}{\partial y^2} \qquad \text{I-3}$$

$$\frac{\partial u}{\partial x} + \frac{\partial v}{\partial y} = 0 \qquad \text{I-4}$$

$$u \frac{\partial t}{\partial x} + v \frac{\partial t}{\partial y} = \alpha \frac{\partial^2 t}{\partial y^2} \qquad \text{I-5}$$

where u = velocity in the x-direction

v = velocity in the y-direction

t = temperature of the fluid

ν = kinematic viscosity $(= \frac{\mu}{\rho})$

α = thermal diffusivity $(= \frac{k}{c\rho})$

x = coordinate in the direction of flow

y = distance from the solid surface.

The boundary conditions are

At $y = 0$; $u = 0$, $v = 0$, $t = t_w$

At $y = \infty$: $u = U$, $t = t_o$

where U = main stream velocity.

The law of continuity is satisfied by introducing a stream function ψ, defined by

$$u = \frac{\partial \psi}{\partial y} \qquad \text{I-6}$$

and

$$v = - \frac{\partial \psi}{\partial x} \qquad \text{I-7}$$

If we introduce

$$\eta = \tfrac{1}{2} \left(\frac{U}{\nu x}\right)^{\frac{1}{2}} \cdot y \qquad \text{I-8}$$

and $$\psi = (U \nu x)^{\frac{1}{2}} \cdot f(\eta) \qquad \text{I-9}$$

then $$u = \tfrac{1}{2} U f' \qquad \text{I-10}$$

and $$v = \tfrac{1}{2} \left(\frac{U\nu}{x}\right)^{\frac{1}{2}} (\eta f' - f) \qquad \text{I-11}$$

where the suffix indicates differentiation with respect to η

Equation (I-3) leads to

$$f''' + ff'' = 0 \qquad \text{I-12}$$

If $$\theta(\eta) = \frac{t - t_w}{t_o - t_w} \qquad \text{I-13}$$

then equation (I-5) becomes

$$\theta'' + \frac{\nu}{\alpha} \eta \theta' = 0 \qquad \text{I-14}$$

The boundary conditions are

At $\eta = 0$; $f = 0$, $f' = 0$, $\theta = 0$

At $\eta = \infty$; $f' = 2$, $\theta = 1$

Equation (I-14) was solved by Pohlhausen, and his final result gives

$$h = 0.664 \quad k \left(\frac{\nu}{\alpha}\right)^{\frac{1}{3}} \left(\frac{U}{L\nu}\right)^{\frac{1}{2}} \qquad \text{I-15}$$

or $$\left(\frac{hL}{k}\right) = 0.664 \left(\frac{c\mu}{k}\right)^{\frac{1}{3}} \left(\frac{UL}{\nu}\right)^{\frac{1}{2}} \qquad \text{I-16}$$

where h = coefficient of heat transfer

L = length of the plate.

Some approximate attempts were made by Boussinesq, King, and Aichli, before Pohlhausen, and by Leveque afterwards. These mathematical attacks on the problem have been thoroughly described by Drew (10).*

FORCED HEAT CONVECTION IN TURBULENT FLOW PARALLEL TO A PLANE PLATE AT UNIFORM TEMPERATURE.

This case was treated by Latzko(30) in 1921. It is assumed that the plate is so thin that the leading edge does not affect the arriving stream. If the heating effect of friction is neglected and uniform pressure is assumed then the velocity field and temperature field are similar.

According to von Karman(28), the velocity distribution and the thickness of the boundary layer may be expressed by

$$u = U \left(\frac{y}{\delta}\right)^{1/7} \qquad \text{I-17}$$

and

$$\delta = 0.37 \left(\frac{\nu}{Ux}\right)^{1/5} x \qquad \text{I-18}$$

where U = velocity at the end of the boundary layer

δ = thickness of the boundary layer

and other symbols have the usual meaning.

The similarity between the velocity field and temperature field gives

$$\theta = \theta_o \left(\frac{y}{\delta}\right)^{1/7} \qquad \text{I-19}$$

---

* Numbers in parentheses refer to Bibliography at the end of the work.

where θ = average temperature difference at cross-section x

θ_o = temperature difference between the surface and the undisturbed stream.

The condition for thermal equilibrium in an element of the boundary layer is

$$\frac{d}{dx}\int_0^\delta \rho u c \theta \, dy - \rho c \theta_o \frac{d}{dx}\int_0^\delta u \, dy + q = 0$$

where q = heat leaving the plate at x

c = specific heat of the fluid.

$$\therefore \frac{d}{dx}\int_0^\delta \rho U \left(\frac{y}{\delta}\right)^{1/7} c\theta_o \left(\frac{y}{\delta}\right)^{1/7} dy - \rho c \theta_o \frac{d}{dx}\int_0^\delta U \left(\frac{y}{\delta}\right)^{1/7} dy + q = 0$$

Introducing the equation (I-18) and solving, we get

$$q = 0.0285 \, \rho c U \theta_o \left(\frac{\nu}{Ux}\right)^{0.2} \qquad \text{I-20}$$

The total amount of heat leaving a plate strip of unit width and length L is then

$$Q = \int_0^L q \, dx$$

$$= 0.0356 \, \rho c U \theta_o L \left(\frac{\nu}{UL}\right)^{0.2}$$

$$= h \theta_o L \qquad \text{I-21}$$

$$\therefore h = 0.0356 \, \rho^{0.8} c\mu^{0.2} L^{-0.2} U^{0.8} \qquad \text{I-22}$$

$$\text{or} \quad \left(\frac{hL}{k}\right) = 0.0356 \left(\frac{\rho UL}{\mu}\right)^{0.8} \left(\frac{c\mu}{k}\right) \qquad \text{I-23}$$

It is noticed that in this theory it was assumed that the flow was turbulent right from the leading edge.

HEAT TRANSFER TO A FLUID IN LAMINAR FLOW BETWEEN TWO PARALLEL WALLS.

This case was treated by Jakob[24] in 1939. The following assumptions were made :

1. The same amount of heat was produced per unit time and surface.
2. Temperature changes were so small that the fluid properties were considered constant.

In the range of streamline motion, the velocity distribution is parabolic according to the equation

$$u = 4\, U_{max} \left(\frac{y}{b} - \frac{y^2}{b^2}\right) \qquad \text{I-24}$$

where u = velocity of the fluid at y

y = distance from the wall

b = gap between the plates

U_{max} = velocity at $y = \frac{b}{2}$

For the part of flow between y and $y + dy$ (Fig.1), the heat balance leads to the differential equation

$$q = k \frac{d^2 t}{dy^2} \qquad \text{I-25}$$

where q = heat received by the fluid through the unit of cross-sectional area in unit time over a unit length of plate

Introducing $H = \int_0^b q\, L\, B\, dy$ and solving, we get

$$t = \frac{H}{LBk} \left(\frac{y^3}{b^2} - \frac{y^4}{2b^3}\right) + c_1 y + c_2 \qquad \text{I-26}$$

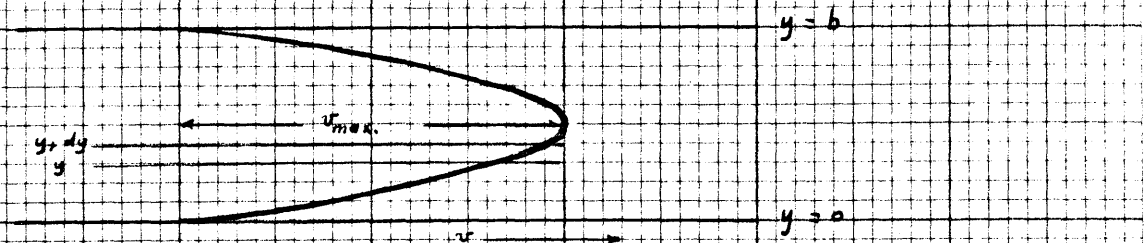

(i) Velocity distribution

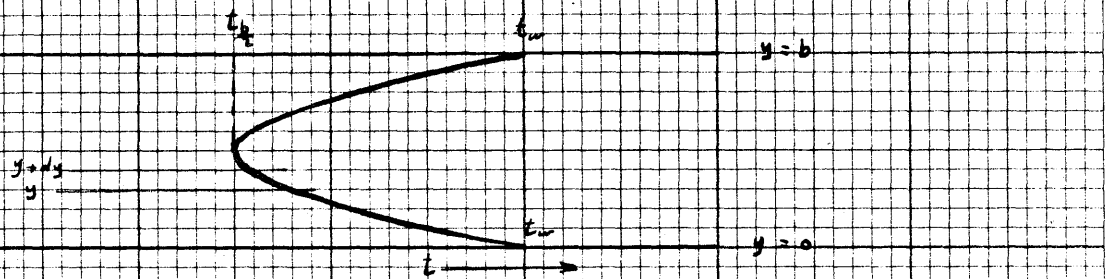

(ii) Temperature distribution; both sides heated.

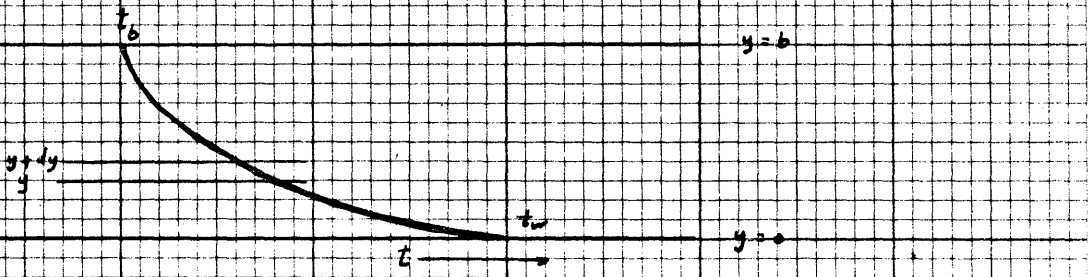

(iii) Temperature distribution; one side heated.

Fig. 1 : VELOCITY AND TEMPERATURE DISTRIBUTIONS IN STREAMLINE FLOW BETWEEN TWO PARALLEL PLATES.

where H = total heat received by the fluid

B = width of the plates

L = length of the plates

t = temperature (w, for wall)

c_1 and c_2 are constants

other symbols have the usual meaning.

In the case of equal heating from both walls, the boundary conditions are :

$$t = t_w \quad \text{at} \quad y = 0 \quad \text{and at} \quad y = b.$$

With these, equation (I-26) becomes

$$t = t_w - \frac{H}{LBk} \left(\frac{y}{2} - \frac{y^3}{b^2} + \frac{y^4}{2b^3} \right)$$

and the minimum temperature at $y = \frac{b}{2}$ is

$$t_{\frac{b}{2}} = t_w - \frac{5}{32} \frac{Hb}{LBk} \qquad \text{I-27}$$

If the coefficient of heat transfer (h) is defined by

$$\frac{H}{2} = h L B \left(t_w - t_{\frac{b}{2}} \right) \qquad \text{I-28}$$

it follows that

$$h = \frac{16}{5} \frac{k}{b} \qquad \text{I-29}$$

In the case of one sided heating, the boundary conditions are :

At $y = 0$, $t = t_w$

At $y = b$, $\frac{dt}{dy} = 0$

With these, equation (I-26) becomes

$$t = t_w - \frac{H}{LBk} \left(y - \frac{y^3}{b^2} + \frac{y^4}{2b^3} \right)$$

and the minimum temperature at $y = b$ becomes

$$t_b = t_w - \tfrac{1}{2} \frac{Hb}{LBk} \qquad \text{I-30}$$

Defining the coefficient of heat transfer (h') in this case by

$$H = h' L B (t_w - t_b) \qquad \text{I-31}$$

it follows that

$$h' = 2 \frac{k}{b} \qquad \text{I-32}$$

The case of heat transfer in laminar flow between two parallel plates was considered later by some other workers. Some of these are Purday[41], Prins and coworkers[40], Bye and Schenk[5] and Schenk and Beckers[46].

HEAT TRANSFER TO A FLUID IN TURBULENT FLOW BETWEEN TWO PARALLEL WALLS.

This case was considered by Lévêque[31]. He treated it as if the fluid were a solid slab moving between fixed heated plates. The following assumptions were made :

1. The y-component of the velocity is everywhere zero.
2. The plate temperature t_w is constant.
3. The plates and the fluid extend indefinitely in the z-direction.
4. The values of the fluid properties are constant.

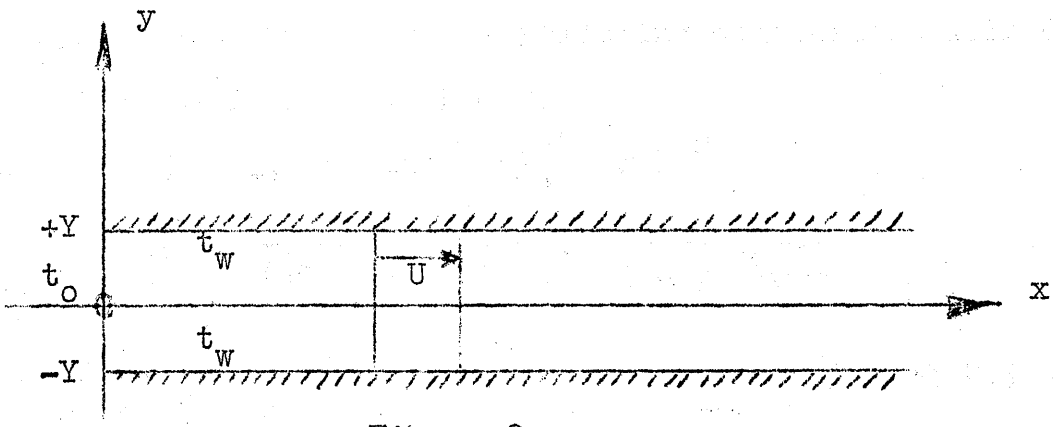

Figure 2.

The boundary conditions are

$t = t_w$ if $y = \pm Y$ and $0 < x < L$

$t = t_o$ if $x < 0$

$t = t_w$ as x goes to infinity and y lies between +Y and -Y.

(The symbols are explained in Fig.2.)

If the thermal conduction in the direction of the fluid motion is neglected the general equation reduces to

$$\frac{\partial t}{\partial x} = \frac{\alpha}{U} \frac{\partial^2 t}{\partial y^2} \qquad \text{I-33}$$

As a type of solution Lévêque chose the formula

$$t = e^{-\frac{(2)^2(\alpha x)}{(m)(U)}\left(\frac{x}{Y^2}\right)} \cos\left(m \frac{y}{Y}\right) \qquad \text{I-34}$$

where m is a parameter such that : $\cos m = 0$.

If the average temperature difference is taken as the arithmetic mean between the initial and final values of temperature difference then the calculation of Leveque for the average coefficient of heat transfer leads to

$$h = \frac{2c\rho UY}{x} \cdot \frac{1 - \frac{8}{\pi^2}\left[e^{-\beta} + \frac{1}{9}e^{-9\beta} + \frac{1}{25}e^{-25\beta} + \cdots\right]}{1 + \frac{8}{\pi^2}\left[e^{-\beta} + \frac{1}{9}e^{-9\beta} + \frac{1}{25}e^{-25\beta} + \cdots\right]} \qquad \text{I-35}$$

where $\beta = \left(\frac{\pi}{2}\right)^2 \frac{\alpha}{U} \frac{x}{Y^2}$

From equation (I-35) the following conclusions were drawn :

1. When β is large, $h \propto U$.
2. When $\beta \leq \frac{1}{4}$, or when $\frac{UY^2}{\alpha x} \gg \pi^2$

$$h = \frac{2}{\sqrt{\pi}} \sqrt{\frac{kc\rho U}{x}} \cdot \frac{1}{1 - \sqrt{\frac{\alpha x}{\pi UY^2}}} \qquad \text{I-36}$$

3. For very small β the case of a flat plate is approached and

$$h = \frac{2}{\sqrt{\pi}} \left(\frac{kc\rho U}{x}\right)^{0.5} \qquad \text{I-37}$$

Lévêque stated that his formulae are not applicable if $\frac{2\rho UY}{\mu}$ is below 2000.

DIMENSIONAL ANALYSIS.

In most applications of heat transfer, the variables affecting the heat transfer coefficient are being grouped in some dimensionless groups so as to facilitate calculations and reduce the number of variables to be dealt with experimentally. Another advantage of dimensional analysis is that in any one set of self-consistent units the numerical value of a dimensionless group is the same as in any other set of self-consistent units.

Considering the general problem of forced convection, the coefficient of heat transfer (amount of heat transferred per unit time per unit surface area per unit temperature difference between the solid surface and fluid) can be assumed to be given

by the equation[16]

$$h = K_1 . U^m . L^b . \mu^d . k^e . \rho^f . c^n \qquad \text{I-38}$$

where U = forced fluid velocity

L = linear scale

K_1, m, b, d, e, f, & n are constants

other symbols have the usual meanings.

Equating the dimensions of both sides of equation (I-38) and solving in terms of m and n, we get

$$h = K_1 . U^m . L^{m-1} . \mu^{n-m} . k^{1-n} . \rho^m . c^n$$

$$= K_1 . \left(\frac{\rho UL}{\mu}\right)^m . \left(\frac{c\mu}{k}\right)^n . \frac{k}{L}$$

$$\text{or } \left(\frac{hL}{k}\right) = K_1 . \left(\frac{\rho UL}{\mu}\right)^m . \left(\frac{c\mu}{k}\right)^n \qquad \text{I-39}$$

These groups are known as

$\frac{hL}{k}$ = Nusselt number (Nu)

$\frac{\rho UL}{\mu}$ = Reynolds number (Re)

$\frac{c\mu}{k}$ = Prandtl number (P_r)

Therefore the heat transfer by forced convection is given by the relation

$$Nu = K_1 . Re^m . P_r^n \qquad \text{I-40}$$

The values of the constants K_1, m and n depend on the geometry of the surface, its surroundings, the conditions of flow and the conditions in which the different properties of the fluid are evaluated. These constants can be obtained

either experimentally or mathematically. If they are to be determined by experiments then, theoretically, for either laminar or turbulent flow three experiments under different conditions should be sufficient to find these three constants, and so would allow the determination of (h) for all possible changes of the six independent variables. Since similarity exists only if the kind of flow is the same, different constants will occur in the laminar and turbulent regions.

Equation (I-40) applies to gases and liquids in forced convection heat transfer. In cases of air (as in the present work) the value of Pr is nearly constant and equal to 0.72. So putting this value in equation (I-40) we get

$$Nu = K. Re^{m} \qquad \text{I-41}$$

which is used for forced convection heat transfer to air.

PHYSICAL SIGNIFICANCE OF DIMENSIONLESS GROUPS:

The Nusselt number ($\frac{hL}{k}$) represents the ratio of the actual convection heat transfer per unit surface area per unit time ($h\theta$) to ($\frac{k\theta}{L}$), which is proportional to the heat transfer by conduction in the fluid at rest.

The Ryenolds number ($\frac{\rho UL}{\mu}$) may be regarded as the ratio of the oncoming fluid momentum per unit area per unit time (ρU^2) to the viscous drag force per unit area ($\frac{\mu U}{L}$) against which it is balanced.

The Prandtl number ($\frac{c\mu}{k}$) is the ratio of the momentum diffusivity (or kinematic viscosity $\frac{\mu}{\rho}$) to the thermal

diffusivity ($\frac{k}{c\rho}$). It represents the ratio of the fluid property governing the transfer of momentum by viscous effects due to a gradient of velocity, to the fluid property governing the transfer of heat by thermal diffusion due to a gradient of temperature.

The Reynolds number is therefore the group which determines the flow pattern, and the Prandtl number determines the relation of the temperature distribution in a fluid to the velocity distribution. Thus in forced convection the fluid motion is fixed by R_e, and the superposition of a temperature difference between the fluid and the boundary surface causes a temperature distribution in the fluid, which is fixed by Pr, together with the original fluid motion.

TEMPERATURE AND PHYSICAL PROPERTIES OF THE FLUID :

There is argument about the temperature at which the values of the physical properties of the fluid have to be taken. Some workers take these values at the mean fluid bulk temperature; others take them at the film temperature. Most of those using the film temperature take it as $\frac{1}{2}(t_w + t_o)$ [where t_w = wall temperature, and t_o = fluid bulk temperature].

In all cases the density of the fluid should be taken at the fluid bulk temperature. In the present experimental work to be described later the writer has taken the other properties also at the fluid bulk temperature.

CHAPTER II.

PREVIOUS EXPERIMENTAL WORK.

The available experimental data for heat transfer between flat surfaces and fluids flowing over them can be summarised as follows:

Relation between velocity and heat transfer.

Fishenden and Saunders[14] stated that they observed from the investigations of different workers that for smooth surfaces the coefficient of heat transfer was proportional to a power of the stream velocity around 0.8. This is in agreement with the theoretical expression derived by Latzko[30](equation I-22).

Jürges[27] measured the heat transfer from smooth and rough copper plates 1.64 feet square to air flowing parallel to the surface. The surface temperature was maintained electrically at 115-140°F. The air temperature was taken as that of the oncoming stream. The plate was in alignment with one of the vertical walls of a duct through which air was blown by means of a fan. The results of Jürges can be represented as follows :

For air stream velocities <16 feet/second

$$h = 0.99 + 0.21\ U \qquad \text{Btu/(ft)}^2\text{(hr)(degF)} \qquad \text{II-1}$$

For air stream velocities >16 feet/second

$$h = 0.5\ U^{0.78} \qquad \text{II-2}$$

(h and U have the usual meanings).

Frank[17] carried out some experiments with a pair of thin vertical polished aluminium plates, each 2.3 x 2.3 feet. The plates were heated electrically and mounted out of doors in such a way that they automatically set themselves parallel to the wind direction. The temperature difference between the plate and the air was about 30°C. An anemometer was used to measure the air speed.

He found that the heat transfer coefficient for wind speeds up to 20 feet/second is given by

$$h = 0.57\ U^{0.656} + 0.67\ e^{-0.58U} \qquad \text{II-3}$$

The second term in the equation (II-3) shows the effect of natural convection in the cases of small air speeds.

Haucke[21] used two parallel cast iron plates, each 6.56 x 1.64 feet, fixed at a distance of 1.89 inches apart. The surface temperatures were maintained at about 212°F by means of steam jacketing.

Air was passed into the space between the plates through an extension of 6.56 feet in length. A pitot tube was used to measure the air speed at different points. The range of air speed was 13 to 66 feet/second. The air temperature was measured by thermocouples at the inlet and outlet of the working section, and the logarithmic mean temperature difference was taken.

The values obtained for the coefficient of heat transfer

can be expressed by

$$h = 0.57\ U^{0.713} \qquad \text{II-4}$$

Slegel and Hawkins[48] measured the heat transfer from a heated vertical plate to an air stream flowing parallel to it at various speeds. The plate was of $\frac{1}{8}$ inch brass and 10 ins long by 8 inches wide. It was placed inside a wind tunnel of cross-section 18 inches square. The plate was heated electrically and an unheated starting length of $39\frac{1}{4}$ inches was used.

The range of air velocity was from 32 to 66 feet/second, and the difference between the plate and air temperatures varied between 22 and 222°F. Calculating the physical properties at the film temperature Slegel and Hawkins correlated their data by the equation

$$Nu = 0.0299\ Re^{0.817} \qquad \text{II-5}$$

Values of the heat transfer coefficient for different air stream velocities are shown in Fig.3.

Ali[1] carried out his experiments for air flowing over a horizontal flat brass plate of dimensions 10 x 5 x $\frac{1}{8}$ inches. The plate was placed in a wind tunnel of square section 16x16 ins. The leading edge of the plate was at a distance of $14\frac{1}{2}$ inches from the inlet of the working section. The air velocity was 5 to 51 feet/second. The plate was heated electrically and radiation and conduction losses were calculated. The average plate temperature varied between 150°F and 380°F. Air

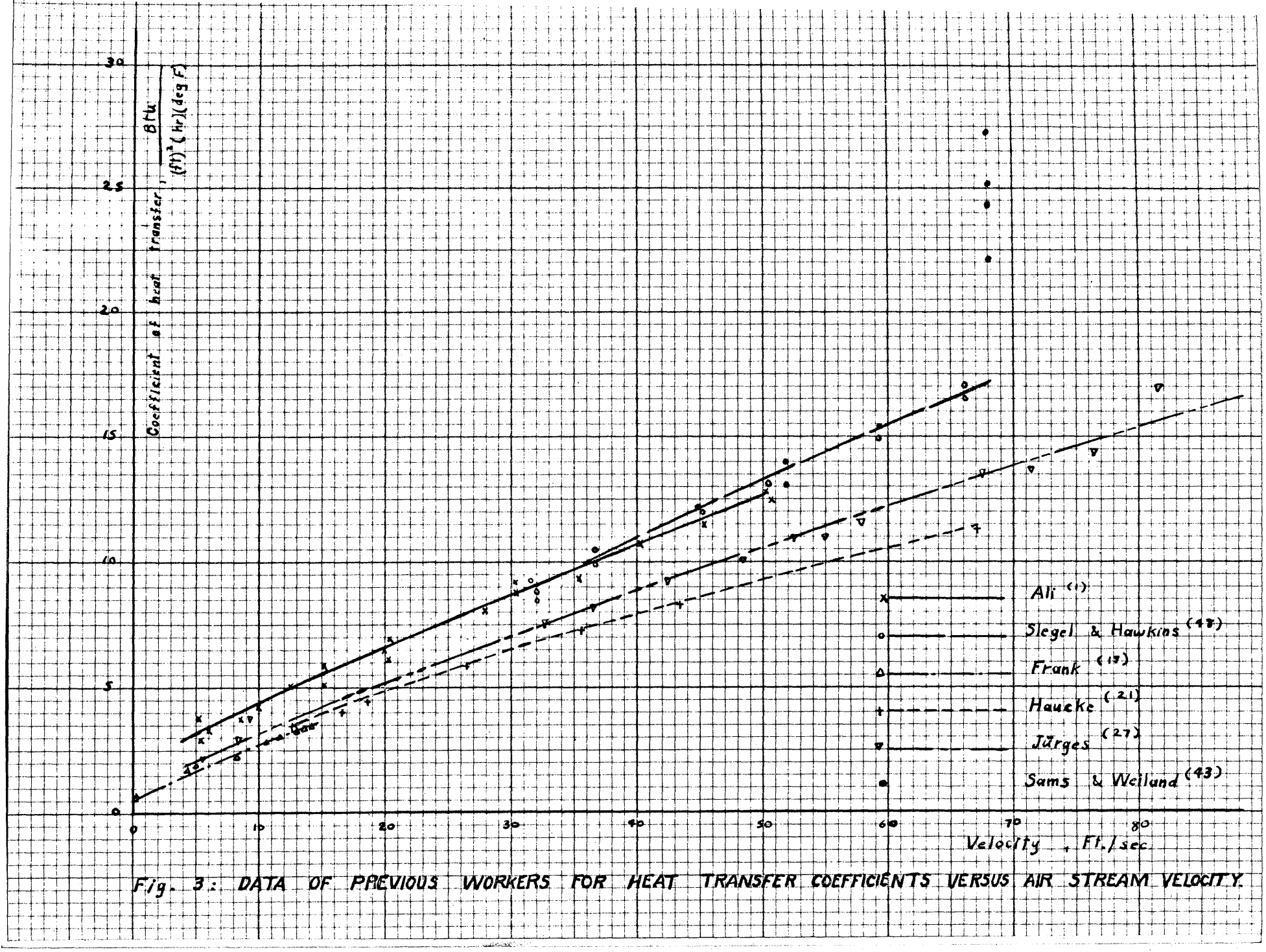

Fig. 3: DATA OF PREVIOUS WORKERS FOR HEAT TRANSFER COEFFICIENTS VERSUS AIR STREAM VELOCITY.

temperature was taken as that of the bulk of the air stream.

He correlated his data by the following relations :

For air stream velocity $<$ 16 feet/second

$$h = 2 + 0.231\ U \qquad \text{II-6}$$

For air stream velocity $>$ 16 feet/second

$$h = 0.945\ U^{0.682} \qquad \text{II-7}$$

Since mass velocity rather than linear velocity is the fundamental variable in forced convection equations, it is recommended[45] that the velocity U be multiplied by $\frac{460 + 70}{460 + t}$ when the temperature t of the air differs materially from 70^{o}f.

Effect of plate length on heat transfer.

Another series of experiments was carried out by Haucke[21] on two parallel plates having differing lengths. Four pairs of plates were used, having lengths 1.64, 3.28, 4.92 and 6.56 feet. In all cases the distance between the plates was kept at 1.89 ins.

He found that the coefficient of heat transfer increased with decreasing the length of the plates according to the expression

$$h = 0.98\ U^{0.71}\ L^{-0.29} \qquad \text{II-8}$$

This can be compared with Latzko's theoretical expression (I-22) which shows that (h) should be proportional to $(L^{-0.2})$.

Ali[1] undertook a second series of experiments to investigate

the effect of the plate length on heat transfer. He used a flat plate 10 x 5 inches, fitted inside the wind tunnel. The heating coil was constructed of six individual heaters, each having the same width as the brass plate (5 inches), with lengths of 1, 1, $1\frac{1}{2}$, $1\frac{1}{2}$, 2 and 3 inches successively. The input to each heater was adjusted separately so as to maintain the temperature of the heating surface constant all over the entire hot surface for all running conditions.

He found that the local coefficient of heat transfer was comparatively high at the leading edge of the plate. Then it decreases gradually till a length of $7\frac{1}{2}$ inches downstream is reached, after which the value of the local coefficient becomes practically constant.

Effect of unheated starting length.

Jakob and Dow[26] conducted an experimental investigation to determine the effect of different hydrodynamic starting lengths on the heat transfer coefficient. The heating surface in their experiments was a copper tube 1.3 inches in diameter and 8 inches long, with an electric heating coil inside. Wooden nose pieces of varying length served to vary the hydrodynamic starting length.

Air was passed through a channel and discharged by a square nozzle 10 x 10 inches into the room. Axes of the nozzle and the heating tube were coincident. The air velocity was varied from 10 to 150 feet/second.

The total heat given to the coil was measured by a wattmeter, and thermal losses were estimated. A pitot tube was used to measure the air stream velocity, which was determined at a single point midway between the ends of the hot cylinder and two inches from its surface. Seven different nose pieces were used. The ratio of the starting length to the total length was varied from 0.101 to 0.606.

Reynolds number (R_e) and Nusselt number (Nu) were defined as

$$R_e = \frac{U.Lt}{\nu_o} \qquad \text{and} \qquad Nu = \frac{h.L_t}{k_f} \qquad \text{II-9}$$

where L_t = total length of cylindrical surface
$= L_s + L_h$

L_s = unheated hydrodynamic starting length

L_h = length of heating surface

ν_o = kinematic viscosity at t_o

t_o = temperature of the bulk air

k_f = thermal conductivity at t_f

$t_f = \frac{1}{2}(t_w + t_o)$

t_w = mean temperature of the heating surface

(other symbols have the usual meanings).

Nu versus R_e was plotted for different cases of $\frac{L_s}{L_t}$. The turbulent region was generally started at R_e between 250,000 and 600,000. Nu was also plotted versus $\frac{L_s}{L_t}$ for two constant values of R_e in the turbulent region. The results were represented by the equation

$$Nu = 0.028\ R_e^{0.8}\left[1 + 0.4\left(\frac{L_s}{L_t}\right)^{2.75}\right] \qquad \text{II-10}$$

If there is no starting length then, by substitution in equation (II-10), we get

$$Nu = 0.028\ R_e^{0.8} \qquad \text{II-11}$$

Effect of solid boundaries on heat transfer.

The difference between the effect of unrestricted and wall bounded flow on heat transfer has not yet been fully studied. It has been recommended by Jakob[48] that more work should be done for comparison of such cases.

Cope[7] cooled air in circular and rectangular pipes with the aim of approximating the three dimensional flow to a two dimensional one. Two rectangular pipes of internal sections 1" x 0.125" and 2" x 0.1" were used. He observed the experimental values of heat transfer, and also calculated them from the mean surface friction by Reynolds' theory that

$$\frac{H}{F} = \frac{C\theta}{U} \qquad \text{II-12}$$

where H = heat transferred per unit area, Btu/ft.^{2}hr.
F = fricitional force per unit area of surface, lb/ft.hr^2
C = specific heat , Btu/lb.$^\circ$F
θ = temperature difference , $^\circ$F
U = mean velocity , ft/hr.

The results of the three dimensional experiments showed an appreciably greater rate of heat transmission than that calculated from Reynolds' theory. The results obtained from the rectangular pipes show that as the flow becomes more two dimensional in

character, the ratio of the observed heat transmission to the calculated one becomes progressively smaller and considerably less than unity.

Bailey and Cope[3] carried out some experiments in heating and cooling water flowing in a series of pipes of circular and rectangular sections in the same apparatus and varying the cross-section from a square down to a rectangle whose (breadth/depth) ratio is comparatively large. The pipes had internal dimensions 0.673" diameter, 0.552" square, 0.748" x 0.355", 0.875" x 0.248" and 1.0" x 0.126". The range of R_e was from 3,000 to 25,000, using the hydraulic diameter* as the length parameter.

Among the conclusions drawn by the authors are :

1. That an increase in surface friction does not necessarily lead to a corresponding increase in heat transmission.
2. That the heat transmission from a narrow rectangular pipe through which water is flowing and being heated is greater than that of a circular pipe under the same conditions. If the water is being cooled the heat transmission of the flat pipe is less than that of the circular pipe. That is to say that the heat transmission decreases under "cooling" and increases under "heating" conditions as the (breadth/depth) ratio increases.

The authors stated that the difference might be due to the increasing relative importance of the boundary layer; under "cooling" conditions the mean temperature of this layer is below that of the main body of the water and in consequence its

---

* Hydraulic diameter $= \frac{4 \times \text{area of cross-section}}{\text{perimeter}}$

viscosity is higher, resulting in a smaller value of its R_e. The reverse would be the case under "heating" conditions

---

Washington and Marks[51] undertook some experiments on air flowing through rectangular passages. They used three horizontal, steam jacketed, copper walled ducts, separated at the edges by strips of transite. The three ducts were all of the same height and length (5 inches and 4 feet respectively), but each had a different gap between the side walls, the gaps being $\frac{1}{8}$", $\frac{1}{4}$" and $\frac{9}{16}$". No calming section was used, but the abruptness of entrance was reduced by the use of an entrance cone. The wall temperature and the inlet and outlet temperatures were recorded by copper-constantan thermocouples. The air velocity was determined by measuring the pressure difference across a calibrated orifice. The apparatus used by Washington and Marks is shown in Fig.4.

The data were correlated by the equivalent diameter $D = \frac{2ab}{a+b}$ (where a = height of duct, and b = gap between the side walls). The air speeds were

9.8 to 131.8 feet/second for the $\frac{1}{8}$" duct

7.46 to 111.1 feet/second for the $\frac{1}{4}$" duct

3.76 to 59.6 feet/second for the $\frac{9}{16}$" duct.

The results for the heat transfer coefficient versus average air velocity for the three ducts are shown in Fig.5. They are shown also in Fig.6 as Nu versus R_e.

The authors stated that the flow was viscous up to

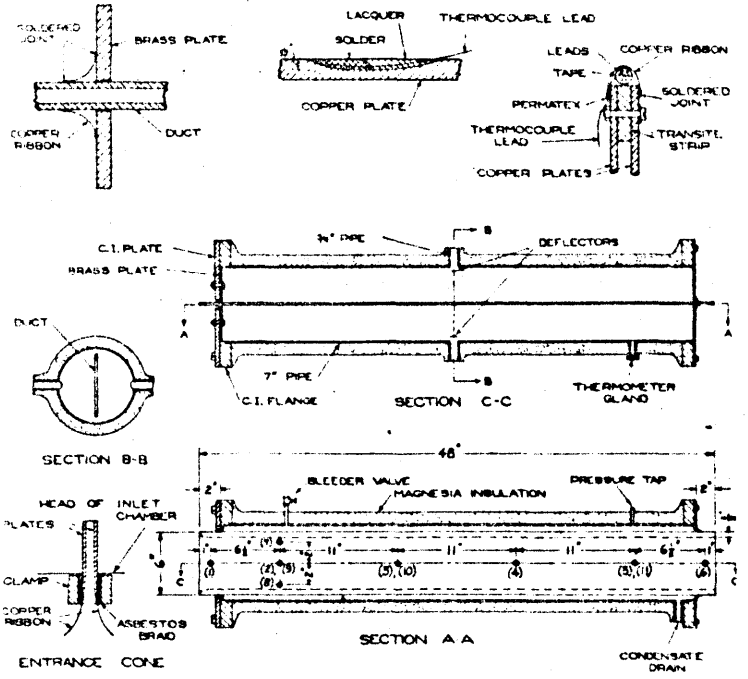

FIGURE 1. CONSTRUCTION DETAILS AND ASSEMBLY OF APPARATUS

Figures in parentheses denote thermocouple junctions. Junctions 1 to 8 are in one wall, junctions 9 to 11 in the other

Fig 4: APPARATUS USED BY WASHINGTON AND MARKS (51).

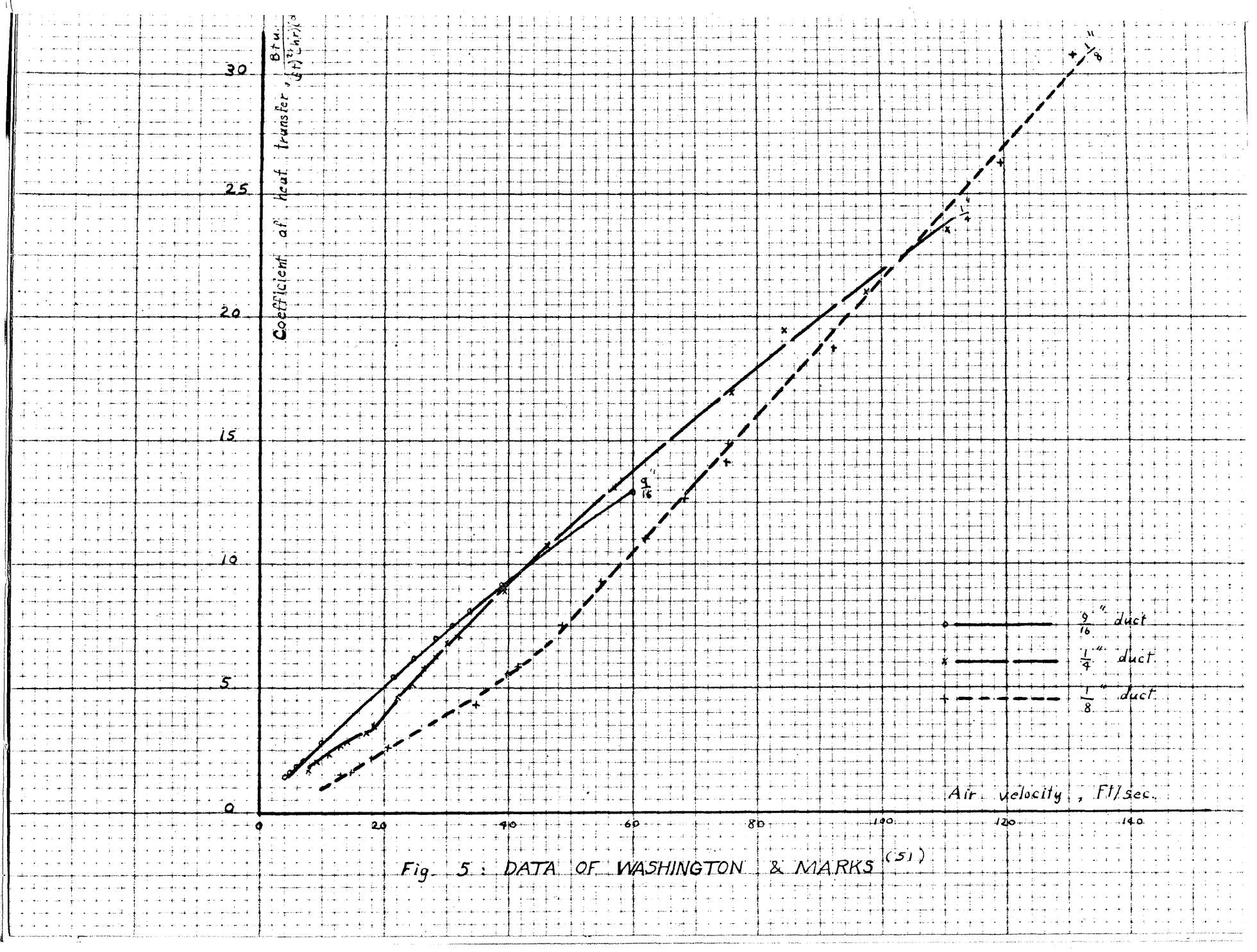

Fig. 5 : DATA OF WASHINGTON & MARKS (51)

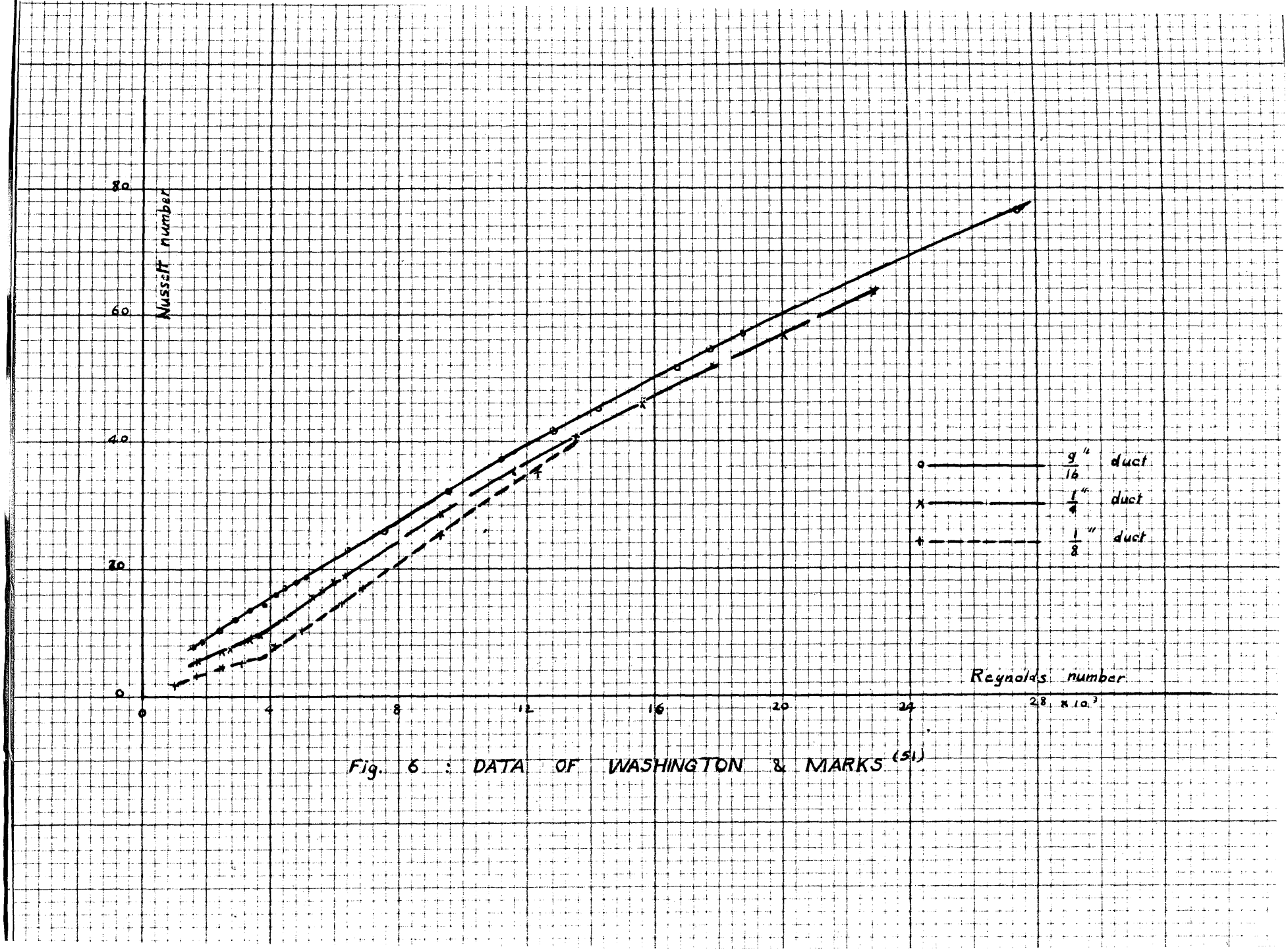

Fig. 6 : DATA OF WASHINGTON & MARKS (51)

$\frac{\rho UD}{\mu} = 3400$. It became fully turbulent when $\frac{\rho UD}{\mu}$ exceeded 13,000, in which case the data were represented by the equation

$$\frac{hD}{k} = 0.0203 \left(\frac{\rho UD}{\mu}\right)^{0.8} \qquad \text{II-13}$$

where U = mean velocity
other symbols have the usual meanings.

It was noticed that in the viscous flow an increase of the gap between the walls produced an increase in the surface coefficient of heat transfer and a decrease in the fricition gradient.

Sams and Weiland[43] conducted some experiments to obtain forced convection heat transfer data for flow of air between parallel flat plates forming passages of short length-to-effective diameter ratios. They used two stacks of thin flat plates, each stack having nine plates. Each plate was 3.5" long, 3" wide and 0.018" thick. The spacing between each two plates was $\frac{1}{4}$". A 24" long wooden approach section was used so as to have a uniform stream at the leading edges of the plates.

The plates were heated electrically till temperatures of about 200 to 220°F. The air temperature was about 58°F. The arithmetic mean temperature of the air (before and after heating) was taken as its bulk temperature. Various gaps between the two stacks were applied, and also the effect of misalignment between the stacks was studied. The effects on heat transfer were small, but generally the heat transfer coefficients were high.

Three mean airstream velocities were applied, namely 68, 108 and 172 feet/second. The corresponding average coefficients of heat transfer were 24.3, 36.7, and 55.4 Btu/ft^{2}hr.^{o}F.

CONCLUSION.

From the results given in this and the preceding chapters it becomes clear that the experimental results for turbulent flow heat transfer coefficients lie, generally, higher than mathematically calculated ones. When a plate is placed in a stream of air in a wind tunnel this stream is not completely smooth, but is, to a greater or less extent, eddying. Thus, in addition to the main velocity of the stream, the air at any point has an eddying or irregular velocity, the mean value of which is zero. In the mathematical treatment of heat transfer in turbulent flow, generally, the mean flow components only are considered.

MacAdams[32] discussed this problem and showed why little success follows attempts to apply mathematical analysis in the prediction of heat transfer from the fundamental equation for heat conduction in moving fluids , unless empirical corrections are introduced. These correction factors may be determined experimentally as the details of the mechanism of turbulent flow are not fully recognised as yet.

However, the experimental results do not agree among themselves. The inlet conditions have much to do with that. The

results are specially dependent upon the overall dimensions and the specific proportions of the equipment. This was pointed out by Fishenden and Saunders[14] who stated that the heat transfer coefficient depends to a considerable extent upon the conditions of flow, such as the depth of stream and the velocity distribution.

In the following chapter some approximate expressions will be derived. They show the effect of some flow conditions on heat transfer.

CHAPTER III.

GENERAL THEORETICAL CONSIDERATIONS

In this chapter a general discussion of the flow parallel to a flat surface and between two parallel flat plates will be given. The effect of the flow conditions on heat transfer will also be discussed.

The case of heat transfer from a flat surface to a fluid flowing in radial direction parallel to the surface has not been considered before. An approximate mathematical solution to this case will also be given. It is hoped that the ideas described here furnish the beginning step in this direction.

Flow parallel to a single flat plate.

When a uniform stream arrives at the forward edge of a thin plate the fluid has, practically, the velocity (U) at all distances from the plate. The fluid next to the plate is then forced to remain at rest while the main stream flows on with velocity U. As a result a thin layer is formed in which the viscosity forces of the fluid bring about a change of velocity. As the stream moves over the surface, the retarding effect of viscosity forces gardually penetrates deeper and deeper into the surrounding fluid so that the boundary layer increases in thickness (Fig.7).

For some distance downstream the flow in the boundary layer is laminar. This laminar flow is followed by a transition to

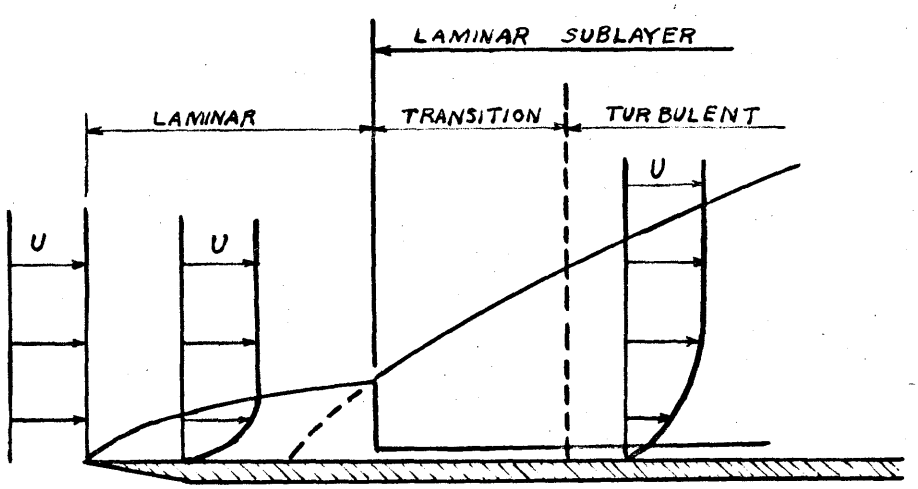

Fig. 7 : DEVELOPMENT OF BOUNDARY LAYER ALONG A FLAT PLATE.

turbulence when $(\frac{Ux}{\nu})$ reaches a certain critical value, where x is the distance from the leading edge of the plate. This critical value depends generally on the disturbances present and on the conditions at the front of the plate. In the turbulent stage, finally, the thickness of the boundary layer increases more rapidly than it did in the laminar range. Within the turbulent boundary layer, however, a very thin laminar film still exists next to the surface, being a permanent feature of any fully established flow.

In problems where it is necessary to consider a boundary layer containing both laminar and turbulent portions it is customary (Ref.19, page 329) to neglect the length of the transition region.

Effect of flow conditions on heat transfer.

The measurements of Elias[12] suggest that the velocity and temperature distributions for the flow in the boundary layer along a heated plate are of the same form. Because of the analogy between momentum transfer and heat transfer the mode of heat transmission depends upon whether the flow in the boundary layer is laminar or turbulent. It may be expected that Pohlhausen's equation (I-15) will be applicable to a certain length of the plate where the boundary layer is laminar, while Latzko's equation (I-22) applies to the remaining length, where the boundary layer is turbulent. An average value of (h) all

along the plate may lie, theoretically, between the values given by the two expressions.

To deduce an average theoretical expression the following definitions are introduced :

L = total length of the plate
X = length subject to laminar boundary layer ($X \leq L$)
U = main stream velocity
h_l = heat transfer coefficient from equation (I-15)
h_t = heat transfer coefficient from equation (I-22)
h_m = overall average coefficient of heat transfer.

The average coefficient of heat transfer is given by

$$h_m = \frac{X}{L} \cdot h_l + \frac{L-X}{L} \cdot h_t$$

$$= h_t + \frac{X}{L} (h_l - h_t) \qquad \text{III-1}$$

or $$h_m = h_t + f(X, L, U) \qquad \text{III-2}$$

The value of f can be zero or either positive or negative.

For small stream velocities (h_l) is larger than (h_t), and (f) is positive. When the stream velocity increases (h_t) increases faster than (h_l). A value of (U) is reached, where $h_l = h_t$. After that value of (U) the value of (h_t) exceeds (h_l) and the value of (f) becomes negative, thus giving a value for (h_m) smaller than (h_t).

Another influence is given by (L). If (L) increases then, for the same value of (U), (f) decreases till it becomes zero.

These two results lead to the conclusion that $\frac{h_m}{h_t}$ is greater than one at small velocities and plate lengths. This ratio decreases when either (U) or (L) increases.

If $h_m = K.U^n$ then n should lie somewhere between 0.5 and 0.8. The value of n will be nearer to 0.5 the shorter the plate. If $L \gg X$ then $n = 0.5$.

The effect of turbulence at the leading edge of the plate is to reduce the value of the critical Reynolds number, thus reducing the value of (X) in equation (III-1). This, for the same values of (U) and (L), makes the value of (h_m) nearer to that of (h_t).

Flow and Heat transfer between two parallel flat plates.

The flow between two parallel flat plates is much affected by the gap between the plates and the distance downstream. When the two plates are widely spaced from each other the thickness of the boundary layer is very small compared with the distance between the plates. In this case none of the plates has an appreciable effect on the other, and each one of them can be considered as a single flat plate placed in the stream.

However, when the two plates become nearer to each other, different conditions begin to exist. Goldstein[19] has shown that with certain types of entry the flow, when it enters a duct, is uniform over a cross-section. Later, the fluid near the wall is retarded, with consequent acceleration of the central portions in order to ensure that the flux is the same across all sections. The retarded layer grows in thickness until it fills the whole duct, and ultimately the final velocity distribution is attained. Therefore, for laminar flow between two parallel

plates, the parabolic distribution of velocity is attained only after a sufficient distance from the entry, and the velocity distribution in this 'inlet length' depends on the conditions at the entry.

If care is taken to have the fluid free from disturbances at the entry, the flow in the duct for some distance x from the entry will be laminar even though turbulence may develop further downstream. The value of $\frac{Ux}{\nu}$ at which the transition starts may be equal to that for flow along a flat plate. After the transition to turbulence takes place, a further distance is required before the velocity distribution across the section takes its final form. After that distance, when the turbulence becomes fully developed, the flow in any one section is the same as that in any other one.

These flow conditions affect the heat transfer seriously. Some cases of sufficiently long plates have been discussed in Chapter I. But, as shown previously, the conditions in the inlet length are entirely different. The heat transfer coefficients close to the entrance are much higher than those found downstream because of the severe temperature gradients in the entrance.

In the case of turbulent flow heat transfer wider gaps have two advantages :

1. Turbulence in the main stream increases as the distance between the plates increases. The fluid particles will have more freedom to move in all directions.
2. As the gap increases the inlet length increases, thus

more heat will be transferred.

An analysis has been made recently by Deissler[8] for turbulent heat transfer in the entrance regions of smooth passages. He studied the effect of (R_e) on the value of $\frac{N_u}{N_{ud}}$ for different values of $\frac{x}{b}$ (where Nud = value of N_u when the fl flow becomes fully developed, x = distance from the entrance). The values of $\frac{Nu}{Nud}$ close to the entrance were higher for the low Reynolds numbers than for high ones. This effect dies gradually as we proceed downstream. This means that, at a point near the entrance, the increase in Nu with R_e is slower than that of Nud. In other words, if

$$Nu \propto R_e^{n_1} \quad \text{and} \quad Nud \propto R_e^{n_2}$$

then n_2 must be bigger than n_1. The difference between n_2 and n_1, decreases as we go downstream. Therefore, for smaller values of $\frac{x}{b}$ we may expect a smaller exponent of the curve. It is to be stressed again that this applies only to the local coefficients of heat transfer near the entrance. If the plates are short this result may be reflected on the average coefficients of heat transfer.

RADIAL FLOW OF A FLUID PARALLEL TO A FLAT SURFACE.

The difference between this case and that of uniform parallel flow lies in the fact that the main stream velocity in this case varies from one point to another in the direction of flow. Accordingly the growth of the boundary layer does not follow the same simple rules. Similarly the heat transfer will not follow the formulae given in Chapter I by Pohlhausen and Latzko.

The heat transfer in this case is much affected by the difference between the radii of the heating surface and the ratio of them. As the main stream velocity varies at different radii a definition is necessary for a certain reference velocity. This will be referred to as the mean velocity of the main stream.

Definition of the effective mean velocity of the main stream (U_m)

The effective mean velocity of the main stream is defined as the uniform velocity at which a particle of the fluid travels between radii r_1 and r_2 in the same interval of time as the actual case of radial flow. Therefore we have

$$\left[t\right]_{r_1}^{r_2} = \frac{r_2 - r_1}{U_m} \qquad \text{III-3}$$

$$\delta t = \frac{\delta r}{U}$$

where δt = interval of time

U = velocity at radius r

$$= \frac{U_1 r_1}{r}$$

$$\therefore \delta t = \frac{r \delta r}{U_1 r_1}$$

$$\therefore [t]_{r_1}^{r_2} = \frac{1}{U_1 r_1} \int_{r_1}^{r_2} r \, dr$$

$$= \frac{r_2^2 - r_1^2}{2U_1 r_1} \qquad \text{III-4}$$

From equations (III-3) and (III-4) we get

$$U_m = \frac{2U_1 r_1}{r_1 + r_2} \qquad \text{III-5}$$

The corresponding mean radius (r_m) is therefore the arithmetic mean between r_1 and r_2.

Heat Transfer between a flat surface and air flowing in radial direction as compared with heat transfer to air in uniform parallel flow.

The theoretical expression derived by Latzko (equation I-22) for heat transfer in uniform parallel flow was based on the assumptions given by von Karman[28] for the thickness of the boundary layer and the velocity distribution inside it. Small velocities were assumed and the pressure outside the boundary layer was considered constant.

However, with variable main stream velocity both theoretical and experimental evidence are at a minimum. The pressure outside the boundary layer is not constant and the growth of the boundary layer is affected by the variation of the mainstream velocity. As a method of prediction of the heat transfer in this case, the use of the flat plate correlation will be made

with some modification. Although it may be a rough approximation the effect of the pressure gradient will be neglected here. The temperature difference between the surface and the fluid outside the boundary layer will also be assumed constant. The growth of the boundary layer will be considered affected by the effective mean velocity of the mainstream. Other assumptions used by Latzko are also assumed here.

If the radial flow starts at a radius r_1 with velocity U_1, the mainstream velocity (U) at any radius (x) will be given by

$$U = \frac{U_1 r_1}{x} \qquad \text{III-6}$$

The velocity distribution in the boundary layer is given by

$$\frac{u}{U} = \left(\frac{y}{\delta}\right)^{1/7} \qquad \text{III-7}$$

where u = velocity inside the boundary layer at x and y
x = radius
y = distance normal to the surface ($\leq \delta$)
δ = thickness of the boundary layer.

The effective mean velocity (U_{mx}) between radii r_1 and x is

$$U_{mx} = \frac{2U_1 r_1}{r_1 + x} \qquad \text{III-8}$$

and the thickness of the boundary layer at a radius x will be

$$\delta = 0.37 \left(\frac{\nu}{U_{mx}}\right)^{0.2} \cdot (x - r_1)^{0.8} \qquad \text{III-9}$$

Similarly the temperature distribution in the boundary layer is given by

$$\frac{\theta}{\theta_o} = \left(\frac{y}{\delta}\right)^{1/7} \qquad \text{III-10}$$

where Θ = temperature difference between the surface and the fluid at y.

Θ_o = temperature difference between the surface and the main stream.

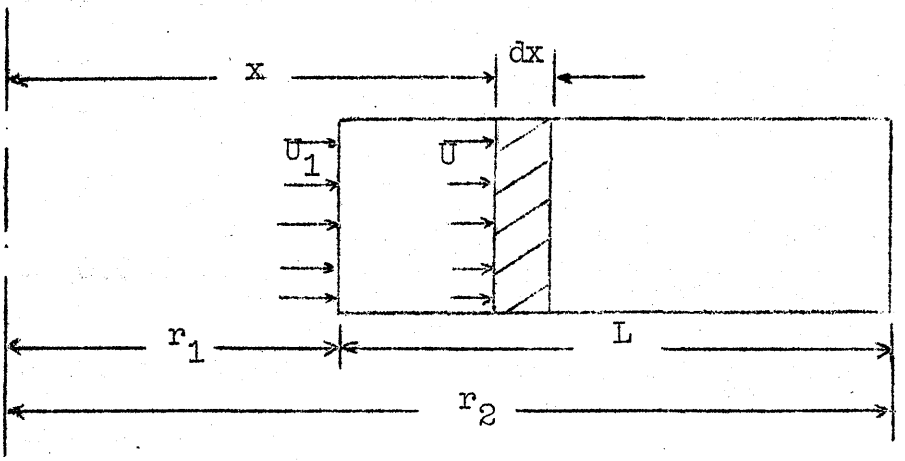

Figure 8.

A flat plate of unit width is now considered (Fig.8). The plate extends between the lines r_1 and r_2. The fluid arrives at r_1 with velocity U_1, and then the velocity varies according to equation (III-6).

Neglecting the heat of friction, the equilibrium in an element of the boundary layer will be given by the equation

$$q = \rho\, c\, \Theta_o \frac{d}{dx} \int_o^\delta u\, dy - \rho\, c \frac{d}{dx} \int_o^\delta u\, \Theta\, dy$$

where q = heat given per unit length of surface.

Substitution for u and Θ from equations (III-7), (III-6) and (III-10) gives

$$q = \frac{7}{72}\, c\rho\, \Theta_o\, U_1\, r_1\, \frac{d}{dx}\left(\frac{\delta}{x}\right) \qquad \text{III-11}$$

From equations (III-9) and (III-8) we get

$$\frac{\delta}{x} = 0.37 \left[\frac{\nu\,(x + r_1)}{2\, U_1 r_1}\right]^{0.2} \frac{(x - r_1)^{0.8}}{x}$$

$$= 0.37 \left(\frac{\nu}{2\, U_1 r_1}\right)^{0.2} \frac{(x + r_1)^{0.2}(x - r_1)^{0.8}}{x} \qquad \text{III-12}$$

It follows from equations (III-11) and (III-12) that

$$q = 0.0356\, c\rho\, \theta_o U_1 r_1 \left(\frac{\nu}{2U_1 r_1}\right)^{0.2} \frac{d}{dx}\left[\frac{(x+r_1)^{0.2}(x-r_1)^{0.8}}{x}\right] \quad \text{III-13}$$

The total heat input is given by

$$Q = \int_{r_1}^{r_2} q\, dx$$

$$= 0.0356\, c\, \theta_o (\rho U_1 r_1)^{0.8} \left(\frac{\mu}{2}\right)^{0.2} \left[\frac{(r_2+r_1)^{0.2}(r_2-r_1)^{0.8}}{r_2}\right]$$

$$= h\, \theta_o (r_2 - r_1) \quad \text{III-14}$$

$$\therefore h = 0.0356\, c(\rho U_1 r_1)^{0.8} \left(\frac{\mu}{2}\right)^{0.2} \left[\frac{(r_2 + r_1)^{0.2}}{r_2 (r_2 - r_1)^{0.2}}\right]$$

$$= 0.0356\, c(\rho U_m)^{0.8} \mu^{0.2} \left(\frac{1}{L}\right)^{0.2} \left(\frac{r_2 + r_1}{2 r_2}\right) \quad \text{III-15}$$

where $L = r_2 - r_1$.

In the dimensionless form equation (III-15) becomes

$$\left(\frac{hL}{k}\right) = 0.0356 \left(\frac{\rho U_m L}{\mu}\right)^{0.8} \left(\frac{c\mu}{k}\right) \left(\frac{r_2 + r_1}{2 r_2}\right) \quad \text{III-16}$$

The influence of the ratio of the radii appears in the term $\left(\frac{r_2 + r_1}{2 r_2}\right)$.

Equation (III-15) may now be compared with Latzko's expression (I-22). If we put

h_r = value of h given by equation (III-15)

and h_u = value of h given by equation (I-22)

then we have

$$\frac{h_r}{h_u} = \frac{r_2 + r_1}{2 r_2} \quad \text{III-17}$$

This means that for radial outward flow the coefficient of heat transfer may be expected to be lower than that when the flow is uniform. When the value of the inner radius (r_1) approaches that of the outer one (r_2) the value of (h_r) approaches (h_u). A graph for the ratio $\left(\frac{h_r}{h_u}\right)$ versus $\left(\frac{r_1}{r_2}\right)$, calculated from equation

(III-17) is shown in Fig.9.

Another trial was made when the boundary layer was considered laminar. For uniform parallel flow the velocity distribution in the boundary layer is given by[19]

$$\frac{u}{U} = \frac{2y}{\delta} - \frac{2y^3}{\delta^3} + \frac{y^4}{\delta^4} \qquad \text{III-18}$$

and the thickness of the boundary layer is[19]

$$\delta = 5.83 \left[\frac{\nu\, l}{U}\right]^{0.5} \qquad \text{III-19}$$

where l = distance from the leading edge of the plate.

Equation (III-18) was also used for radial flow, and the thickness of the boundary layer given by

$$\delta = 5.83 \left[\frac{\nu (x - r_1)}{U_{mx}}\right]^{0.5} \qquad \text{III-20}$$

(all symbols have the usual meanings)

The temperature distribution is

$$\frac{\theta}{\theta_o} = \frac{2y}{\delta} - \frac{2y^3}{\delta^3} + \frac{y^4}{\delta^4} \qquad \text{III-21}$$

The same procedure for the turbulent boundary layer was applied here, and the final result is

$$h = 0.686\, c \left(\frac{\rho U_m \mu}{L}\right)^{0.5} \cdot \left(\frac{r_2 + r_1}{2 r_2}\right) \qquad \text{III-22}$$

and

$$\left(\frac{hL}{k}\right) = 0.686 \left(\frac{\rho U_m L}{\mu}\right)^{0.5} \cdot \left(\frac{c\mu}{k}\right) \left(\frac{r_2 + r_1}{2 r_2}\right) \qquad \text{III-23}$$

A similarly derived expression for uniform parallel flow gives

$$h = 0.686\, c \left(\frac{\rho U_m \mu}{L}\right)^{0.5} \qquad \text{III-24}$$

The ratio between the results given by expressions (III-22) and (III-24) is also equal to $\left(\frac{r_2 + r_1}{2 r_2}\right)$.

In this simplified treatment the effect of the pressure

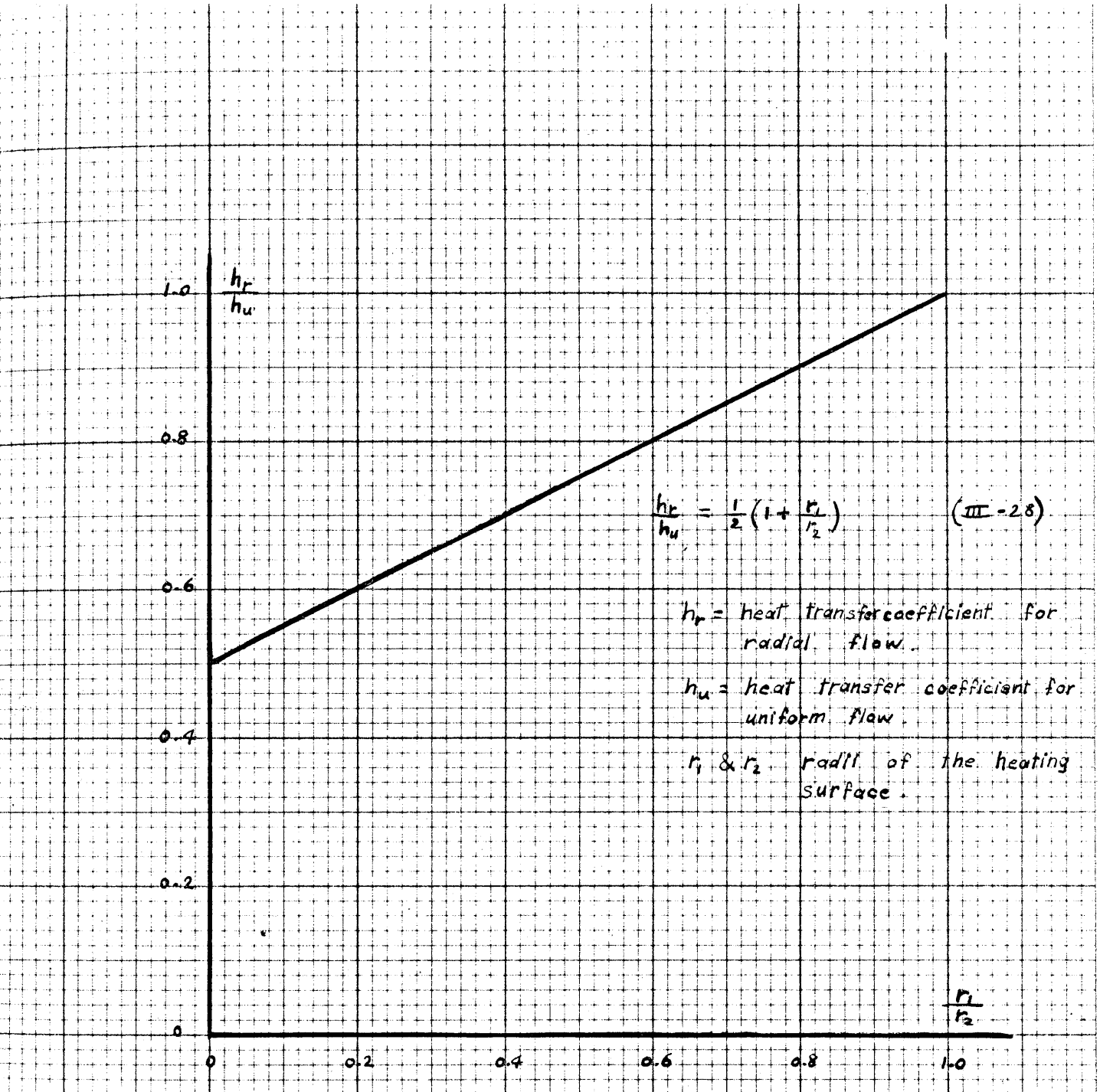

$$\frac{h_r}{h_u} = \frac{1}{2}\left(1 + \frac{r_1}{r_2}\right) \qquad (III-28)$$

h_r = heat transfer coefficient for radial flow.

h_u = heat transfer coefficient for uniform flow.

r_1 & r_2 radii of the heating surface.

Fig. 9 : EFFECT OF RATIO OF RADII ON HEAT TRANSFER. (theoretical)

gradient was neglected. Equation (III-17) may not represent the right values, but it generally gives an indication of the tendency of heat transfer. There is also experimental evidence that the heat transfer in uniform parallel flow is generally higher than that in outward radial direction. This will be shown later.

CHAPTER IV.

DESCRIPTION OF APPARATUS.

The apparatus consists mainly of three components :

1. Air passage
2. Heating unit
3. Measuring instruments.

AIR PASSAGE.

(i) Main pipe :

This was a horizontal circular galvanised pipe of diameter 6 inches and length 6 feet. One of its ends was connected to an air blower, and the other end led to the working section. Inside the pipe were two honey-combs, a nozzle and a bearing support. The pipe was supported on the bench by three wooden supports, its axis being $9\frac{3}{4}$ inches above the bench.

(ii) Air blower :

It was of the centrifugal type and driven by a direct current motor. Air was sucked from the room and blown into the main pipe. The diameter of the blower outlet was 6 inches. Its axis was in the same horizontal line as that of the pipe axis.

Some of the experiments were carried out with a motor and the blower connected together by means of a solid coupling. They were both supported on one solid base which was fixed to the floor. Later, it was found of much interest to extend the range of air discharge, and another motor was used. This was mounted on a special base; and the power was transmitted to the

blower through an endless V-belt.

(iii) Nozzle (for measuring the air flow):

The nozzle was made of brass and generally in accordance with British Standard 726 (1937) and British Standard 1042(1943). It was fixed inside the main pipe, at 22 inches from its inlet. The axes of the nozzle and pipe were coincident. Details of the nozzle are shown in Fig.10.

(iv) Honey-combs:

Two honey-combs, having octagonal cells $\frac{3}{8}$ inch side and of length 3 inches, were introduced, one being placed at the inlet of the pipe and the other at the downstream of the nozzle. The aim was to prevent swirl induced by the fan impeller about the direction of flow parallel to the axis of the pipe.

(v) Bearing support :

This was placed 6 inches before the outlet of the pipe and fixed to it by 8 screws. It served to carry one end of the shaft carrying the unheated disc. The support was made of brass and wood so as to be solid, light and causing the least possible disturbance to the air stream.

(vi) Inlet to working section :

This was designed so as to reduce inlet disturbances and to achieve a uniformly converging airstream resulting in a flow parallel to the plates. A smooth bell-mouthed piece of wood (Fig.11) was fixed with 4 screws to the unheated disc. Its maximum diameter was 7 inches.

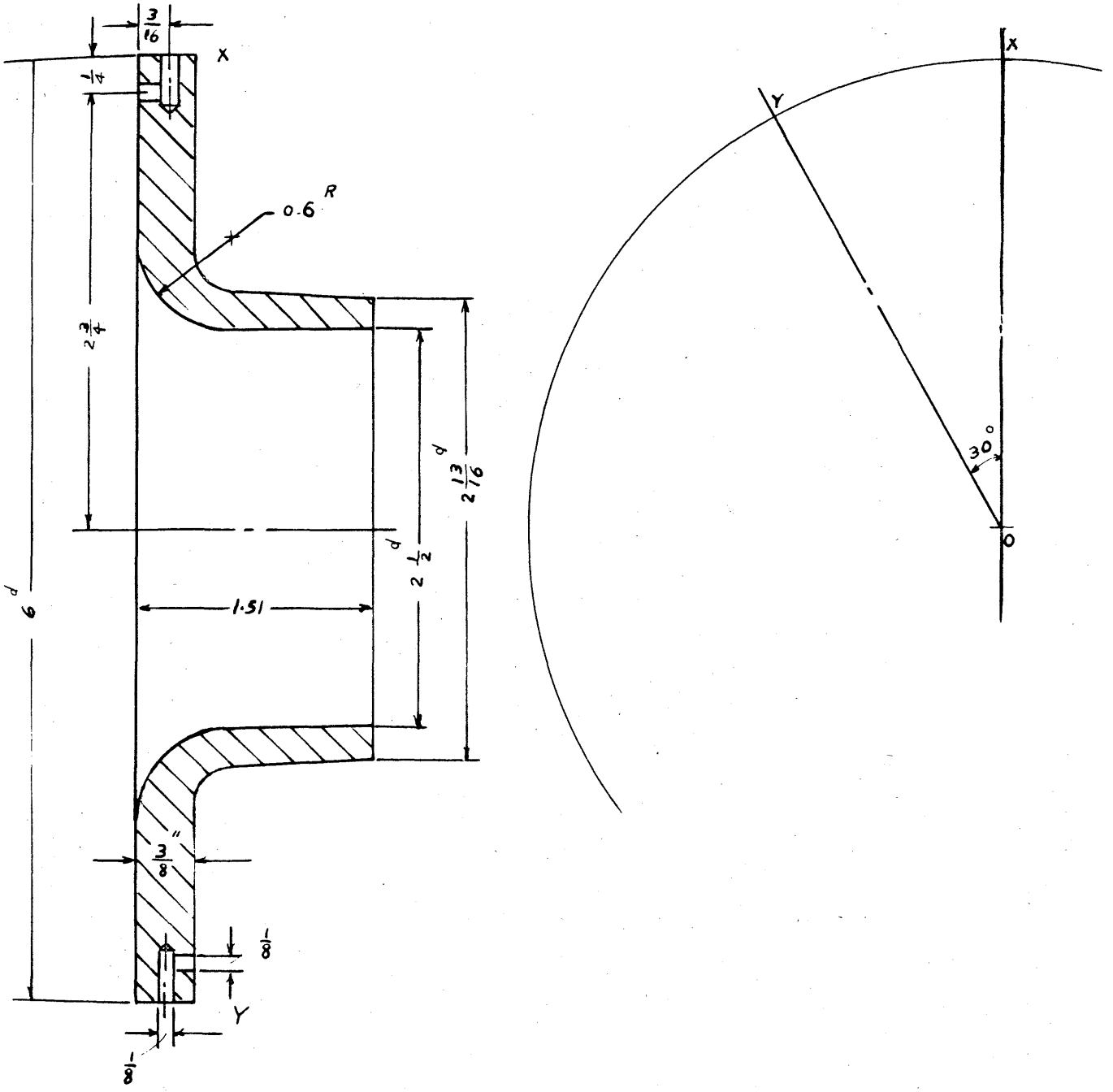

SECTION XOY

dimensions in inches

FIG. 10 : FLOW NOZZLE.

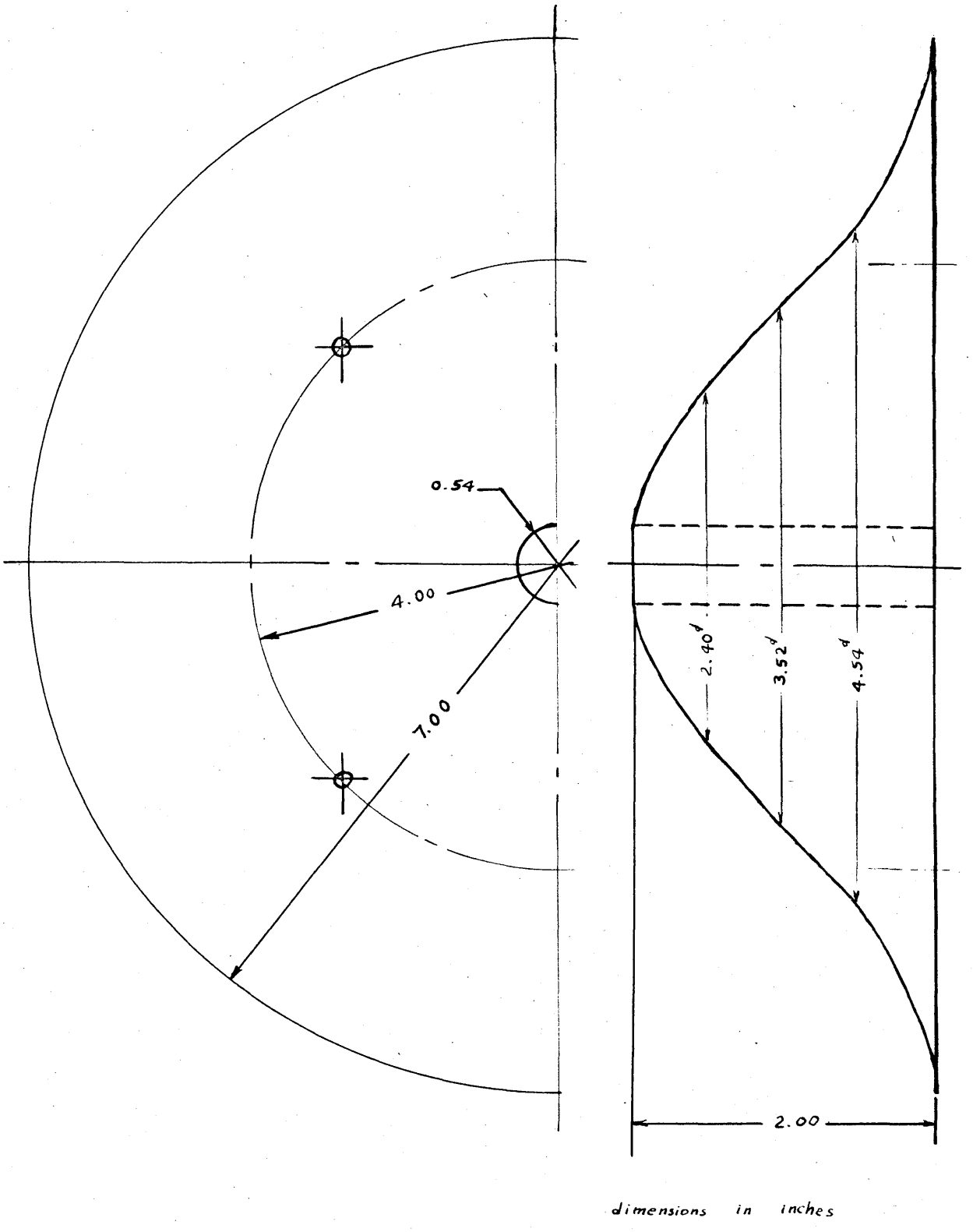

FIG. 11 : BELL-MOUTHED INLET TO THE WORKING SECTION.

(vii) Working section and unheated disc :

One side of the working section was formed of the heating unit. The heating surface had radii $4\frac{1}{2}$" and 8". It was surrounded by an asbestos ring of outer diameter 18 inches. The space between the heating surface and the pipe outlet was filled with another asbestos ring which formed a part of the bell-mouthed inlet.

The other side of the working section was the unheated disc (Fig.12). This was simply a brass disc of 18" diameter and $\frac{1}{8}$" thickness. Seven thermocouples were placed at different points on the unheated disc to determine its temperature. Their positions are shown by numbers 15, 16, 17, 18, 19, 20 and 21 in Fig.12. The technique followed in fitting these thermocouples was the same as that of the heating plate; and it will be described later. Two holes (mark A in Fig.12) were made at radii $4\frac{1}{2}$ and 8 inches to allow for thermocouple leads to pass to measure the air temperature at the beginning and end of the heating surface. To prevent heat conduction, the wires of the two thermocouples were passed through two glass tubes 3/32" diameter. The glass tubes could move through tufnol tubes which were screwed into the holes (A). Two other holes (B in Fig.12) of diameter 0.028" were made at radii $4\frac{5}{8}$ and $7\frac{7}{8}$ inches to measure the static heads at those two points. Other holes C and D will be described later.

A brass boss of 2" diameter and $3\frac{1}{2}$" length was fixed to the disc with 3 screws. Both the disc and boss were mounted on a steel shaft of diameter $\frac{1}{2}$", the shaft being mounted on two supports.

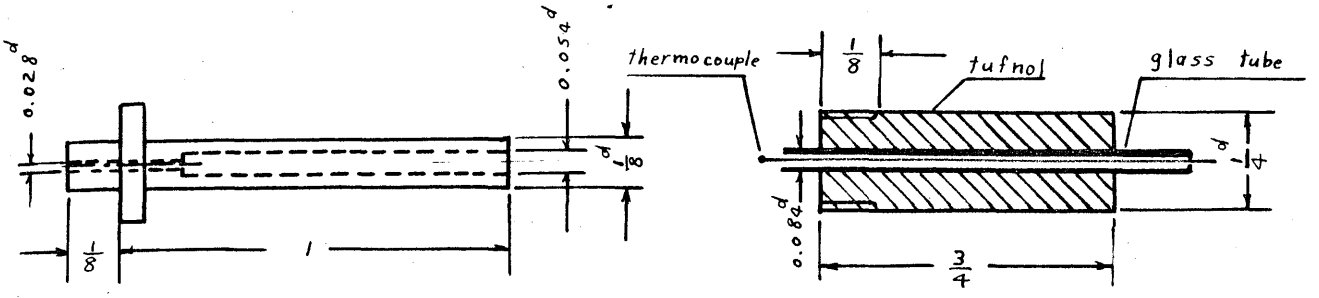

CONNECTED TO HOLES B

CONNECTED TO HOLES A

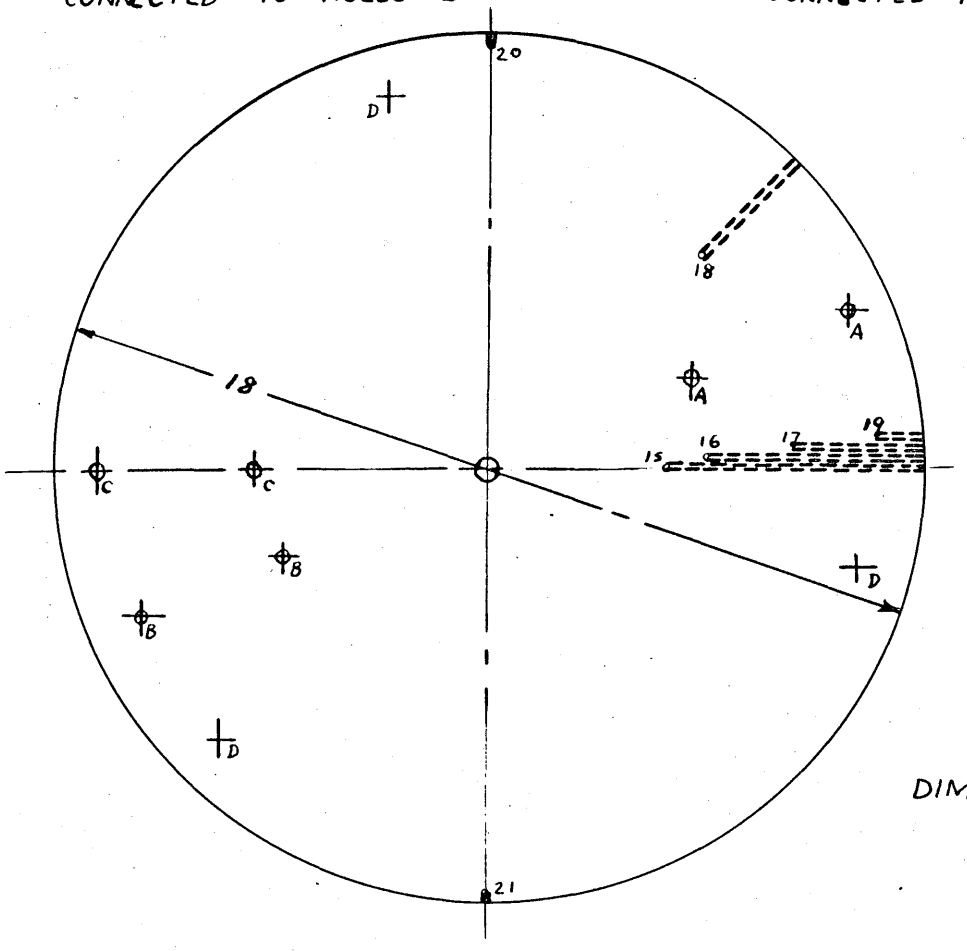

DIMENSIONS IN INCHES

MARK	DESCRIPTION
15, 16, 17, 18, 19, 20, 21	Thermocouple holes & grooves
A	Measurement of air temperature
B	Measurement of static pressure
C	Fitting micrometer arrangement
D	Gap adjustment

Fig. 12 : UNHEATED DISC.

One of these supports was inside the pipe, and the other was fixed to the bench.

A diagram of the air passage is shown in Fig.13.

HEATING UNIT.

The heating unit consists of the following main components:

(i) The heating plate
(ii) The main heater
(iii) The guard heater
(iv) Asbestos between the main heater and the guard heater
(v) Brass frame & asbestos sheets and rings.

The construction of the heating unit is shown in Fig.14.

(i) The heating plate :

This was a circular brass plate of thickness $\frac{1}{8}$" and inner and outer diameters 9 and 16 inches respectively. Ten holes, 0.052" diameter, were drilled in the plate in the positions shown by numbers 1, 2, 3, 4, 5, 6, 7, 8, 9, and 10 in Fig.14. A 60^0 cone was made at the front surface of each hole. At the other surface of the plate ten grooves were provided.

The copper constantan thermocouples, which were made of 26 gauge wire, were positioned in this manner : The ends of the two wires forming a thermocouple were twisted and then fused together by means of an electric spark in an atmosphere free from oxygen; thus forming the hot junction. They were then placed in a hole and fixed by soldering, and slightly hammered to fill the 60^o cone. Each thermocouple was then embedded in its groove, the

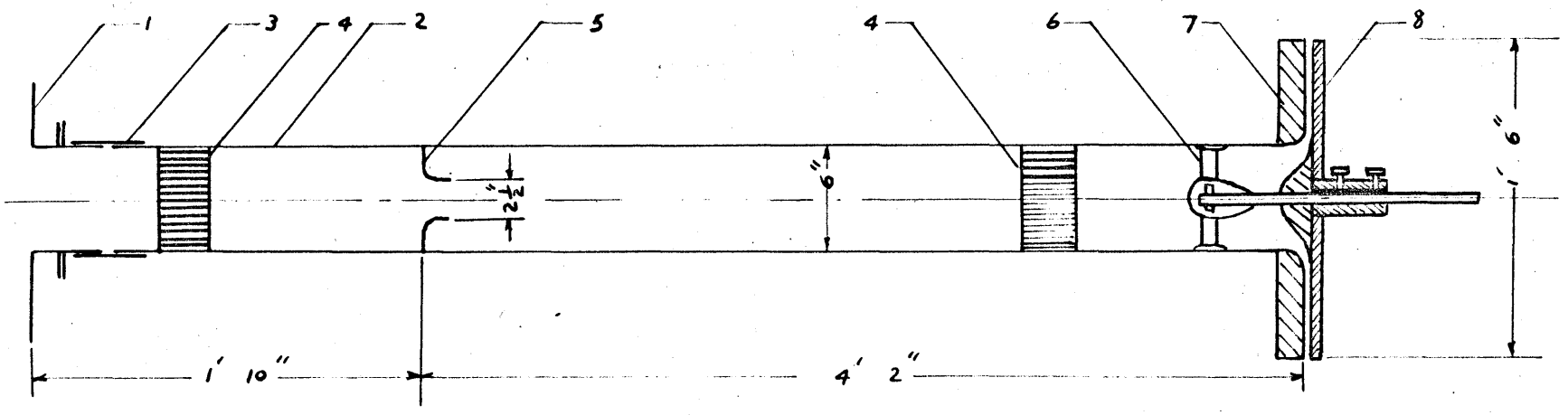

1- AIR BLOWER
2- MAIN PIPE
3- RUBBER PIPE
4- HONEY-COMBS
5- FLOW NOZZLE
6- BEARING SUPPORT
7- HEATING UNIT
8- UNHEATED DISC

FIG. 13 : DIAGRAM OF THE AIR PASSAGE

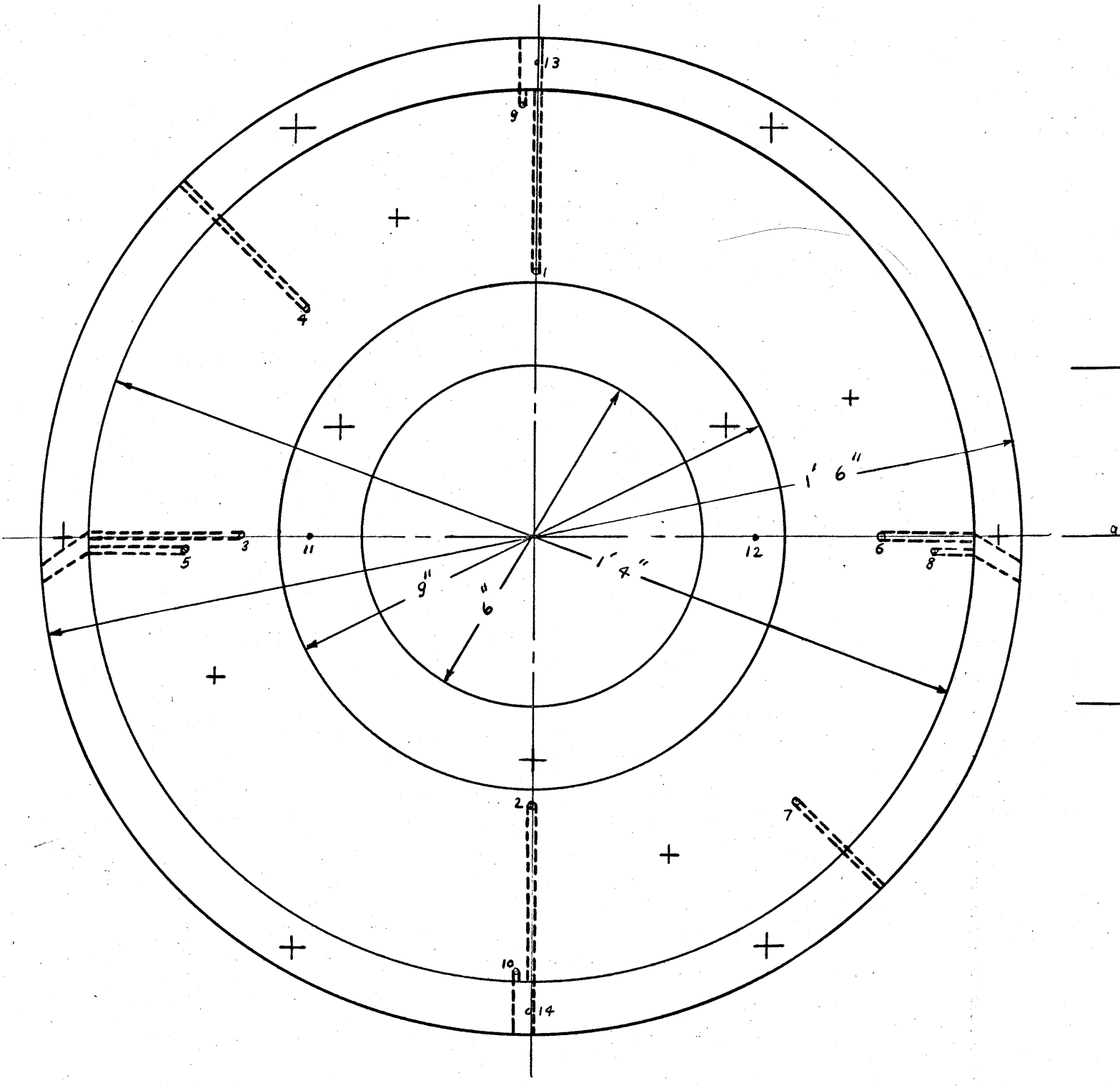

FIG. 14 : CONSTRUCTION OF THE HEATING

groove was then filled with a solution of asbestos powder and water glass. The thermocouples then passed from the plate through holes in the asbestos and frame. The conducting wires were insulated with glass spun fibre which appears quite satisfactory up to temperatures of the order 300°C.

(ii) The main heater :

Two mica rings of thickness 0.01" were used. One of them had inner and outer diameters 9 and 12 inches, the other 13 and 16 inches. A nickel chromium heating tape of cross-section 0.050" x 0.008" was wound in series over them. The mean pitch over the two rings was $\frac{3}{8}$". This unit was then placed between two mica rings, each of thickness 0.01", and inner and outer diameters 9 and 16 inches respectively.

(iii) The guard heater:

Mica rings used for the guard heater were of the same dimensions as those used for the main heater. The only difference between the two heaters was that the nickel-chromium tape used for the guard heater had cross-section 0.025" x 0.006".

(iv) Asbestos between the two heaters :

This was a circular sheet of inner and outer diameters 9 and 16 inches and thickness $\frac{1}{4}$". Three thermocouples were placed and embedded on each side in such a way that three pairs of identical thermocouples were formed. The heads were placed at radii $5\frac{3}{8}$, $6\frac{1}{4}$ and $7\frac{1}{8}$ inches.

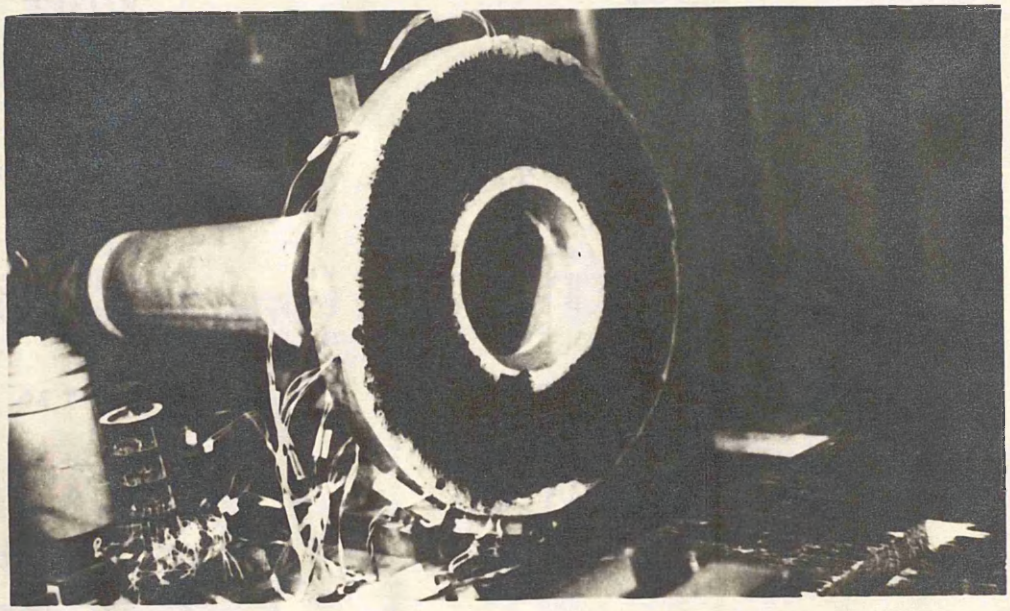

Fig. 15 : THE HEATING UNIT IN POSITION.

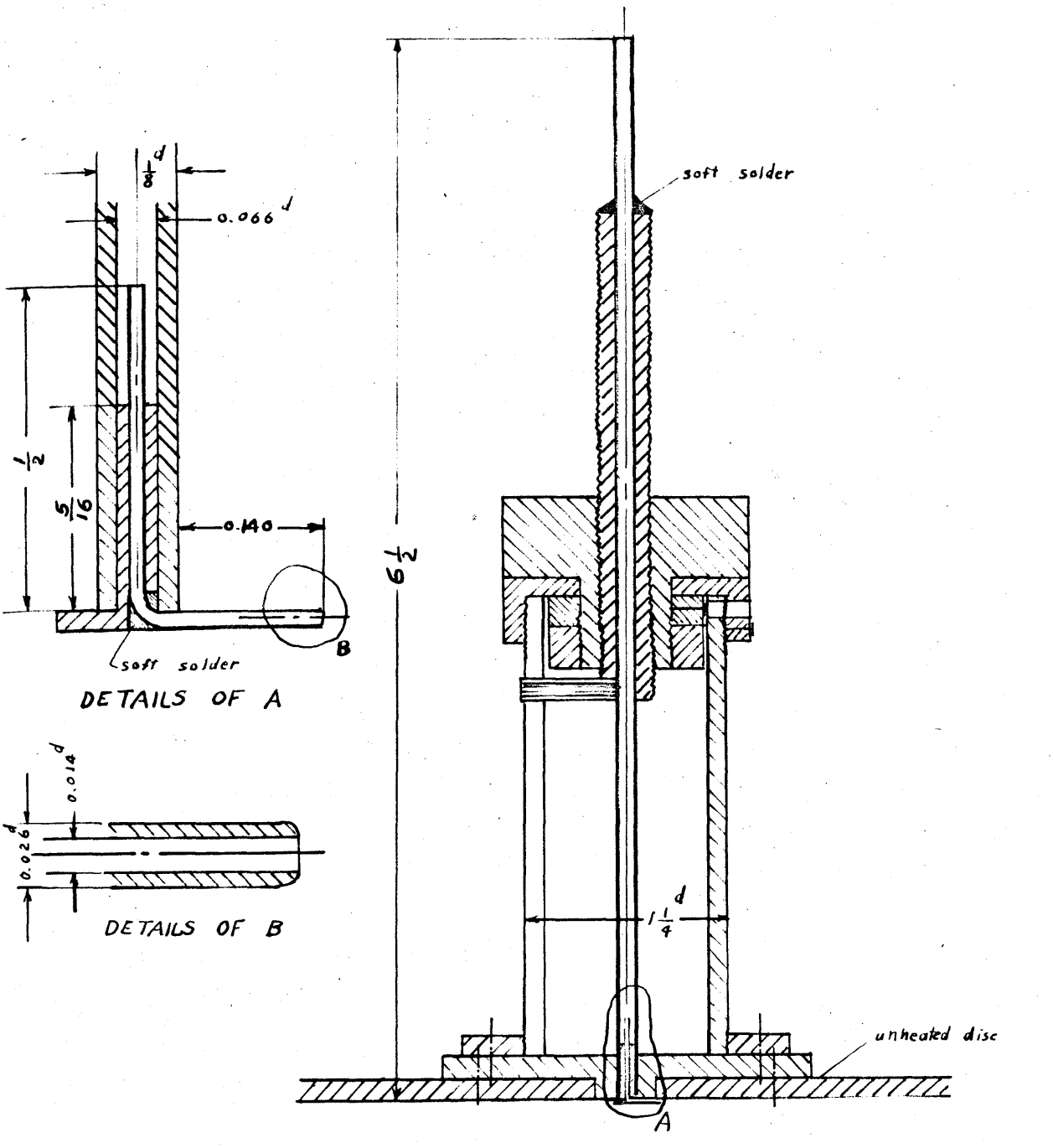

FIG. 16 : PITOT TUBE AND MICROMETER ARRANGEMENT.

copper tube was then soldered to a specially designed micrometer with one division representing 0.001". The construction of the pitot tube and micrometer arrangement is shown in Fig.16.

The micrometer was designed to be carried by the body of the unheated disc (holes C, Fig.12). In this way the distance of the point of measurement from the surface would be easily determined from the micrometer initial reading and a single measurement of the distance corresponding to one particular reading. The head branch of the pitot tube was aligned with its axis along the wind direction; that is, towards the axis of the 6" pipe. The other end of the $\frac{1}{8}$" copper tube was connected to one side of a Casella micromanometer whose opposite side was connected to a static head hole at the same radius as that of the leading end of the total head tube (holes B, Fig.12).

Other measuring instruments were :

1. Voltmeter
2. Ammeter
3. Potentiometer set (reading 5 micro-volt)
4. Selector switch
5. Thermos flask with ice
6. Wet and dry bulb hygrometer
7. Tachometer
8. Two inclined tube manometers
9. Casella micromanometer.

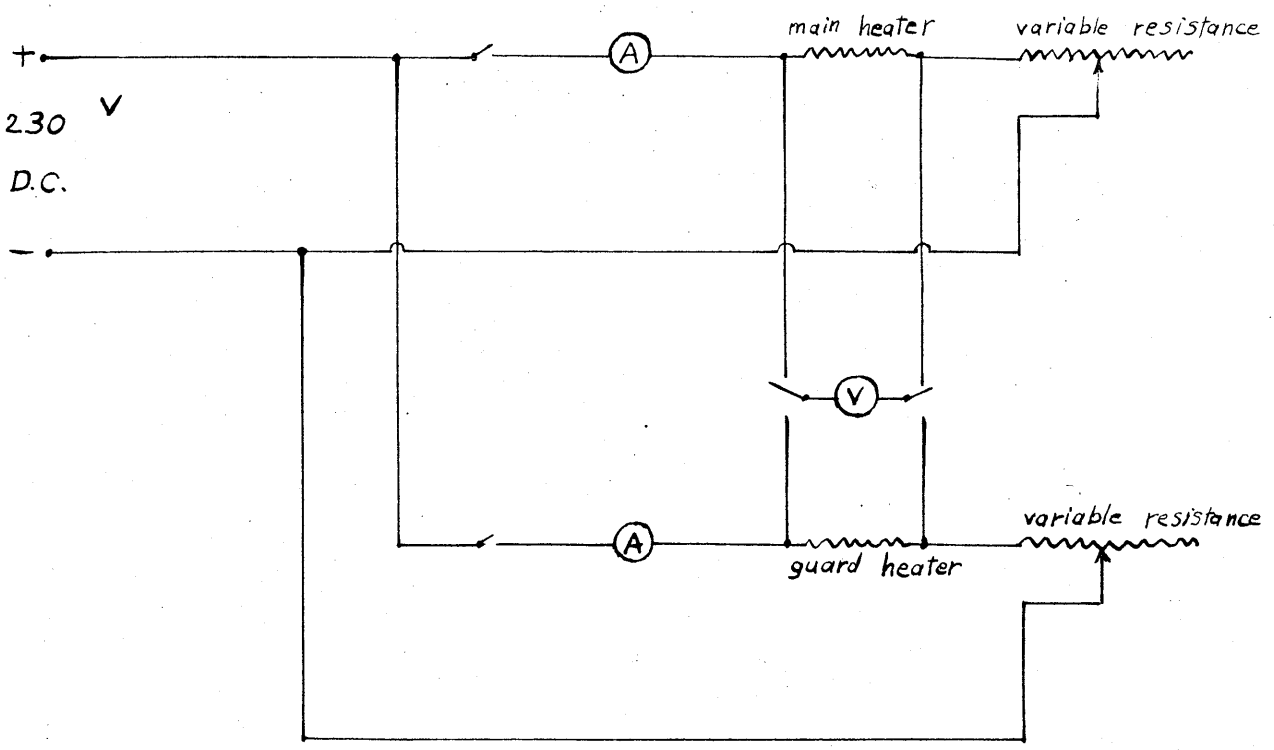

Fig. 17 : ELECTRICAL CONNECTION TO MAIN AND GUARD HEATERS.

the heaters to measure the voltage drop across it.

The rear surface of the unheated disc (Fig.12) was covered by an asbestos disc of diameter 18" and thickness $\frac{1}{2}$". To adjust the distance between the heating surface and the unheated disc, three $\frac{1}{8}$" screwed holes (marked D in Fig.12) were made equidistant from each other at a diameter $15\frac{7}{8}$" in the unheated disc. Then the distance was adjusted by the number of turns made by the screws.

Because of the wide range of emissivity of brass, the surfaces of the heating brass plate and the unheated disc were covered with a thin layer of matt black paint, thus assuming an emissivity of 0.97[16].

A selector switch and a thermocouple potentiometer set were used to measure the electomotive force of each thermocouple to an accuracy of 0.005 millivolt. The connection diagram for the thermocouples, selector switch, potentiometer set and common cold junction (ice in thermos) is shown in Fig.18.

It is to be mentioned here that the two thermocouples used for measuring the temperature of the flowing air were of different wire from the rest of the thermocouples. These two were copper constantan of 30 gauge (0.012" diameter). They were made in the same manner as the others and similar calibration was carried out on them. The juntions were polished, and during the actual experimental work care was taken that the junctions were always clean. This was necessary to reduce the heat radiation between them and the heating surface to a minimum.

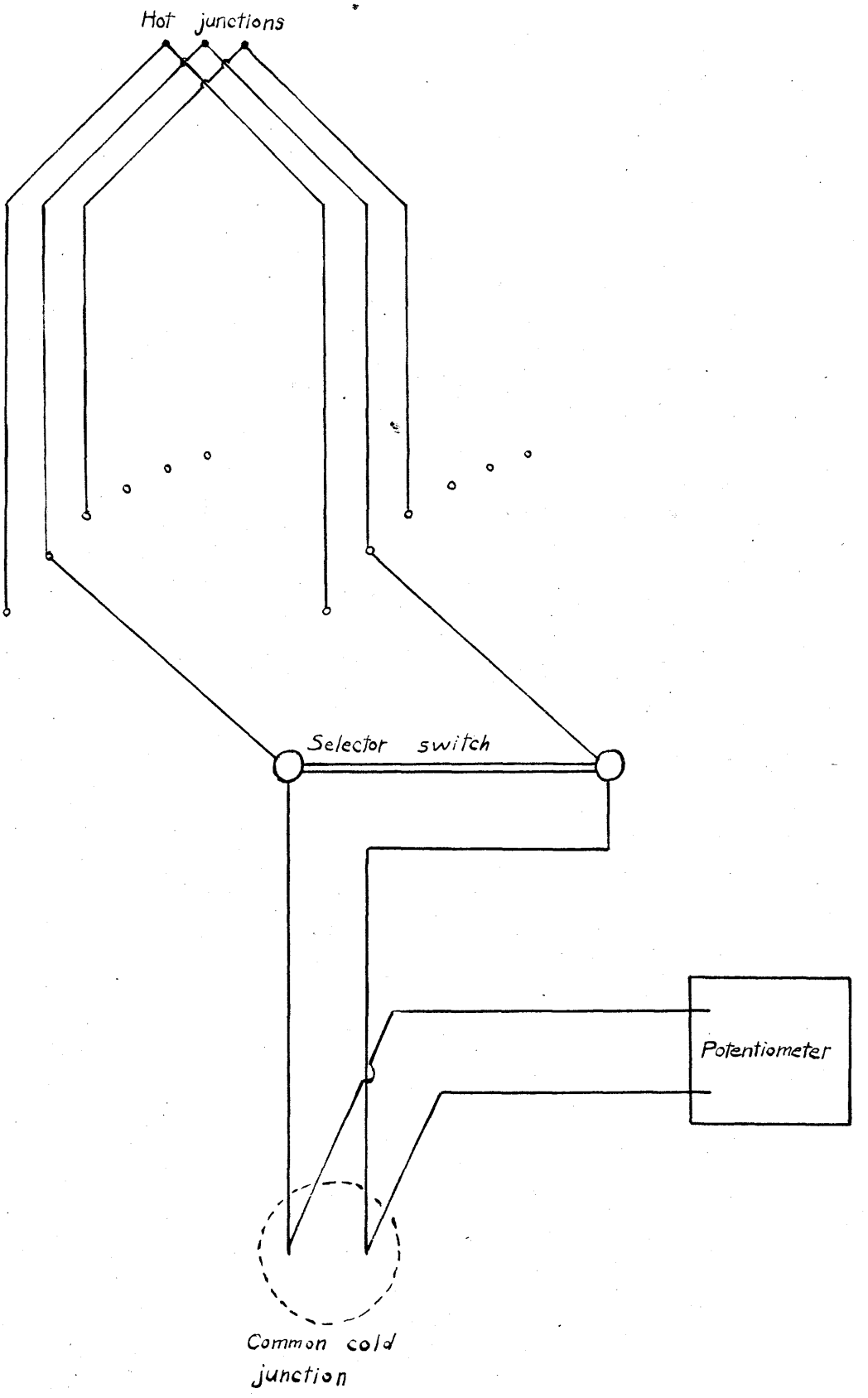

Fig. 18 : THERMOCOUPLES' CONNECTION DIAGRAM.

Generally, the temperature of the flowing air was taken nearer to the unheated disc than to the heating surface.

A wet and dry bulb hygrometer was placed near the inlet to the air blower to indicate the wet and dry bulb temperatures. A photograph of the final set-up is shown in Fig.19.

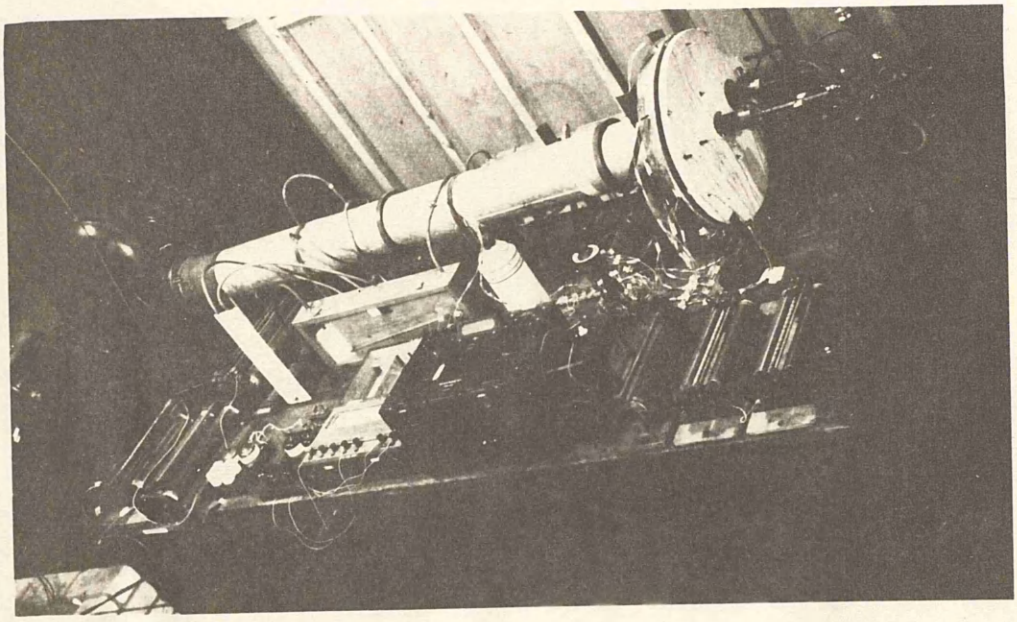

Fig. 19 : PHOTOGRAPH OF FINAL SET-UP.

CHAPTER V.

CALIBRATION OF MEASURING DEVICES.

Calibration was carried out on the following :

1. Thermocouples
2. Nozzle
3. Small total head tube.

CALIBRATION OF THERMOCOUPLES.

There are three distinct ways of calibrating a thermocouple. The first is by direct comparison with a standard thermometer over its working range. The second is to determine the response for certain accurately known fixed points and to fit an equation to these. The third is the deviation method where responses are measured at some fixed points over the range, the deviation from the response of a standard thermocouple calculated and a curve of deviation against standard response drawn. From this deviation curve and the standard curve a calibration curve for the particular thermocouple is drawn.

In the present work* the deviation method was chosen. Calibration was carried out with a suitable glass jar and condenser, known as a hypsometer. The fixed points chosen were the boiling points at atmospheric pressure of water and naphthalene. The

---

* The calibration described here was for all the thermocouples used to measure solid body temperatures. Similar calibration was carried out for the two thermocouples used for measuring the temperature of the flowing air.

Temperature	Response	Standard response	Deviation
100.2	0.003975	0.004289	-0.000314
218.2	0.009508	0.010264	-0.000756

From these values the deviation curve has been plotted, Fig.20, giving the deviation against the standard response. From this curve, deviations from the standard at all temperatures have been read off to give the calibration curve shown in Fig.21.

Fig.22 shows the calibration curve of the thermocouples used for measuring the temperature of the flowing air.

CALIBRATION OF NOZZLE.

For the calibration of the nozzle, a method similar to that recommendedby Ower[38] was applied. The nozzle described in Chapter IV was placed inside the pipe, and the calibration process took place. Upstream and downstream tappings were connected to the opposite sides of the manometer, to give the pressure difference across the nozzle. A standard pitot tube was used to measure the velocity distribution downstream in the pipe in vertical and horizontal planes at the same cross-section. Two honey-combs, having octagonal cells $\frac{3}{8}$" side and 3" length, were placed far upstream and downstream of the nozzle. Fig.23 shows the relative positions of the pipe, nozzle, honey-combs and Pitot tube.

The velocity head was measured by a Casella micromanometer. From the velocity distribution in the two perpendicular planes an average velocity distribution curve was obtained. Different

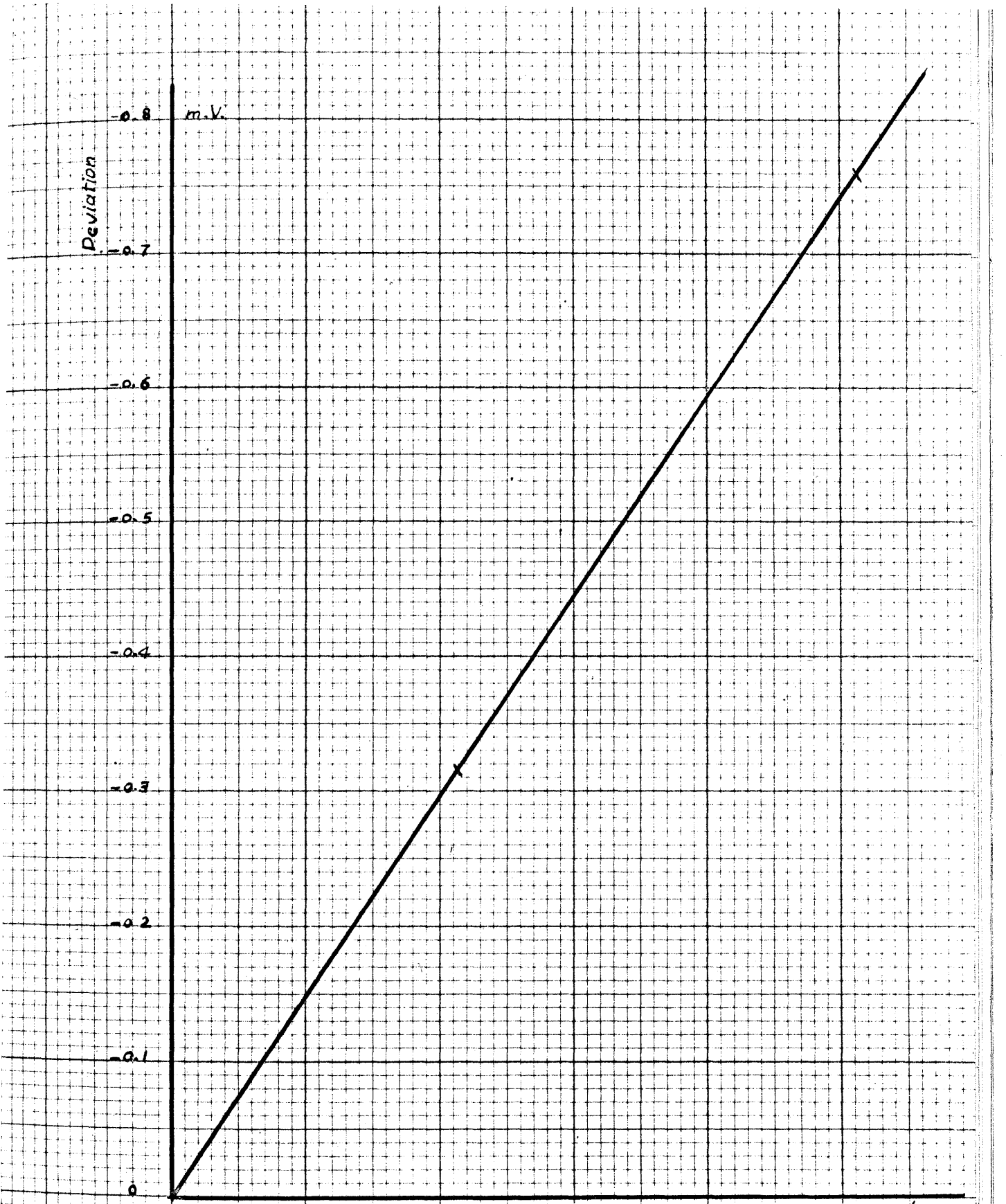

Fig. 20 : CALIBRATION OF THERMOCOUPLES.

(deviation curve).

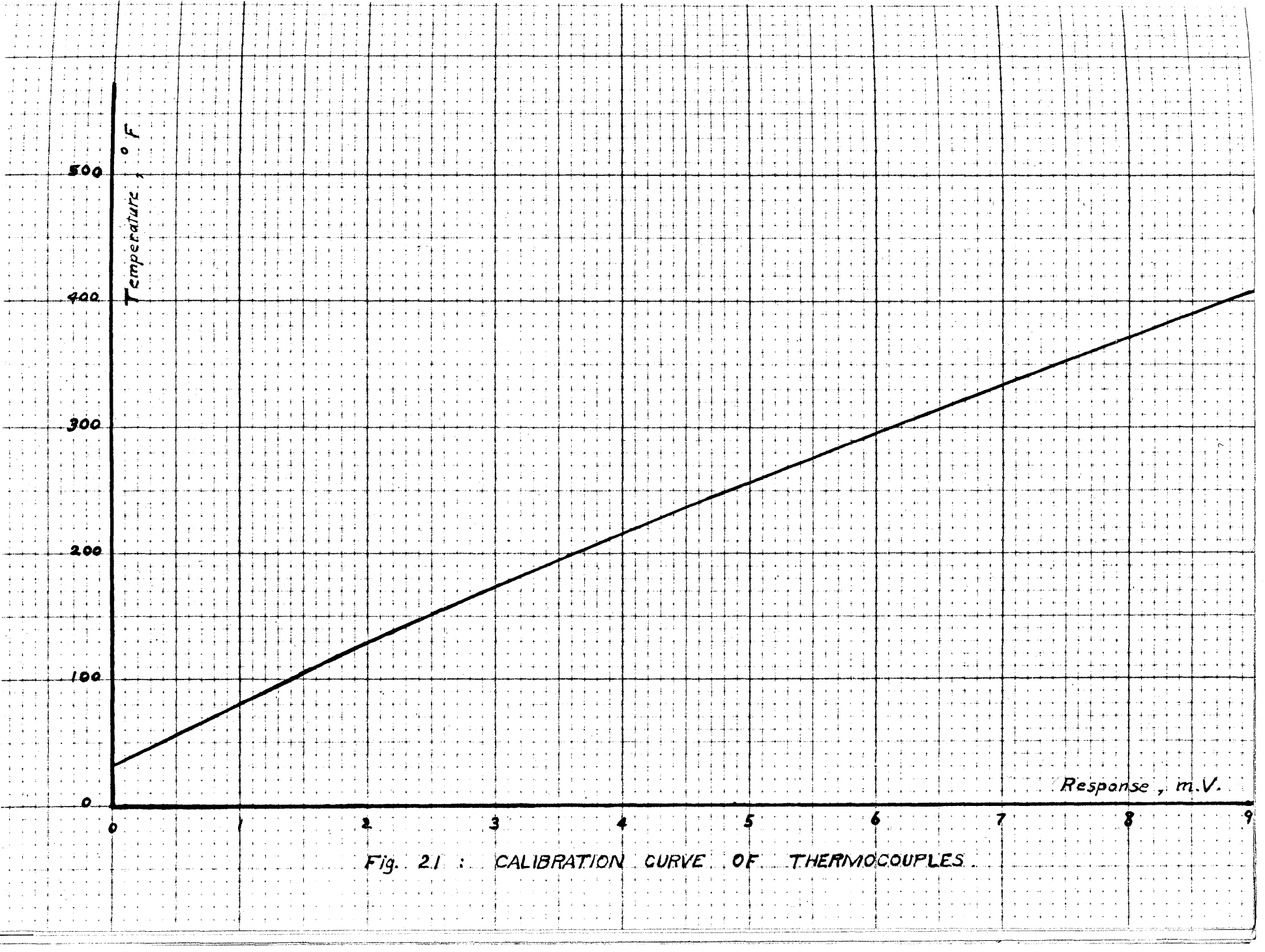

Fig. 21 : CALIBRATION CURVE OF THERMOCOUPLES.

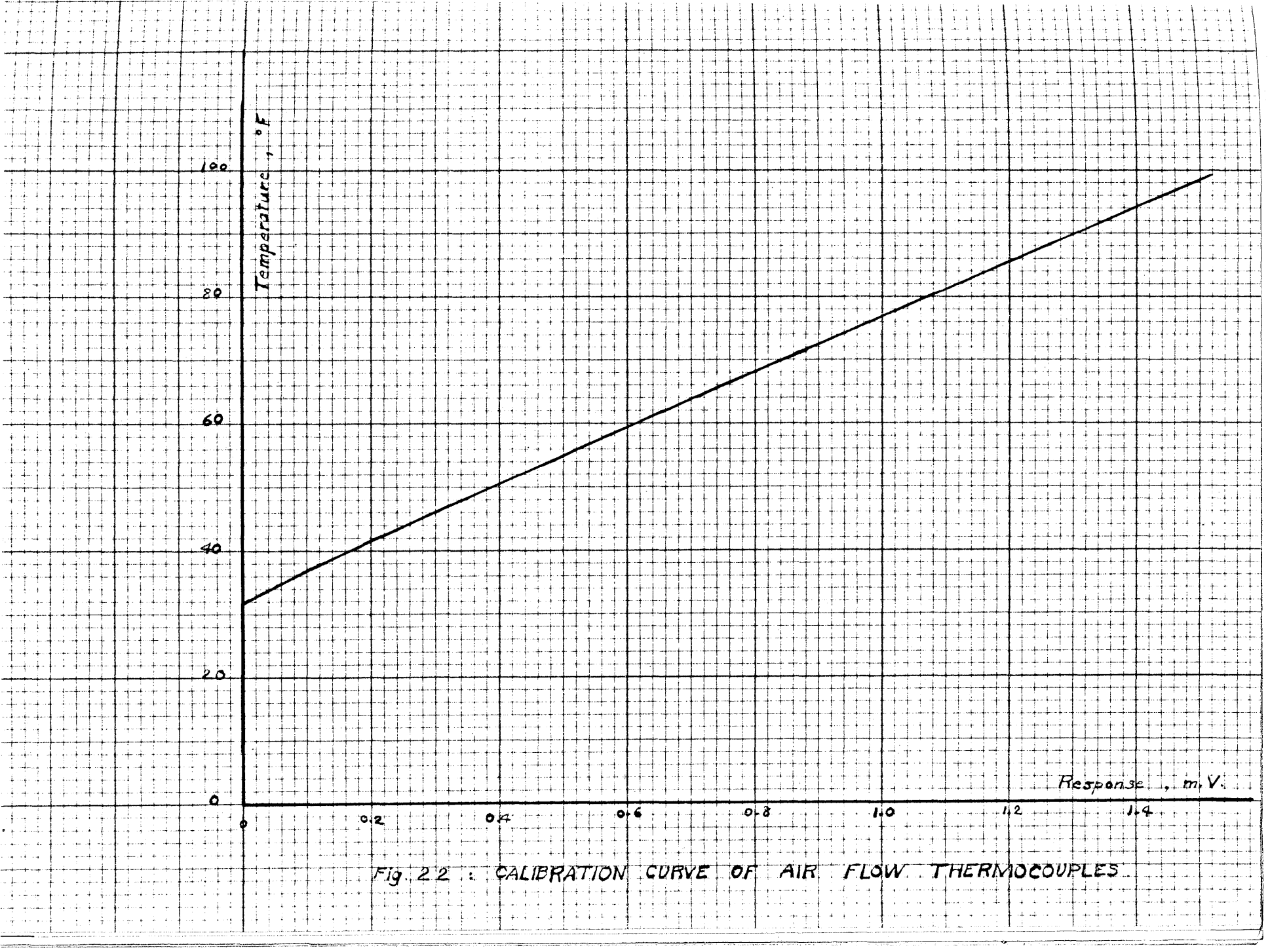

Fig. 22 : CALIBRATION CURVE OF AIR FLOW THERMOCOUPLES

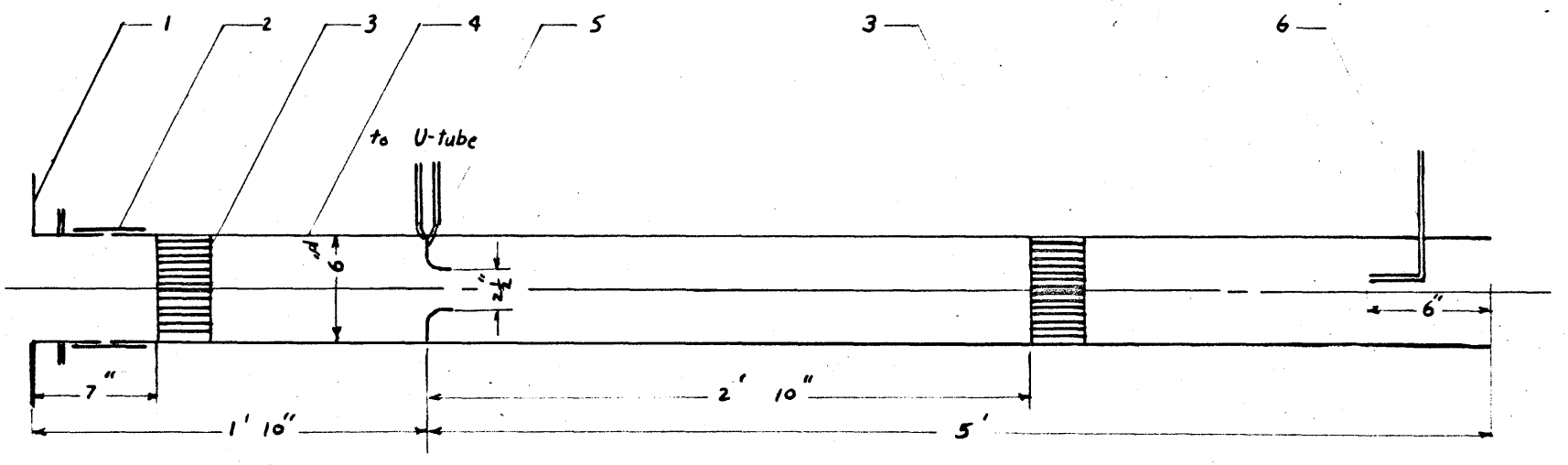

1 - AIR BLOWER
2 - RUBBER PIPE
3 - HONEY-COMBS
4 - MAIN PIPE
5 - FLOW NOZZLE
6 - PITOT TUBE.

FIG. 23 : ARRANGEMENT FOR THE CALIBRATION OF THE NOZZLE.

velocity traverses were made corresponding to different pressure differences across the nozzle, the pressure difference being kept constant during each experiment. The steady rotation of the air blower was checked by means of a tachometer every 15 minutes.

To calculate the amount of air flowing per unit time, the pipe was divided into nine circular zones with centres at the axis by circles of radii 1.5, 1.7, 1.9, 2.1, 2.3, 2.5, 2.7, 2.9 and 3.0 inches. The areas of each zone and the mean velocity through it were calculated. By multiplication, the discharge through each zone was obtained. Addition, and then multiplication by the air density, gave the total discharge through the pipe.

Ten experiments were carried out for the calibration of the nozzle. These correspond to ten different air discharges. The observations and results are shown in tables 1 to 4 in Appendix II. Fig.24 shows the velocity distribution curves for two different discharges (experiments 1 and 10) in the vertical and horizontal planes and the average velocity distribution. A curve for the air discharge in pounds per minute versus the pressure difference across the nozzle in inches of water is shown in Fig.25.

The density of the air, as affected by the barometric pressure and moisture in the air, was calculated as follows :

From the dry and wet bulb temperatures the relative humidity of the air was calculated[22]. The saturation pressure at the dry bulb temperature was determined from the 1939 Callendar Steam Tables[18]. Then by multiplying this by the relative humidity the vapour pressure of moisture in the air was obtained. The density of the air was calculated form the formula[22].

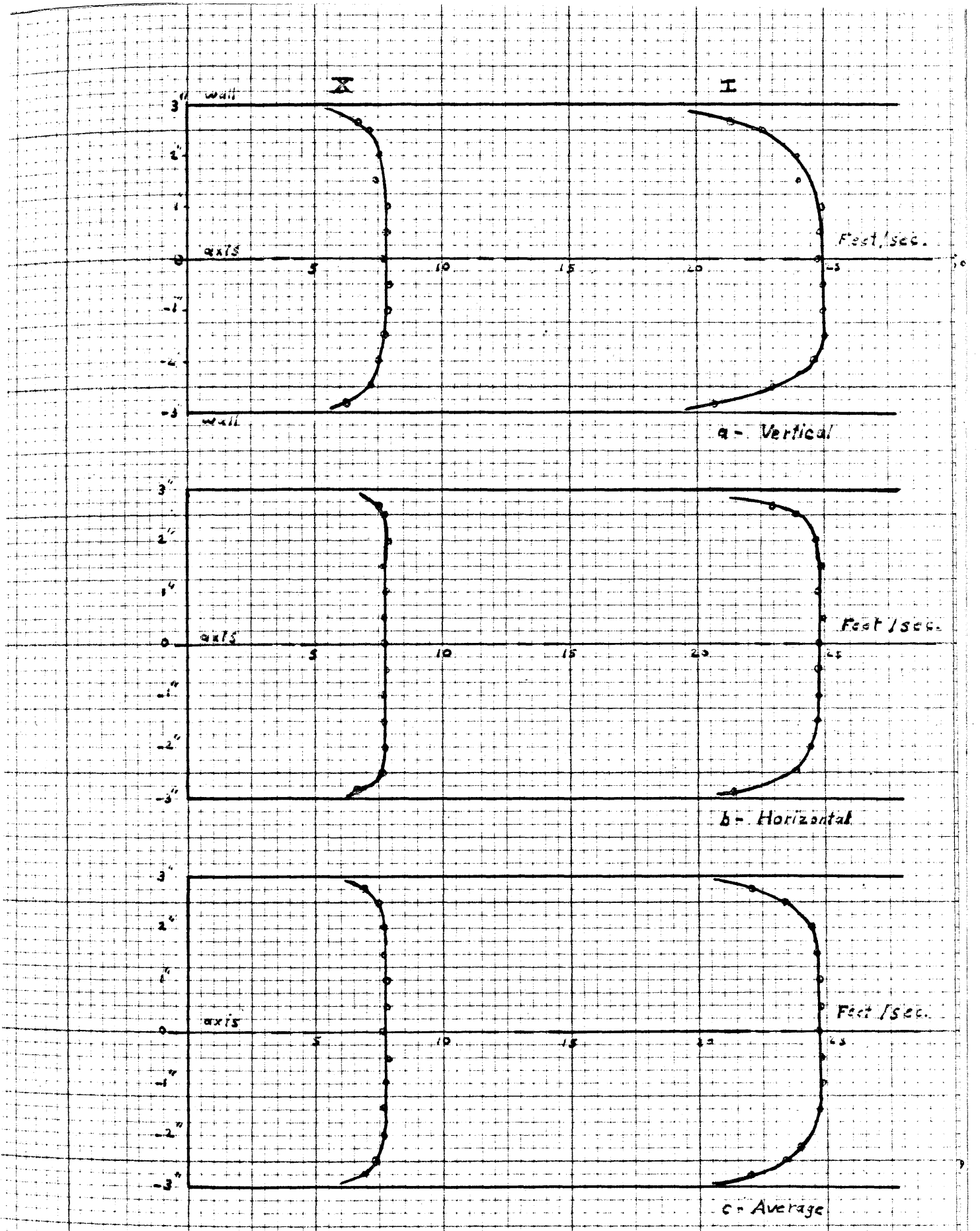

Fig. 24 : Velocity distribution in the main pipe.

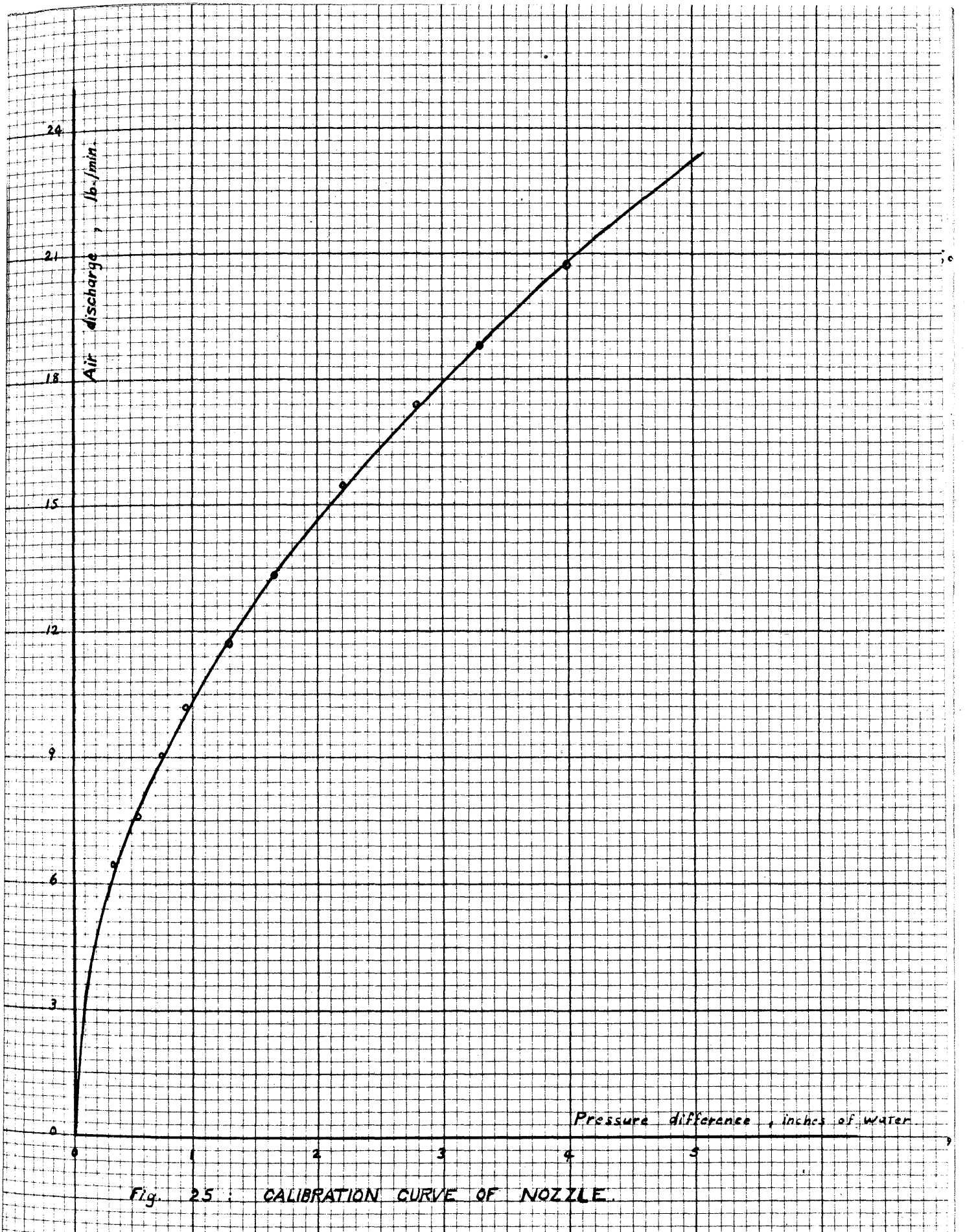

Fig. 25 : CALIBRATION CURVE OF NOZZLE.

Density of moist air $= 1.2929 \times \frac{273.13}{T} \times \frac{B-0.3783\,e}{760}$ V-2

where T = absolute temperature in ^{o}C absolute.
B = barometric pressure in m.m. Hg.
e = vapour pressure of moisture in the air.in m.m. Hg.

This equation is for the C.G.S. system of units and gives the density in grams/litre. The final result was converted to the F.P.S. system.

The air velocity was calculated from the velocity head as follows :

$$U = a\sqrt{2\,g\,H_v} \qquad \text{V-3}$$

where U = air velocity, feet/second.
a = coefficient of the Pitot tube (=1)
g = acceleration due to gravity,
= 32.2 ft./sec.^{2}.
H_v = velocity head, ft. of air.

By substitution we get

$$U = 3.63\sqrt{\frac{H_m}{\rho}} \qquad \text{V-4}$$

where H_m = velocity head, m.m. of water.
ρ = density of air, lbs./ft.^{3}.

CALIBRATION OF TOTAL HEAD TUBE

The idea applied here was to make comparison between the readings given by the small total head tube and those given by a standard one. The calibration took place before soldering the tube to the micrometer.

The two Pitot tubes were supported near the end of a 6" pipe, with their axes parallel to the pipe axis, and their leading ends at the same plane and facing the air stream. The two tubes were

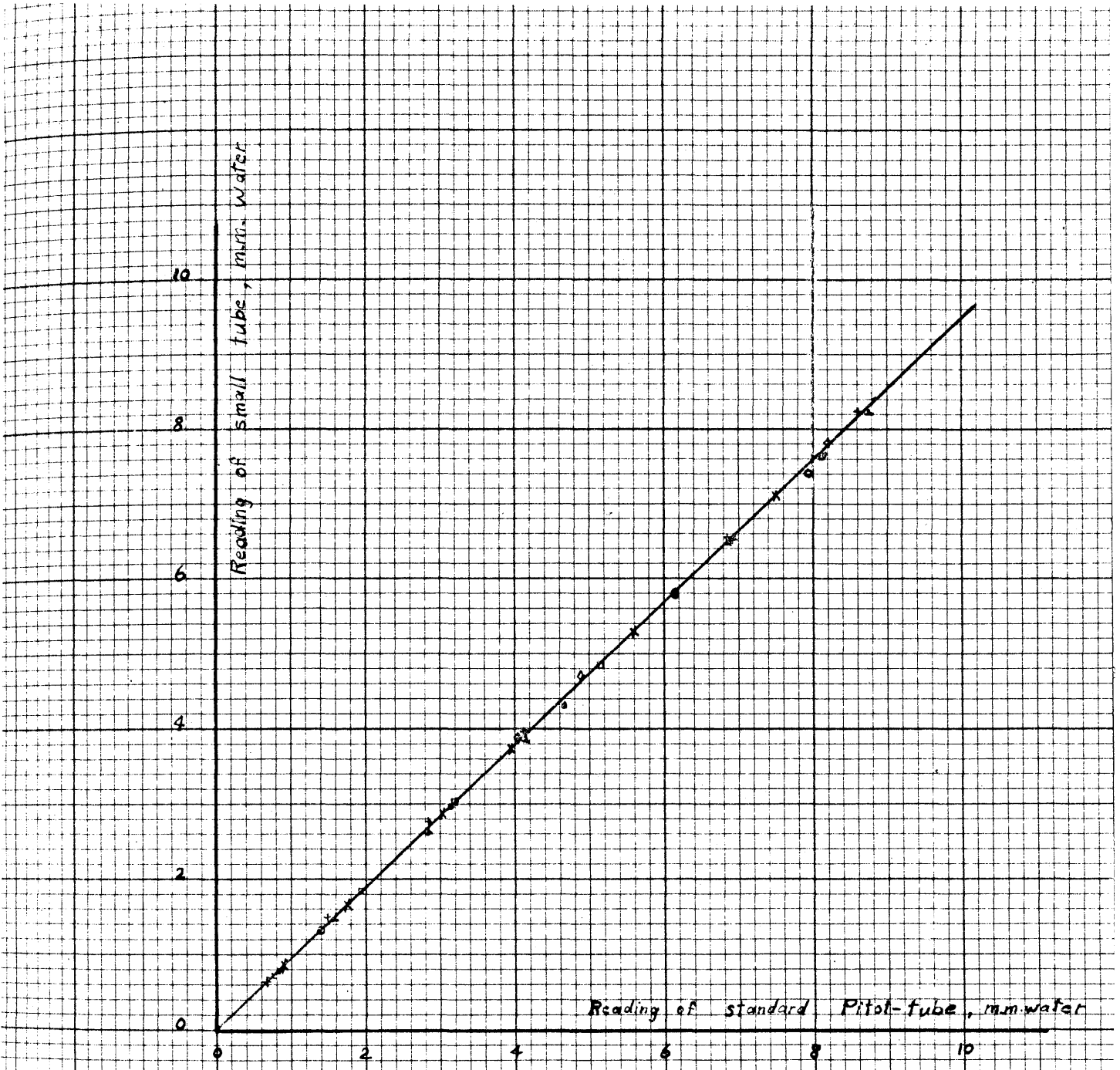

Fig. 26 : CALIBRATION CURVE OF SMALL TOTAL HEAD TUBE.

CHAPTER VI.

EXPERIMENTAL PROCEDURE AND METHOD OF CALCULATION.

A - MEASUREMENTS.

The measurements required during the experiment were recorded as follows :

1. Pressure difference across the nozzle :

Pressure differences less than 1.3" of $w_a$ter were measured by an inclined tube manometer (each division = 0.01" water). One tenth of each division could be estimated. Pressure differences more than 1.3" of water were measured by a vertical U-tube. This pressure difference was used to determine the quantity of air flowing per unit time. It also served as an indication of any fluctuationof the motor speed during the experiment.

2. Blower speed:

This was measured by a tachometer every 15 minutes so as to check the stability of the air blower.

3. Electrical input:

The voltage and current of both the main and the guard heaters were measured separately by calibrated voltmeter and ammeter.

4. Temperature of the heating surface :

It was determined by measuring the electromotive forces of nine thermocouples fixed as described in Chapter IV (Thermocouple number 10, Fig.14, did not give any readings and the average of the other nine was taken).

5. Temperature of the unheated disc:

This was determined by measuring the electromotive forces of seven thermocouples fixed as described in Chapter IV.

6. Flow of heat in the asbestos:

This was prevented at the rear surface of the main heater by adjusting the electrical input to the guard heater to a certain value such that the three pairs of thermocouples placed at both surfaces of the asbestos between the two heaters gave identical readings.

Heat flowing from the edges of the heating plate was determined by four thermocouples embedded in the asbestos; two before the working section and two after it.

7. Air temperature and humidity:

Wet and dry bulb temperatures at the intake of the air blower were measured. The air flow temperature was also measured at the inlet and outlet of the working section as described in Chapter IV.

8. Velocity distribution between the plates:

The velocity head was measured by the small total head tube at different points between the two plates. The tube was connected to a Casella micromanometer which gives readings to 0.01 m.m. of water.

B - EXPERIMENTAL PROCEDURE.

For a certain required rate of discharge of air in the working section, the pressure difference across the nozzle was

determined. The speed of the direct current motor was adjusted to give that pressure difference. Throughout the test this pressure difference was kept constant, and the motor speed was checked at intervals of 15 minutes.

For a given electrical input to the main heater, the electrical input to the guard heater was adjusted to obtain the equilibrium condition. Then the voltage across both heaters was kept constant during the test.

At intervals of 30 minutes during the experiment, the following data were observed:

6 thermocouple readings of the asbestos between the heaters.
9 thermocouple readings giving the heating surface temperature
2 thermocouple readings for the heat flow to the inner asbestos ring.
2 thermocouple readings for the heat flow to the outer asbestos ring.
7 thermocouple readings for the unheated disc temperature.
2 thermocouple readings for the air flow temperature.

Near the end of each experiment the barometric pressure and the wet and dry bulb temperatures were recorded.

In some experiments the velocity distribution between the plates was measured. This process always started after reaching the thermal steady state. The two opposite sides of the Casella micromanometer were connected to the total head tube and the static head hole. This process was repeated at two radii, $4\frac{5}{8}$" and $7\frac{7}{8}$".

The average time required to reach a thermal steady state was about three hours.

C - METHOD OF CALCULATION.

Analysis of heat flow.

The heat input to the main heater is distributed into the following parts :

1. Heat lost by radiation from the heating surface.
2(a) Heat lost by conduction to the inner asbestos ring.
2(b) Heat lost by conduction to the outer asbestos ring.
3. Heat transferred to the flowing air by forced convection.

---

1. Heat lost by radiation.

Saunders[44] and Hottel[23] considered the problem of radiant heat interchange between finite surfaces. Hottel found that the formulation of point to point radiation in differential form, and the integration between the desired limits lead in all cases to an equation of the general form

$$H_r = S \cdot F_g \cdot F_b \cdot \sigma \cdot (T_w^4 - T_d^4) \qquad \text{VI-1}$$

where H_r = rate of heat transfer by radiation, Btu/hour.
S = Area of one of the two surfaces, ft^2.
F_g = geometric factor, which allows for the average angle throughout which one surface sees the other.
F_b = factor that makes allowance for the departure of the two surfaces from complete blackness.
σ = Stefan-Boltzman constant.,
= 1.723×10^{-9} Btu/ft^2.hr.$^oR^4$
T_w = average temperature of the hot surface, ^oF abs.
T_d = average temperature of the tunnel walls, ^oF. abs.

F_g depends on which surface is chosen for use in the area term, and F_b is a function of the individual emissivities of both surfaces.

One of the cases considered by Hottel was the radiation from an element dS to a circular disc in a plane parallel to that of dS. For this case he gave

$$F_g = \frac{1}{2}\left[1 - \frac{x^2 + 1 - R^2}{\sqrt{x^4 + 2(1 - R^2)x^2 + (1 + R^2)^2}}\right] \qquad \text{VI-2}$$

and $F_b = \epsilon_1 \epsilon_2$ VI-3

where $R = \dfrac{\text{radius of disc}}{\text{distance between planes}}$

$x = \dfrac{\text{distance from dS to the normal thro' centre of disc}}{\text{distance between planes}}$

ϵ_1 & ϵ_2 = individual emissivities of the two surfaces.

In the present work, S is taken as the area of the heating surface, T_w as the average temperature of the heating surface and T_d as the average temperature of the unheated disc.
Thus S = 0.955 sq.ft.

The radiation from the heating surface is received partly by the unheated disc and partly by the surroundings. The part received by the disc can be estimated from equation (VI-2) by putting the distance from dS to the normal through the centre of the disc as $\frac{1}{2}(4.5 + 8) = 6.25"$. Fig.27 shows that amount for different values of the gap between the plates. As the part received by the surroundings is comparatively very small, and the difference between the room temperature and that of the unheated disc is actually small, then the error in assuming $F_g = 1$ is very small and can be neglected.

The emissivity factor F_b is generally taken between 0.97 and 0.94. An average value of 0.95 was chosen.

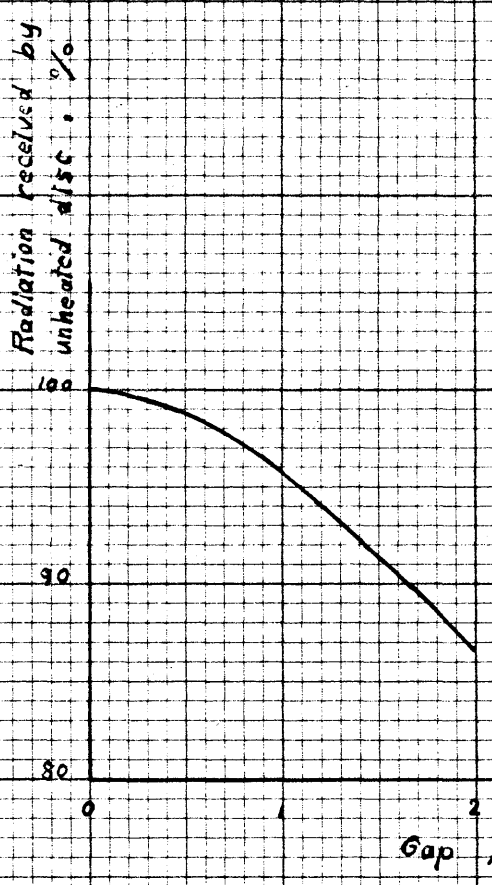

Fig. 27 : PERCENTAGE OF RADIATION RECEIVED BY UNHEATED DISC.

Therefore the heat lost by radiation is

$$H_r = 0.955 \times 1 \times 0.95 \times 1.723 \times 10^{-9}(T_w^4 - T_d^4)$$
$$= 1.563 \times 10^{-9}(T_w^4 - T_d^4) \qquad \text{VI-4}$$

2. Heat lost by conduction from the plate sides to the asbestos rings:

Heat transfer by conduction is expressed by the equation

$$H_c = - k.A. \frac{\Delta t}{\Delta x} \qquad \text{VI-5}$$

where H_c = heat flow by conduction, Btu/hr.
k = thermal conductivity, Btu/ft.hr.^{o}F.
A = area, ft^2.
Δt = temperature difference, ^{o}F.
x = distance, feet.

In the present case there is heat conduction from the inner and outer sides of the heating plate. So we have

$$H_c = - k \left(A_i \frac{\Delta t_i}{\Delta x_i} + A_o \frac{\Delta t_o}{\Delta x_o}\right) \qquad \text{VI-6}$$

where i and o denote inner and outer sides respectively.
Average value for k = 0.1 Btu/ft.hr.^{o}F (32)
A_i = 0.025 ft^2. , A_o = 0.044 ft^2.
$\Delta x_i = \Delta x_o$ = 1/24 feet.
Δt_i = t_w - mean temperature of thermocouples 11 & 12 (Fig.14)
Δt_o = t_w - mean temperature of thermocouples 13 & 14 (Fig.14)

3. Net normal heat flow to the air stream :

This is given by

$$H = H_o - (H_r + H_c) \qquad \text{VI-7}$$

where H_o = total heat input to the main heater.

Average coefficient of heat transfer

$$h = \frac{H}{S.(t_w - t_m)} \quad Btu/ft^2.hr.^oF. \qquad VI-8$$

where t_m = mean bulk air temperature
= mean temperature given by thermocouples B* (chapter IV).

Rate of discharge of air

This was directly determined from the calibration curve of the nozzle (Fig.24).

Point values of the stream velocity

These were calculated from equation V-4, H_m being the head given by the total head tube divided by the coefficient of that tube (Fig.25).

Average value of air velocity at radius (r).

This was determined by dividing the amount of air discharge by the cross-sectional area at radius (r).

Effective mean airstream velocity along the surface.

This was calculated as defined in equation (III-5),

$$U_m = \frac{2\,U_1 r_1}{r_2 + r_1} \qquad VI-9$$

---

* After Fishenden and Saunders (ref.15) and Rehsenow (ref.42) it was found unnecessary to make any correction in the readings given by thermocouples B as the error would be very small.

D - DIMENSIONLESS GROUPS.

The values of the thermal conductivity and viscosity of air used in the calculation of the dimensionless groups were taken from graphs plotted from the data of several workers. These graphs are given in Figs. 28 & 29. The properties were always evaluated at the mean bulk temperature of the air stream.

Calculation of Reynolds number.

In the present work, generally, the characteristic dimension of length is the gap between the heating surface and the unheated disc. At any radius (r) of the working section the air discharge is given by

$$Q = 2\pi r b U = 2\pi r_1 b U_1$$

$$Q \propto U_1 r_1 b$$

If Reynolds number is proportional to $\frac{\rho U b}{\mu}$, then it can be put in the form

$$R_e = \frac{\rho U_1 b}{\mu} \cdot \frac{Q}{U_1 r_1 b} = \frac{Q}{r_1 \mu} \qquad \text{VI-10}$$

where all the symbols have the usual meaning.

Equation VI-10 was used in calculating Reynolds number.

Calculation of Nusselt number

The formula chosen to calculate Nusselt number is

$$Nu = \frac{hb}{k} \qquad \text{VI-11}$$

where all the symbols have the usual meaning.

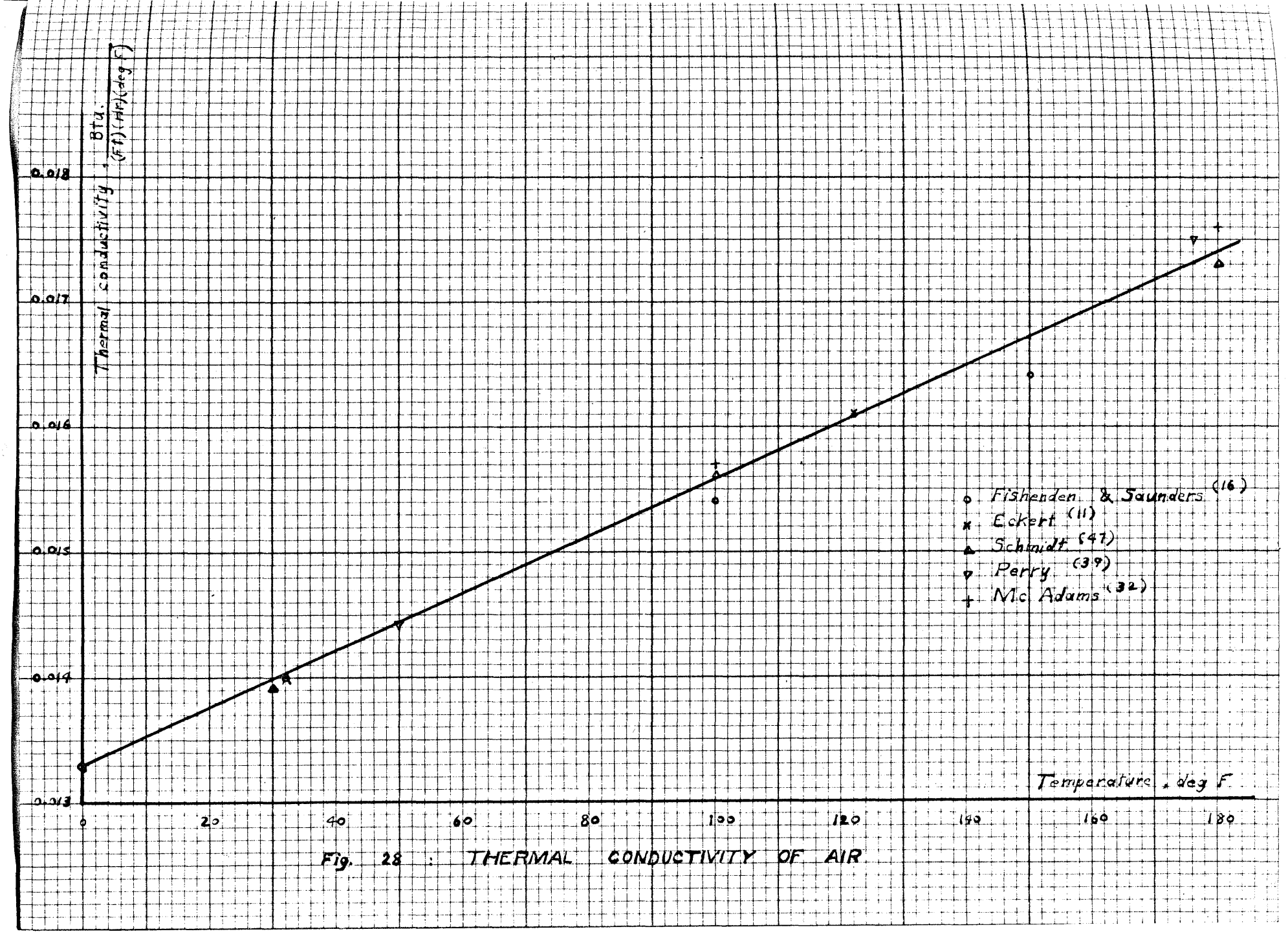

Fig. 28 : THERMAL CONDUCTIVITY OF AIR

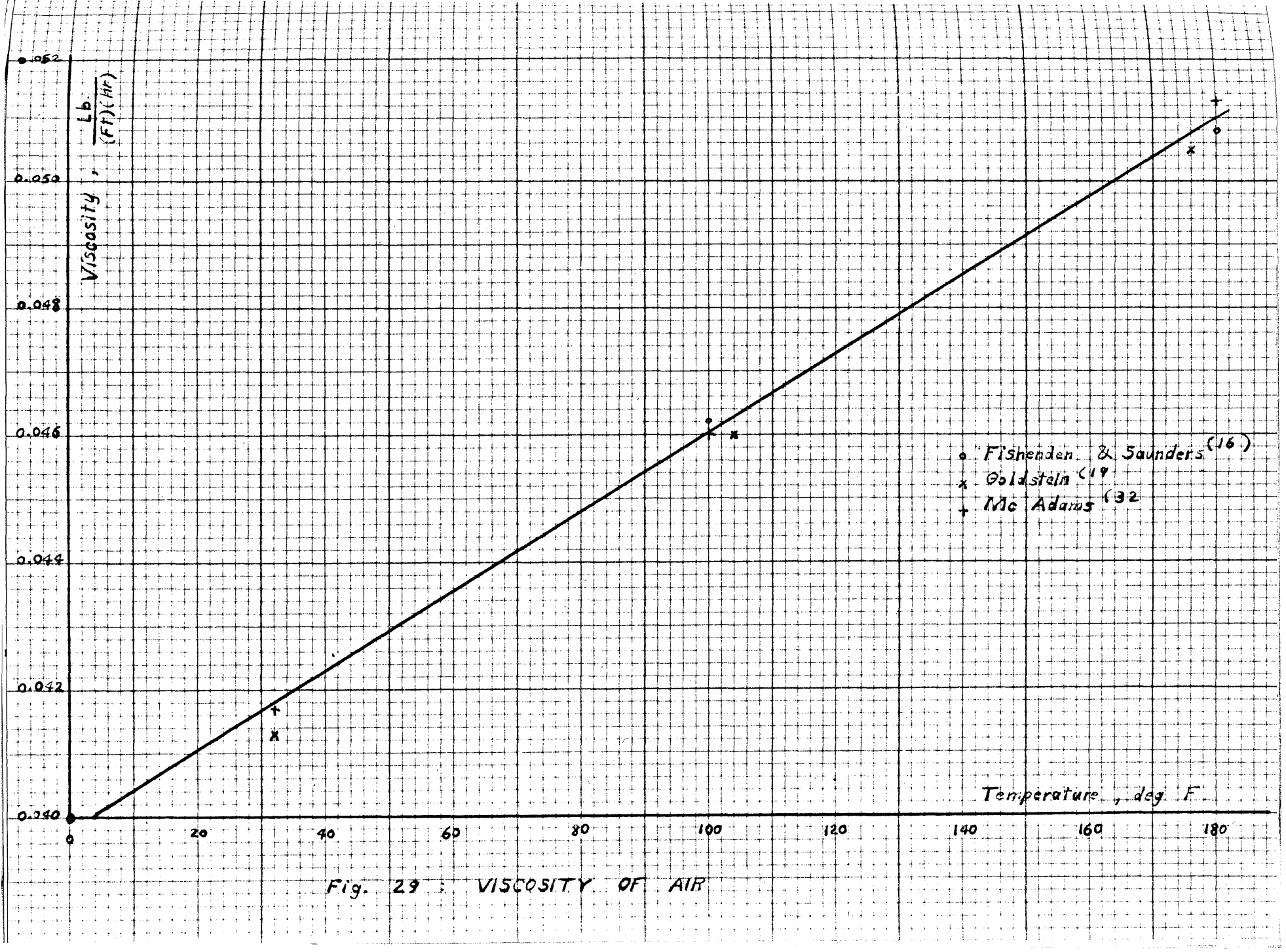

Fig. 29 : VISCOSITY OF AIR

E - SAMPLE OF CALCULATION.

Gap = $\frac{1}{4}$" , experiment number 1.

The following data were observed :

Pressure difference across nozzle	= 1.5" of water.
Voltage of main heater	= 195.1 volts
Current of main heater	= 2.481 amperes.
Room temperature	= 64°F.
Air flow temperature at r_1	= 66.0°F
Air flow temperature at r_2	= 70.9°F

Thermocouple readings for equilibrium between main and guard heaters were :

Main heater side	7.68	7.45	7.29
Guard heater side	7.69	7.45	7.27

Readings of the thermocouples of the heating surface (1 to 9) :

2.85, 2.86, 2.89, 2.86, 2.89, 2.89, 2.90, 2.90 and 2.89

Readings of the thermocouples of the unheated disc (15 to 21):

0.75, 0.76, 0.77, 0.77, 0.77, 0.77 and 0.76.

Readings of thermocouples of inner asbestos ring (11 and 12):

1.88 and 1.87.

Readings of thermocouples of outer asbestos ring (13 and 14):

1.43 and 1.40.

From the preceding data the following calculations are made

Amount of air discharge	= 761 pounds per hour
Heat input to the main heater	= 1651 Btu. per hour
Mean temperature of the heating surface	= 166.0°F.
Mean temperature of the unheated disc	= 69.7°F.
Mean temperature of inner asbestos ring	= 121.5°F
Mean temperature of outer asbestos ring	= 100.5°F
Mean bulk temperature of the flowing air	= 68.45°F

Heat lost by radiation = $1.563 \times 10^{-9}[(625.7)^4-(529.4)^4]$

= 117 Btu. per hour.

Heat lost by conduction = $0.1 \times 24(0.025 \times 44.5 + 0.044 \times 65.5)$

= 10 Btu. per hour.

Total heat loss = 117 + 10 = 127 Btu/hour

Net heat of convection = 1651 - 127 = 1524 Btu/hour.

Coefficient of heat transfer = $\frac{1524}{0.955(166.0 - 68.4)}$

= 16.34 Btu/sq.ft.hr.^{o}F

Cross-sectional area at arithmetic mean radius (r = 6.25")

= 0.0682 sq.ft.

Effective mean velocity of air = $\frac{761}{0.0682 \times 3600 \times 0.0748}$

= 41.5 ft/sec. (corrected to 70^{o}

Dimensionless groups:

At 68.4^{o} we have (from Figs 28 & 29)

k = 0.01482 Btu/ft.hr.^{o}F

and μ = 0.044 lbs/ft.hr

$R_e = \frac{761 \times 12}{0.044 \times 4.5} = 46,120$

$Nu = \frac{16.34 \times 1}{0.01482 \times 48} = 22.95$

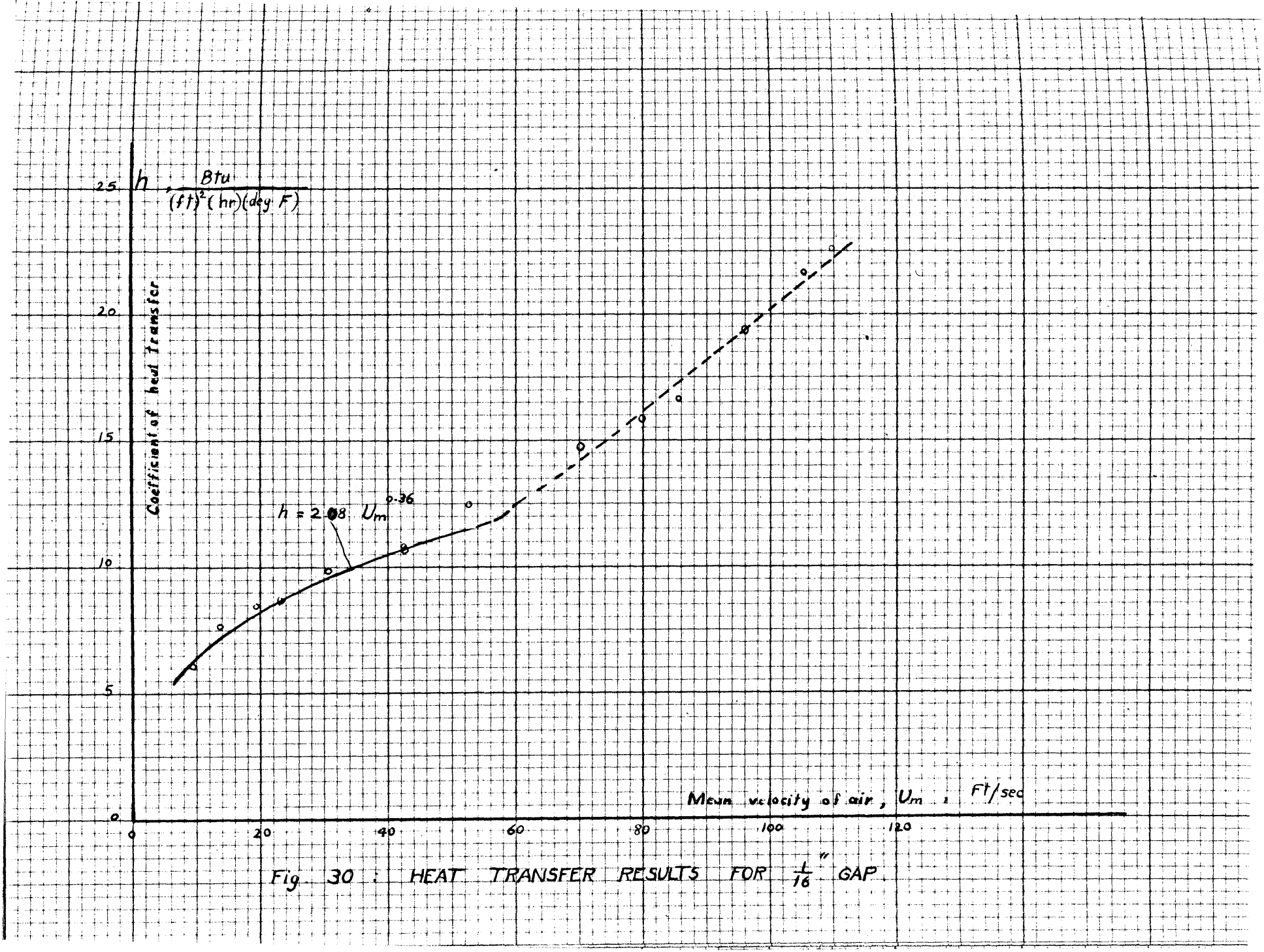

Fig. 30 : HEAT TRANSFER RESULTS FOR $\frac{1}{16}$" GAP

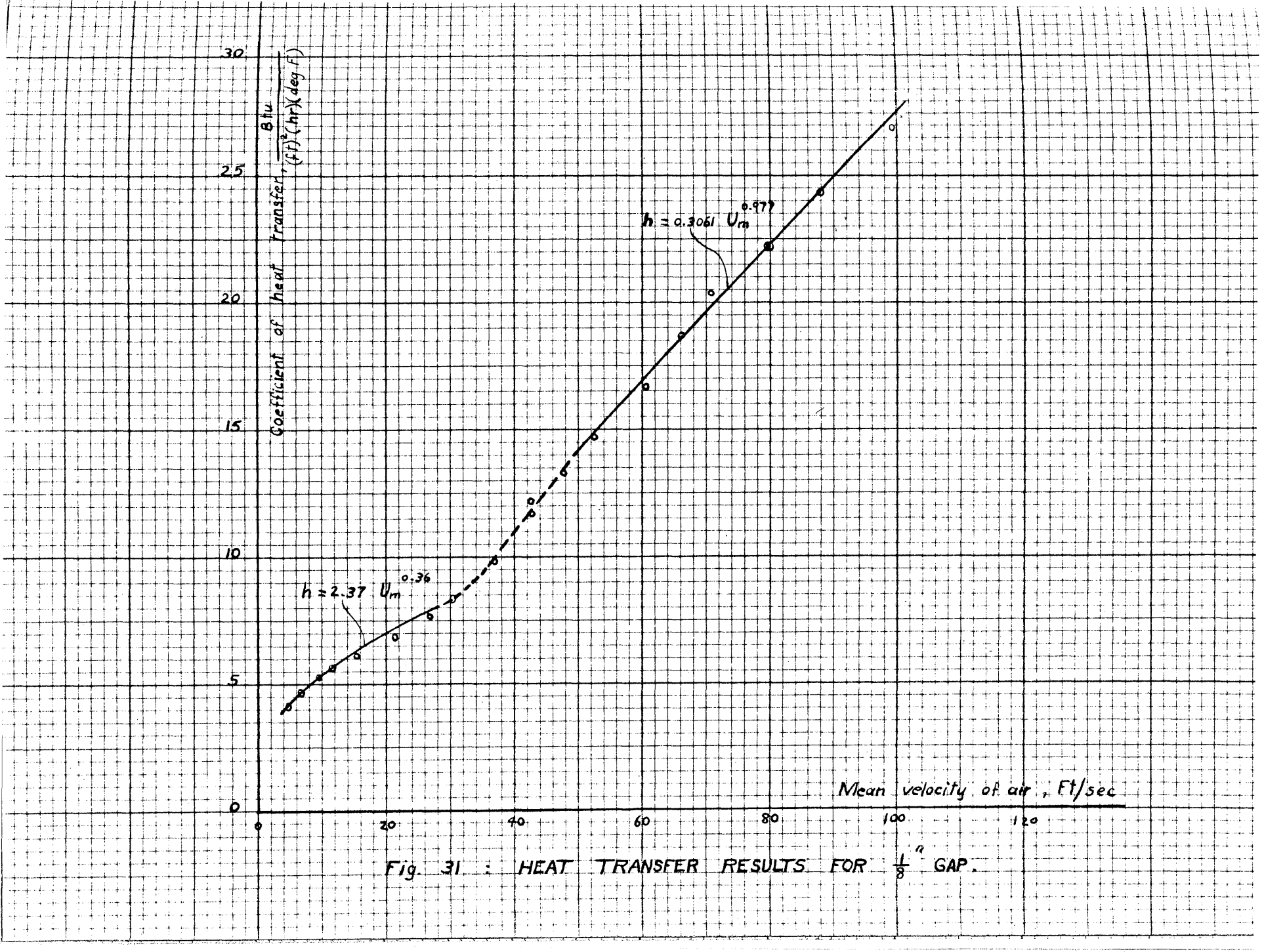

Fig. 31 : HEAT TRANSFER RESULTS FOR $\frac{1}{8}$" GAP.

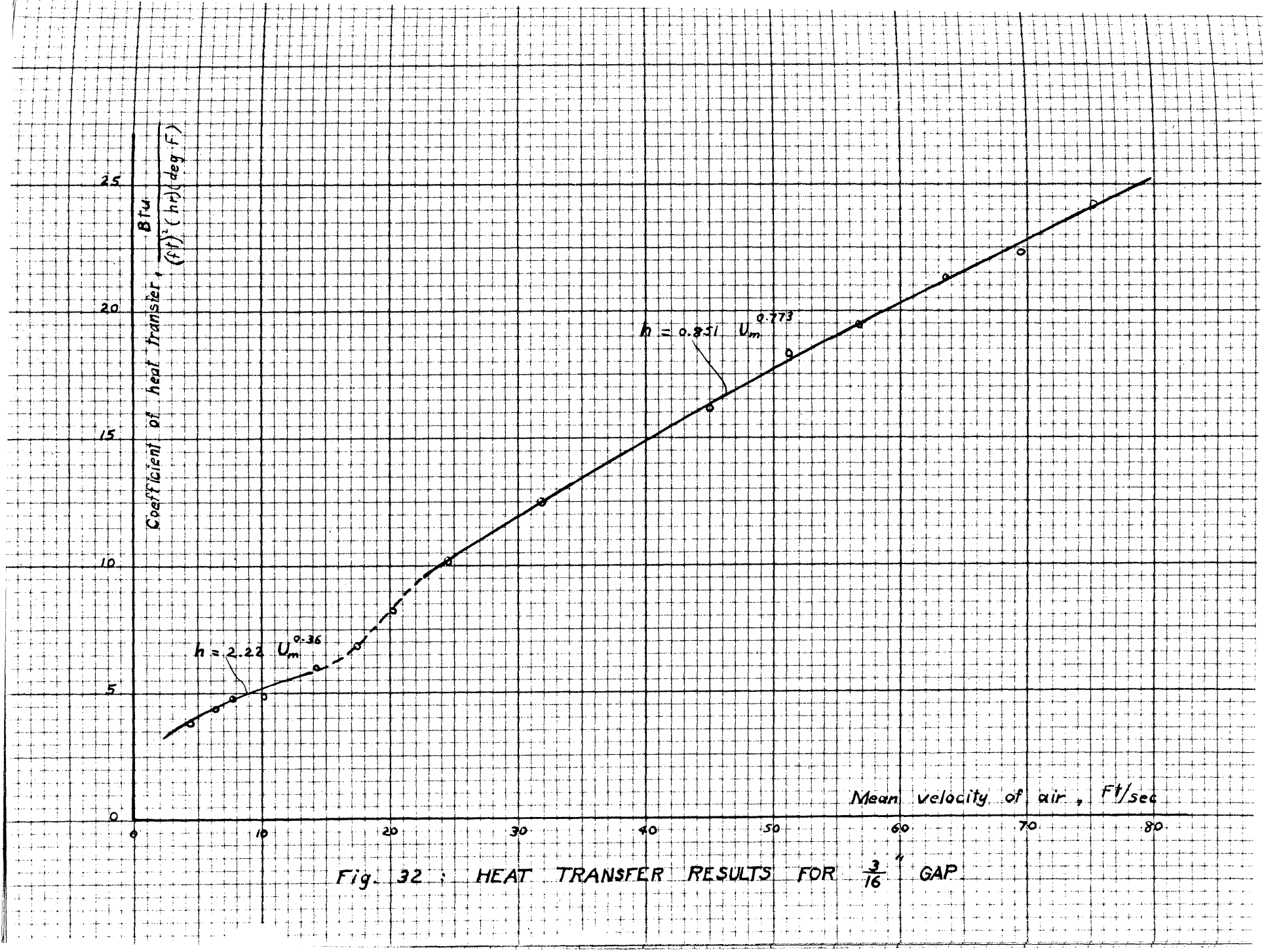

Fig. 32 : HEAT TRANSFER RESULTS FOR $\frac{3}{16}$" GAP

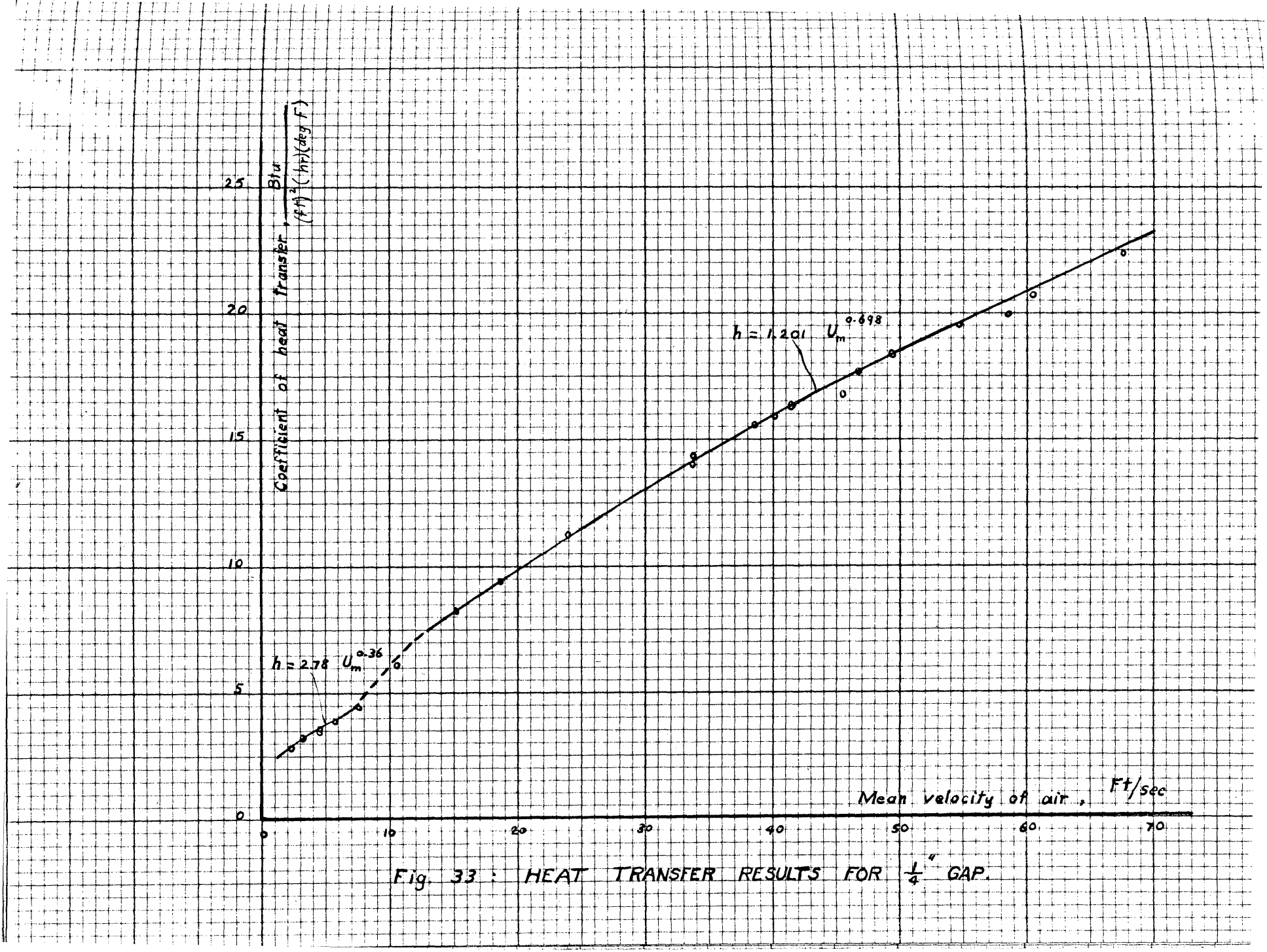

Fig. 33 : HEAT TRANSFER RESULTS FOR $\frac{1}{4}$" GAP.

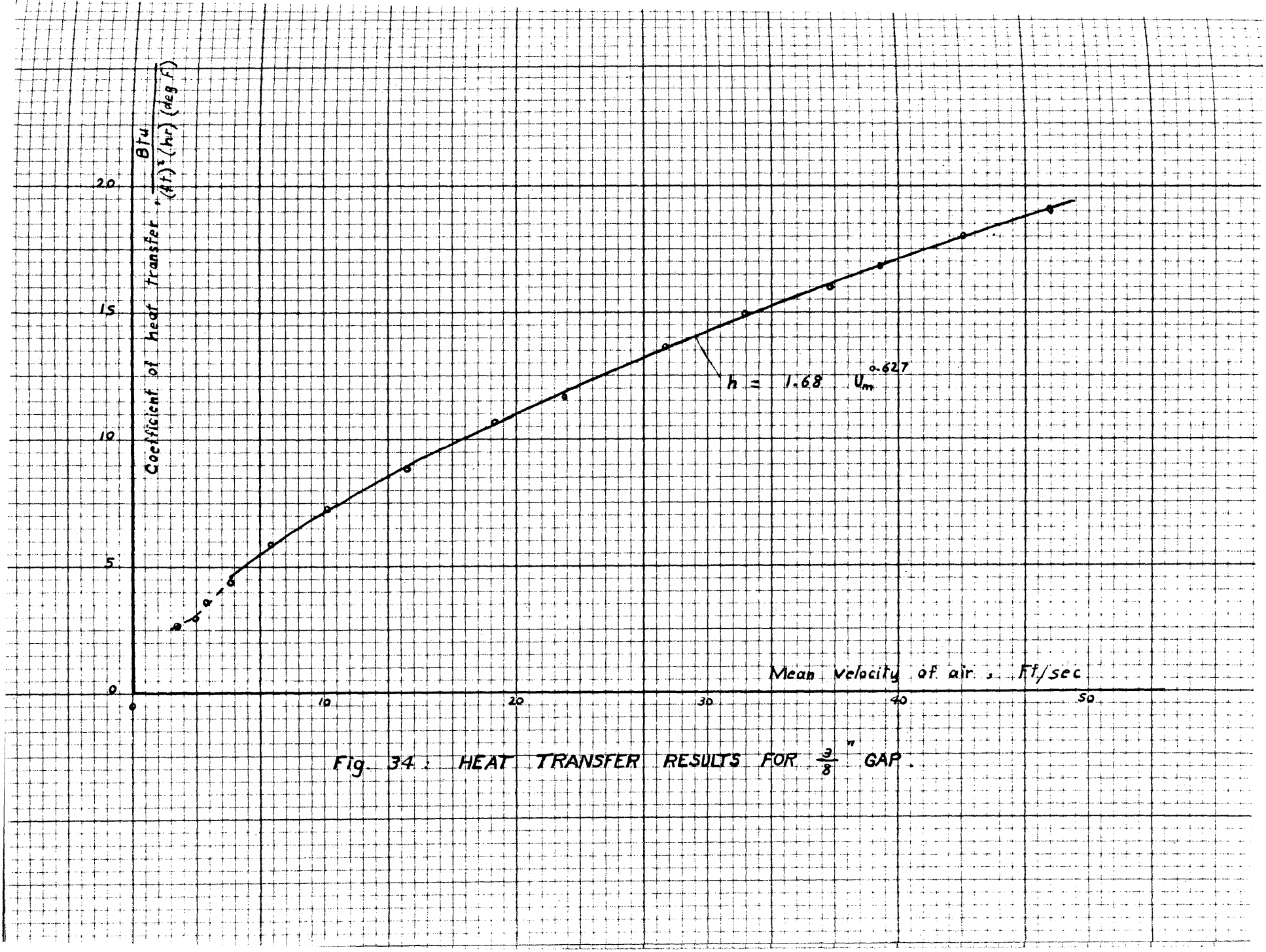

Fig. 34 : HEAT TRANSFER RESULTS FOR $\frac{3}{8}$" GAP.

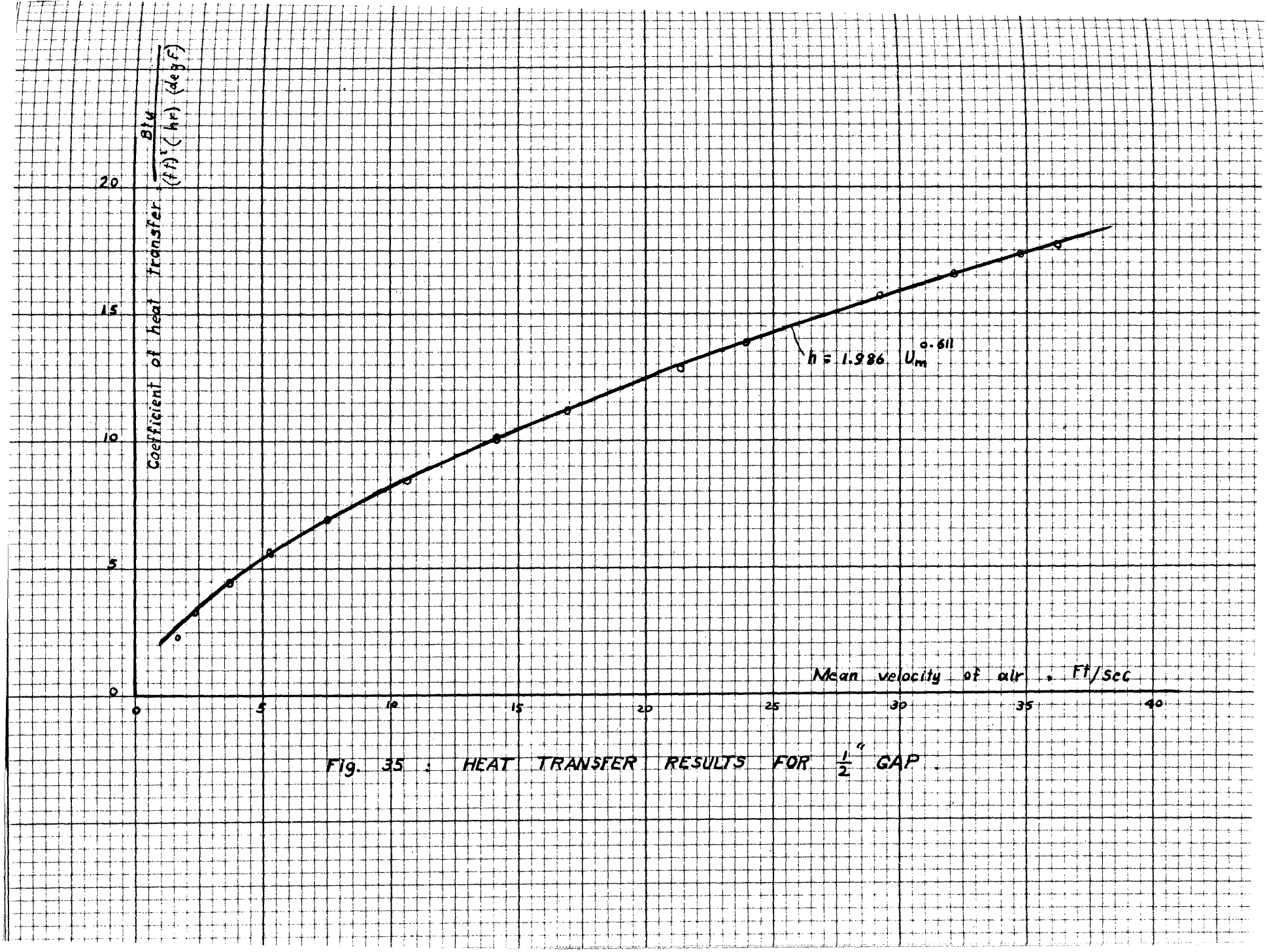

Fig. 35 : HEAT TRANSFER RESULTS FOR $\frac{1}{2}$" GAP .

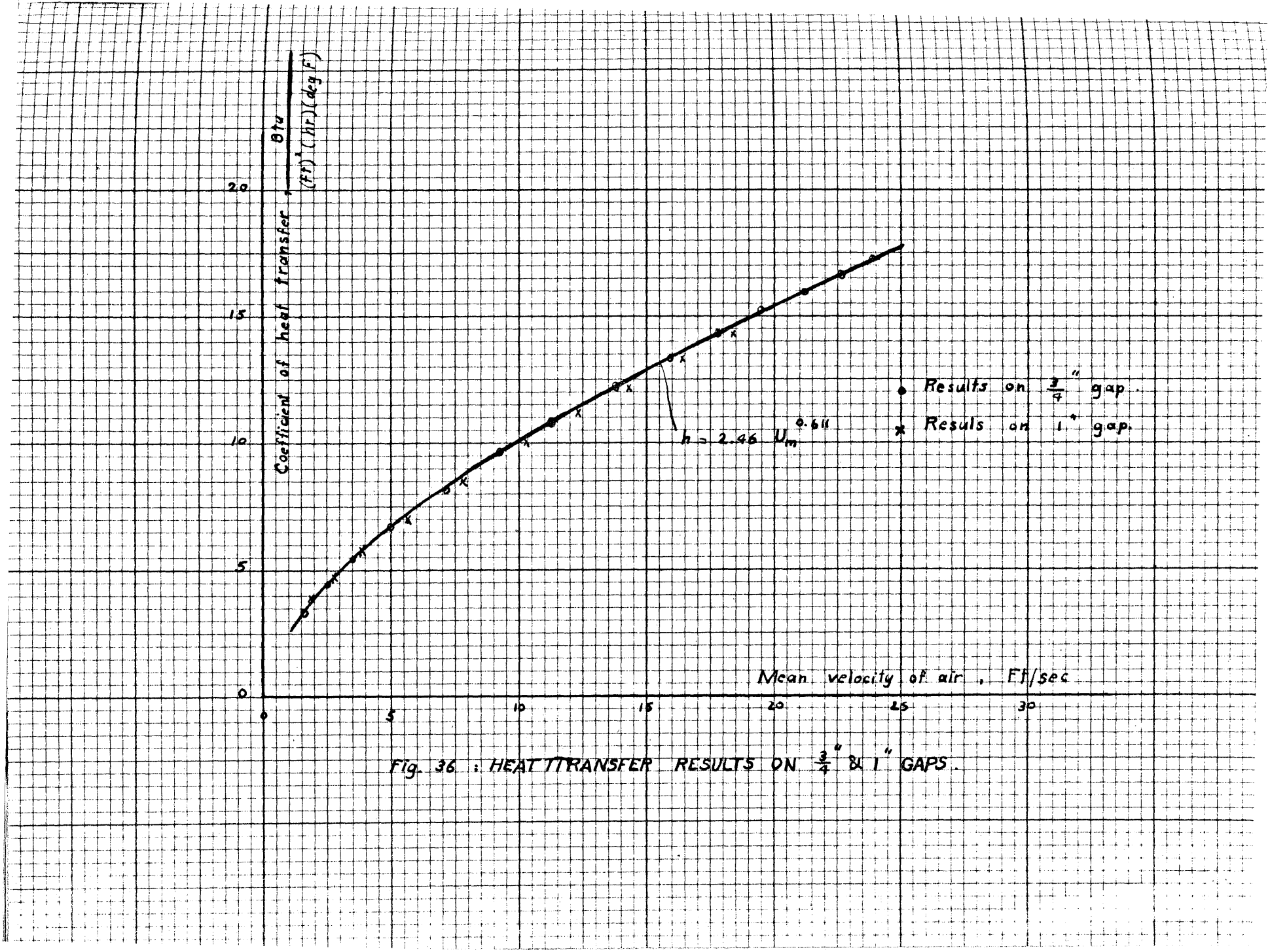

Fig. 36 : HEAT TRANSFER RESULTS ON $\frac{3}{4}$" & 1" GAPS.

for the 1" gap were nearly the same as those for ~~that of~~ the $\frac{3}{4}$" one. Results of the first are shown in Fig.36 so as to be compared with those of the latter. All the results for all the gaps were replotted in Figs.37 to 44, in the form of Nu as a function of R_e, both as defined in Chapter VI.

There was no definite indication for any change in the local temperature of the heating surface at different radii. The readings of the nine thermocouples were very close to each other, and the averages were taken.

Table (VII-2) shows some other data from the observations and results. (Meanings of the different lines of the table are shown below).

Table (VII-2)

Gap	1/16	$\frac{1}{8}$	3/16	$\frac{1}{4}$	$\frac{3}{8}$	$\frac{1}{2}$	$\frac{3}{4}$	1
Line 1	14	20	15	24	15	14	14	10
2	9	4.5	4	2				
3	56	28	16	8				
4	2500	2500	3500	2500				
5	16000	15800	13000	8000				
6		49	22	13	7	2.5	2	2
7		100	76	68	48	36	24	18
8		23000	19000	14000	10300	5500	5000	
9		55000	62000	76000	80000	80000	80000	80000
10	161.4	155.2	162.5	163.5	169.8	167.6	170.1	171.4
11	183.5	177.1	183.5	185.1	181.9	176.6	175.1	178.0

The different lines are as follows :

1. Number of experiments
2. Minimum value of U_m for laminar flow, ft/sec.
3. Maximum value of U_m for laminar flow, ft/sec.
4. Minimum value of R_e for laminar flow.
5. Maximum value of R_e for laminar flow.
6. Minimum value of U_m for turbulent flow, ft/sec.
7. Maximum value of U_m for turbulent flow, ft/sec.

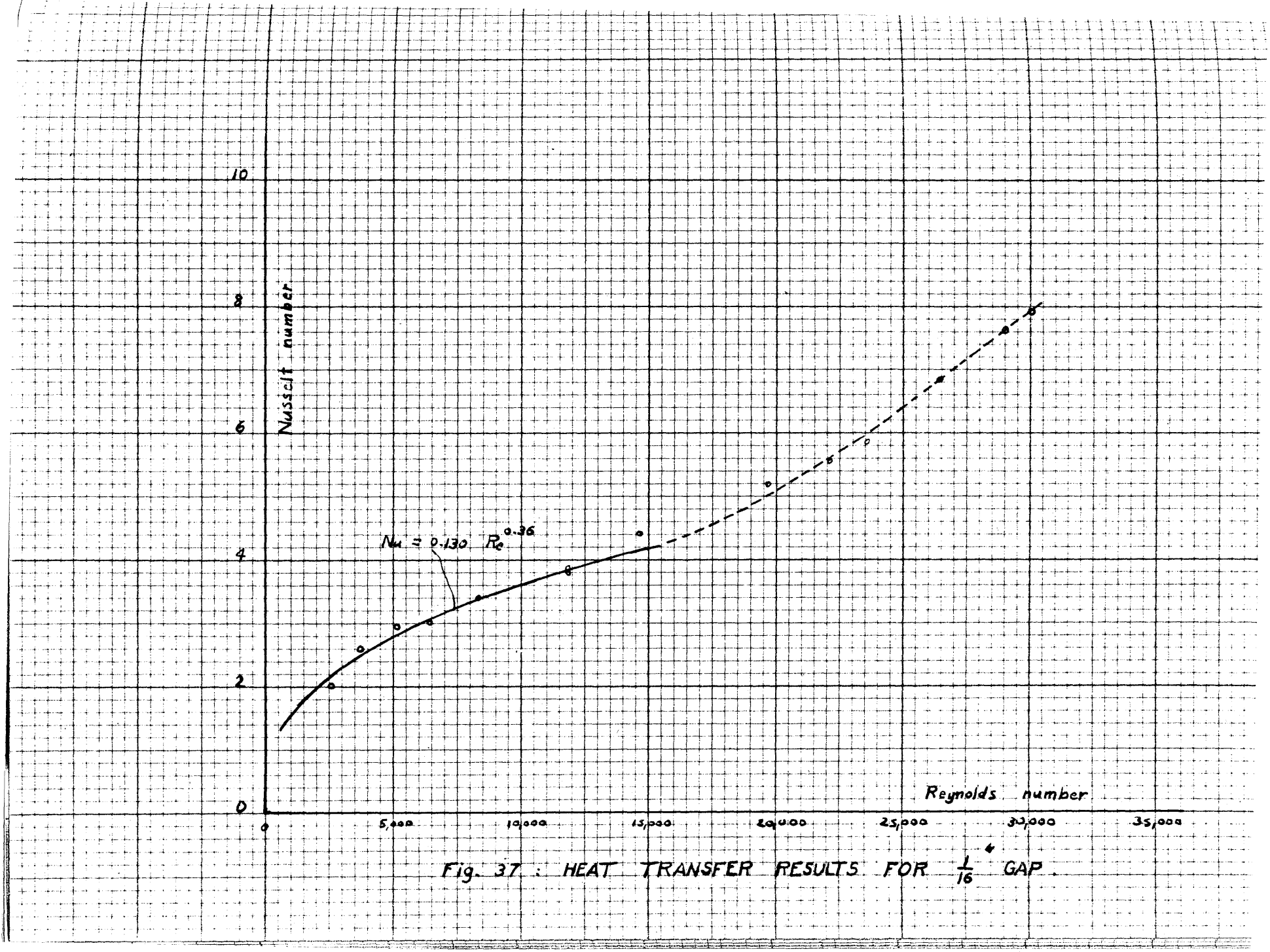

Fig. 37 : HEAT TRANSFER RESULTS FOR $\frac{1}{16}$" GAP.

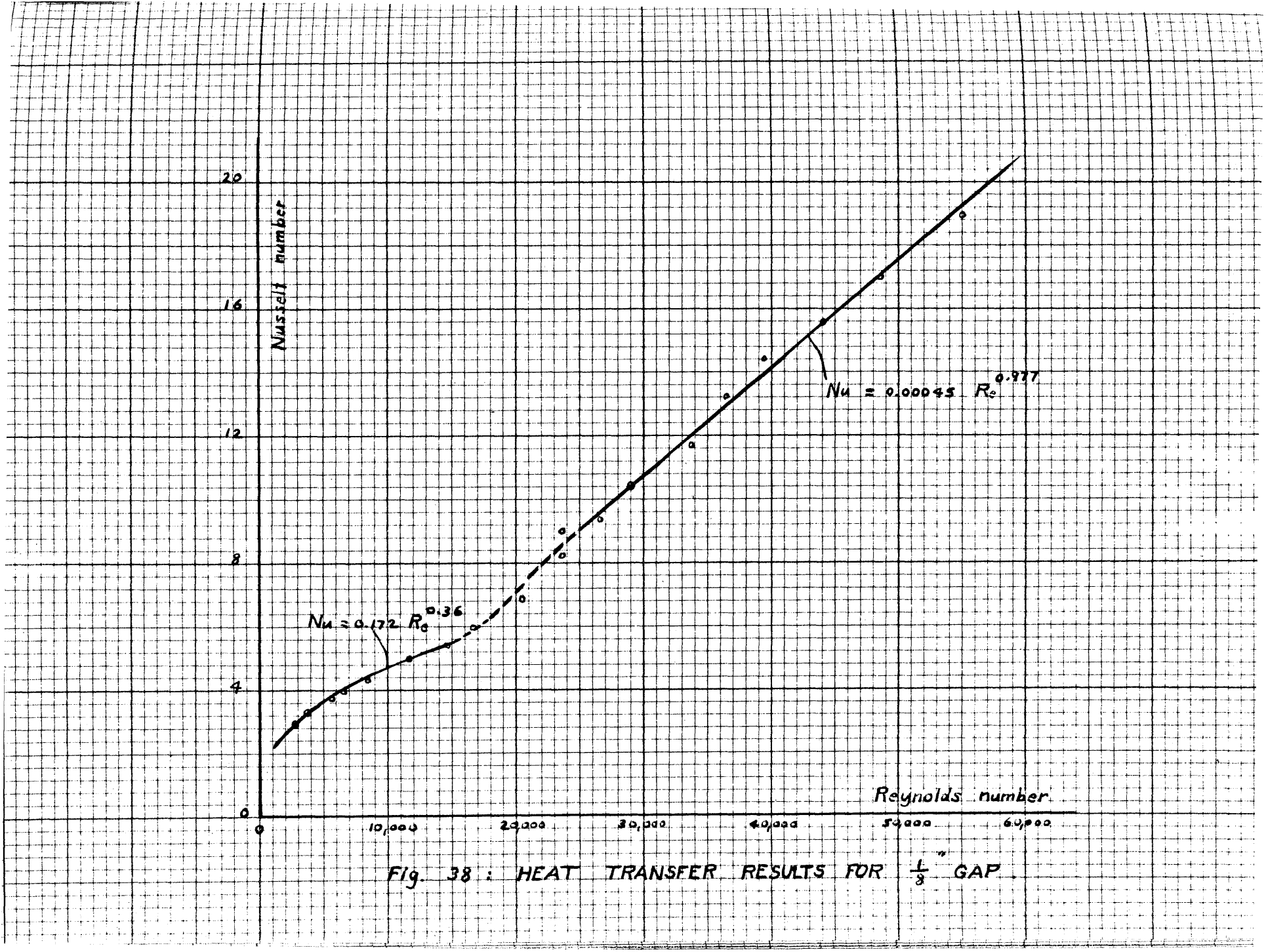

Fig. 38 : HEAT TRANSFER RESULTS FOR $\frac{1}{8}$" GAP

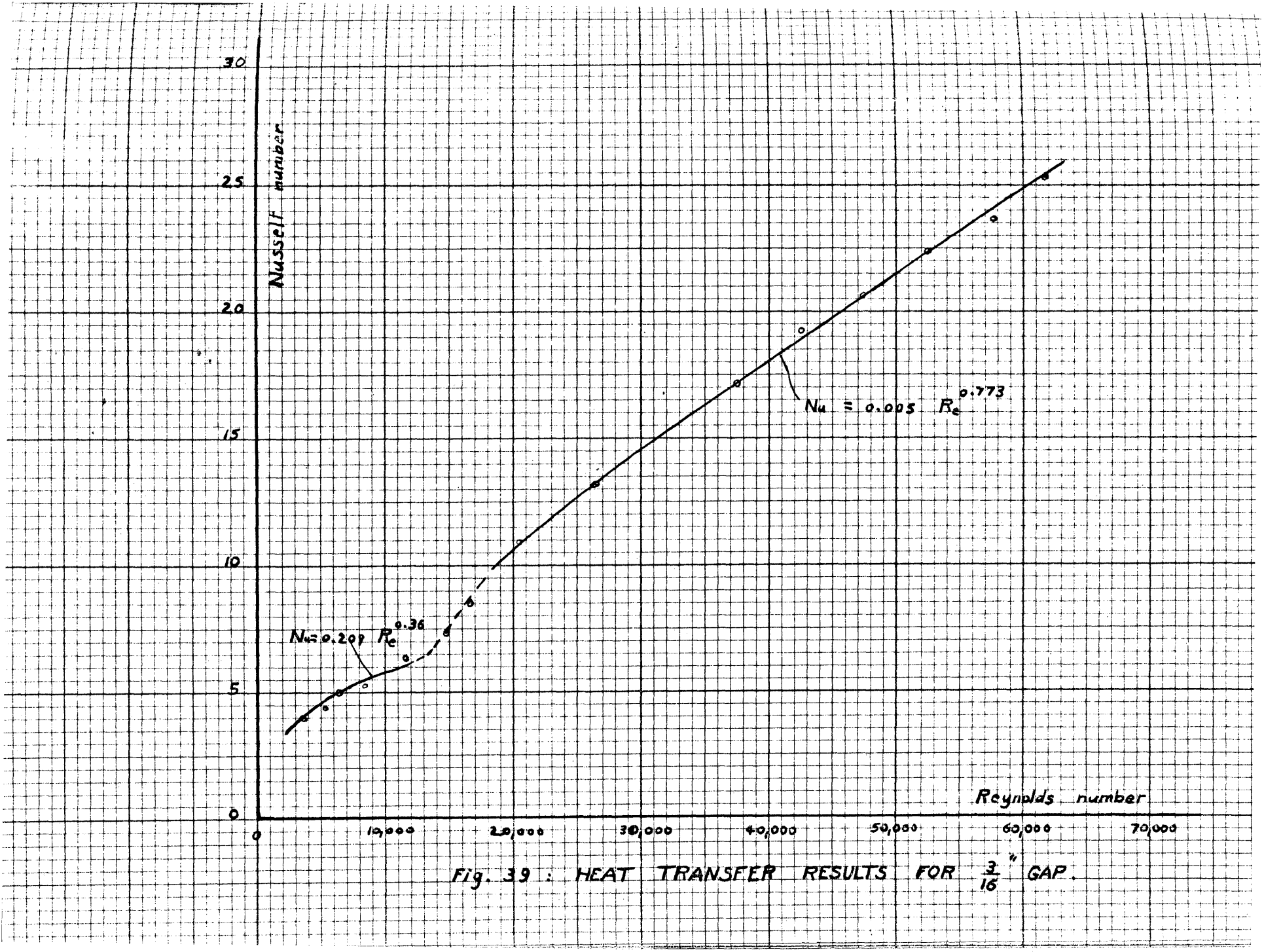

Fig. 39 : HEAT TRANSFER RESULTS FOR $\frac{3}{16}$" GAP.

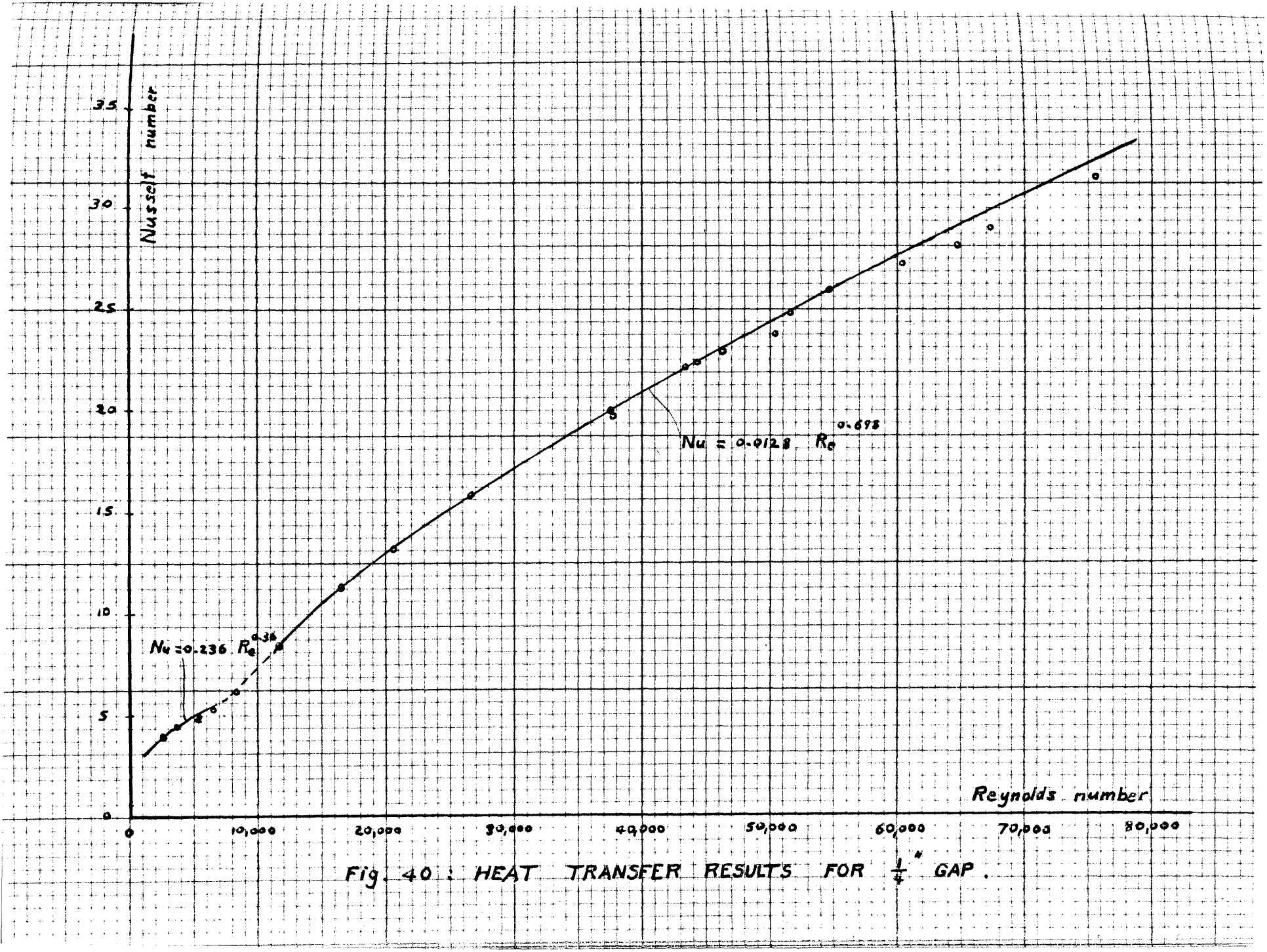

Fig. 40 : HEAT TRANSFER RESULTS FOR $\frac{1}{4}$" GAP.

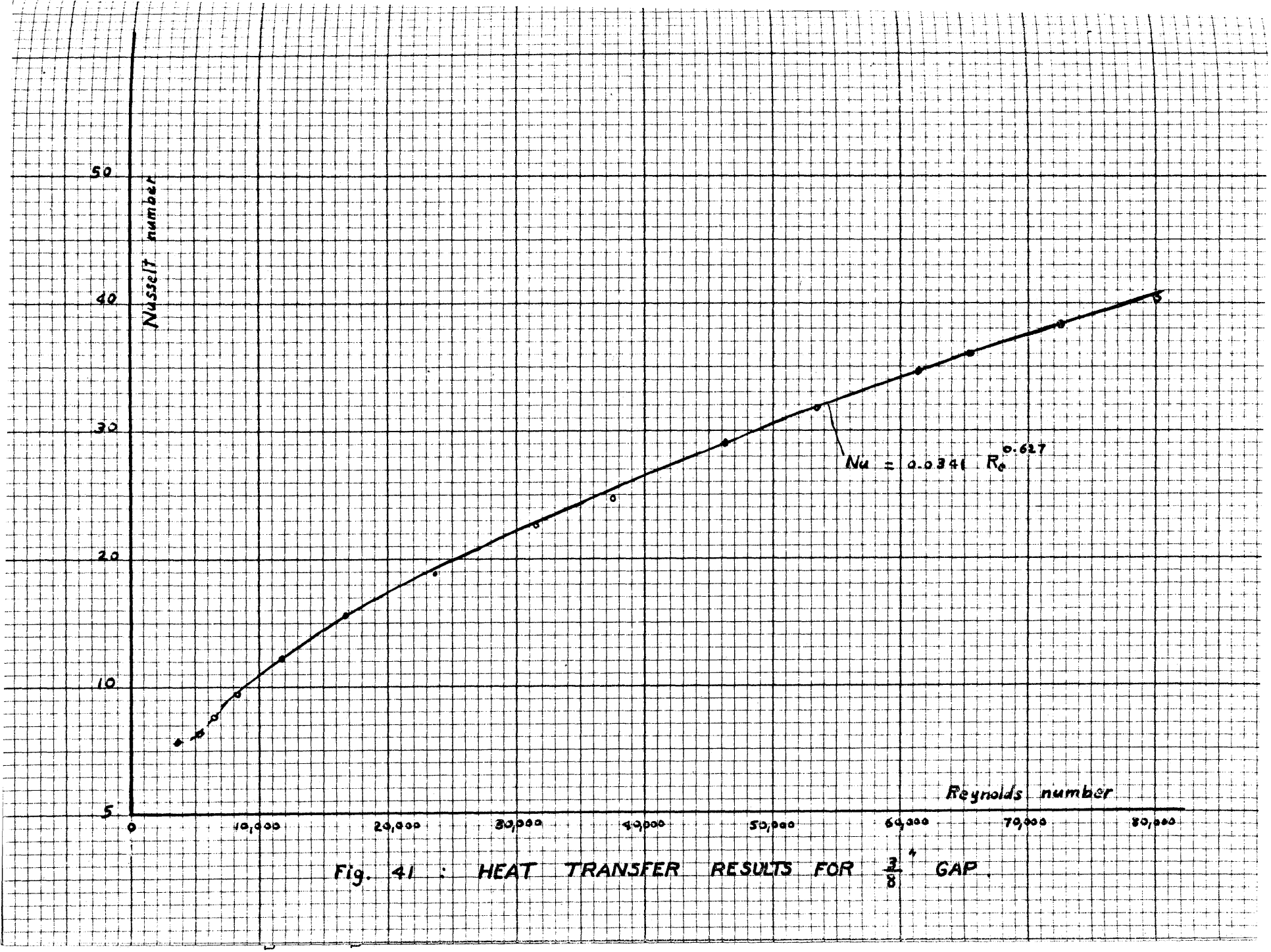

Fig. 41 : HEAT TRANSFER RESULTS FOR $\frac{3}{8}$" GAP.

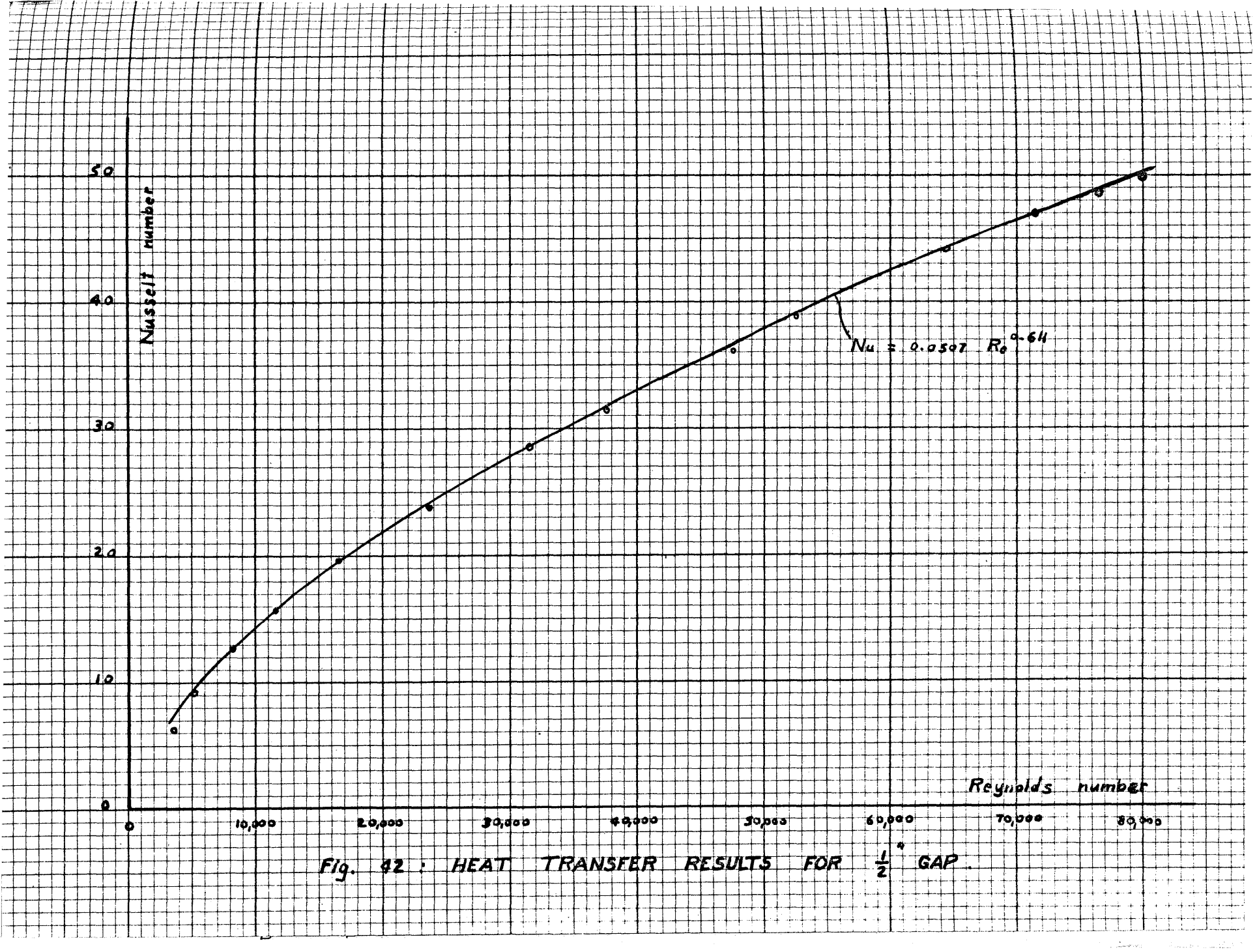

Fig. 42 : HEAT TRANSFER RESULTS FOR $\frac{1}{2}$" GAP.

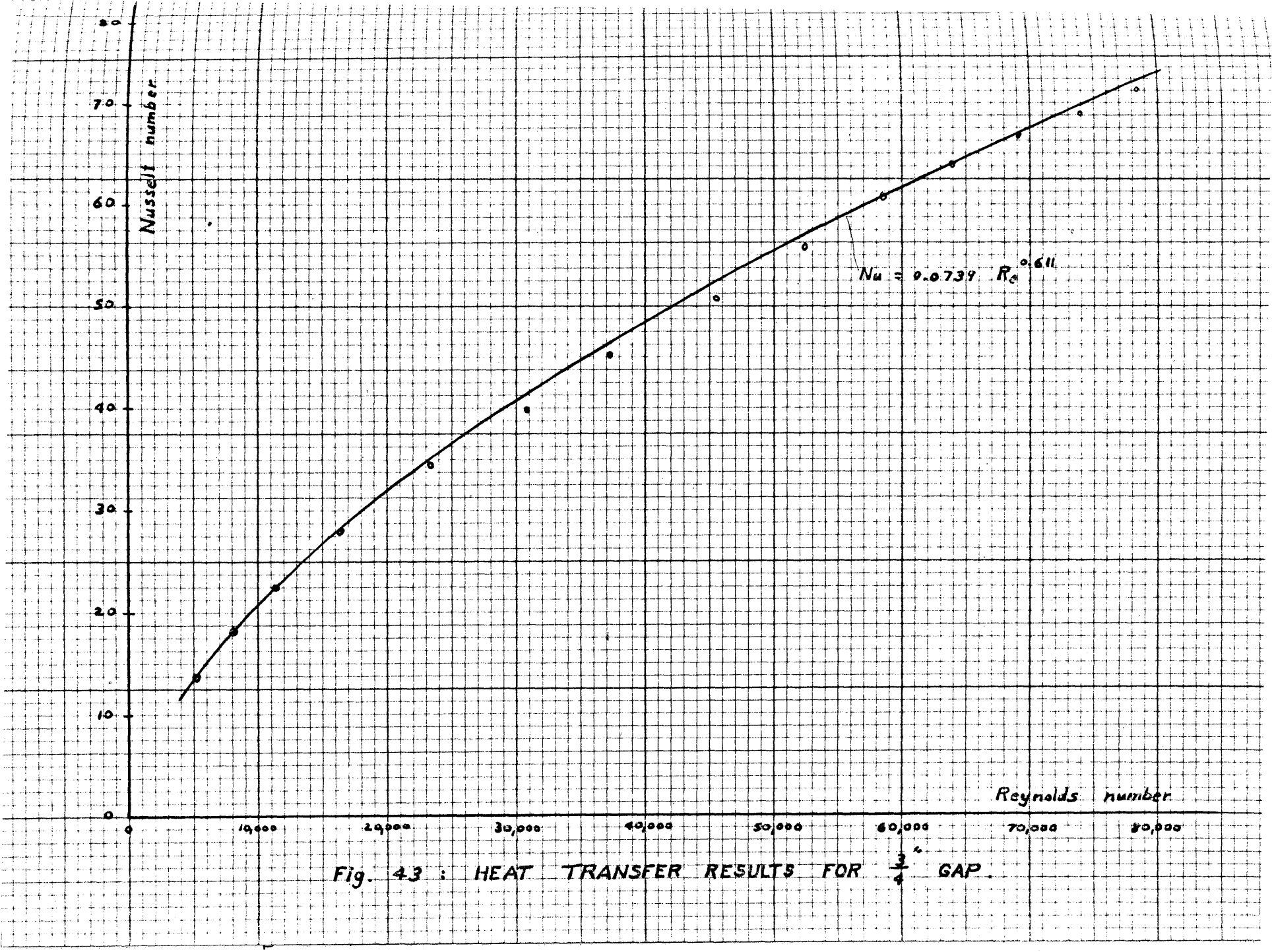

Fig. 43 : HEAT TRANSFER RESULTS FOR $\frac{3}{4}$" GAP.

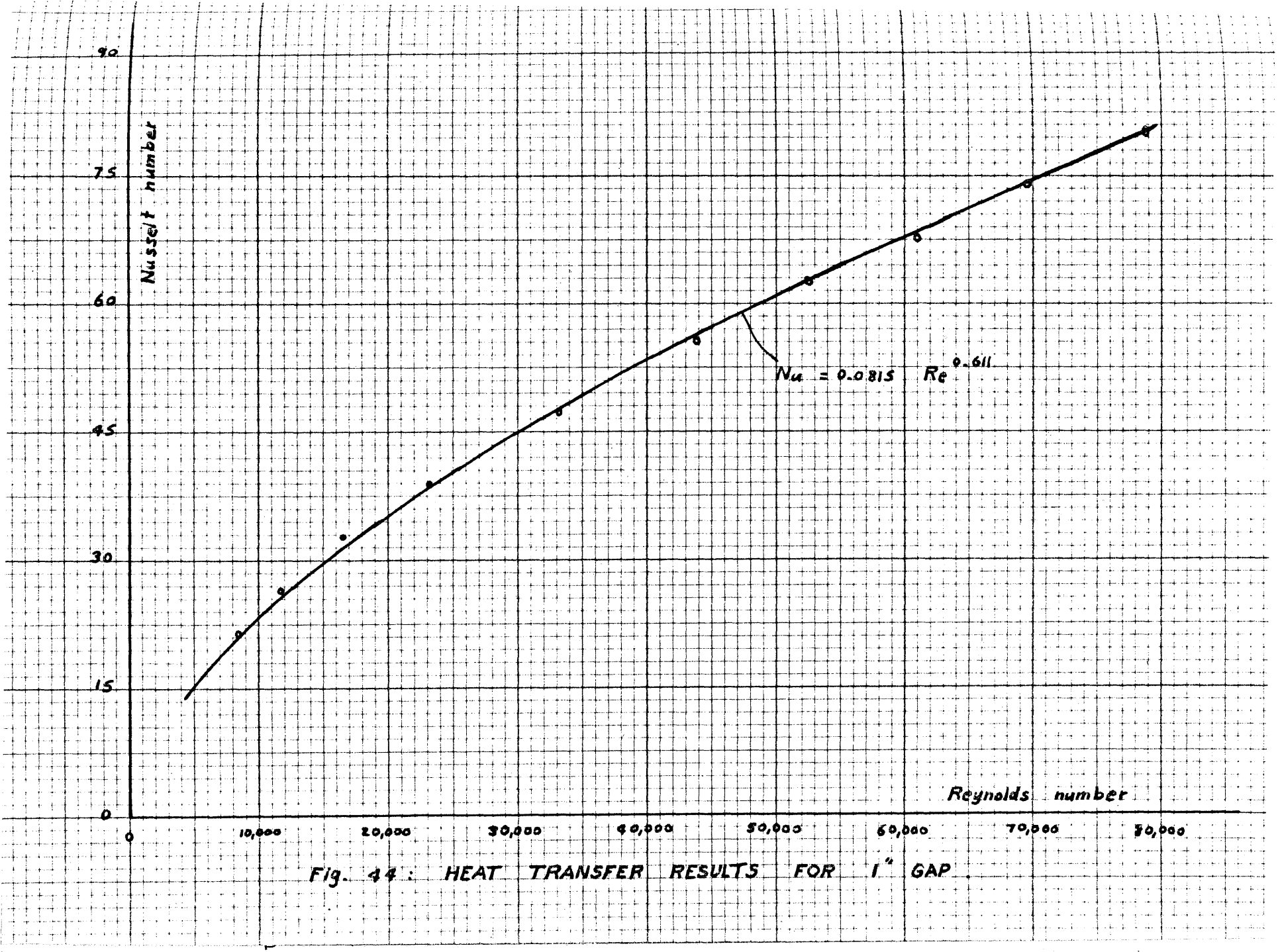

Fig. 44 : HEAT TRANSFER RESULTS FOR 1" GAP.

8. Minimum value of R_e for turbulent flow.
9. Maximum value of R_e for turbulent flow.
10. Minimum average value of t_w, ^oF.
11 Maximum average value of t_w, ^oF.

The difference between the temperature of the heating surface and the room temperature ranged between 94 and 124^oF. For large air discharges the heat lost by radiation from the heating surface was about 4.4 percent of the total heat given to the main heater, while for the smallest discharges this ratio reached about 34 percent. The heat lost by conduction was only between 0.35 and 2.5 percent. The electrical input to the guard heater was generally between 20 and 45 percent of that given to the main heater.

B - VELOCITY DISTRIBUTION BETWEEN THE PLATES.

Fourteen pairs of velocity distribution traverses were carried out on six different gaps, namely, $\frac{1}{8}$, 3/16, $\frac{1}{4}$, $\frac{3}{8}$, $\frac{1}{2}$ and $\frac{3}{4}$ inches. The observations and results are shown in tables 22 to 28 and figures 45 to 50.

Average velocities at radii $4\frac{5}{8}$" and $7\frac{7}{8}$" were calculated from the velocity distribution curves (dashed lines in Figs.45 to 50) and from the quantity of air discharge as given by the calibration curve of the flow nozzle. Agreement was found within $\pm$ 3%.

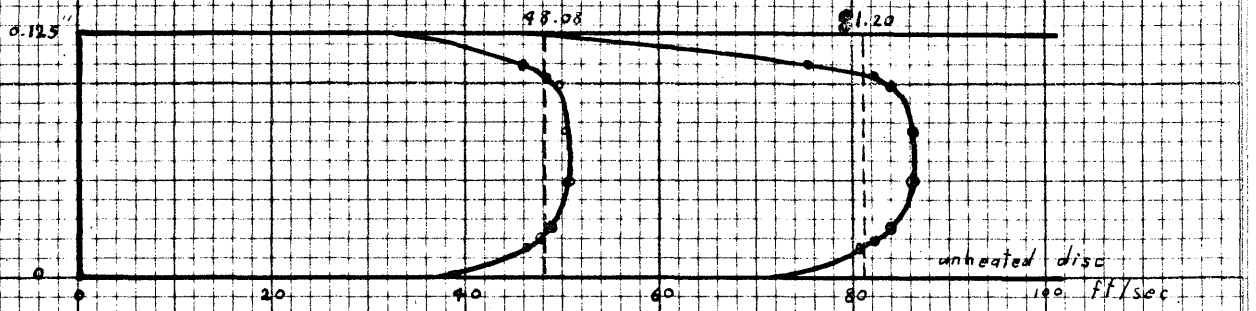

Experiment (3) : Air discharge = 555 lbs./hour

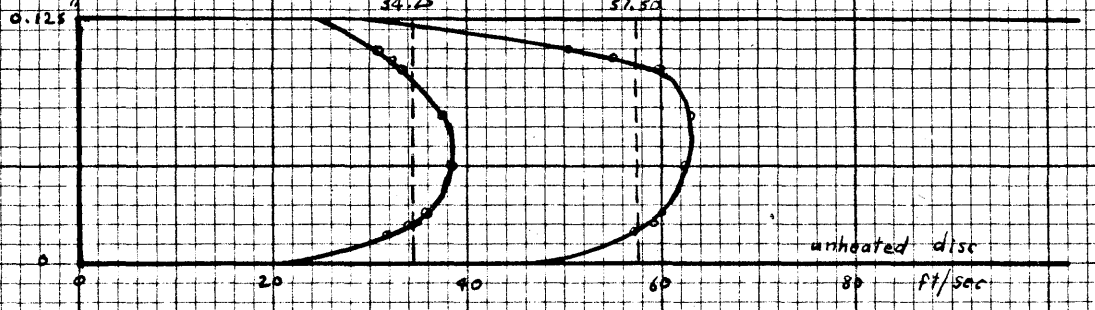

Experiment (2) : Air discharge = 393 lbs/hour

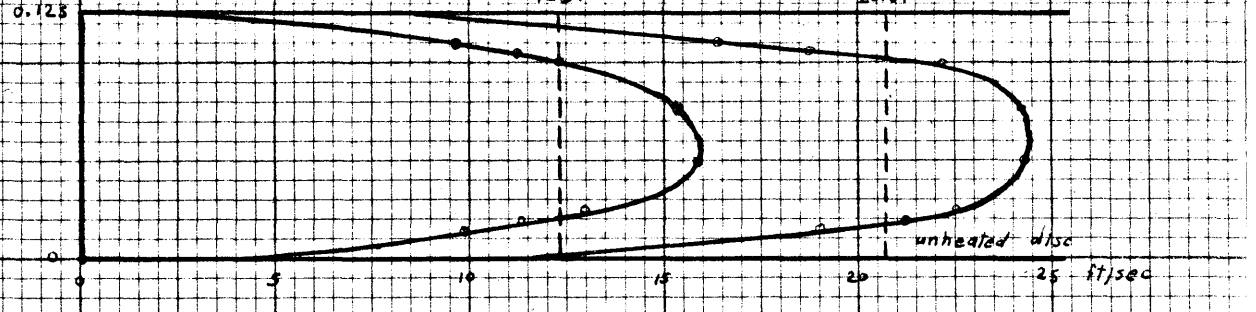

Experiment (1) : Air discharge = 139.2 lbs./hour

Fig 45 : VELOCITY DISTRIBUTION BETWEEN THE PLATES

gap = $\frac{1}{8}$"

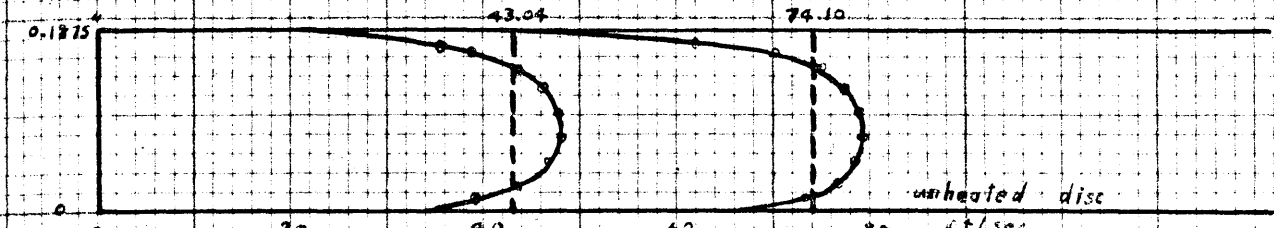

Experiment (6) : Air discharge = 760.8 lbs/hour

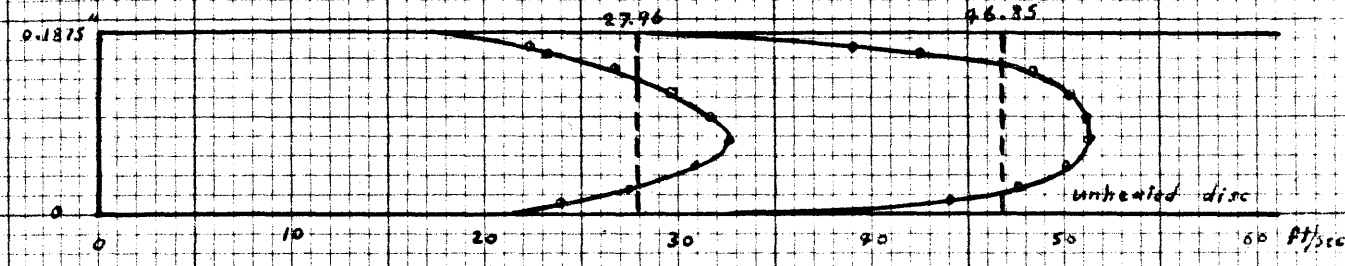

Experiment (5) : Air discharge = 480.6 lbs/hour

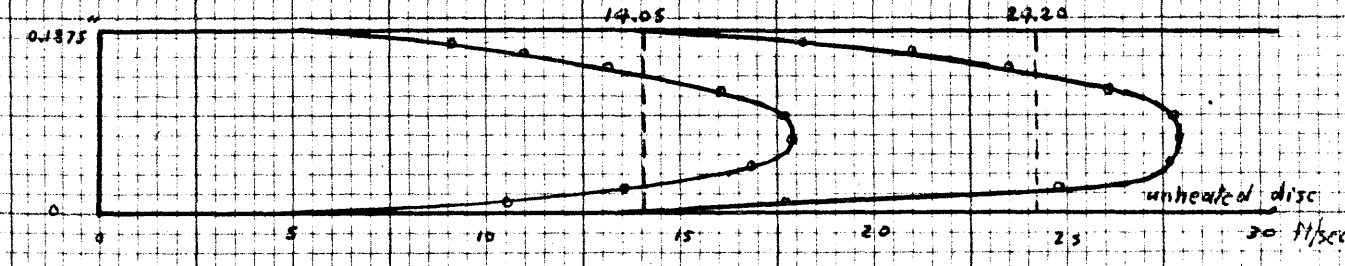

Experiment (4) : Air discharge = 240.3 lbs/hour

Fig. 46 : VELOCITY DISTRIBUTION BETWEEN THE TWO PLATES

gap = $\frac{3}{16}$"

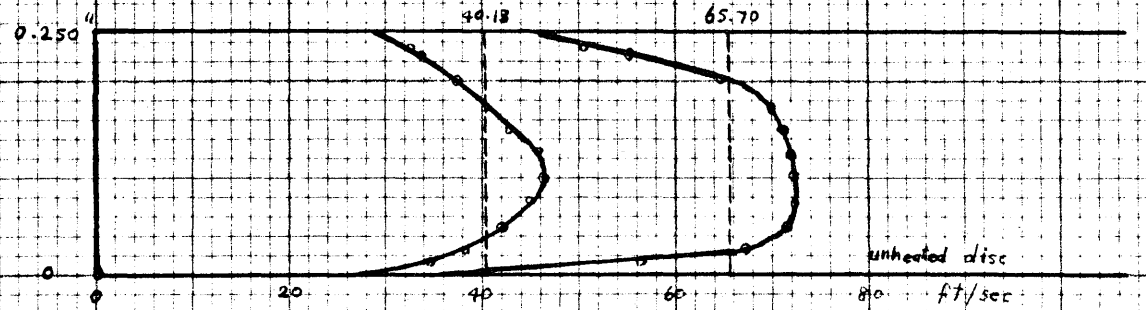

Experiment (9). Air discharge = 900 lbs./hour

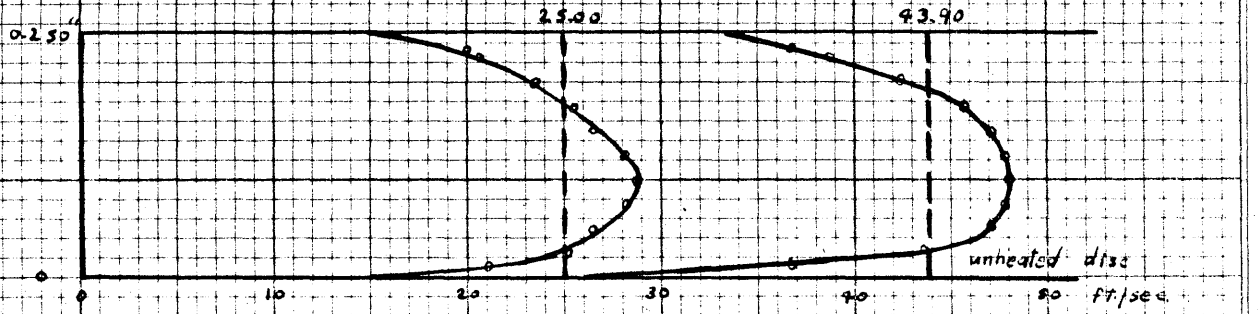

Experiment (8) Air discharge = 590.2 lbs./hour

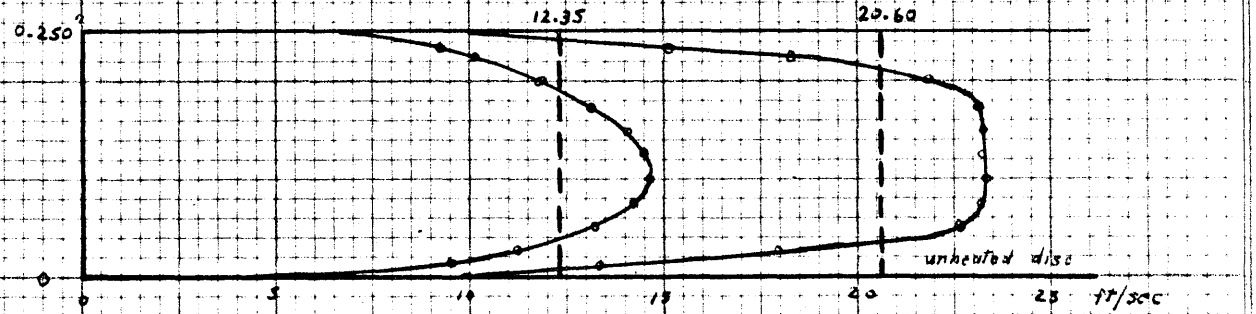

Experiment (7). Air discharge = 277.8 lbs./hour

Fig 47: VELOCITY DISTRIBUTION BETWEEN THE TWO PLATES.

gap = $\frac{1}{4}$"

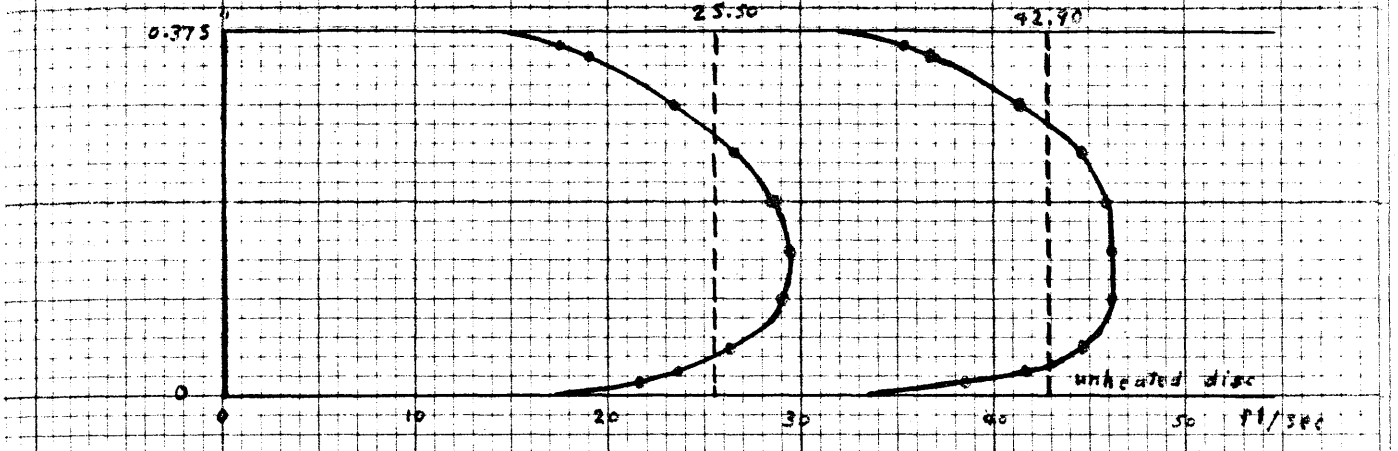

Experiment (11) ; Air discharge = 877.8 lbs/hour

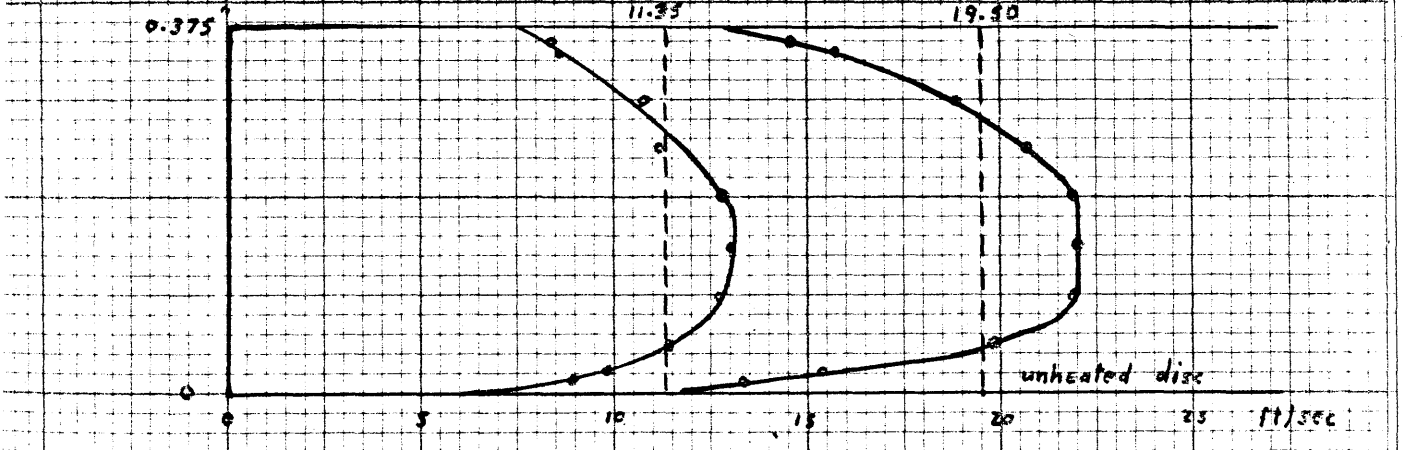

Experiment (10) ; Air discharge = 393.0 lbs/hour

Fig. 48 : VELOCITY DISTRIBUTION BETWEEN THE TWO PLATES.

gap = $\frac{3}{8}$"

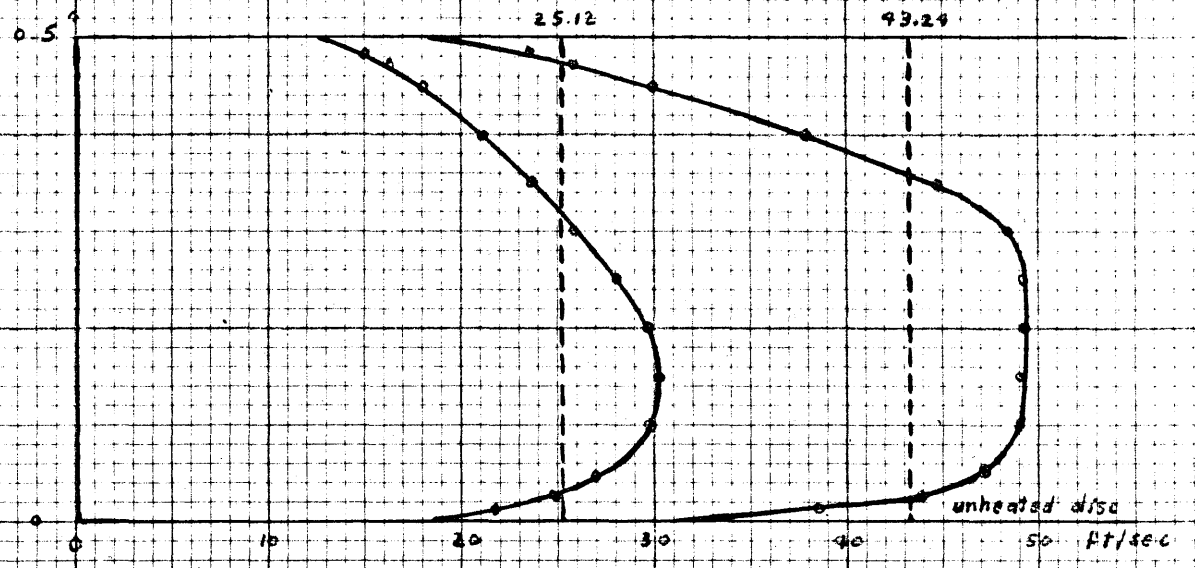

Experiment (13) : Air discharge = 1176.6 lbs./hour

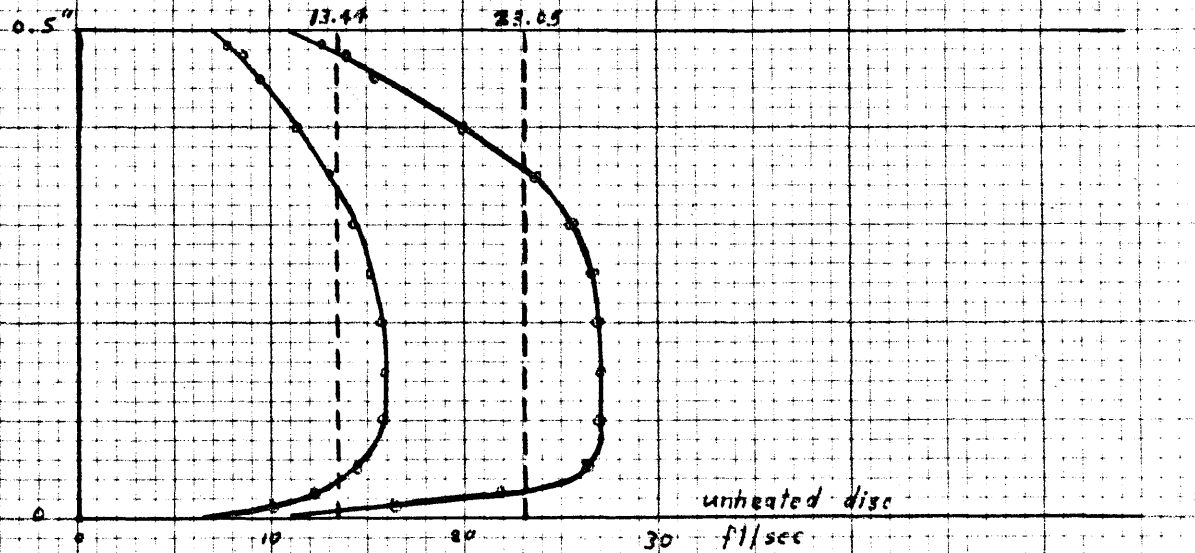

Experiment (12) : Air discharge = 621 lbs./hour

Fig. 49 : VELOCITY DISTRIBUTION BETWEEN THE THE TWO PLATES.

gap = $\frac{1}{2}$"

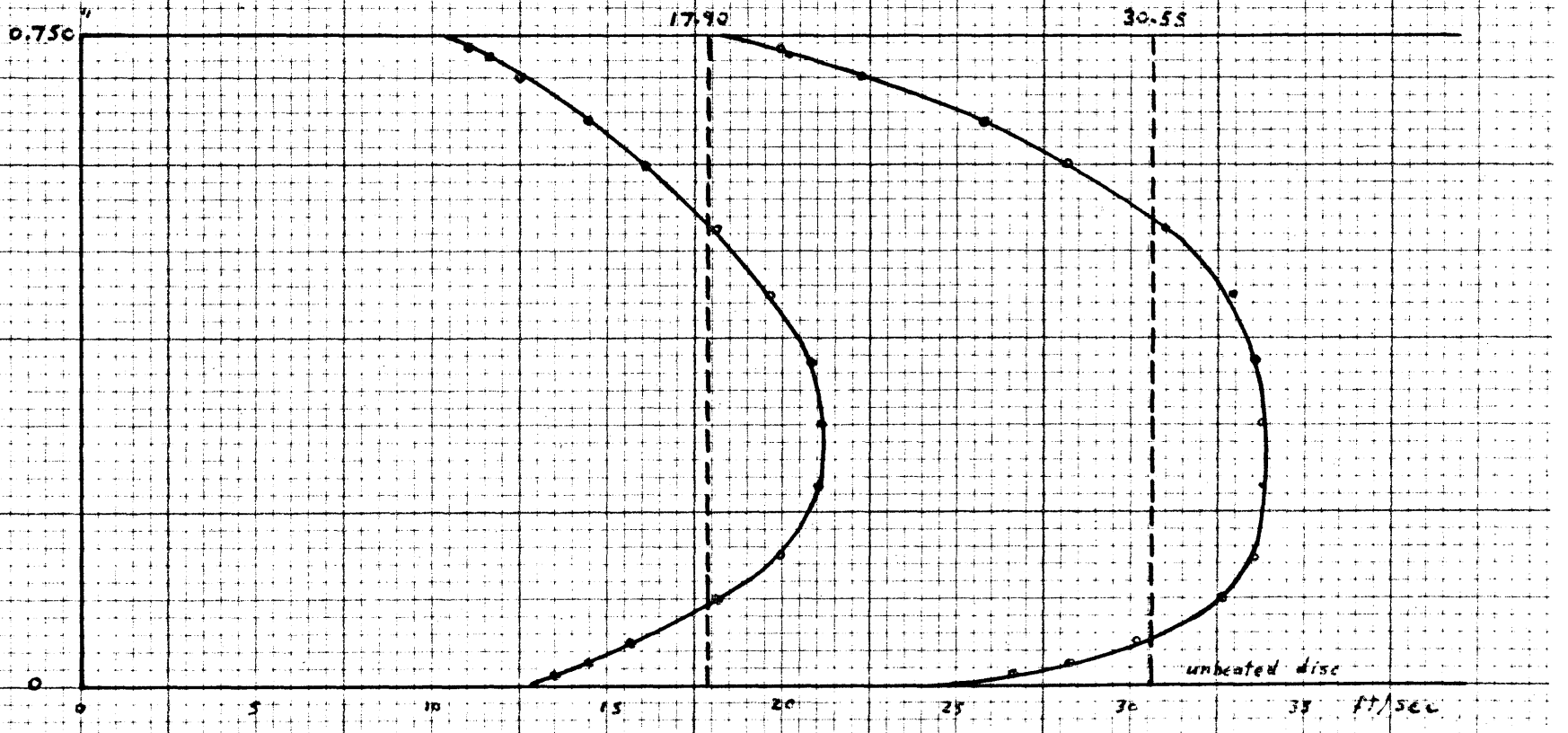

Experiment (14): Air discharge = 1242 lbs/hour

Fig. 50 : VELOCITY DISTRIBUTION BETWEEN THE TWO PLATES

gap = $\frac{3}{4}$"

C - ANALYSIS OF HEAT TRANSFER RESULTS.

I - Laminar Flow.

The value of the constant (n) of the general equations (VII-1) and (VII-2) was the same for all the gaps in the laminar flow range. As the gap increased the constant K (in equation VII-1) decreased according to the equation

$$K = 1.233 \left(\frac{b}{L}\right)^{-0.2} \qquad \text{VII-3}$$

where b = gap between the plates

$L = r_2 - r_1$

r_2 & r_1 = radii of the heating surface.

On the other hand, the variation of the constant A (in equation VII-2) with the gap followed the law

$$A = 0.755 \left(\frac{b}{L}\right)^{0.44} \qquad \text{VII-4}$$

The values of K and A were plotted against b in Fig.51. The solid lines represent equations (VII-3) and (VII-4)

After equations (VII-3) and (VII-4) the general equations (VII-1) and (VII-2) for laminar flow become

$$h = 1.233 \left(\frac{b}{L}\right)^{-0.2} \cdot U_m^{0.36} \qquad \text{VII-5}$$

and

$$Nu = 0.755 \left(\frac{b}{L}\right)^{0.44} \cdot R_e^{0.36} \qquad \text{VII-6}$$

The values of $\left[\frac{Nu}{\left(\frac{b}{L}\right)^{0.44}}\right]$ were calculated from equation (VII-6) and plotted versus R_e in Fig.52. The experimental values of Nu for different gaps were divided by $\left(\frac{b}{L}\right)^{0.44}$ and the results shown on the same graph.

It is noticed that the critical Reynolds number at which the laminar flow ceases to continue is not constant for all the gaps. It generally decreases as the gap increases. This will be discussed later, but the relation between that critical (R_e) and

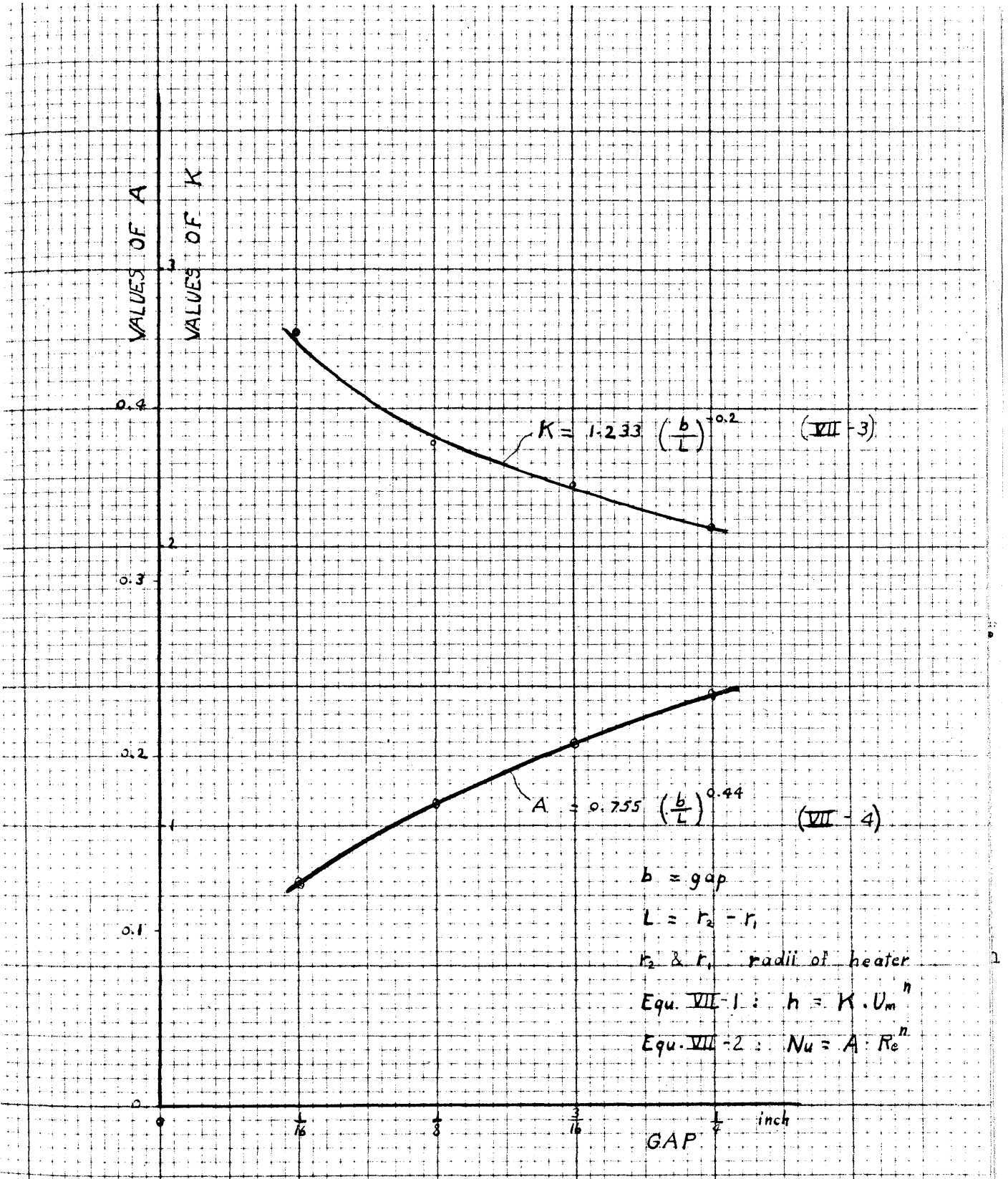

Fig. 51 : EFFECT OF GAP ON K & A (equations VII-1 & VII-2) IN LAMINAR FLOW RANGE.

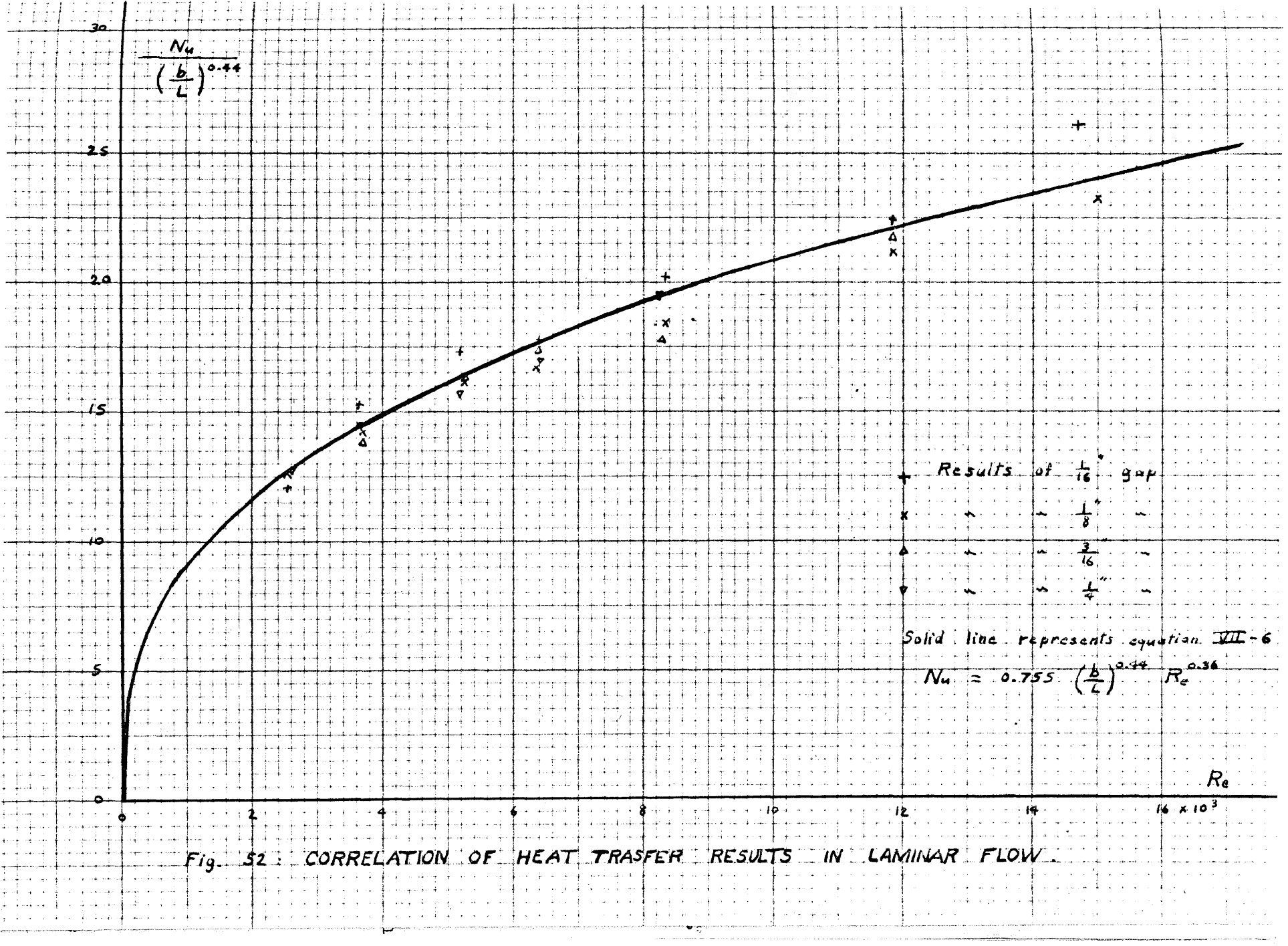

Fig. 52 : CORRELATION OF HEAT TRASFER RESULTS IN LAMINAR FLOW.

the gap is shown by the solid line in Fig.53.

II - Turbulent Flow.

The value of the Reynolds number at which turbulence starts changes from one gap to another. In the range of experiments for the 1/16" gap no clear turbulence started. At $\frac{1}{8}$" gap turbulence started at R_e about 28,000. This critical value decreased as the gapincreased, until it reached the value of about 6,000 for the $\frac{1}{2}$" gap. For wider gaps no definite value of critical Reynolds number could be found.

Different values of critical (R_e) required to start turbulence versus the gap (b) are shown in Fig.53, by the dashed line. This variation of the critical value will be discussed later.

Another feature in the turbulent range is the variation of the value of the exponent (n) in equations (VII-1) and (VII-2) with the gap. In the $\frac{1}{8}$" gap the value of n was 0.977. It then decreased as the gap increased until the value 0.611 was reached when the gap was $\frac{1}{2}$". Further increase in the gap did not change the value of n. In Fig.54 the variation of (n) with (b) is shown. This curve will be discussed later.

According to the variation of the exponent of the Nu-R_e curves no simple equation like (VII-6) was found for turbulent flow. An equation of the form

$$Nu = A. R_e^{n} \times f \qquad \text{VII-7}$$

(where f is a function of $\frac{b}{L}$ and R_e)

might be the simplest possible to collect all the data of all the gaps together. The exponent 0.611 was chosen as it is the perm-

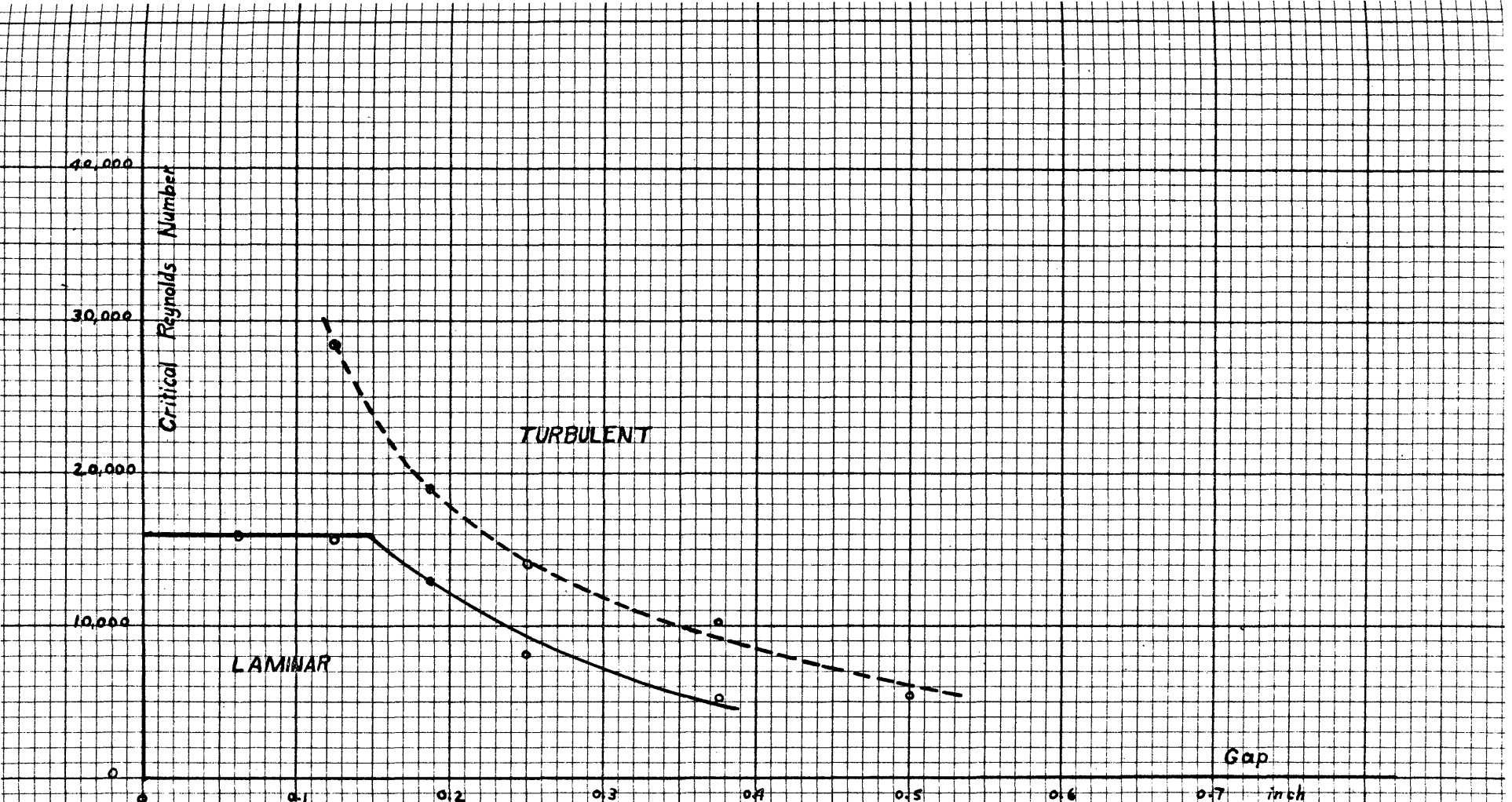

Fig. 53 : EFFECT OF GAP ON CRITICAL REYNOLDS NUMBER.

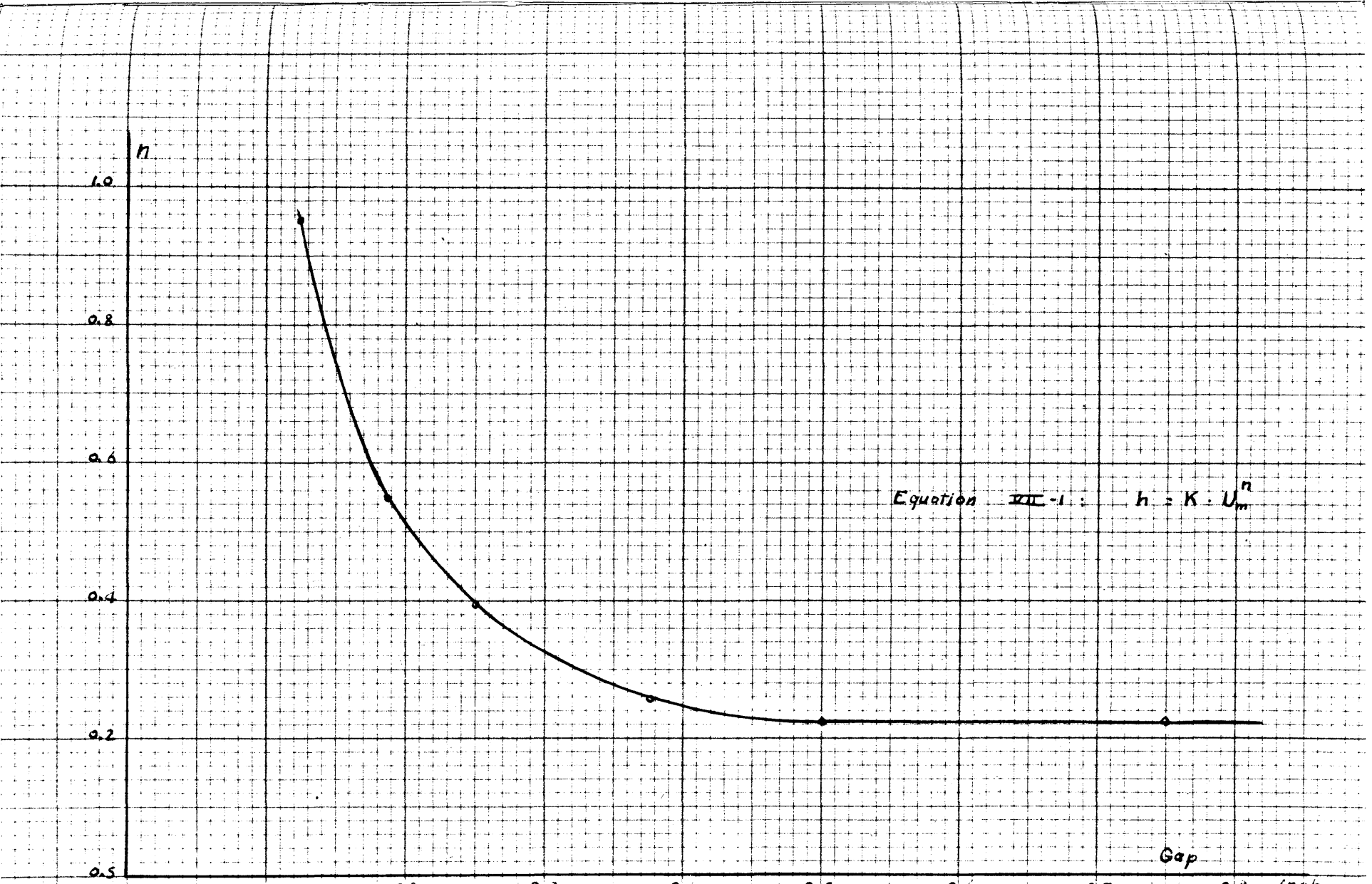

Fig. 54 : VARIATION OF (n) IN EQUATION VII-1 WITH THE GAP IN THE TURBULENT FLOW RANGE

anent value of (n) reached for the wide gaps. The best value of (A) was found to be0.075, and (f) given by the equation

$$f = 1 - 1.516\left[1 - 4.67\frac{b}{L}\right]^{0.8} \cdot R_e^{-0.06} \qquad \text{VII-8}$$

Thus, equation (VII-7) becomes

$$Nu = 0.075\, R_e^{0.611} \cdot \left[1 - 1{,}516\left(1 - 4.67\frac{b}{L}\right)^{0.8} \cdot R_e^{-0.06}\right] \qquad \text{VII-9}$$

The writer suggests this experimental equation for turbulent flow up to R_e = 80,000 and for gaps between $\frac{3}{4}$" and $\frac{1}{8}$", or for values of $\frac{L}{b}$ = 4.67 to 28.

Fig.55 shows values of $(\frac{Nu}{f})$ plotted against (R_e) according to equations (VII-8) and (VII-9). The results of the experiments on the six gaps ($\frac{1}{8}$" to $\frac{3}{4}$") were corrected by dividing (Nu) by the value of (f) for different gaps and Reynolds numbers. Those corrected values are shown in Fig.55 so as to be compared with equation VII-9.

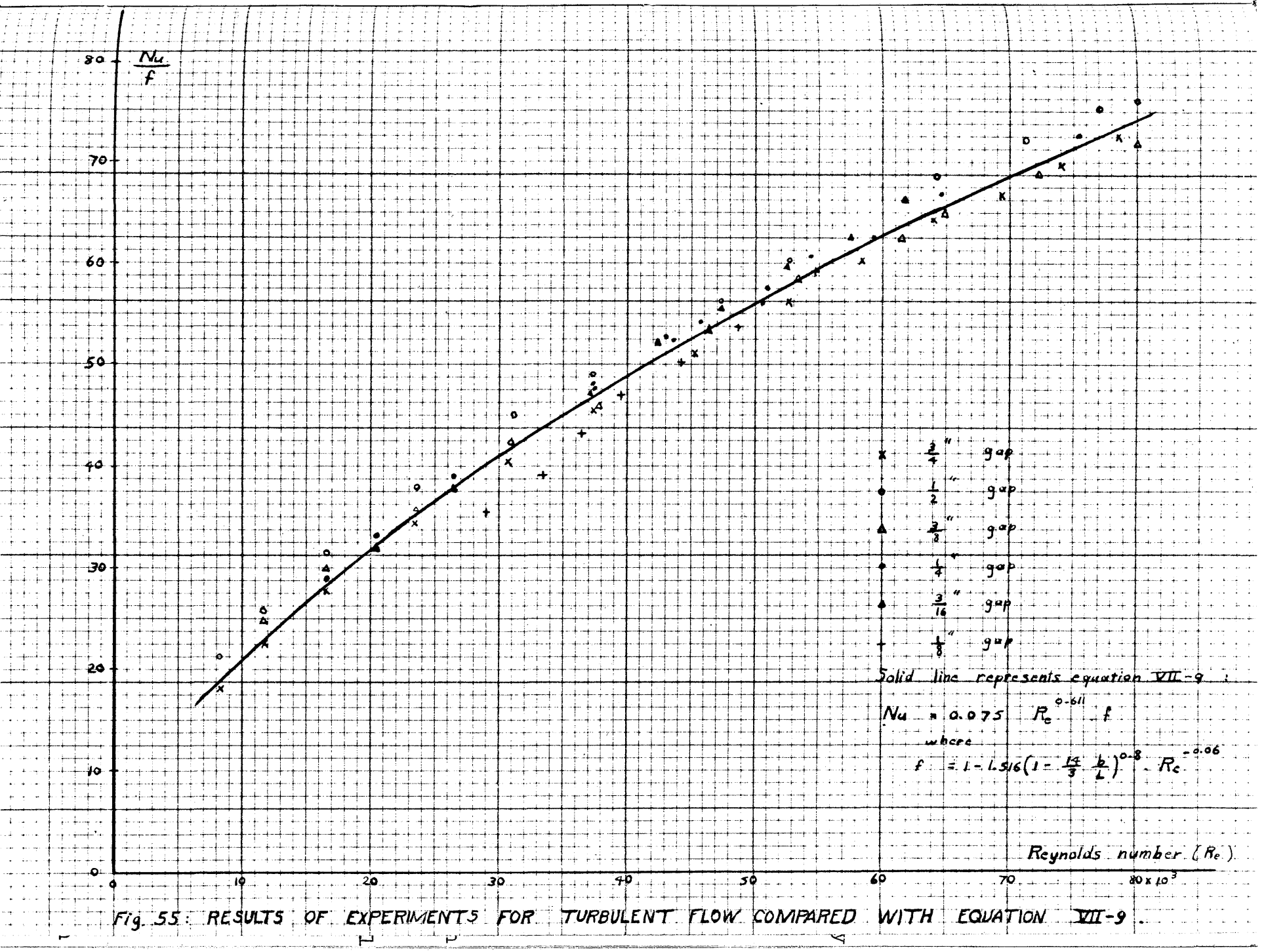

Fig. 55: RESULTS OF EXPERIMENTS FOR TURBULENT FLOW COMPARED WITH EQUATION VII-9 .

CHAPTER VIII.

DISCUSSION OF RESULTS.

A - CRITICAL REYNOLDS NUMBER.

The change of the critical Reynolds number in the present work has been shown in Fig.53 against the gap (b). For the commencement of transition from laminar to turbulent flow the critical value is nearly constant (= 16,000) when the gap is very small. Later, after a gap of about 0.15" is reached, that critical value begins to decrease as the gap increasss. After a certain region of transition turbulence starts. The Reynolds number necessary to start turbulence is greater for small gaps. As the gap increases the value of (R_e) decreases till, at last, the flow is completely turbulent for the widest gaps.

Similar results were obtained by Davies and White[9] who measured the friction when water was passed in very flat ducts. They found, in seven out of ten different gaps, that the deviation from the viscous flow line generally occurs earlier when the gap is increased if all other conditions remain the same. The critical value was constant for the smallest three gaps. For a different reason they represented their results in a way different from that of Fig.53, but the shape of their results agrees completely with the solid line in Fig.53.

Davies and White explained this result by introducing what they called the "entrant length" (l). This entrant length was constant in all the tests, and the ratio $\frac{l}{b}$ (where b is the depth of duct)varied with each change of depth, and therefore true

geometrical similarity was not secured. After a certain value of $\frac{l}{b}$ is reached this factor ceases to have any effect on the position of the first deviation from true viscous flow.

It has been shown by Goldstein[19] that the value of (R_e) at the commencement of the transition region depends, to a large extent, on the inlet conditions and on the turbulence producing mechanism. It can be expected that the critical Reynolds number at a certain cross-section depends on the type of entrance and on the distance of the cross-section considered from the entrance.

It may be stated, therefore, that the early transition with wider gaps is due to the fact that the parabolic flow is not established yet. As the gap increases more eddying is likely to occur. The conditions approach those of flow past flat plates. When the gap decreases, however, the parabolic flow has more chance to form. Turbulence is being somewhat suppressed and the critical value therefore increases.

B - DISCUSSION OF LAMINAR FLOW RESULTS.

In laminar flow of fluids heat is transferred mainly by conduction. According to the equation of heat conduction the rate of heat transfer increases with the thermal conductivity and decreases with the increase of the distance travelled. From this it can be assumed that the surface conductance (h) decreases as the gap (b) increases. This was verified experimentally as equation (VII-5) shows.

Theory [36] suggests that, for laminar flow in

flat ducts *, the coefficient of heat transfer (h) increases proportional to a one-third power of the velocity until, at sufficiently long distance downstream, the local coefficient approaches a limiting value independent of the velocity. At that limit the heat transfer can be represented by Jakob's equations (I-29) and (I-32).

The exponent in the present work was found to be 0.36 instead of $\frac{1}{3}$. Probably this is because the velocity distribution at the inlet was not completely parabolic. In such cases Norris and Streid[36] suggest that Pohlhausen's equation (I-15) for laminar flow parallel to a flat plate can be used for the transition length until the flow becomes parabolic. If this is accepted then the (average) exponent (n in equation VII-1) will be somewhere between $\frac{1}{3}$ and $\frac{1}{2}$. The value 0.36 looks to be reasonable.

As for the influence of the gap (b) Norris and Streid suggest that $\left[h \propto b^{-\frac{1}{3}} \right]$ if the length (L) of the duct remains the same. In the present work the value (-0.2) was found instead of $(-\frac{1}{3})$. This may have been caused by natural convection currents. With wider gaps there is more chance for these currents to form, thus counteracting, to an extent, the effect of the gap on heat transfer.

Although exact comparison cannot be made because of the difference in the flow conditions, the present experimental values obtained for laminar flow for different gaps were

---

* The words "flat duct" were used in the paper of Norris & Streid to denote the case of flow between flat parallel plates of infinite extent perpendicular to the flow direction.

recalculated on the basis of $Nu^{+} - \Phi$ of the paper of Norris & Streid and shown in Fig.56, compared with the theoretical values for flat ducts (h based on the arithmetic mean temperature difference). The method of recalculation is shown in Appendix I. The present resultsare about 20% higher than the theoretical ones. This is believed to be, partly, due to free convection currents. The authors themselves predicted that experimental results would be higher for that reason, and they suggested that the correction factor by which the theoretical results are to be multiplied is $1.15(\frac{\mu_m}{\mu_f})^{0.14}$, where μ_m = viscosity of the fluid at its bulk temperature, and μ_f = viscosity at the film temperature. This factor makes the theoretical results higher by about 14 percent.

C - DISCUSSION OF TURBULENT FLOW RESULTS.

1. Variation of heat transfer with the gap :

The present results in the turbulent range show, generally, an increase in the heat transfer as the gap (b) increases. This can be explained as follows:

In the case of turbulent flow the greater part of heat transfer takes place by means of convection currents towards and away from the heating wall. The rate of heat transfer by such currents is obviously proportional to the component of velocity normal to the wall. This component of velocity will be increased by the eddies resulting from the disturbance of the fluid flow, and the heat transfer will therefore increase as a result of this action.

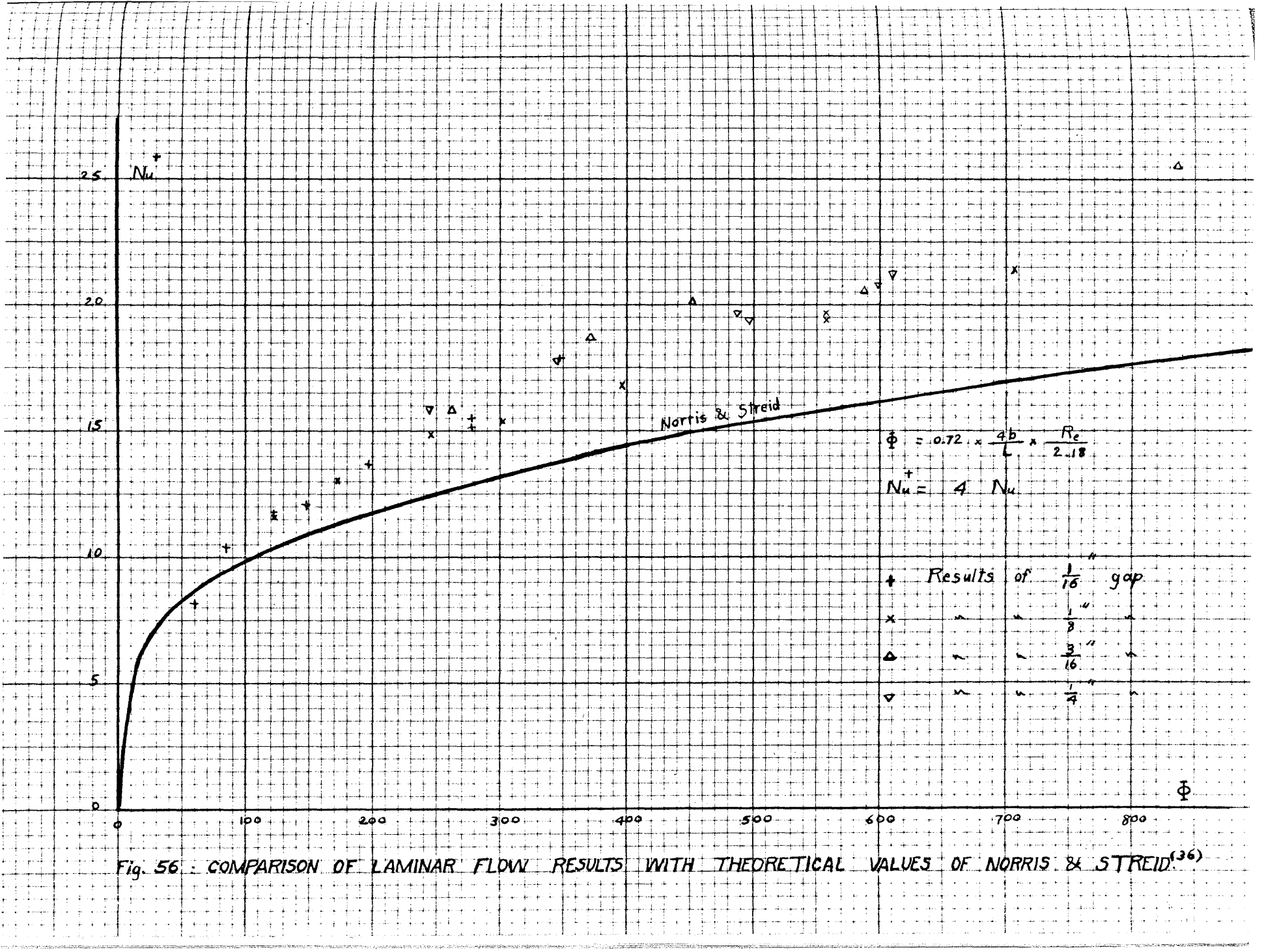

Fig. 56 : COMPARISON OF LAMINAR FLOW RESULTS WITH THEORETICAL VALUES OF NORRIS & STREID[36]

Where a fluid enters a duct under certain conditions, eddies are set up. As the fluid proceeds along the duct, these eddies subside and the stream assumes undisturbed turbulent flow with uniform heat transfer coefficient. Schack[45] has shown that these inlet eddies persist for longer distances in large ducts than in small ones, so that for ducts of equal length (as in the present case) the mean "surface conductance" would tend to be higher for larger gaps. This effect would tend to couteract the effect of the gap alone, which is to reduce the heat transfer with increase in the gap.

In very narrow ducts the proximity of the walls tends to minimize the velocity components normal to the walls. In other words, the different particles of the fluid have, for wider gaps, more freedom to move here and there as they have a wider path. When the gap is small, however, the freedom of the particles to move will be restricted, and turbulence suffers some kind of suppression. It will be expected, therefore, that wider gaps give higher heat transfer coefficients than narrow ones.

Yet, this factor of more freedom is not unlimited. There may be a certain gap at which the effect of the depth of the air stream vanishes completely. As found in the present work this critical gap was $\frac{3}{4}$". This corresponds to an $(\frac{L}{b})$ ratio of 4.67. The values of the heat transfer coefficient for different air speeds were nearly the same when the gap was increased from $\frac{3}{4}$" to 1"

Probably if the gap is further increased, the values of the heat transfer coefficient might be the same, or even less than those of the $\frac{3}{4}$" and 1" gaps. This may result from the expected

reduction in the velocity component touching the heating surface normally. No trial was made with gaps larger than one inch as this would render the maximum airstream velocity comparatively very small.

2. Comparison of the results with theory.

Like the common findings in the comparison of theoretical and experimental heat transfer results in turbulent flow, the present experimental results are higher than those given by the theoretical expression (III-15). This was expected because in the mathematical solution, for the sake of simplification, the flow is assumed two-dimensional. Actually, only the mean flow may be two-dimensional, but there are fluctuating values of velocity in the three perpendicular directions. This will cause an increase in the heat transfer.

To account for the high experimental values three factors may be considered :

1. Natural convection currents.
2. The presence of an unheated starting length.
3. Turbulence.

The effect of the natural convection currents may be appreciable only when the air speeds are small. But as the air velocity increases this effect becomes less and less important.

The unheated starting length may be considered approximately as the difference between the main pipe radius and the inner radius of the heating surface. This distance is 1.5". If the expression (II-10) given by Jakob and Dow[26] is accepted, then the unheated starting length would be responsible for only

about1.5% of the amount of heat transferred, had the unheated length been absent.

The writer believesthat the high coefficients of heat transfer found in the present work are mainly due to turbulence. The 90° deflection of the air passage at a short distance before the working section is likely to cause a flow fluctuation normal to the heating surface. Such fluctuations, obviously, increase the heat transfer. They may be damped, however, on their way downstream across the working section.

The problem of "super-turbulence" has been studied by Arabi (2). He worked on heat transfer to water flowing in tubes and investigated the effect of different inlet conditions on heat transfer. He differentiated between normal turbulence and super turbulence, and stated that if any turbulence promoter such as bends existed before the heat transfer section the results would be, no doubt, higher than those for normal turbulence.

Arabi found that the local heat transfer increased with super-turbulence, and the excess over normal turbulence decreased as the former gradually dissipated. There was a critical value of $\frac{l}{d}$ (where l = length of the working section, d = diameter of tube) below which the effect of super-turbulence was obvious. Arabi found that what he called 'the coefficient of increase of heat transfer due to super-turbulence' was a function of Reynolds number.

In spite of the difference in the nature of Arabi's work and the present one, Arabi's results may be useful here. In the

present work the 90° change in the direction of the air stream might have been a turbulence promoter. The unsymmetry noticed in the curves of the velocity distribution between the plates supports this idea. If this is the case then there will be a critical value of $\frac{L}{b}$ after which the effect of super-turbulence will vanish. Because of the small length (L) of the heating surface in the present work the effect of super-turbulence is great.

Yet, it is noticed that the values given by equation (III-15) lie below the experimental values of all the gaps. With narrow gaps, as the flow becomes more and more two-dimensional in character, the experimental values approach the theoretical ones.

The theoretical expression (III-15) was derived for the case of radial flow parallel to a flat surface. This case corresponds to the $\frac{3}{4}$" and 1" gaps as the maximum heat transfer coefficients were obtained and no effect of the gap was present. Equation (III-16) is

$$\frac{hL}{k} = 0.0356 \left(\frac{\rho U_m L}{\mu}\right)^{0.8} \left(\frac{c\mu}{k}\right).\left(\frac{r_2 + r_1}{2 r_2}\right) \qquad \text{VIII-1}$$

As shown in Chapter II, an empirical correction may be necessary for theoretical expressions to be successful. This correction factor is naturally a function of Reynolds number. If we assume that the turbulent boundary layer is formed right from the leading edge then the results of the $\frac{3}{4}$" and 1" gaps suggest that the values given by equation (VIII-1) be multiplied by (F), where

$$F = 1 + 42.35\ R^{-0.26} \qquad \text{VIII-2}$$

$$\text{where } R = \frac{\rho U_m L}{\mu} \qquad \text{VIII-3}$$

Thus equation (VIII-1) becomes

$$\frac{hL}{k} = 0.0356 \left(\frac{\rho U_m L}{\mu}\right)^{0.8} \left(\frac{c\mu}{k}\right) \left(\frac{r_2 + r_1}{2 r_2}\right) \left[1 + 42.35 \left(\frac{\rho U_m L}{\mu}\right)^{-0.26}\right] \qquad \text{VIII-4}$$

$$\text{or} \quad N = 0.0356\, R^{0.8}\, P_r (1 + 42.35\, R^{-0.26}) \left(\frac{r_2 + r_1}{2 r_2}\right) \qquad \text{VIII-5}$$

$$\text{where} \quad N = \frac{hL}{k} \qquad \text{VIII-6}$$

Equation (VIII-5) is represented by the solid line in Fig.57. The results of the $\frac{3}{4}$" and 1" gaps were recalculated to give (N) and (R), and are shown in Fig.57.

3. Comparison with the results of other workers.

This comparison is based on two points :

1. The present work isconsidered as heat transfer from a flat plate to an airstream. The mean stream velocity is taken as defined in equation (III-5).
2. The results of other workers were corrected to a plate length 3.5 inches according to Haucke's equation (II-8).

The comparison is shown in Fig.58. For the middle values of gap the agreement is satisfactory. For large gaps the present results are somewhat higher, while for small gaps they are lower. It may be added that in the work of every investigator, generally, one set of moderate flow conditions was taken. Probably a change in such conditions might result in either higher or lower heat transfer values, reaching the present extremes.

The work of Sams and Weiland[43] was carried out on a similar plate length (= 3.5 inches). The gap between their plates was $\frac{1}{4}$". Their results are not shown in Fig.58, but the present results on the $\frac{1}{4}$" gap fall about 8% lower than the values of Sams and Weiland, though there is more chance for turbulence

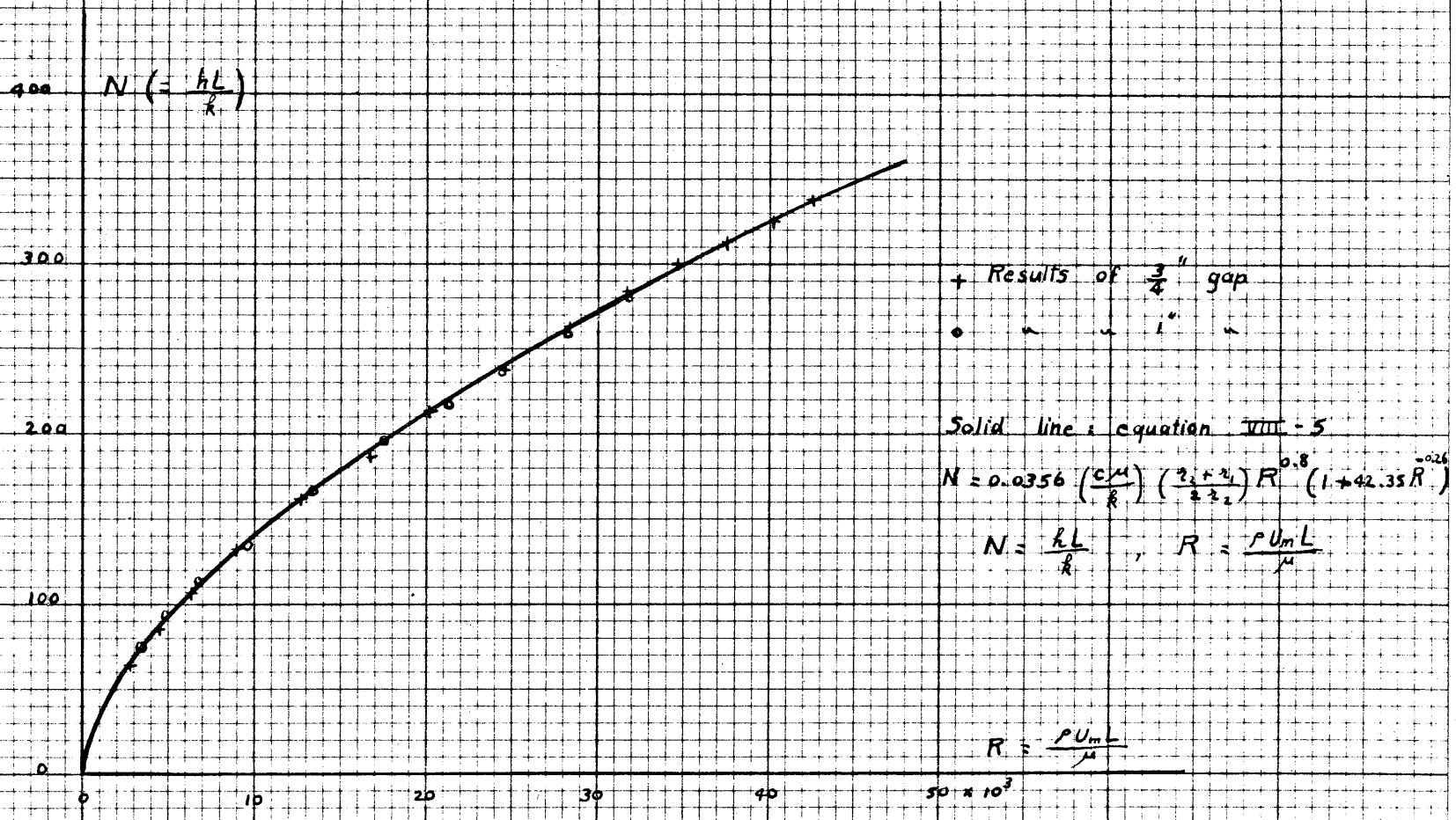

Fig. 57 : EXPERIMENTAL RESULTS COMPARED WITH EQUATION (VIII - 5)

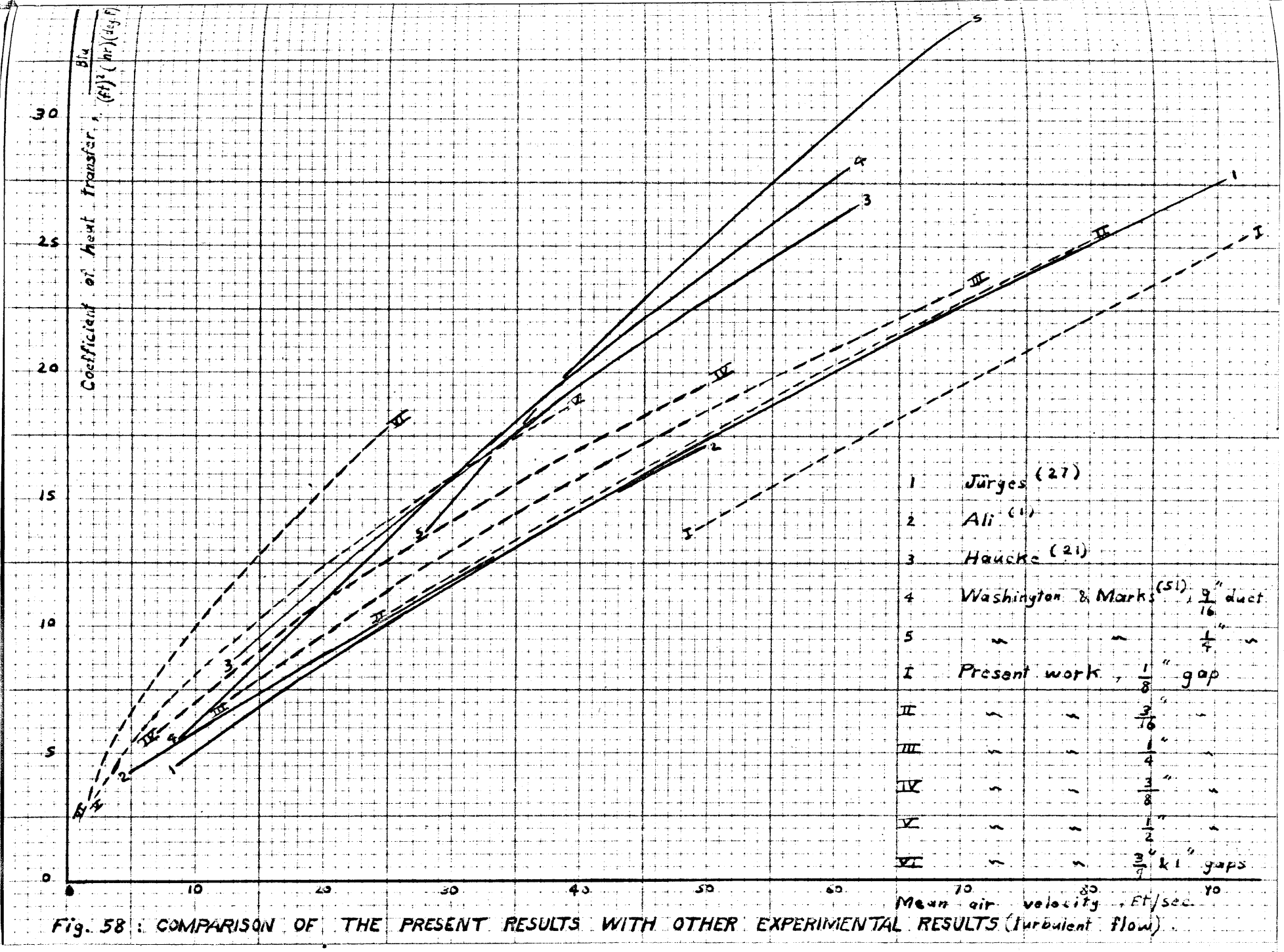

Fig. 58 : COMPARISON OF THE PRESENT RESULTS WITH OTHER EXPERIMENTAL RESULTS (Turbulent flow).

in the present work. This, again, gives support to the theoretical result reached in Chapter III, which shows that the heat transfer in radial outward flow is lower than that in uniform parallel flow, other conditions being the same.

4. Steepness of the curves.

It is well noticed in the present results that the exponent of the ($Nu - R_e$) curves varies from one gap to another, being greater as the gap decreases. This variation is in agreement with the conclusions drawn by Leveque[31] and explained in Chapter I.

In his search for similar cases the writer found similar results in the work of some other investigators. Ser (see Leveque[31], page 208) studied heat convection to air at the inside of circular tubes of small diameters. He reached the general equation ($h \propto U^n$). The value of (n) ranged between 0.5 and 1, being smaller for larger diameters.

Also, Washington and Marks[51] noticed an increasing steepness of their results with the decrease of the gap. They stated that the variation was only below $\frac{\rho UD}{\mu} = 13{,}000$ (where D = equivalent diameter of the duct) and it was believed to be due to a dampening of the free convection currents as the walls are brought together. They stated also that for $(\frac{\rho UD}{\mu})$ above that value the turbulence was fully developed and all the results follow equation (II-14).

The results of Washington and Marks were shown in Figs. 5 and 6. It seems that their results after $\frac{\rho UD}{\mu} = 13{,}000$ are not

sufficient to show whether they follow the same equation or not for the different ducts.

In dealing with similar cases in pipes McAdams[32] stated that as $(\frac{\rho UD}{\mu})$ increases beyond 2100, the curve must rise rapidly in order to reach the line of the turbulent flow. In this semi-turbulent range the exponent n (in $h = K.U^n$) can exceed unity. However, when $(\frac{\rho UD}{\mu})$ becomes sufficiently large (about 10,000), n becomes 0.8.

It is interesting to compare this with the results of Green and King[20] who investigated the heat transfer in tubes of originally 0.23" inside diameter, which were flattened to about half this size. The length of both circular and flattened tubes was 12 inches. Taking the equivalent diameter as the characteristic length, they found that the transition region for such tubes extended only from $(\frac{\rho UD}{\mu}) = 2000$ to 3500, whereas the upper limit for cylindric tubes was about 8000.

It is also interesting to give here the results of El-Sayed[13], who worked on flow in annuli. He went to a conclusion that the effect of reducing the length in the direction of the flow and the gap between solid parallel boundaries on the turbulent velocity profiles, is to give the profiles transitional shapes between the laminar and turbulent distributions.

In the present case, in some of the $Nu-R_e$ curves (shown in Fig.59 on logarithmic scale) there was a clear transition between two clearly different behaviours. These two behaviours were considered laminar and turbulent. The points in the considered

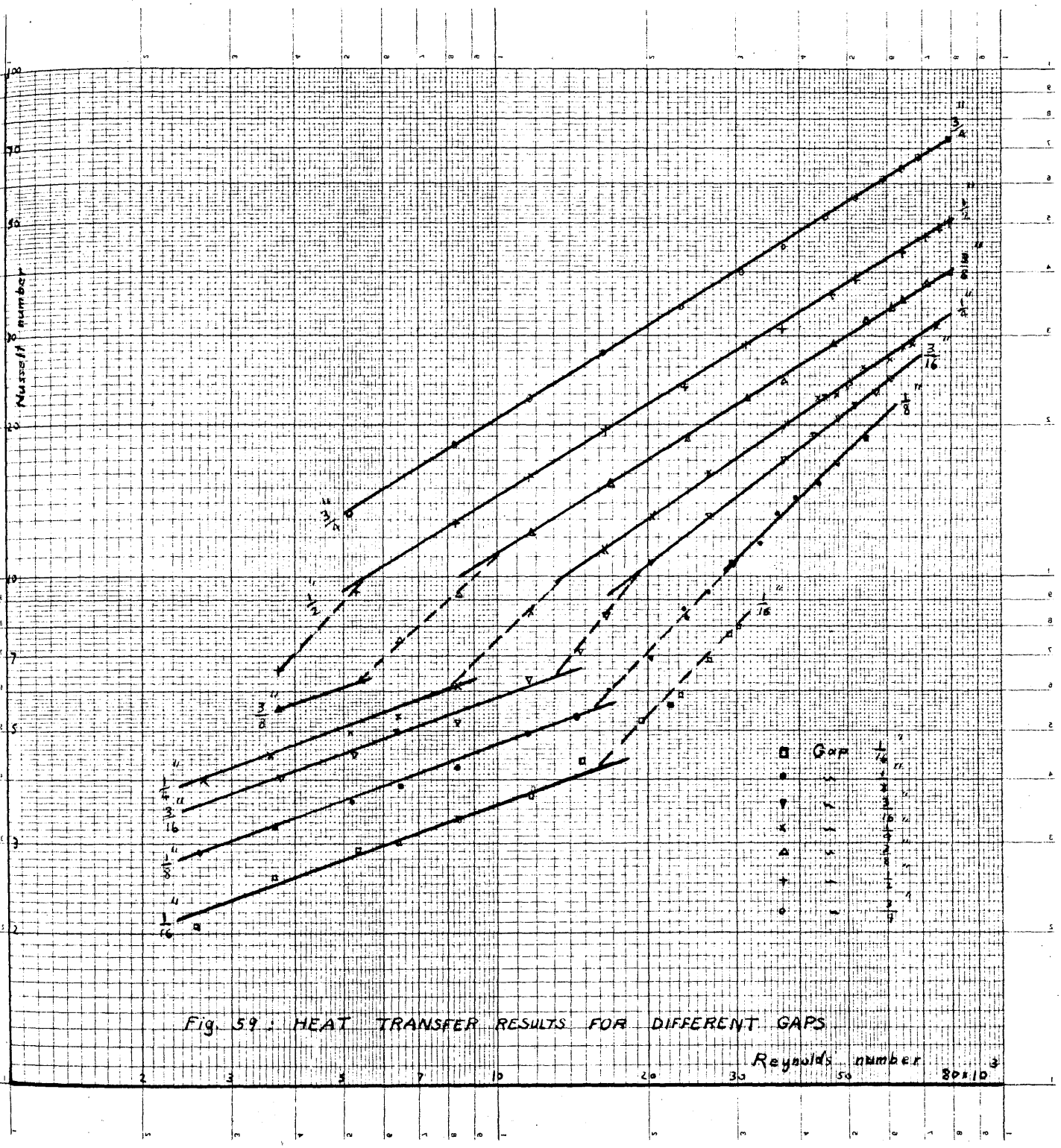

Fig. 59 : HEAT TRANSFER RESULTS FOR DIFFERENT GAPS

turbulent range can better form straight lines than curves. The range of R_e is long enough for a judgement ot be given. It is also noticed that the results, with exception of the smallest two gaps, are rather consistent.

As the length of the present heating surface (difference between radii) is small the discussion given in Chapter III may be introduced here. In the inlet length the boundary layer at each wall is still growing and the central part is being accelerated. As shown by Deissler[8] and confirmed by the present velocity distribution measurements, the growth of the boundary layer is slower for larger Reynolds numbers. This means that, for the same gap, the inlet length increases as Reynolds number increases. When the gap between the plates is sufficiently large all the heating surface lies in the entrance region. Therefore, the ratio of inlet length to total length (= 1) will not be affected by the increase in Reynolds number. The increase in Nu with R_e will be slower than for the fully developed turbulent part. This explains the constant exponent in the largest three gaps. However, when the gap decreases the ratio of inlet length to total length becomes smaller than one. This ratio increases as Reynolds number increases, and accordingly the increase in Nusselt number will be faster than for large gaps.

To sum up two results are pointed out :

1. When the gap is large the increase in heat transfer with Reynolds number is slower than the increase in the fully developed case as there is no increase in the inlet length.
2. When the gap is small an increase in Reynolds number causes an increase in the inlet length thus giving rise to heat transfer at a higher rate than with large gaps.

CHAPTER IX.

FLOW AND HEAT TRANSFER DUE TO ROTATING DISCS.

Since the heat transfer is much related to the flow conditions of the fluid near the disc, previous investigations dealing with this part of the problem will be first summarized. These will be followed by a short account of work# dealing with the actual heat transfer.

A - THE FLOW DUE TO ROTATING DISCS.

The s teady motion of an incompressible viscous fluid, due to an infinite rotating plane lamina, was first considered by von Karman[28]. If r, θ, z are cylindrical polar coordinates, the plane lamina is taken to be (z = 0); and it is rotating with constant angular velocity (ω) about the axis (r = 0). The motion of the fluid is considered on the side of the plane for which (z) is positive; the fluid is infinite in extent. If u, v, w are the components of the velocity of the fluid in the directions of r, θ, z increasing respectively, and P is the pressure then the equation of motion is

$$\left.\begin{aligned} u\frac{\partial u}{\partial r} + w\frac{\partial u}{\partial z} - \frac{v^2}{r} &= -\frac{1}{\rho}\frac{\partial P}{\partial r} + \nu\left[\frac{\partial^2 u}{\partial r^2} + \frac{\partial}{\partial r}\left(\frac{u}{r}\right) + \frac{\partial^2 u}{\partial z^2}\right] \\ u\frac{\partial v}{\partial r} + w\frac{\partial v}{\partial z} + \frac{vu}{r} &= \nu\left[\frac{\partial^2 v}{\partial r^2} + \frac{\partial}{\partial r}\left(\frac{v}{r}\right) + \frac{\partial^2 v}{\partial z^2}\right] \\ u\frac{\partial w}{\partial r} + w\frac{\partial w}{\partial z} &= -\frac{1}{\rho}\frac{\partial P}{\partial z} + \nu\left[\frac{\partial^2 w}{\partial r^2} + \frac{1}{r}\frac{\partial w}{\partial r} + \frac{\partial^2 w}{\partial z^2}\right] \end{aligned}\right\} \quad \text{IX-1}$$

(ρ and ν have the usual meanings)

The equation of continuity is

$$\frac{\partial u}{\partial r} + \frac{u}{r} + \frac{\partial w}{\partial z} = 0 \qquad \text{IX-2}$$

To satisfy these equations von Karman takes

$$u = r.\, f(z)\ ,\quad v = r.g(z)\ ,\quad w = h(z)\ ,\quad P = P(z) \qquad \text{IX-3}$$

thus yielding for the three funations f, g and h the differantial equations

$$\left.\begin{aligned} f^2 - g^2 + h\frac{df}{dz} &= \nu\frac{d^2f}{dz^2} \\ 2fg + h\frac{dg}{dz} &= \nu\frac{d^2g}{dz^2} \\ h\frac{dh}{dz} &= -\frac{1}{\rho}\frac{dP}{dz} + \nu\frac{d^2h}{dz^2} \\ \frac{dh}{dz} + 2f &= 0 \end{aligned}\right\} \qquad \text{IX-4}$$

and the boundary conditions are

$$\left.\begin{aligned} f(o) &= 0\ ,\quad f(\infty) = 0 \\ g(o) &= w\ ,\quad g(\infty) = 0 \\ h(o) &= 0 \end{aligned}\right\} \qquad \text{IX-5}$$

For non-dimensionsal representation, von Karman puts

$$\zeta = z.\left(\frac{w}{\nu}\right)^{\frac{1}{2}} \qquad \text{IX-6}$$

and the new functions

$$F = \frac{f}{w}\ ,\quad G = \frac{g}{w}\ ,\quad H = h\left(\frac{1}{\nu w}\right)^{0.5} \qquad \text{IX-7}$$

Then equations (IX-4) become

$$\left.\begin{aligned} F^2 - G^2 + HF' &= F'' \\ 2FG + HG' &= G'' \\ 2F + H' &= 0 \end{aligned}\right\} \qquad \text{IX-8}$$

(where the primes denote differentiation with respect to ζ)

and the boundary conditions become

$$\left.\begin{aligned} F(0) &= 0\ ,\quad F(\infty) = 0 \\ G(0) &= 1\ ,\quad G(\infty) = 0 \\ H(0) &= 0 \end{aligned}\right\} \qquad \text{IX-9}$$

$H(\infty)$ must tend to a finite negative limit, say $(-K)$, as (ζ) tends to infinity. Next to the wall the fluid is continuously carried to the outside, to be replaced by axial flow.

The integration of equations (IX-8), with $F'(\infty) = G'(\infty) = 0$

leads to

$$\left.\begin{aligned} -F'(0) &= \int_0^\infty (3F^2 - G^2)\, d\zeta \\ -G'(0) &= 4\int_0^\infty FG\, d\zeta \end{aligned}\right\} \qquad \text{IX-10}$$

Von Karman now assumes that F and G fall off sufficiently rapidly so that a good approximation can be found by replacing the upper limit in the integrals by some finite value (ζ_0) of (ζ), or rather by supposing (F) and (G) zero for values of (ζ) greater than (ζ_0). We must then have

$$\begin{aligned} F(\zeta_0) &= 0 \quad , \quad F'(\zeta_0) = 0 \\ G(\zeta_0) &= 0 \qquad\quad G'(\zeta_0) = 0 \end{aligned} \qquad \text{IX-11}$$

By putting $\zeta = 0$ in equation (IX-8) we obtain the conditions

$$F''(0) = -1 \quad \text{and} \quad G''(0) = 0 \qquad \text{IX-12}$$

Further boundary conditions, obtained by differentiating equations (IX-8) before putting $\zeta = 0$ are ignored, and so are the conditions that the second and higher derivatives of (F) and (G) must vanish at $\zeta = \zeta_0$. Then if $F'(0) = a$, expressions satisfying (IX-9), (IX-11) and (IX-12) are

$$\left.\begin{aligned} F &= (1 - \frac{\zeta}{\zeta_0})^2 \cdot \left[a\zeta + (\frac{2a}{\zeta_0} - \tfrac{1}{2})\zeta^2\right] \\ G &= (1 - \frac{\zeta}{\zeta_0})^2 \cdot (1 + \frac{\zeta}{2\zeta_0}) \end{aligned}\right\} \qquad \text{IX-13}$$

These expressions are then substituted in equation (IX-10) with the upper limits in the integrals replaced by ζ_0. Thus we get a pair of simultaneous equations for (a) and (ζ_0), which are solved to give the approximate solution.

The values given by von Karman are

$$a = 0.4 \quad \text{and} \quad \zeta_0 = 2.58 \qquad \text{IX-14}$$

and therefore the thickness of the boundary layer is

$$\delta = 2.58\,(\frac{\nu}{w})^{0.5} \qquad \text{IX-15}$$

Later, Cochran[6] considered the same problem and obtained an exact solution. The boundary conditions he satisfied were

$$\begin{aligned} F(0) &= 0 \ , \quad G(0) = 1 \ , \quad H(0) = 0 \\ F(\infty) &= 0 \ , \quad G(\infty) = 0 \ , \quad H(\infty) = -K \\ F'(0) &= a \ , \quad G'(0) = b \end{aligned} \qquad \text{IX-16}$$

To satisfy equations (IX-8) and the conditions at infinity he put

$$\left.\begin{aligned} F &= Ae^{-c\zeta} - \frac{(A^2+B^2)}{2c^2} e^{-2c\zeta} + \frac{A(A^2+B^2)}{4c^4} e^{-3c\zeta} - \frac{(A^2+B^2)}{144\,c^6}(17A^2+B^2) e^{-4c\zeta} + \cdots \\ G &= Be^{-c\zeta} - \frac{B(A^2+B^2)}{12c^4} e^{-3c\zeta} + \frac{AB(A^2+B^2)}{18\,c^6} e^{-4c\zeta} + \cdots \\ H &= -c + \frac{2A}{c} e^{-c\zeta} - \frac{(A^2+B^2)}{2\,c^3} e^{-2c\zeta} + \frac{A(A^2+B^2)}{6\,c^5} e^{-3c\zeta} - \\ &\qquad - \frac{(A^2+B^2)(17A^2+B^2)}{288\,c^7} e^{-4c\zeta} + \cdots \end{aligned}\right\} \qquad \text{IX-17}$$

To satisfy equations (IX-8) and the conditions at the origin we have

$$\left.\begin{aligned} F &= a\zeta - \tfrac{1}{2}\zeta^2 - \tfrac{1}{3}b\zeta^3 - \frac{1}{12}b^2\zeta^4 - \frac{1}{60}a\zeta^5 + \left(\frac{1}{360} - \frac{ab}{90}\right)\zeta^6 + \cdots \\ G &= 1 + b\zeta + \tfrac{1}{3}a\zeta^3 + \frac{1}{12}(ab-1)\zeta^4 - \frac{1}{15}b\zeta^5 - \left(\frac{a^2}{90} + \frac{b^2}{45}\right)\zeta^6 + \cdots \\ H &= -\left[a\zeta^2 - \tfrac{1}{3}\zeta^3 - \frac{1}{6}b\zeta^4 - \frac{1}{30}b^2\zeta^5 - \frac{1}{180}a\zeta^6 + \cdots\right] \end{aligned}\right\} \qquad \text{IX-18}$$

where A, B, a, b and c are constants to be determined. These constants have to be chosen so that F, G, H, F' and G' are continuous; and it will follow from the differantial equations that all other derivatives are continuous. Cochran calculated the values of the constants, and his graphs for F, G and H are shown in Fig.60.

In 1951, Batchelor[4] generalized von Karman's solutions and obtained differential equations which may be used to determine the flow hear a rotating disc when the fluid at infinity is rotating

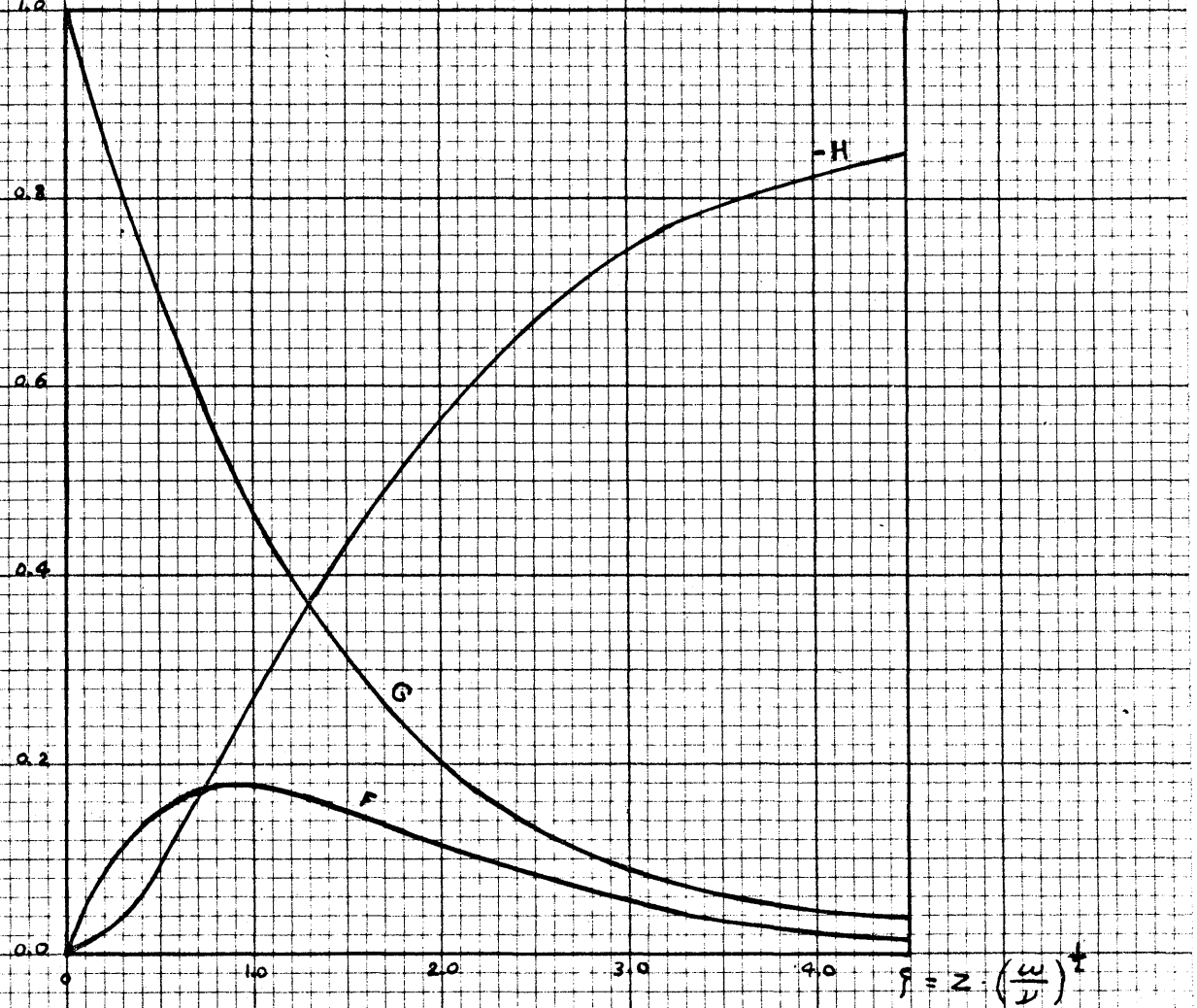

Fig. 60 : COCHRAN'S SOLUTION FOR F, G & H,
(equations IX-17 & IX-18)

about the same axis. He considered also the flow between two coaxial rotating discs. He does not obtain any explicit solutions but, using physical arguments and general properties of the ordinary differential equations, he predicts the general nature of the flow. The chief characteristic of the predicted flow is that in almost all cases the main body of the fluid is also rotating, and transition from one rate of rotation to another takes place in a narrow layer.

In the two-parameter family Batchelor predicts that when one of the discs is stationary there will be a radial inward velocity near that disc, and outwards near the rotating one, which acts in this case as a centrifugal fan.

Stewartson[49] studied the steady motion of a viscous fluid confined between two coaxial discs. His apparatus consisted of two smooth cardboard discs, each of diameter 6 inches, mounted on lathe chucks. One of the discs was attached to the motor of the lathe, and the other to the carriage on which was fixed a small electric motor. Angular velocities given to each disc in either sense were up to about 250 radians per second, and the distance between the discs varied from zero up to about 5 inches. A light smooth propeller and a piece of cotton-wool attached to a thread were used to examine the motion of the fluid between the discs. The apparatus was designed to give only qualitative information.

Stewartson found that when one disc was at rest the main body of the fluid had no angular velocity, with the exception of a thin layer near the rotating disc. Yet he stated that it had been noticed that, while no force was exerted on the disc at rest, as

soon as it was given a slight angular velocity in the same sense as the rotating disc, it and the main body of the fluid rapidly took up a considerable angular velocity.

In the theoretical discussion, Stewartson considered 3 cases

1. The two discs rotate in the same direction,
2. The two discs rotate in opposite directions,
3. One of the discs is at rest.

For the third case the author stated that the main body of the fluid is also at rest. He did not prove this, but it was in agreement with his experiments. His exact solution for the case when the two discs rotate in the same direction breaks down when the slower disc stops. However, an approximate solution leads to the formula

$$\frac{w}{w_2} = 0.425 \left(\frac{w_1}{w_2}\right)^{\frac{1}{3}} \qquad \text{IX-19}$$

where w = angular velocity of the main fluid
w_1 = angular velocity of the slower disc
w_2 = angular velocity of the faster disc.

When $w_1 = 0$ and $\frac{w_2 b^2}{\nu}$ (where b = gap between the discs) is very small, Stewartson gives another approximate expression for the tangential velocity of the fluid; that is,

$$G = \frac{w_2 y}{b} \qquad \text{IX-20}$$

where y = distance from the stationary disc.

When $\frac{w_2 b^2}{\nu}$ increases the changes in the tangential velocity tend to occur near the rotating disc. This is more appreciable when $\frac{w_2 b^2}{\nu}$ exceeds 10.

B - HEAT TRANSFER FROM ROTATING DISCS.

As far as the knowledge of the writer is, there is neither theoretical nor experimental work in the case of heat transfer between a stationary disc and a fluid possessing a motion composed of radial and tangential components. However, very little work has been done only recently for the case of heat transfer from rotating discs to air. The following is a summary of such work.

Wagner[50] extended von Karman's approximate solution for the laminar case to develop an expression for the surface coefficient of heat transfer by convection from a heated rotating plate. He first derived an expression for the temperature distribution. Then the average coefficient of heat transfer was obtained by considering the heat balance

heat lost from the surface = heat carried away radially in the boundary layer.

His approximate expression is

$$h = C.335\ k\ (\frac{w}{\nu})^{0.5} \qquad \text{IX-21}$$

These values hold true as long as the flow in the boundary layer is laminar. This corresponds to a value of $\frac{wr^2}{\nu}$ up to 40,000 (where r = radius of disc, w = angular speed). The coefficient of heat transfer is independent of the radius.

Another solution for the laminar case has been published by Millsaps and Pohlhausen[33]. They used Cochran's results for the Navier-Stokes equations to solve the energy equation for viscous flow by numerical integration. Their solution gives the coefficient of heat transfer as a function of the radius, the distance from

the disc and the Prandtl number. The variation with the radius is very small.

Oudant[37] used Cochran's values for the velocity profiles and expressed the temperature distribution as the sum of two polynomials. The radial variation for the temperature profile was very small and practically unimportant. His expression for the heat transfer coefficient reduces to

$$h = 0.267\, k\left(\frac{w}{\nu}\right)^{0.5} \frac{\mu_o}{\mu_\infty} \qquad \text{IX-22}$$

(for Pr = 0.733)

where μ_o = viscosity of the air at the surface temperature

μ_∞ = viscosity at the ambient air temperature.

Some experimental work has been carried out by Young[52]. He used a polished aluminium disc 12" diameter and facing upwards His experiments were made in conditions up to $\frac{w\, r^2}{\nu}$ of about 80,000 (where r = radius of the disc). He observed that for $\frac{w\, r^2}{\nu}$ less than 40,000 both natural convection and forced convection were of importance, while at $\frac{w\, r^2}{\nu}$ above 40,000 forced convection alone was of prime importance. In this part the data were represented by the equation

$$h = 0.35\, N^{0.38} \quad \text{Btu/ft}^2\text{.hr.}^\circ\text{F} \qquad \text{IX-23}$$

where N = disc speed, r.p.m.

Another kind of work has been carried out by Aktiebolaget Motala Verkstad[34] of Sweden. They worked on heat transfer to and from gases flowing between two parallel rotating discs. The idea was to utilize the properties of the rapidly rotating disc to give a high coefficient of heat transfer due to the great difference of speed between the disc and the gas and to achieve

a certain fan action. The discs had inner and outer radii 11.94" and 35.83", The distance between the discs was 0.59". The initial motion of the gas (at the inner radius) was in the radial direction.

In Fig.61 the coefficient of heat transfer was plotted against the mean radial component of the velocity of the air flowing between the discs when the speed of rotation was 480 r.p.m.

C - HEAT TRANSFER FROM A STATIONARY DISC TO A FLUID IN COMBINED RADIAL AND TANGENTIAL MOTIONS.

This is the case when the fluid particles move in planes parallel to the heating surface with the velocity of each particle composed to two components :

1. Radial component, caused by fluid flow from the centre outwards.
2. Tangential component, caused by an external stirring force.

In the experimental work of this part the heating surface is stationary. The radial flow of air will be maintained by discharge from the air blower. The tangential component of the air velocity is produced by a rotating disc parallel to the heating surface and mounted on the same axis. The surface friction only would be relied upon to give the tangential component. The radial component due to the rotation of the disc would be neglected. Thus the average radial component at any point depends on

1. The amount of air discharged by the blower.
2. The gap between the heating surface and the rotating disc
3. The radius at which the considered point lies.

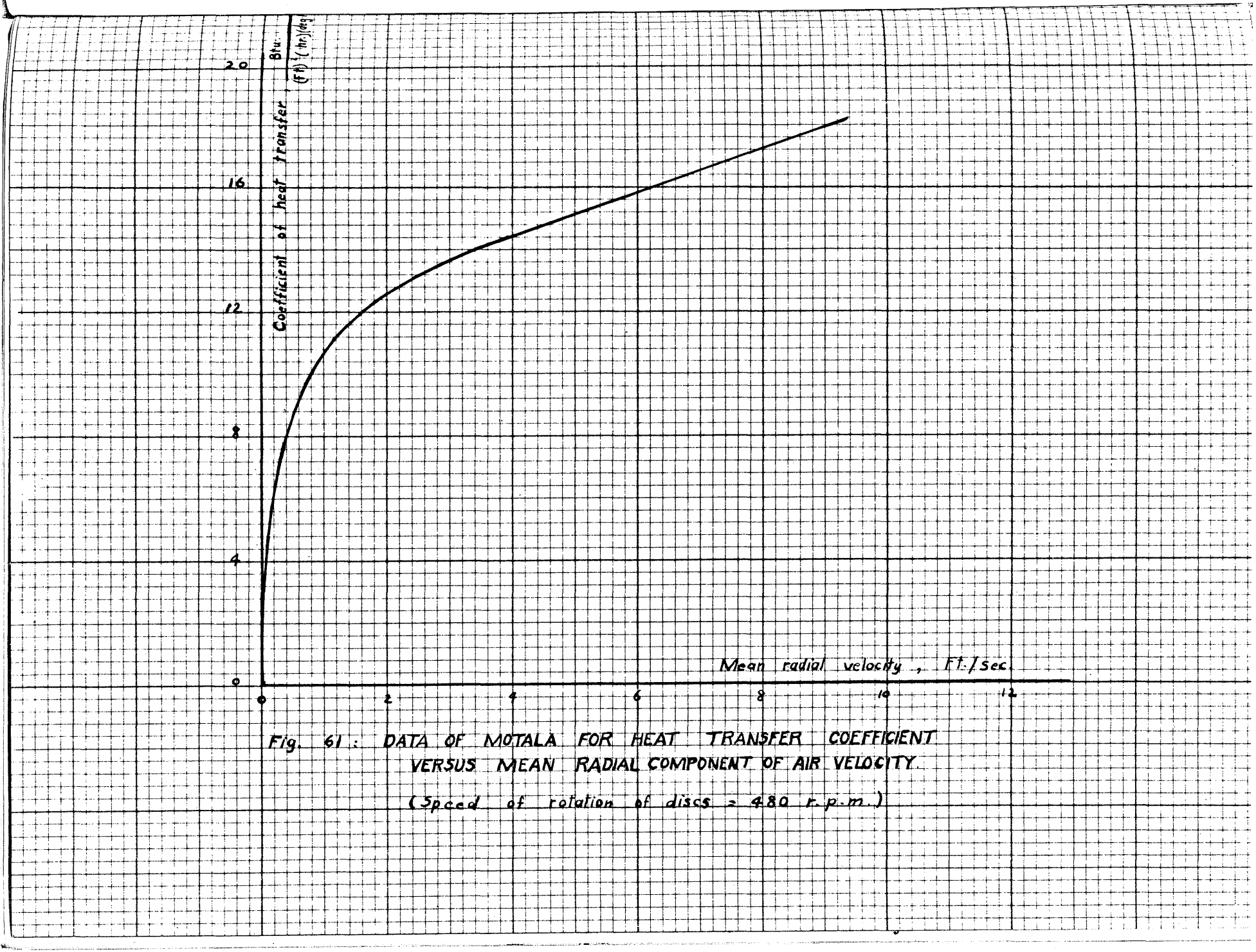

Fig. 61 : DATA OF MOTALA FOR HEAT TRANSFER COEFFICIENT VERSUS MEAN RADIAL COMPONENT OF AIR VELOCITY.

(Speed of rotation of discs = 480 r.p.m.)

The tangential component of velocity depends on

1. The speed of rotation of the disc.
2. The distance away from the rotating disc.
3. The radius at which the considered point lies.

The effect of this motion on heat transfer comes from the fact that the path of the air particles will be longer than the difference between the radii of the heating surface. This longer path, being covered in the same interval of time, means greater mean velocity and, consequently, higher coefficient of heat transfer.

The following is the mathematical derivation of the equation of the path of fluid particles. It is assumed that the motion starts at radius (r_1) without tangential component. If the co-ordinates at any point are r,θ (Fig.62) then the radial component of velocity at any radius is given by

$$u = \frac{dr}{dt} = \frac{K}{r}$$

where K = constant ($= U_1 r_1$)

t = time

$$\therefore \frac{r^2}{2} = Kt + K_1$$

At $t = 0$, $r = r_1$ $\quad\therefore K_1 = \frac{r_1^2}{2}$

$$\therefore r^2 = 2Kt + r_1^2 \qquad \text{IX-24}$$

The tangential component (v) is given by

$$v = r\frac{d\theta}{dt} = \lambda r$$

where λ = constant, dependent upon the disc speed and the distance away from the rotating disc.

$$\therefore \theta = \lambda t + K_2$$

At $t = 0$, $\theta = 0$, $\quad\therefore K_2 = 0$

$$\therefore \theta = \lambda t \qquad \text{IX-25}$$

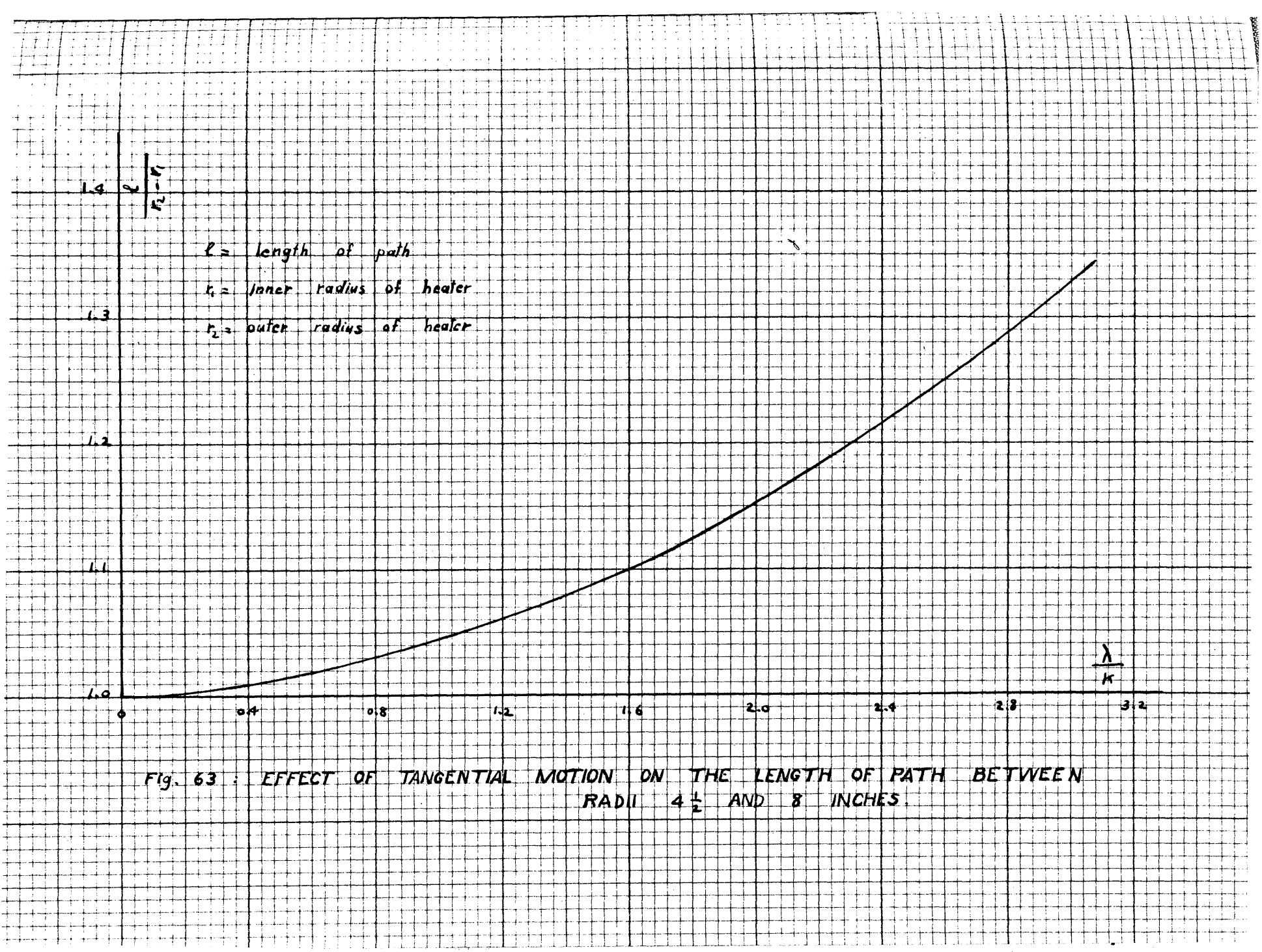

Fig. 63 : EFFECT OF TANGENTIAL MOTION ON THE LENGTH OF PATH BETWEEN RADII $4\frac{1}{2}$ AND 8 INCHES.

As shown before, the increase in the mean velocity is followed by an increase in heat transfer given by the equation

$$\frac{h}{h_o} = \left(\frac{U_{ml}}{U_m}\right)^n = \left(\frac{1}{r_2 - r_1}\right)^n \qquad \text{IX-30}$$

where h = coefficient of heat transfer when the disc is rotating with velocity N

h_o = coefficient of heat transfer when N = 0

The constant (n) in equation (IX-30) will be determined experimentally later.

CHAPTER X.

THE ROTATING DISC

A - CONSTRUCTION OF THE ROTATING ELEMENT.

As shown in Fig.64 the rotating element consists of the following main parts.

1. Rotating discs.
2. Base.
3. Belt drive.
4. Slip-rings and brushes.

The base block on which the rotating element was carried is a casting with two bearing supports five inches apart. The casting was fixed rigidly with five bolts to two steel angles of length 9 inches and cross-section 6 x 6 x $\frac{1}{2}$ inches. The angles were fixed rigidly onto the bench to prevent any movement of the base block.

The shaft was a mild steel tube of length 16 inches, and outside & inside diameters 15/16 and 9/16 inch respectively. One end of the shaft was rigidly fixed into the flange and the rotating discs (Fig.65), while from the other end came the thermocouples' rotating air junctions as will be explained later.

The shaft was fitted in the two bearing supports of the base block. Smooth running was ensured by fitting two phosphor bronze sleeves into the bearing supports. Holes and grooves for lubrication were made in the base and sleeves. Axial movement of the shaft relative to the baseblock was prevented by using two steel rings at the two sides of one of the bearings. The rings were fixed on the shaft by grub screws.

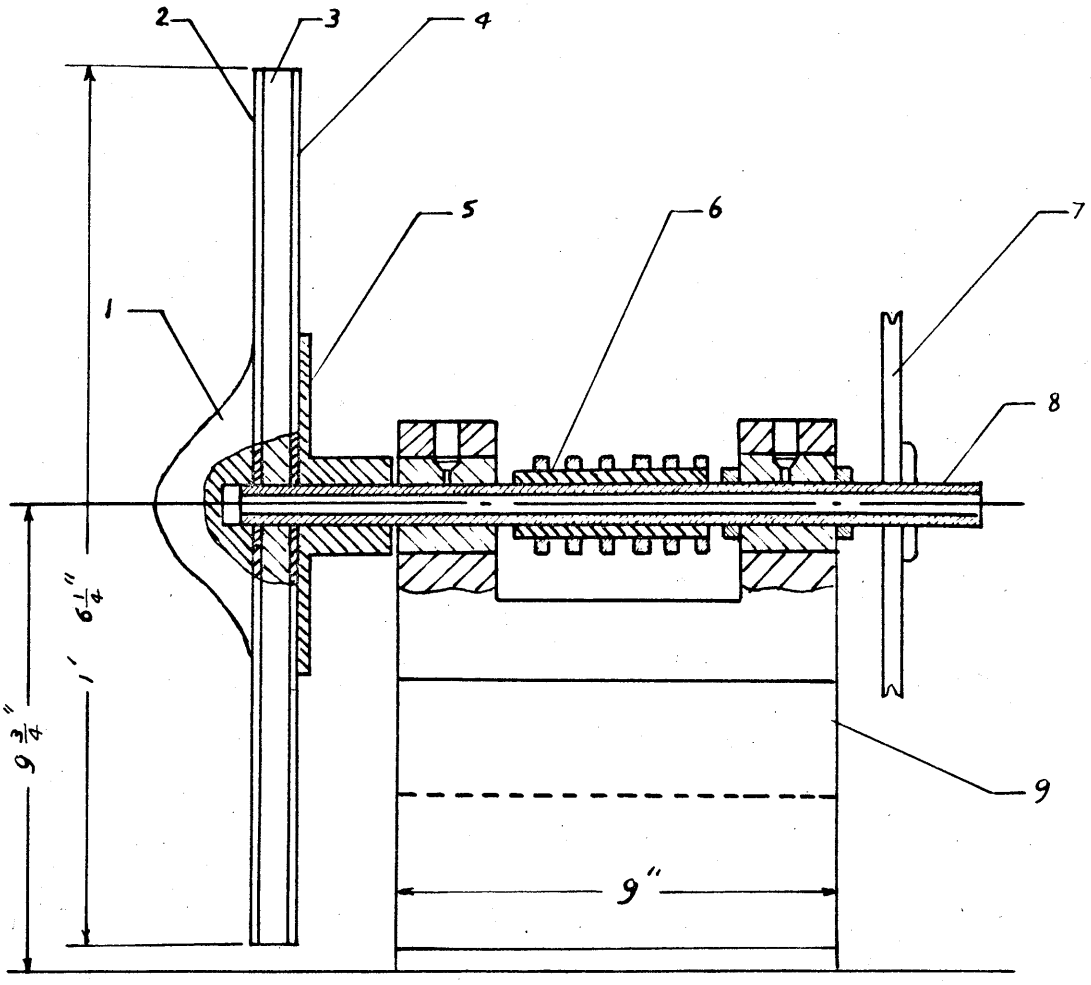

1- inlet cone
2- brass disc (A)
3- asbestos disc
4- brass disc (B)
5- flange
6- slip rings and insulation
7- pulley
8- shaft
9- base block

Fig. 64: ASSEMBLY OF THE ROTATING ELEMENT.

SCALE 1 : 4

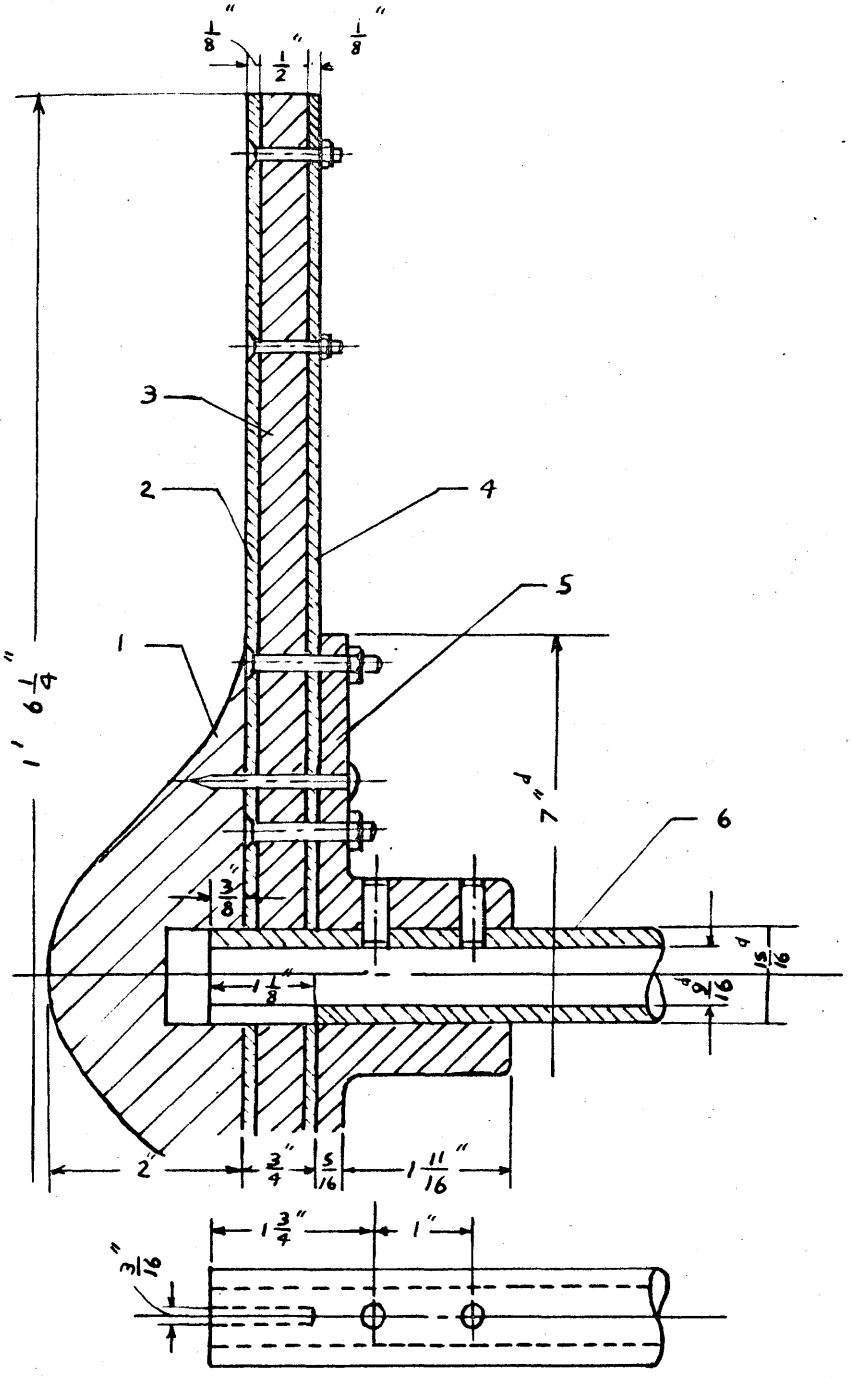

1 - inlel cone

2 - brass disc (A)

3 - asbestos disc

4 - brass disc b

5 - flange

6 - shaft

SCALE 1 : 2

FIG. 65 : FIXED END OF THE SHAFT.

Fixed on the shaft between the two bearings were the slip rings and their insulation. Six $\frac{1}{8}$" holes were drilled in the shaft and insulation for the thermocouple wires. Details of these will be given later.

Near the free end of the shaft an 8" pulley was placed. The pulley could be moved from one place to another along the shaft; but it could be fixed at any required position by means of a grub screw.

A direct current motor was fixed on the floor below the bench. A 3-inch V-pulley was placed on the shaft of the motor. It could be fixed at any required position along the shaft. A link brammer belt was used to transmit the power from the motor to the rotating element. A slot of 12 x 1.5 inches was cut from the bench top to allow for the motion of the belt.

Rotating Discs.

The brass disc (A) was $18\frac{1}{4}$ inches diameter and $\frac{1}{8}$" thickness. It formed one side of the working section. A hole 15/16 inches was drilled at the centre. Three thermocouples were fixed into the brass disc (A) in the same way as those described in Chapter IV, but this time with the grooves going towards the centre instead of towards the circumference. The thermocouples' hot junctions were placed at radii $4\frac{1}{4}$, $6\frac{1}{4}$, and $8\frac{1}{4}$ inches. The six wires were gathered in one groove and then led to the inside of the shaft through a slot at its end.

The brass disc (B) had the same overall dimensions as (A).

The asbestos disc was $\frac{1}{2}$" thick. The steel flange had 7 inches diameter (in contact with the brass disc B), and 2 inches length (In contact with the shaft).

Six stiffeners were rigidly fixed to the brass disc (B). Each stiffener was a steel angle of cross-section $\frac{1}{2}$ x $\frac{1}{2}$ x $\frac{1}{8}$ inch, and length $5\frac{7}{16}$ inches. They were placed radially at six equal angles on the brass disc (B) between radii $3\frac{5}{8}$ and $9\frac{1}{16}$ inches. Each stiffener was fixed to the disc with three screws.

Nine holes of 0.185" diameter (2BA) were drilled in the flange and asbestos and brass discs to allow for nine countersunk screws and their nuts to hold them together. Twelve holes of 0.142" diameter (4BA) were drilled in the brass and asbestos discs to allow for twelve screws and nuts to fix them together. All the holes in the brass disc (B) were screwed, thus serving as lock nuts.

Three equidistant screwed holes of 0.142" diameter (4BA) were drilled in the brass and asbestos discs at $15\frac{7}{8}$ inches diam.. The screws were used to adjust the gap between the brass disc (A) and the heating surface.

The inlet cone in the rotating element was the same one used with the stationary unheated disc. It has been described in Fig 11

After the thermocouples had been fixed in position and the brass and asbestos discs, the flange and the inlet cone had been assembled together, all the assembly was carried on the lathe and the surface of the brass disc (A) skimmed, care being taken that the thermocouples' heads were safe. Later, and before the rotating element was placed over the bench, the skimmed surface

was given a matt black cover to assure black body absorption of heat.

This assembly and the shaft were fixed rigidly together by means of two $\frac{1}{4}$" diameter grub screws which passed into the boss of the flange and the shaft.

Fig.65 shows the fixed end of the shaft and the relative positions of the flange, discs and inlet cone. Fig.66 shows the positions of the holes and grooves in the brass disc (A).

Slip rings and insulation.

Six brass rings were used; all had $\frac{1}{4}$" thickness and $1\frac{7}{8}$ inches outer diameter. The inner diameters were 1.50, 1.51, 1.52, 1.53, 1.54 and 1.55 inches. As shown in Fig.67 a 0.110" diameter (6 BA) screwed hole was made in each ring. A layer of 0.004" silver plating was then given at the outer circumference of each ring.

The insulation sleeve between the rings and the shaft (Fig.67) was made of tufnol. It was fixed on the shaft by means of three 0.185" (2 BA) grub screws. The inner diameter of the insulation was the same as that of the shaft. The outer surface was formed of six different diameters so that the slip rings could be fixed by press fitting them over the sleeve. After the tufnol sleeve was fitted in position on the shaft, six $\frac{1}{8}$" diameter holes were drilled in the sleeve and shaft. Then the six slip rings were forced in position. Six 0.110" (6BA) screws were placed inside the holes in the slip rings, at the same angular position as the holes in the shaft and insulation sleeve.

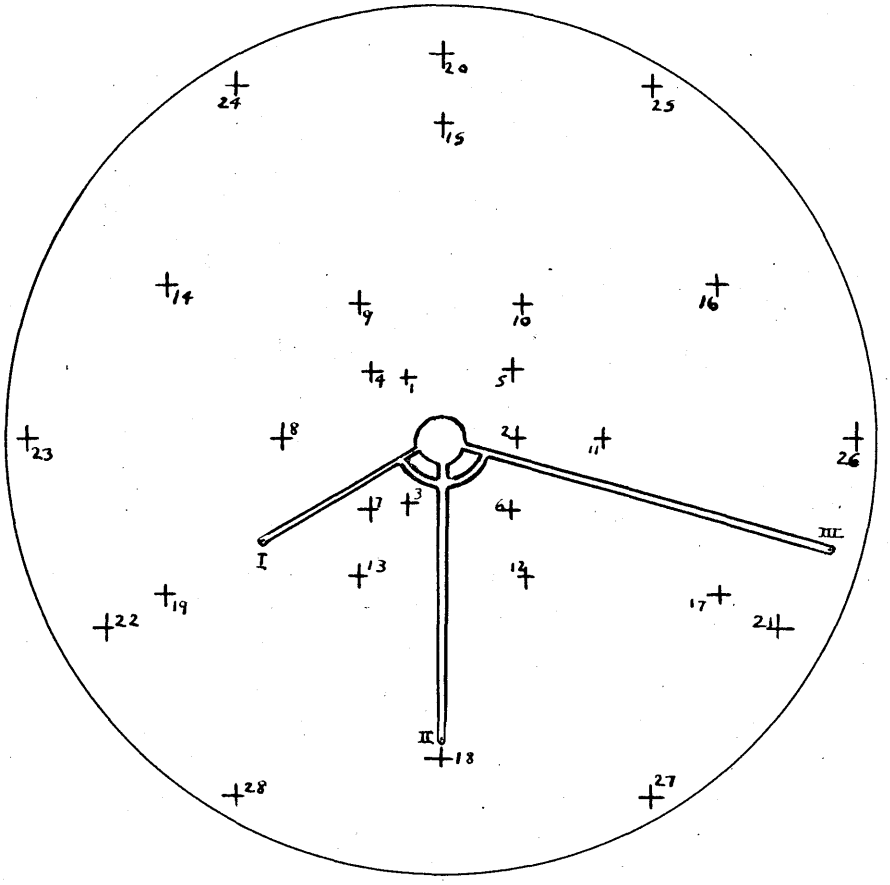

MARK	DESCRIPTION	RADIUS
I	FOR THERMOCOUPLE HEAD	$4\frac{1}{4}$ inches
II	"	$6\frac{1}{4}$ "
III	"	$8\frac{1}{4}$ "
1, 2, 3	HOLES 0.185" d	$1\frac{1}{2}$ "
4, 5, 6, 7	HOLES 0.185" d	2 "
8, 9, 10, 11, 12, 13	HOLES 0.185" d	$3\frac{1}{4}$ "
14, 15, 16, 17, 18, 19	HOLES 0.142" d	$6\frac{1}{2}$ "
20, 21, 22	SCREWED HOLES 0.142" d	$7\frac{15}{16}$ "
23, 24, 25, 26, 27, 28	HOLES 0.142" d	$8\frac{1}{2}$ "

FIG. 66 : BRASS DISC (A).

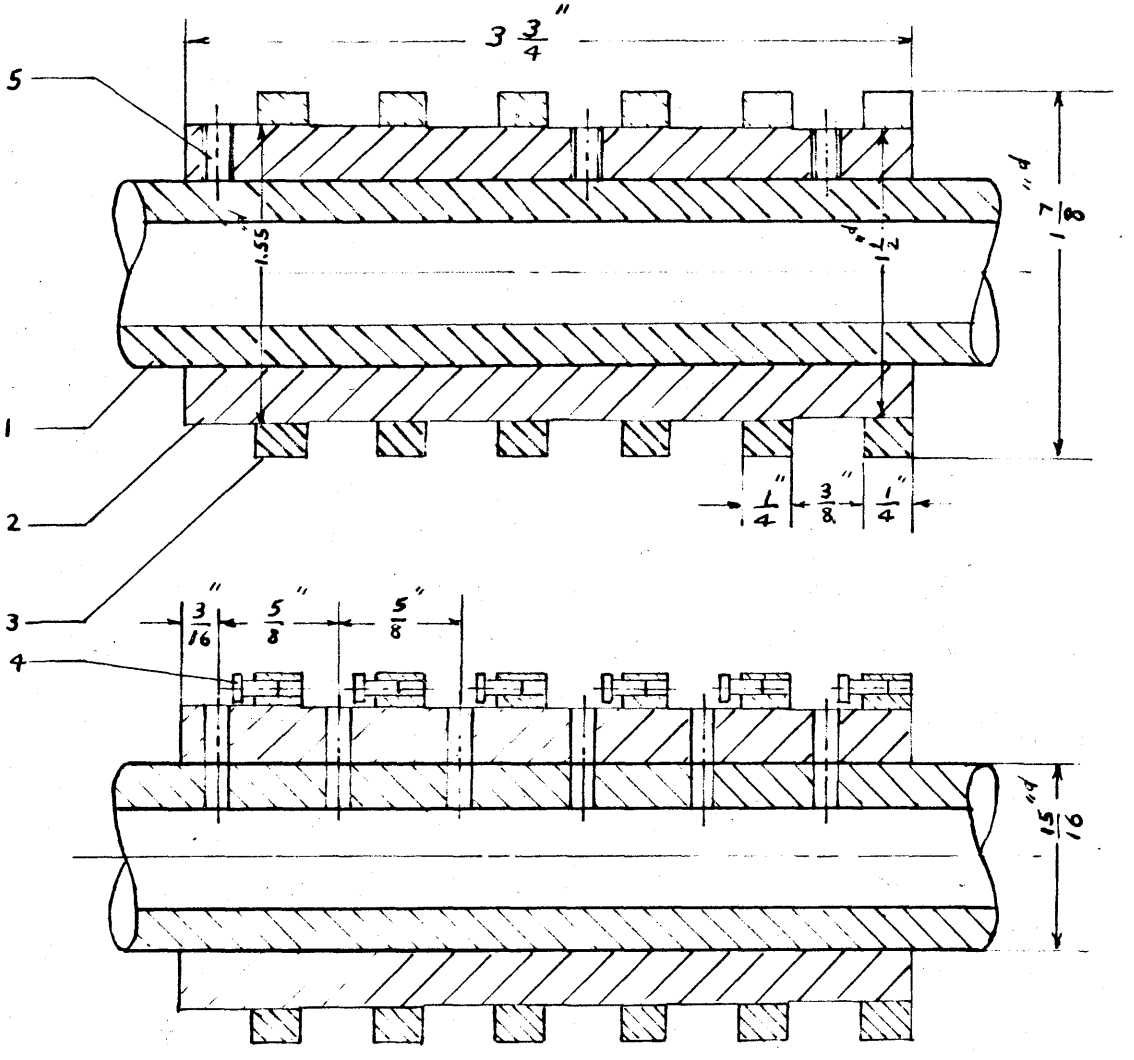

1 - SHAFT
2 - SLEEVE (tufnol)
3 - SLIP RING
4 - SCREW
5 - GRUB SCREW 3/16" Φ

FIG. 67 : SLIP RINGS AND INSULATION

The thermocouples wires were driven into the shaft, the constantan wires to the end of the shaft, while the copper ones came out through the first three holes in the shaft and insulation. Three other copper wires came from the free end of the shaft to the other three holes of the shaft and insulation. Then all the six copper ends were wound around the six screws and soldered in position.

The three couples of constantan and copper wires at the free end of the shaft formed the three rotating air junctions.

Brushes and brush holders:

The sliding contacts were composed of the slip rings and six copper-graphite brushes; each having dimensions $\frac{3}{4}$ x 3/16 x $\frac{1}{4}$ ". Each brush holder had the overall dimensions $1\frac{11}{16}$ x $\frac{1}{2}$ x 9/16 ". The six brush holders were fixed together by means of two $\frac{1}{8}$" rods into a frame. Tufnol insulation in the form of six small sleeves and seven $\frac{1}{8}$" plates was used to insulate the brush holders from each other and from the rods and the frame.

The frame was then fixed into the base block by means of four $\frac{1}{4}$" screws. The position of the brush holders relative to the base block is shown in Fig.68, which is a photograph of the assembly of the rotating element.

Thermocouple circuit:

The thermocouple circuit is shown in Fig.69. The copper end of each couple was soldered indirectly to one of the slip rings, while the constantan end passed through a plug at the end of the

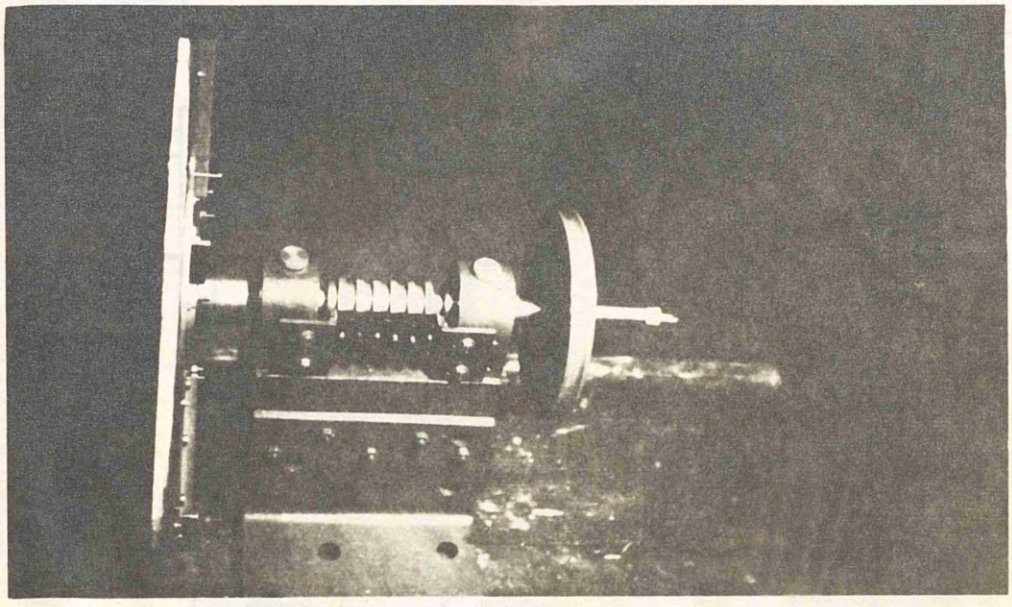

Fig. 68 : PHOTOGRAPH OF THE ROTATING ELEMENT.

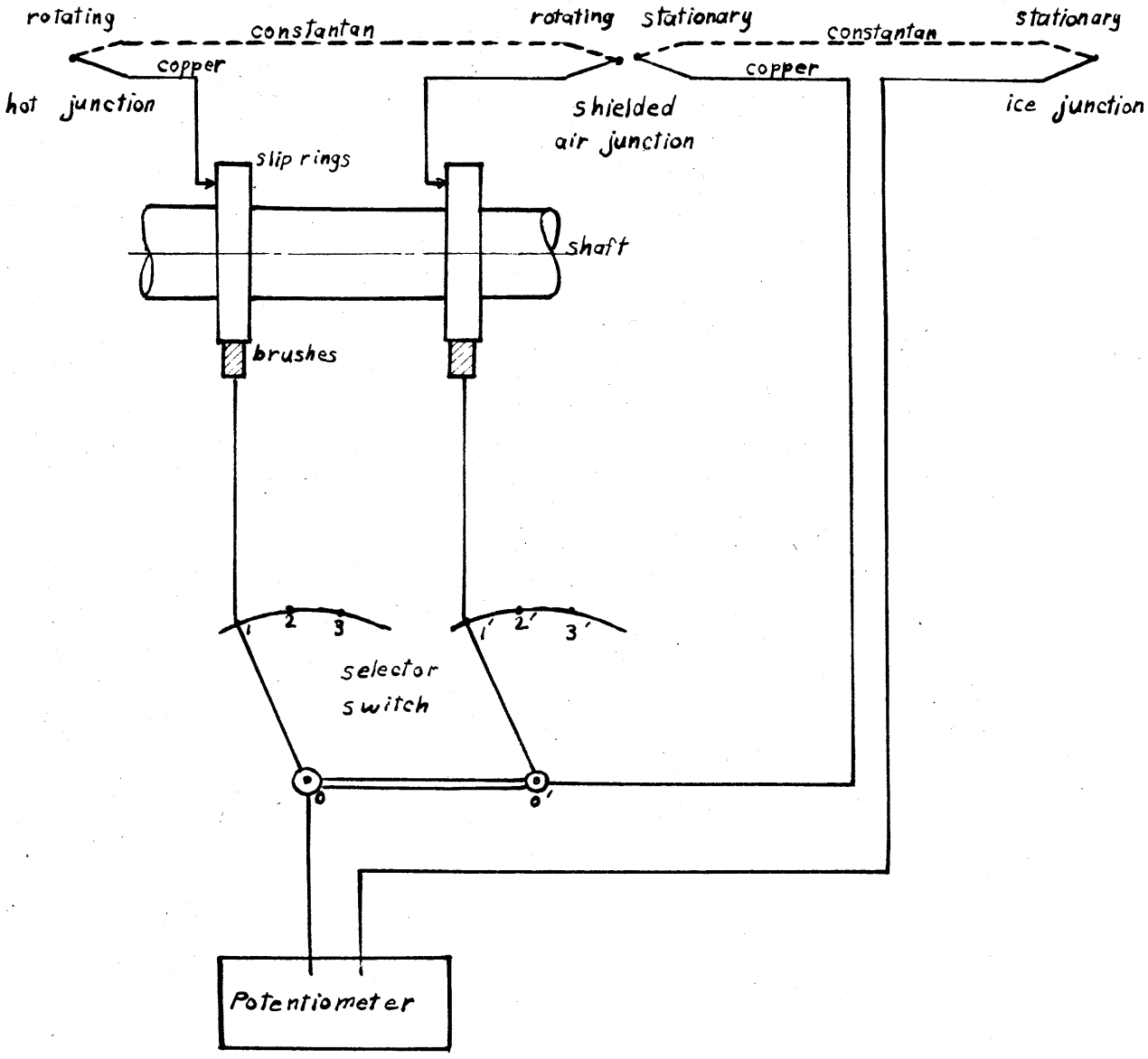

Fig. 69 : DIAGRAM OF THERMOCOUPLE CIRCUIT.

steel shaft and was welded to a copper lead making a rotating air junction. The copper lead of the air junction was then brought back into the shaft and soldered indirectly to a slip ring. From this slip ring a copper lead was run from the brush to one point of the selector switch, while the common point of the switch was connected to a stationary air junction fixed adjacent to the rotating air junction. From the first slip ring ran a copper lead to a selector switch whose common point was connected to the potentiometer. The second terminal of the potentiometer was connected to a thermos ice junction. Between the stationary air junction and the thermos ice junction ran a constantan lead.

Therefore, for the three rotating hot junctions there were three rotating air junctions, one stationary common air junction and one common ice junction. The four air junctions were enclosed together inside a shield.

To check the circuit and the contacts some readings of the electromotive force were taken when no heat was given to the heaters. These readings were found to agree with the room temperature which was measured by a thermometer.

The pressure on the brushes could be adjusted and it was found best to work with as light a pressure as possible to inhibit the formation of a film on the slip ring surfaces. Also, the slip rings were cleaned at the start of each test to ensure that no film was built up by wear of the brushes.

After the rotating element was fixed in position it was surrounded by a guard for the sake of safety. The final set up is shown in Fig. 70.

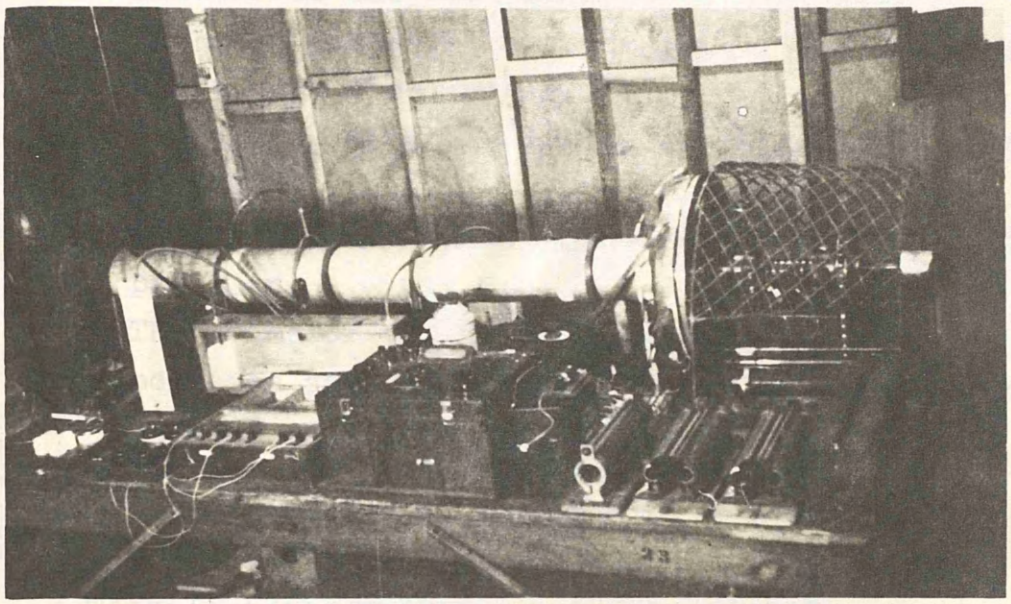

Fig. 70 : PHOTOGRAPH OF FINAL SET - UP.

Adjustment of the gap:

To fix the rotating element in a position to give a certain gap between the heating surface and the rotating disc the following steps were taken;

1. The brushes and the bolts fixing the frame of the brush holders to the base block were loosened.
2. The grub screws fixing the pulley and the rings on the shaft were also loosened.
3. The shaft, with the discs, was then moved to the required position.
4. The pulley and the rings were again fixed in the new right position.
5. The frame of the brush holders was moved to a suitable position and then fixed. Light spring pressure was then exerted on the brushes.

Speed of rotation:

Tensile tests on asbestos were carried out on a tensile test machine. Four different specimens were cut in such a way that the direction of the fibres took different positions in the different specimens. The tests were made on all specimens and it was then decided that the maximum rotational speed should be . . . 400 r.p.m.

B - OBSERVATIONS.

In each experiment the following observations were taken:

1. Pressure difference across the nozzle. This was read on the inclined tube manometer.
2. Speed of rotation of the air blower. It served as a check for the stability of running.
3. Heat input to the main heater.
4. Heat input to the guard heater.

5. Room temperature. The thermometer was placed near the intake of the air blower.
6. Speed of rotation of the rotating element. This was calculated from the speed of the driving motor which was measured by a tachometer.
7. Thermocouple readings. Twenty-two thermocouple readings were taken. They are distributed as follows :
   6 thermocouples for the asbestos between the main and guard heaters.
   9 thermocouples for the heating surface.
   2 thermocouples for the outer asbestos ring.
   2 thermocouples for the inner asbestos ring.
   3 thermocouples for the unheated rotating disc.

C - TEST PROCEDURE.

The following steps were taken in every experiment:

1. With the rotating element stationary the air blower was driven to give the required amount of air flow.
2. Heat was then supplied to the main heater at the required rate.
3. Heat was supplied to the guard heater at the rate necessary to stop any heat conduction across the asbestos between the main and guard heaters.
4. The rates of air discharge and heat inputs were kept constant, while the thermocouple readings were noticed every 30 minutes.
5. After all the steady conditions have been established and recorded, the rotating element was driven to the required speed, and the same readings were taken until the new steady conditions were established.
6. The readings were recorded and the speed of the rotating element was changed to another required speed.
7. The same procedure was repeated for disc speeds 100, 200, 300 and 400 r.p.m.

In some experiments it was necessary to change the amount of heat input to the main heater in order to keep the temperature of the heating surface in the required range. On the other hand, it was sometimes found unnecessary to apply four different disc speeds, and two were considered sufficient.

The time required foracomplete experiment of one air discharge and four disc speeds varied from eight to eleven hours.

D - METHOD OF CALCULATION.

The method of calculation applied here was generally the same as that applied in the case of the stationary unheated disc. The only difference was that the air temperature was taken as that of the room.

CHAPTER XI.

HEAT TRANSFER RESULTS.

Experiments on four different gaps were carried out. Those gaps were $\frac{1}{4}$, 3/16, $\frac{1}{8}$ and 1/16 inches. With the exception of the 1/16 inch gap, when the smallest amount of air discharge from the air blower was applied there was no effect for the rotation on heat transfer from the heating surface. The temperature of the unheated rotating disc changed with rotation, but the coefficient of heat transfer from the stationary heating surface was practically constant. The observations and results are given in Tables 29 and 30 in Appendix II.

However, for the 1/16 inch gap the coefficient of heat transfer was affected by the rotation of the disc. Seven experiments were carried out, and the observations and results are shown in Tables 31 and 32. Fig.71 shows the increase in the heat transfer for different disc speeds versus the mean radial velocity component (U_m). At values of (U_m) above 40 ft/sec. the effect of rotation is almost negligible for the highest speed of rotation (400 r.p.m.).

Other experiments were carried out when there was no air discharge from the blower. The observations and results of these are shown in Tables 33 and 34. The average coefficient of heat transfer was found to increase linearly with the disc speed according to the equation

$$h = 1.20\ (1 + a\,N) \qquad \frac{Btu}{Ft.^2.Hr.^oF} \qquad \text{XI-1}$$

where N = disc speed, r.p.m.

a = constant, given by Table XI-1.

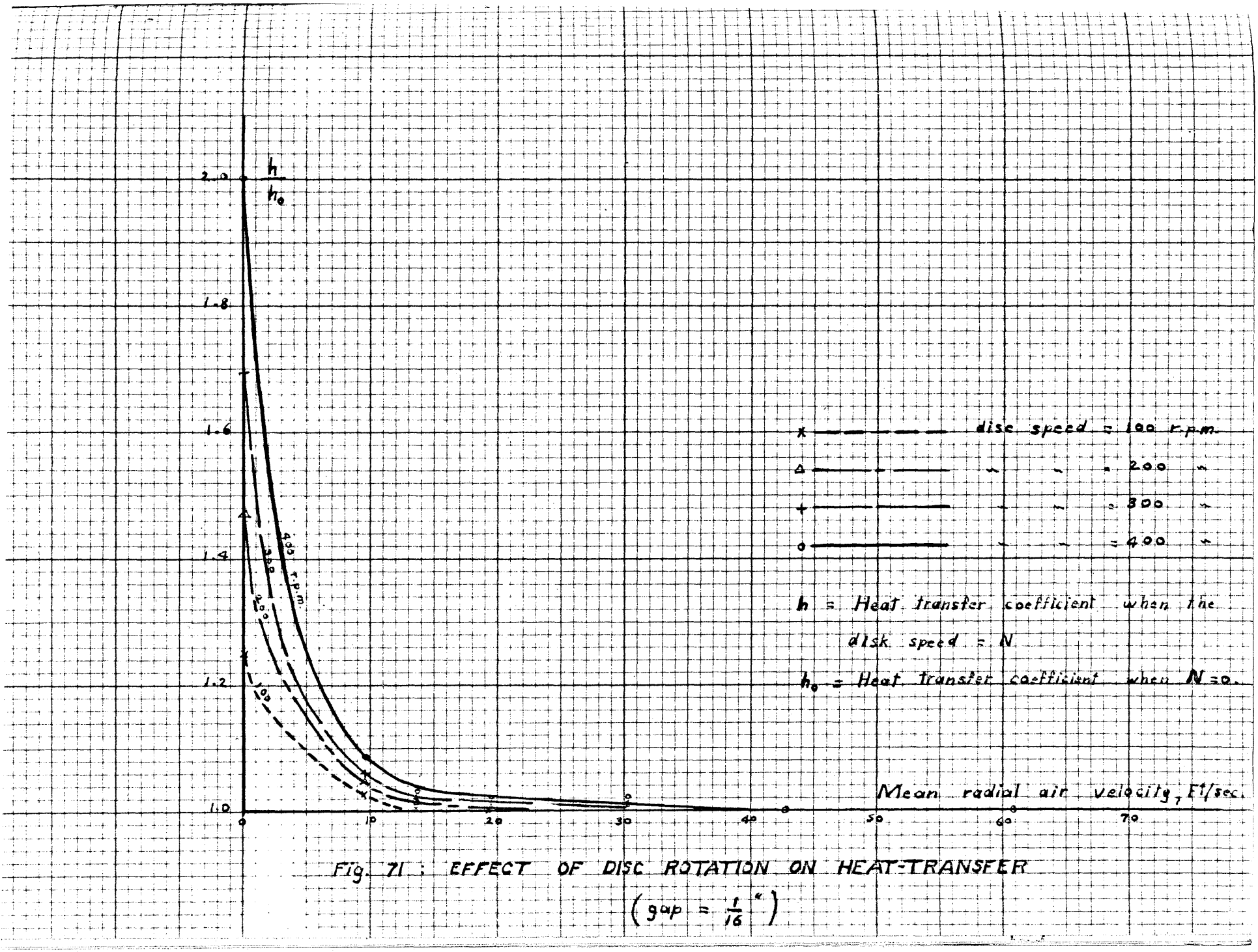

Fig. 71 : EFFECT OF DISC ROTATION ON HEAT-TRANSFER

(gap = 1/16")

Table XI-1 : [Values of (a) in equation (XI-1) for different gaps]

Gap (inches)	1/16	1/8	3/16	1/4
a	0.00375	0.00275	0.00175	0.00087

The values of the coefficient of heat transfer were plotted in Fig.72 against different disc speeds. They were plotted again in Fig.73 against the gap (b).

After these results for the effect of the disc rotation on heat transfer it was necessary to make some investigations on the flow conditions as affected by the rotation of the unheated disc. This work will be described in the following chapter. Discussion of the present heat transfer results will be postponed until the effect of the rotation on the flow conditions is explained.

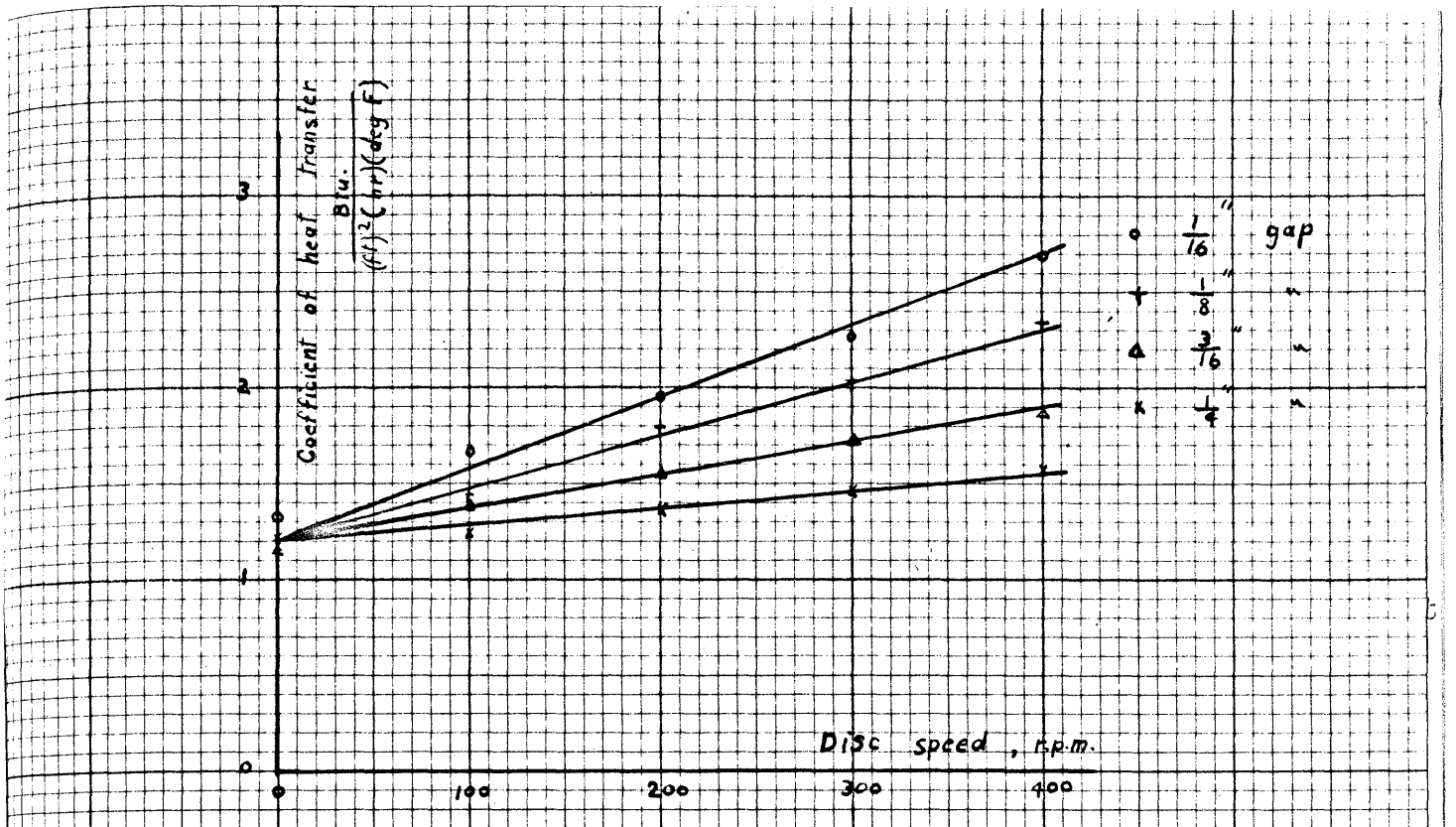

Fig. 72 : EFFECT OF DISC ROTATION ON HEAT TRANSFER WITH NO AIR DISCHARGE.

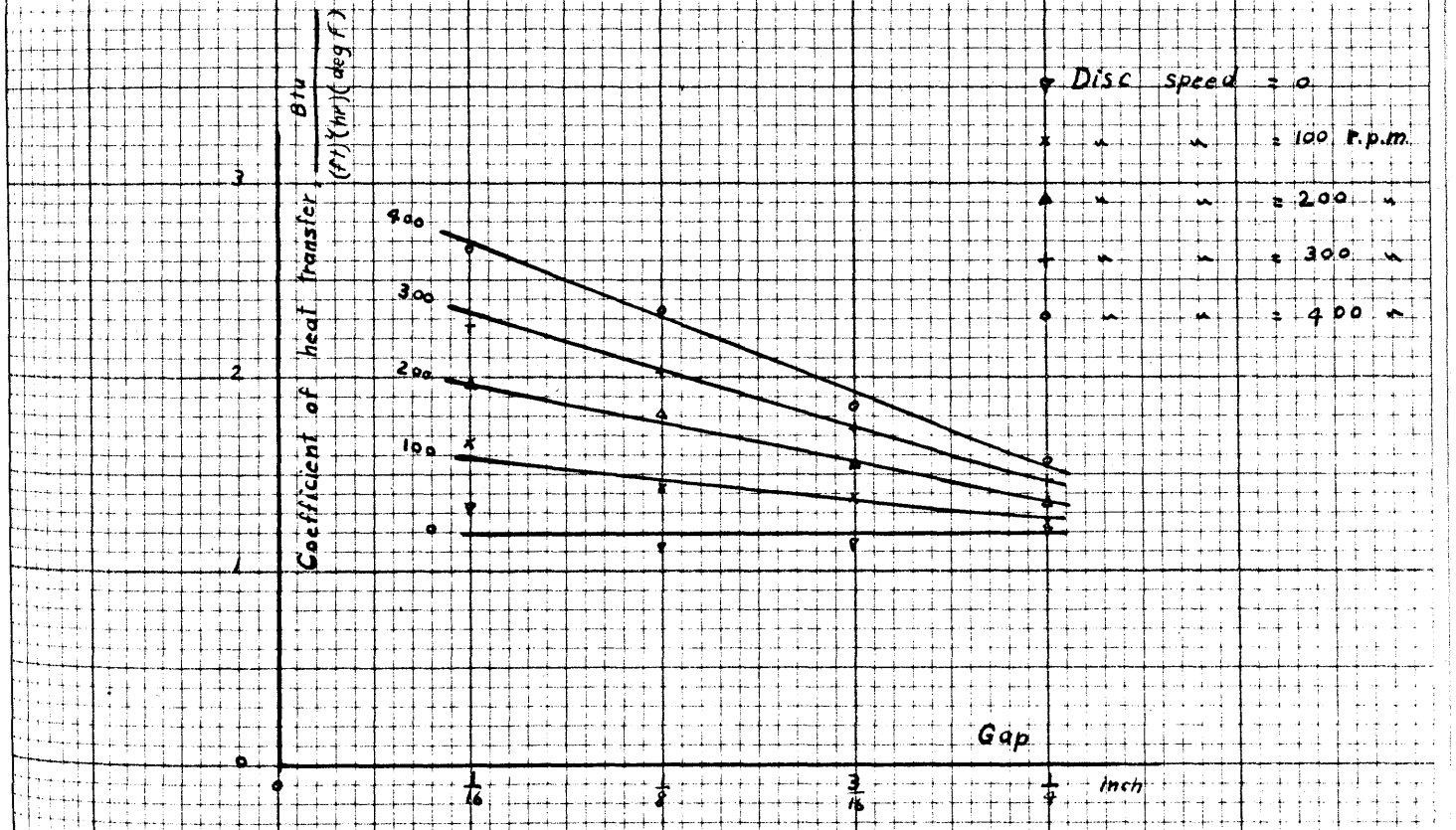

Fig. 73 : EFFECT OF GAP ON HEAT TRANSFER
(Air discharge = 0.)

CHAPTER XII

MEASUREMENTS ON THE FLOW AS AFFECTED BY THE ROTATING DISC.

A - APPARATUS AND EXPERIMENTAL WORK.

General idea:

It was believed to be of some importance to measure the velocity head of the air flowing near the rotating disc in different positions. Such measurements can show how far the effect of rotation is on the direction of the flowing air in different planes parallel to the disc. This will, surely, help to understand the effect of the rotation of the unheated disc on heat transfer.

The idea applied here gives qualitative and quantitative results. The technique is not too accurate, but it gives a fairly good idea about the flow pattern.

The idea is that if a pitot tube is aligned with its axis in the directionof an airstream, with its inlet end facing the stream, then the reading of the kinetic pressure is an indication of the velocity of the stream. If the axis of the tube is not in the directionof the stream then the reading does not give correctly the velocity head.

Now if the direction of the stream is not known and it is required to find it, then the pitot tube can be rotated in different directionsand different corresponding readings are obtained. Plotting the pressure readings versus the angular position, we obtain a curve from which, using the rule of symmetry, the direction of the stream can be found.

The curve shown in Fig.74 (see Goldstein[19]) shows, for a total head tube, the variation in the kinetic pressure reading with rotation about the axis of the stem.

Construction of the small total head tube and micrometer arrangement

Like the small total head tube described in Chapter IV the present one was made. There was only one difference; the length of the tube was $\frac{5}{8}$", and a new $\frac{1}{8}$" copper tube was used.

After some modification the micrometer described in Chapter IV was also used here. This modification allowed for an easy rotational motion of the $\frac{1}{8}$" tube inside the micrometer, thus changing the angular position of the small tube relative to the body of the micrometer.

As shown in Fig.75, the two rings (A) and (B) were placed around the $\frac{1}{8}$" tube at the ends of the micrometer spindle. They were then soldered to the tube. A pointer, which was a stiff steel wire, was soldered to the ring (B) so that the pointer was directed towards the axis of the $\frac{1}{8}$" tube. The circular scale (C) was divided into 36 divisions, each division representing 10 degrees; and it was fixed positively to the spindle.

Now, the micrometer scale and the circular scale (C) form one rigid body. Turning the micrometer nut gives the axial movement. Angular movement can be obtained by turning the $\frac{1}{8}$" tube. Then the steel wire, turning with the tube, indicates, on the circular scale, the angular position of the small tube.

The micrometer and the tube arrangement was carried onto a stand which allowed for movement in all directions. Fig. 76 shows

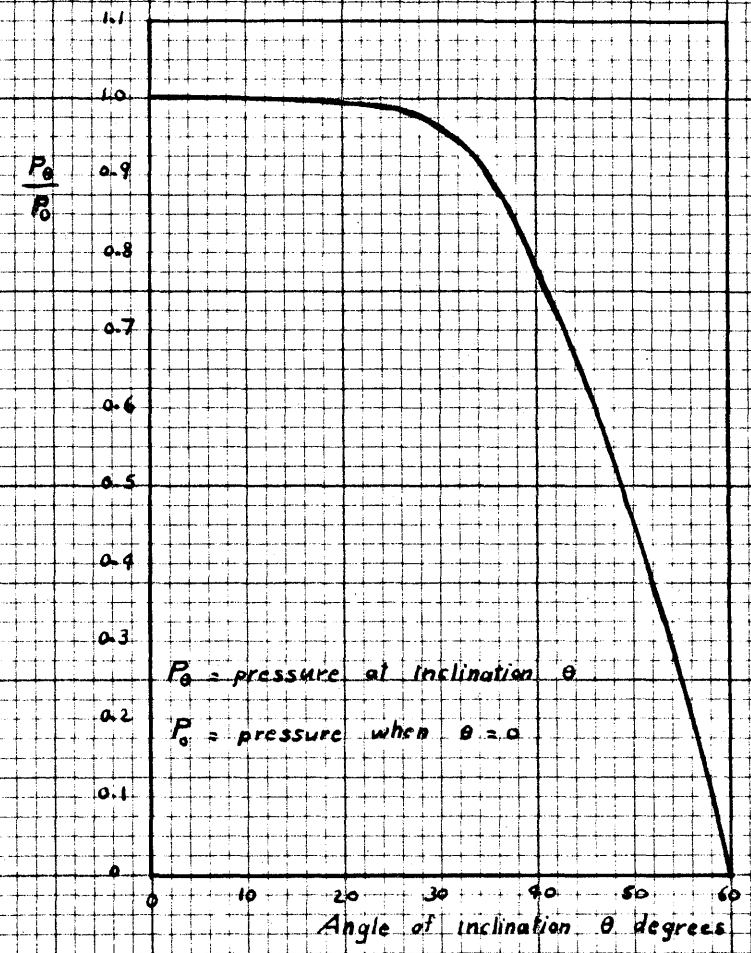

Fig. 74 : VARIATION OF THE KINETIC PRESSURE READING WITH ROTATION ABOUT THE AXIS OF THE STEM.
(reproduced from Goldstein[19])

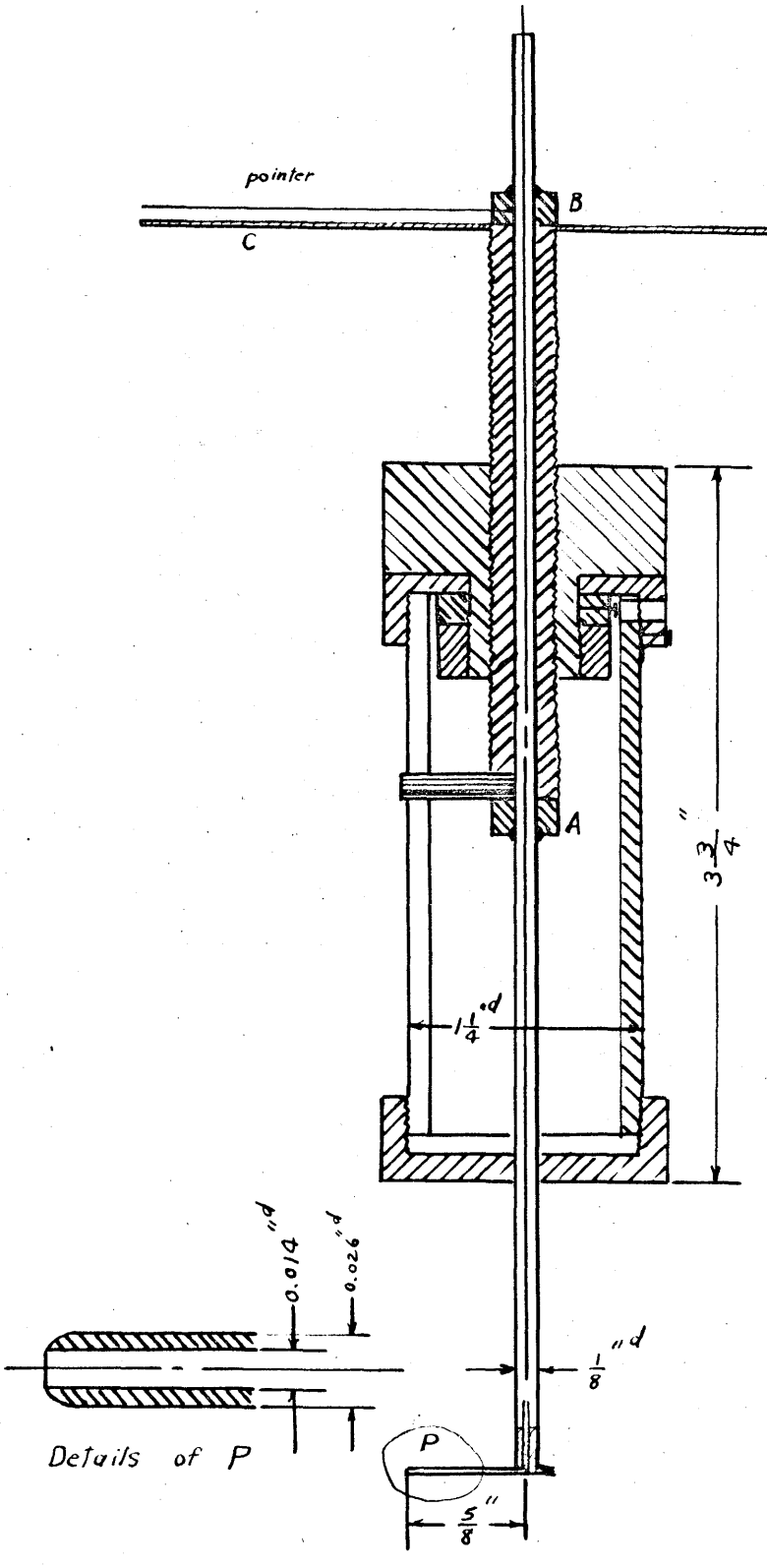

A & B : Rings

C : Circular scale

Fig. 75 : MICROMETER AND TOTAL HEAD TUBE ARRANGEMENT

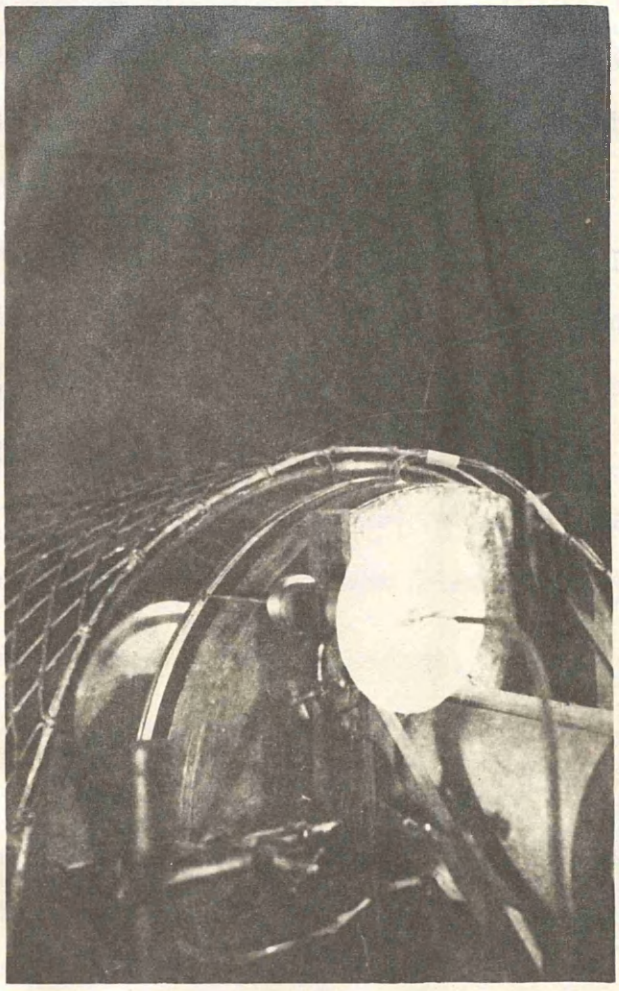

Fig. 76 : MICROMETER ARRANGEMENT IN POSITION.

a photograph of the arrangement in position.

Direction of experiments:

In the present work the Pitot tube was placed near the rotating disc with its axis parallel to the plane of the disc. With the inlet end of the tube at the same position the direction of the axis was changed, but it was still parallel to the plane of the disc. Different total heads were taken for different directions. The total angle moved by the axis of the small tube was 110 degrees. The results were plotted and the direction of the air at that particular point was determined.

For the same amount of air discharge this process was repeated for different disc speeds, namely, 0,100, 200, 300, and 400 r.p.m. For every discharge and every disc speed the same procedure was repeated for various distances between the tube axis and the plane of the disc. Five planes were chosen, their distances from the disc being 0.025, 0.040, 0.065, 0.100 and 0.150 inches.

Five different air discharges were applied. These were, 0, 196.2, 310.5, 440 and 621 pounds per hour. The gap between the disc and the heating surface was kept at $\frac{1}{4}$". All the readings of the total head in the different planes were to be taken with the inlet end of the tube at the same distance from the axis of the disc. That distance was 9 inches; that is the same as the radius of the heating unit. The static pressure at that position was nearly atmospheric, and accordingly the total head would be nearly equal to the velocity head.

Adjustment of the direction and position of the small tube.

A small mark (o) was made on a point on the surface of the disc at a radius of 9 inches. Before adjustment of the direction of the small tube the disc was kept stationary at a certain position, thus giving a certain fixed position (in space) for the mark (o). The small tube was then adjusted in the required direction with its inlet end on the point (o). Then the tube was moved in a plane perpendicular to that of the disc until the required distance apart was reached.

For any change of direction of the small tube the same procedure was applied so that the inlet end would always be in the same place.

Test procedure:

In these measurements the following procedure was taken:

1. The air blower was driven to give the required air discharge.
2. The small tube was aligned in the required direction with its axis at a distance from the disc = 0.025 inch.
3. With the disc stationary the velocity head was taken.
4. The disc was then rotated at 100 r.p.m. and the corresponding kinetic pressure taken.
5. Step 4 was repeated with disc speeds 200, 300 and 400 r.p.m
6. The small tube was then moved (by turning the nut of the micrometer) to a position such that the distance between its axis and the disc = 0.040". Then steps 3, 4 and 5 were repeated.
7. Step 6 was repeated for distances between the disc and the tube axis equal to 0.065", 0.100" and 0.150".
8. The direction of the small tube was then changed, and the steps from 2 to 7 were repeated.

9. Step 8 was repeated for all the required angular positions of the small tube.

If the radial direction is denoted by 0°, the range of the angular positions of the tube lies between -10° and 100°.

B - OBSERVATIONS AND RESULTS

The results of these experiments are given in Tables 35 to 39 and Figs.77 to 81. The planes I, II, III, IV, and V are parallel to the unheated disc and at distances 0.025, 0.040, 0.065, 0.100 and 0.150 inch respectively. In the graphs no representation was shown for plane V as the effect of rotation on the readings was negligible.

The values in Table (XII-1) give the direction of the maximum radings of kinetic pressure; that is, the angle which the stream at the mark (o) makes with the radial direction for different air discharges, different planes parallel to the disc and different disc speeds.

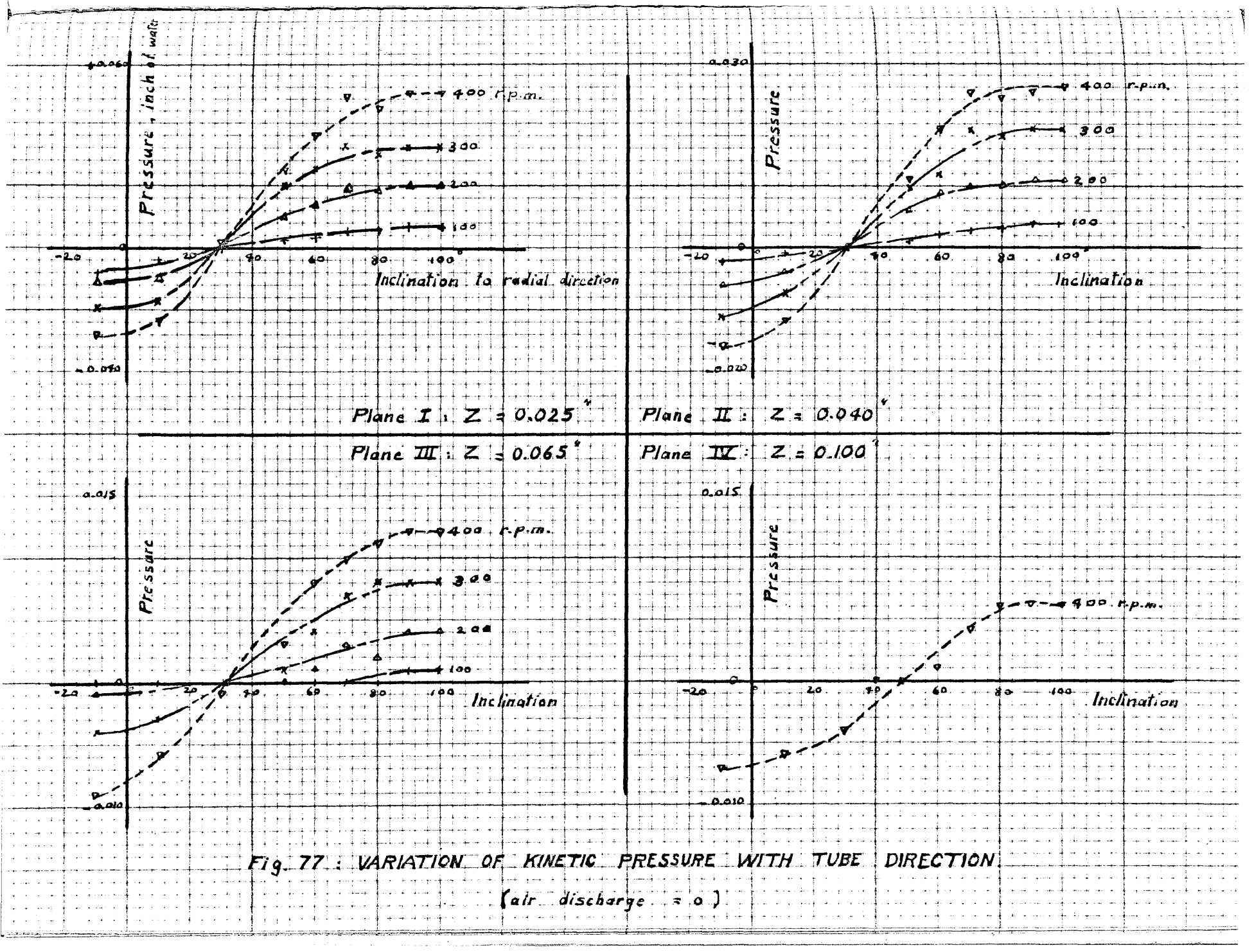

Fig. 77 : VARIATION OF KINETIC PRESSURE WITH TUBE DIRECTION

(air discharge = 0)

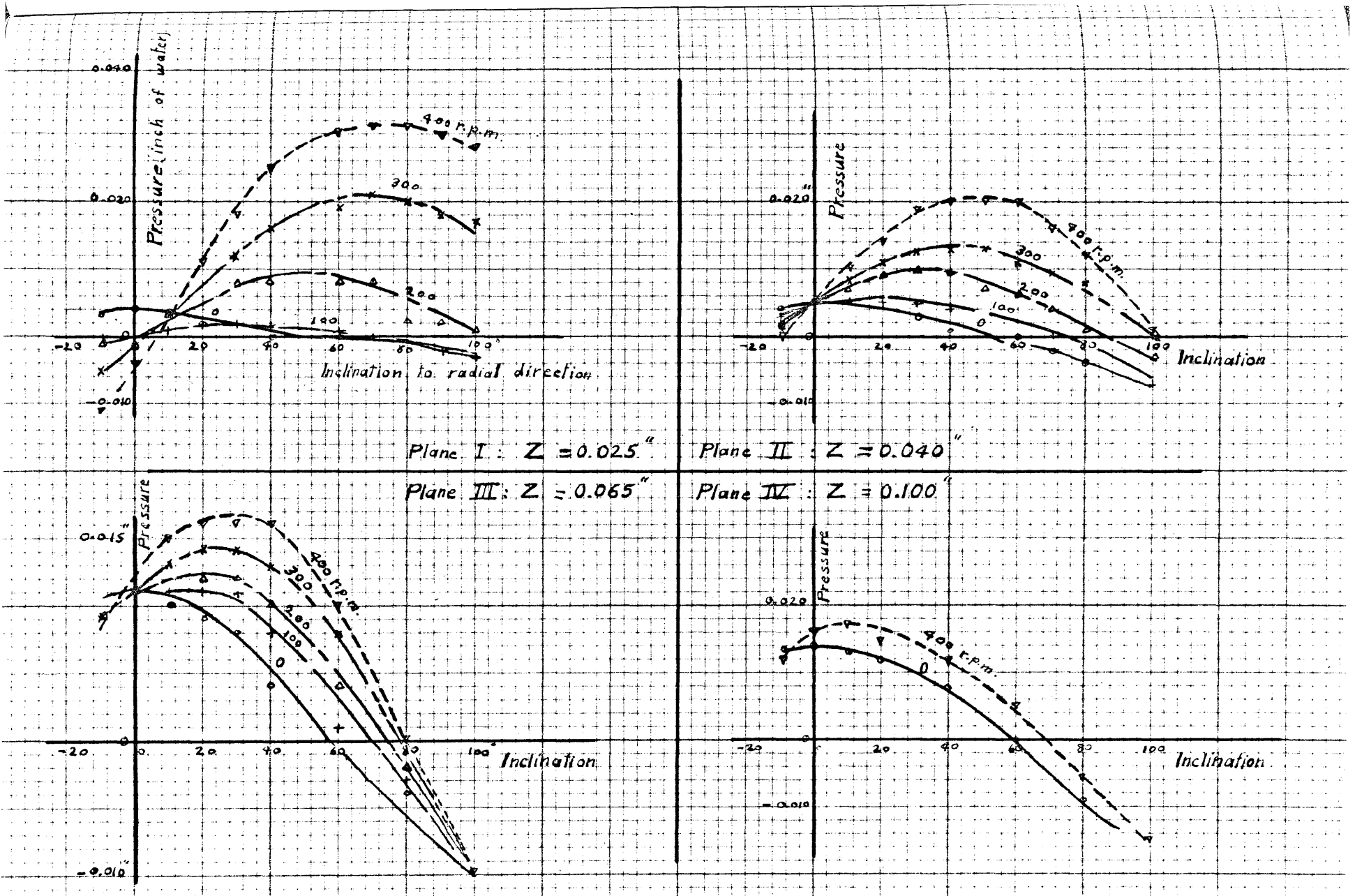

Fig. 78 : VARIATION OF KINETIC PRESSURE WITH TUBE DIRECTION.

(air discharge = 196.2 lbs./hour)

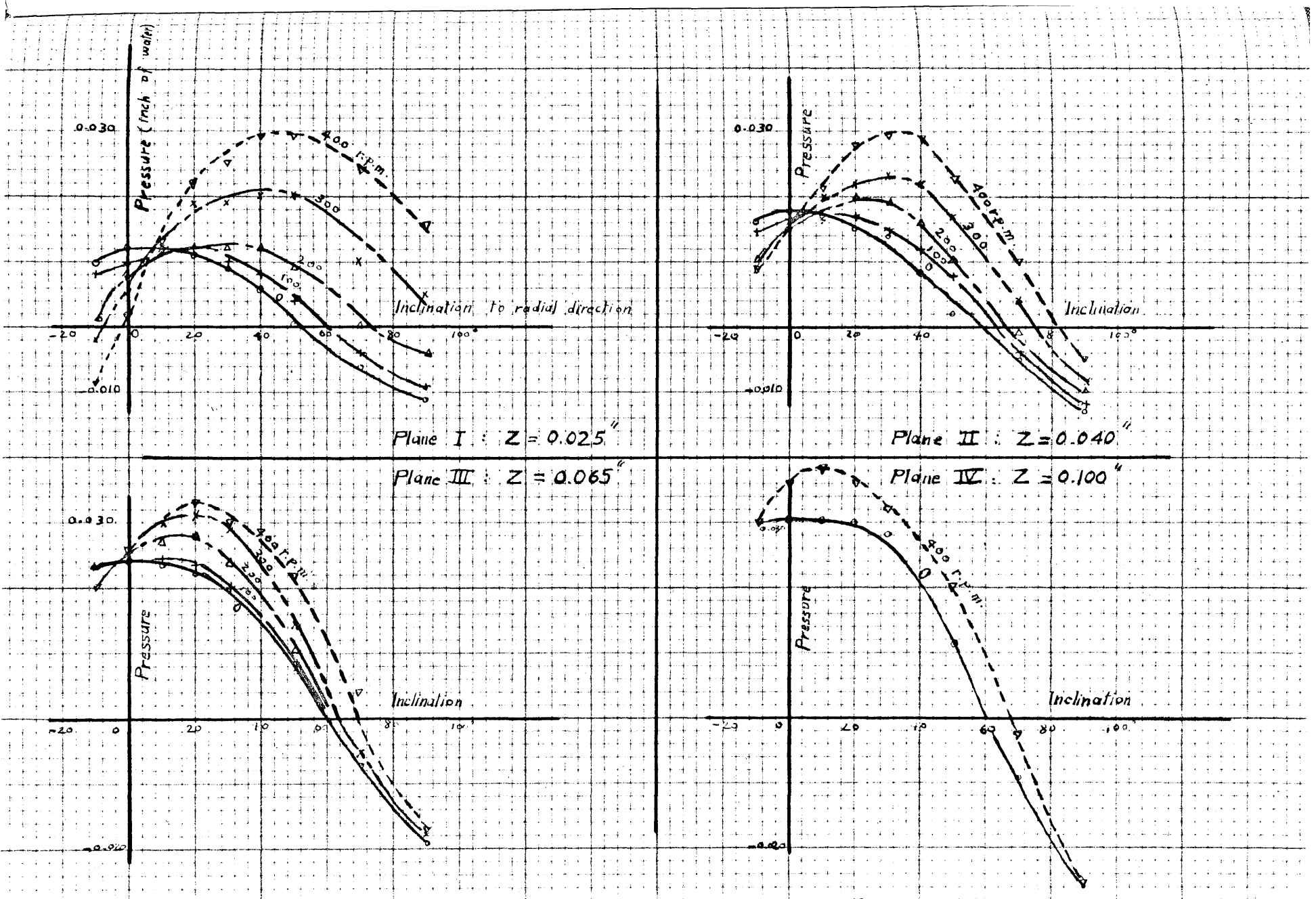

Fig. 79 : VARIATION OF KINETIC PRESSURE WITH TUBE DIRECTION.

(air discharge = 310.5 lbs/hour)

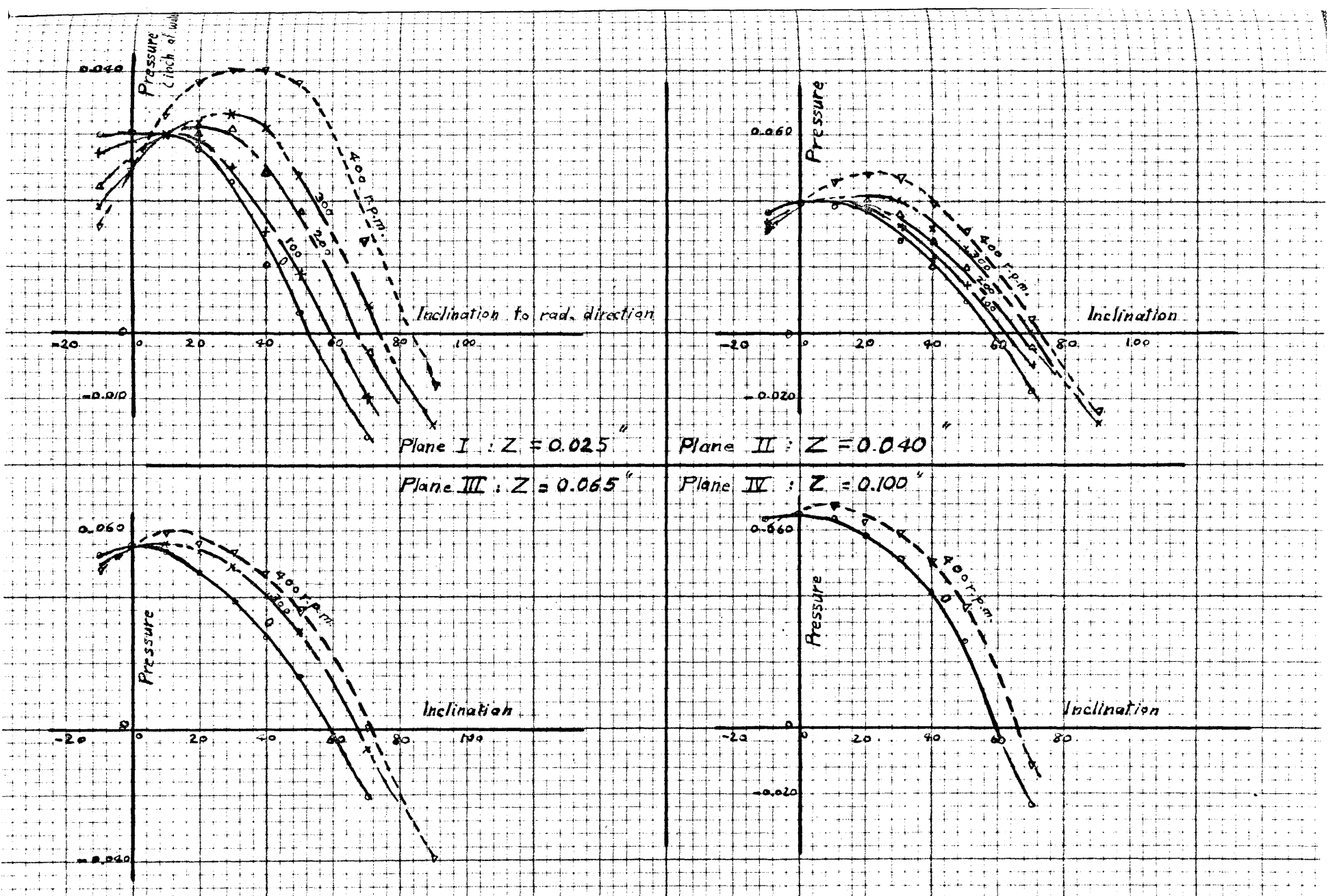

Fig. 80 : VARIATION OF KINETIC PRESSURE WITH TUBE DIRECTION.

(air discharge = 440 lbs/hour)

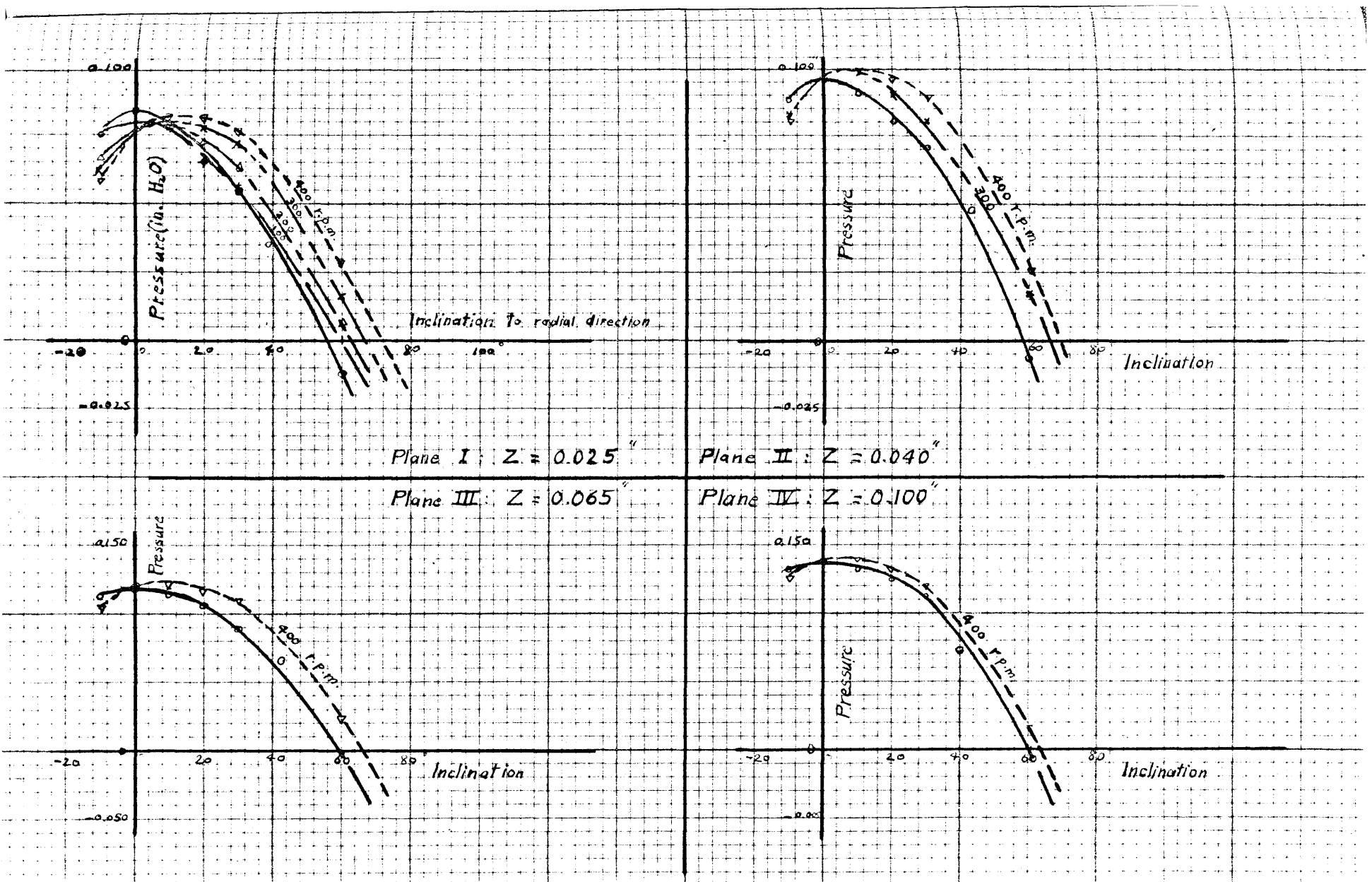

Fig. 81 ; VARIATION OF KINETIC PRESSURE WITH TUBE DIRECTION.

(air discharge = 621.0 lbs./hour)

Table XII-1 : (Angles between the airstream and radial direction at radius 9 inches).

Plane number	Disc Speed r.p.m. \ Discharge lbs/hr.	0	196.2	310.5	440	621
I	0	-	0	0	0	0
	100	90	30	19	10	4
	200	90	50	32	25	10
	300	90	70	42	30	14
	400	90	75	47	35	16
II	0	-	0	0	0	0
	100	90	20	16	10	
	200	90	30	24	17	
	300	90	43	30	21	8
	400	90	50	34	24	10
III	0	-	0	0	0	0
	100	90	19	10		
	200	90	24	15		
	300	90	25	17	10	
	400	90	27	20	12	9
IV	0	-	0	0	0	0
	400	90	10	10	9	7

These angles were again calculated by using Cochran's solution given in Chapter IX. The method of calculation and comparison with the experimental results will be given in the following chapter.

CHAPTER XIII

DISCUSSION OF FLOW AND HEAT TRANSFER RESULTS

A - DISCUSSION OF FLOW RESULTS.

The results shown in Chapter XII are here analysed in another form. Fig.82 represents the maximum pressure readings against the distance from the disc when there is no air discharge from the blower *. These curves show that the effect of rotation is great near the surface of the disc. It then diminishes rapidly as we go farther from the wall. The effect becomes almost negligible at a distance of about $\frac{1}{8}$" from the surface. This result is in agreement with the results of Stewartson[49] who stated that when one of the discs was at rest the main body of the fluid was also at rest, with the exception of a thin layer near the rotating disc.

Figs. 83 to 86 represent the angle between the airstream and the radial direction at radius 9 inches against different air discharges. These show that for very small air discharges the stream is nearly tangential. As the discharge increases the angle between the airstream and the radial direction decreases until, for sufficiently large discharges, the whole stream becomes nearly radial and the effect of rotation becomes very small.

The angle (ϕ) which the airstream makes with the radial direction at a radius 9 inches and different distances from the

---

* For no air discharge from the blower the maximum pressure readings are in direction perpendicular to the radial.

Fig. 82 : EFFECT OF DISC ROTATION AT DIFFERENT DISTANCES FROM THE DISC.

(discharge = 0)

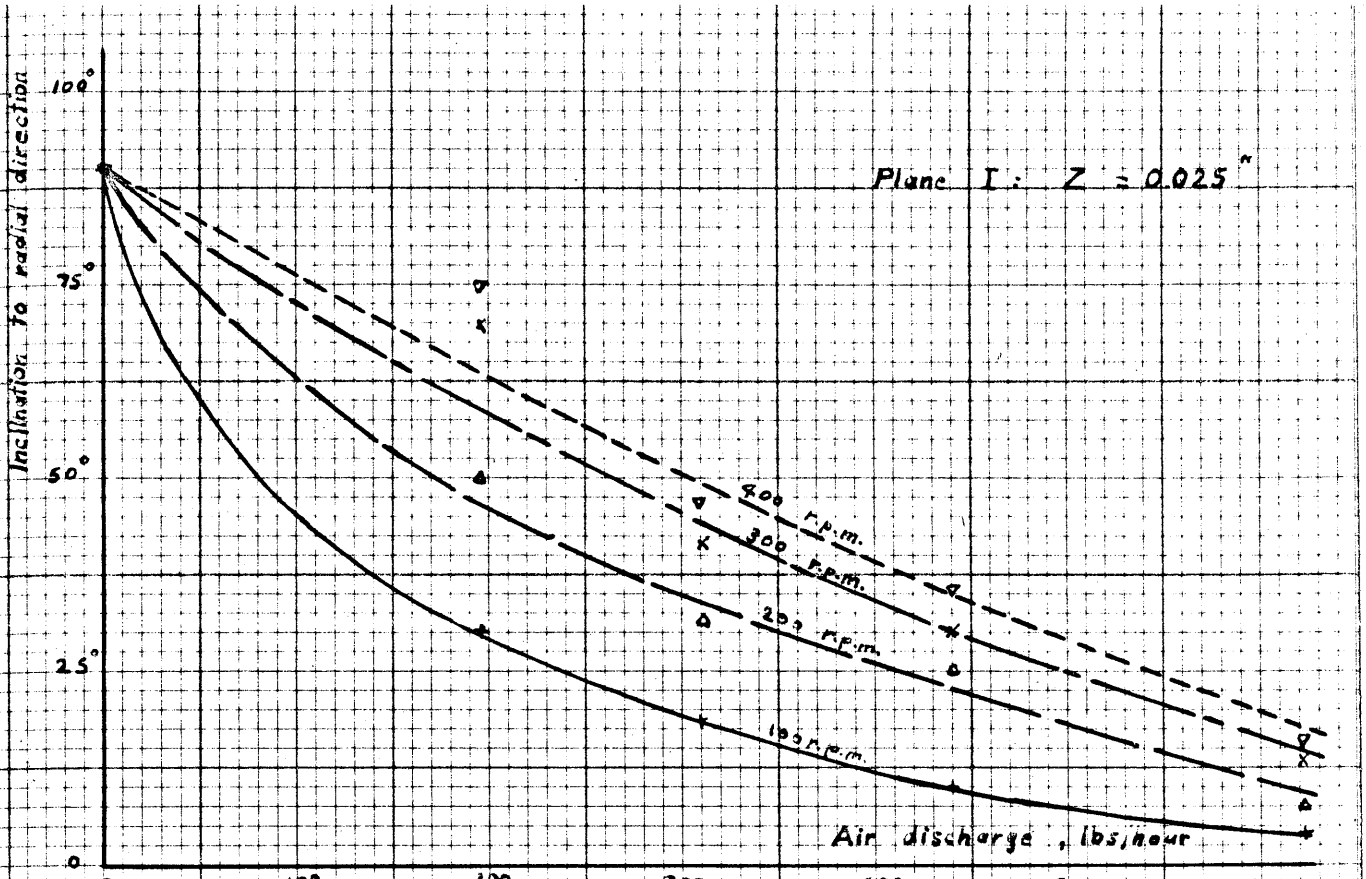

Fig. 83 : EFFECT OF AIR DISCHARGE AND DISC SPEED ON STREAM DIRECTION.

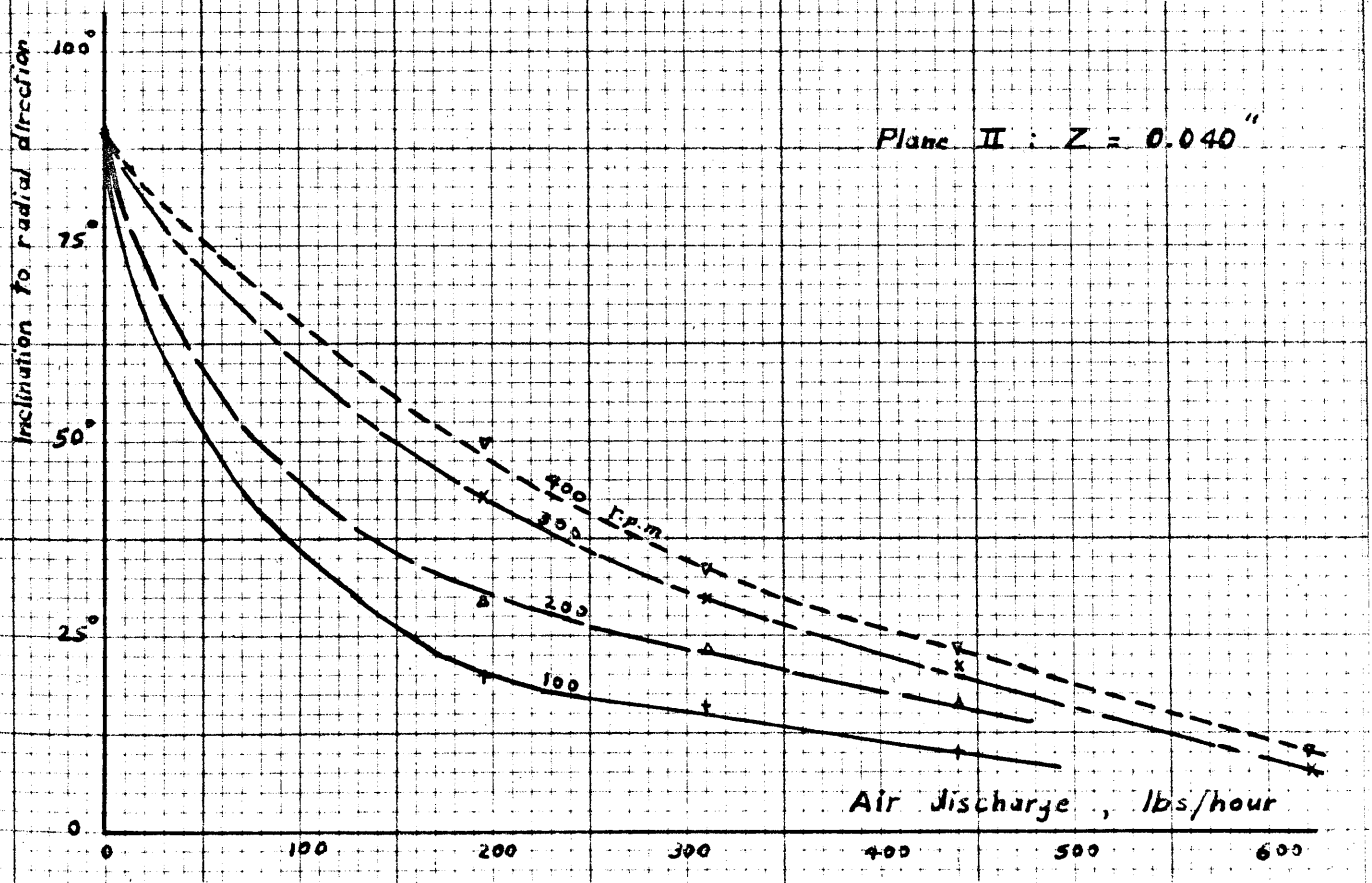

Fig. 84 : EFFECT OF AIR DISCHARGE AND DISC SPEED ON STREAM DIRECTION.

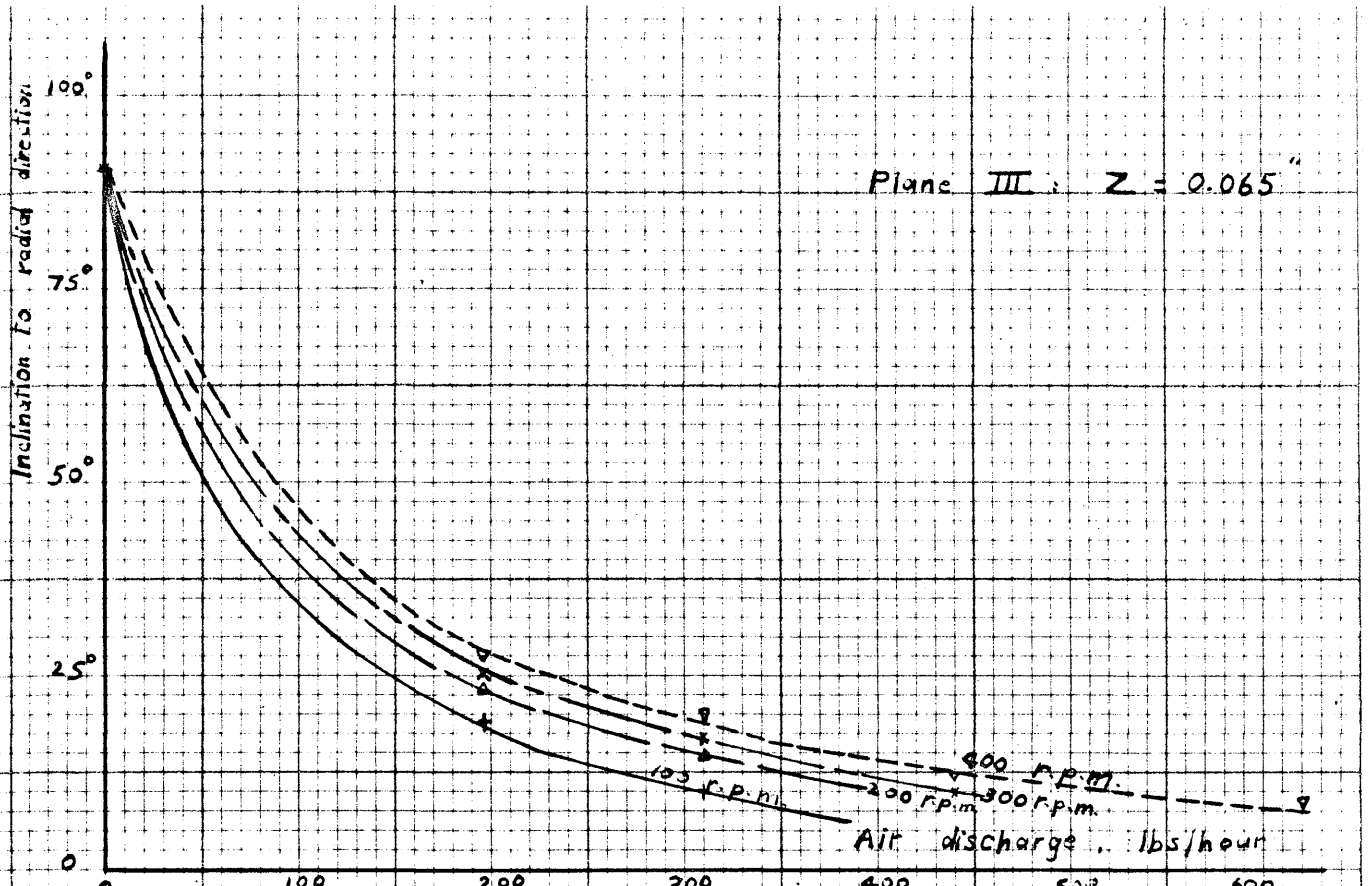

Fig. 85 : EFFECT OF AIR DISCHARGE AND DISC. SPEED ON STREAM DIRECTION

Fig. 86 : EFFECT OF AIR DISCHARGE AND DISC SPEED ON STREAM DIRECTION.

disc were calculated from equation (IX-27) for different values of λ and K. Equation (IX-27) gives

$$\tan \phi = \frac{\lambda}{K} r^2 \qquad \text{XIII-1}$$

The values of K were calculated from the amount of air discharge assuming uniform radial velocity distribution at all radii. Thus

$$K = U_1 r_1 \qquad \text{XIII-2}$$

where U_1 is the velocity at the inner radius r_1.

The values of λ were calculated from Cochran's [6] results given in Fig.60 by putting

$$\lambda = w G \qquad \text{XIII-3}$$

where w = disc speed

G = part of that speed transmitted to the air particles at a certain point.

A value of w was assumed. Then $\left[= z \left(\frac{w}{\nu}\right)^{0.5} \right]$ was calculated by putting the required value of z and the value of ν at the room temperature. G was then determined from Fig.60.

The calculated values of the angle (ϕ) are given in Table (XIII-1). The agreement between the calculated values and those found experimentally (Table XII-1) is generally fair.

From the preceding results it can be stated that :

1. The effect of disc rotation is maximum at the surface of the disc. As soon as the surface is left this effect diminishes rapidly until it practically vanishes at about $\frac{1}{8}$" from the disc.
2. The effect of rotation increases as the disc speed increases. In the present range of disc speeds no weakness was noticed in the effect of increasing speeds.

3. When there is no air discharge from the blower the effect of rotation is predominant. It begins to decrease rapidly as soon as air discharge begins to take place.

Table (XIII-1) ; (Calculated values of $\emptyset$ for different air discharges and different disc speeds).

Distance from Disc (inch)	Discharge lbs/hr. / Disc Speed r.p.m.	196.2	310.5	440	621
0.025	100	33	23	17	12
	200	51	38	29	21
	300	58	45	35	27
	400	62	50	40	31
0.040	100	30	20	14	10
	200	40	28	21	15
	300	46	33	24	18
	400	51	36	27	20
0.065	100	20	13	9	7
	200	24	16	11	8
	300	25	17	12	8
	400	25	17	12	8
0.100	400	11	7	5	4

B - DISCUSSION OF HEAT TRANSFER RESULTS.

After the effect of the disc rotation on the flow conditions has been explained the results of the heat transfer experiments are not surprising. The effect of rotation on flow conditions practically vanishes at a distance of about $\frac{1}{8}$" from the disc. The same result has taken place in the case of heat transfer.

When the gap between the heating surface and the rotating disc was 1/16" the effect of rotation on heat transfer was shown in Fig.71. It can be seen that :

1. The effect of rotation on heat transfer is appreciable when the radial component of the velocity is small. As the radial component increases the effect of rotation decreases rapidly until it vanishes completely at a value of (U_m) of about 40 ft./sec.
2. For the same radial component, the effect of rotation on heat transfer increases as the disc speed increases.

These results are in agreement with the results of the flow measurements. As the air discharge increases the influence of the tangential component decreases. This restricts the increase in the length of path of the air particles as explained before.

Equation (IX-30) is now introduced. We have

$$\frac{h}{h_o} = \left(\frac{1}{r_2 - r_1}\right)^n \qquad \text{XIII-4}$$

This equation gives the increase in the heat transfer as a function of the increase in the path length. The experimental values of $\frac{h}{h_o}$ for all the experiments on the 1/16" gap were calculated corresponding to different values of $\frac{\lambda}{K}$. $K(= U_1 r_1)$ was based on the assumption that the distribution of the radial component of the velocity was uniform. The values of λ were calculated from Cochran's[6] results shown in Fig. 60 by putting $\lambda = w G$. (G) was taken at the middle plane between the heating surface and the rotating disc, that is, at $z = 1/32"$. The results are shown in Fig.87.

For the same values of $\frac{\lambda}{K}$; the values of $\frac{1}{r_2 - r_1}$ were determined from Fig.63. From these values the exponent (n) in equation (XIII-4) was found to be (0.28). Thus equation (XIII-4) becomes:

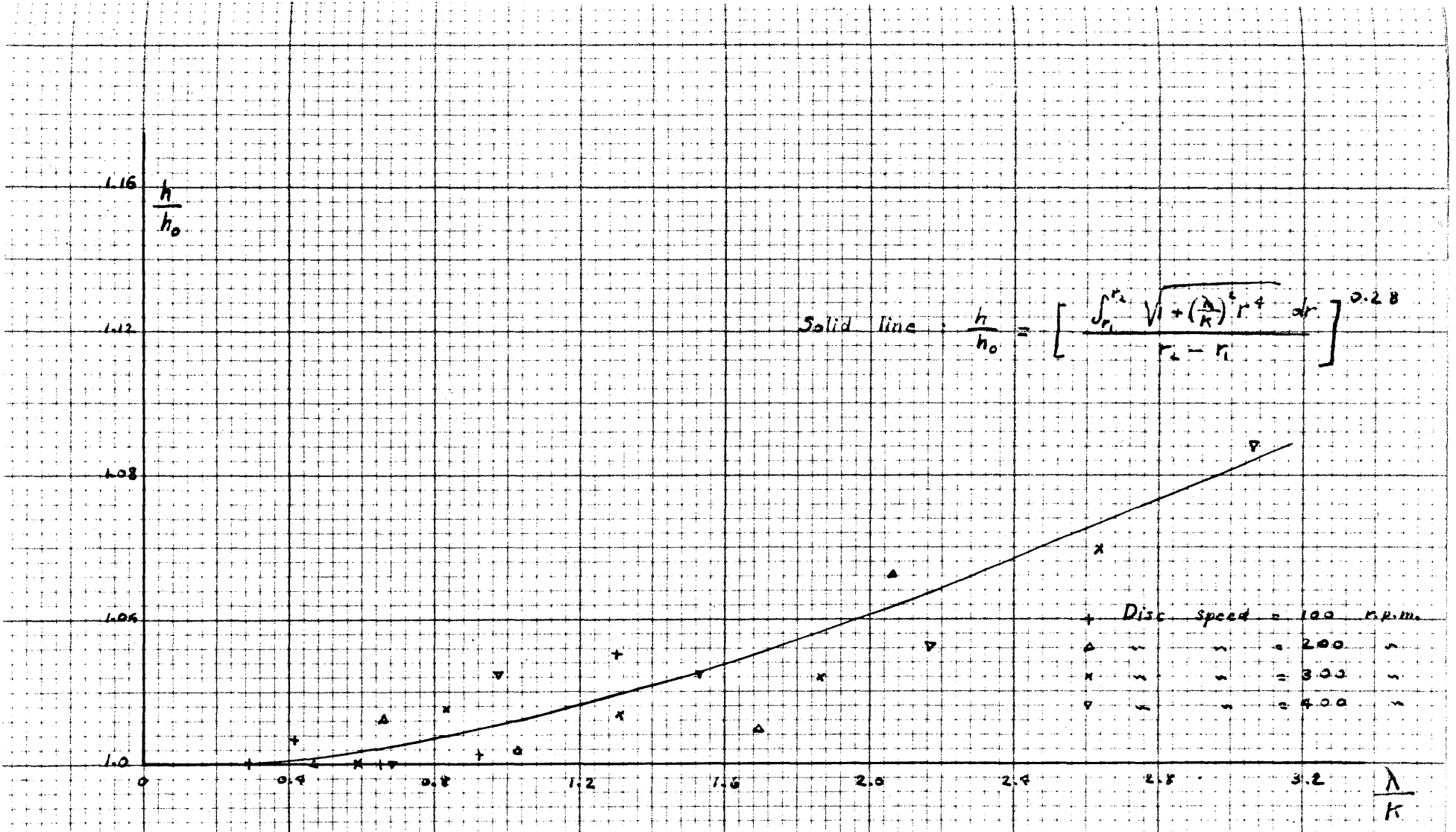

FIG. 87 : EFFECT OF DISC ROTATION ON HEAT-TRANSFER.

$$\frac{h}{h_o} = \left(\frac{l}{r_2 - r_1}\right)^{0.28} \qquad \text{XIII-5}$$

where $$l = \int_{r_1}^{r_2} \sqrt{1 + \left(\frac{\lambda}{K}\right)^2 r^4}\, dr$$

Equation (XIII-5) is represented by the solid line in Fig.87.

When there was no air discharge form the blower the rotation of the disc had an appreciable effect on heat transfer in all the gaps tested (the widest was $\frac{1}{4}$"). This, in fact, does not contradict the previous conclusions. When the disc is at rest and the conditions are isothermal there is no air movement at all. This is true because the air at all the points has practically the same temperature, and therefore the same density. As soon as heating is applied natural convectiontakes place. The air between the two discs becomes hot due to its restricted motion. Also the unheated disc becomes hot due to radiation from the heating surface. However, when the disc starts to rotate the particles of the air adjacent to the disc undergo tangential and radial * components. Such particles are pushed outwards and new ones, having the room temperature, come in their place. These secondary currents have been predicted by Batchelor(4). They have two results :

1. Such currents, though very weak, cause a direct increase in the heat transfer coefficient.
2. The temperature of the air filling the gap decreases, thus asking for more heat from the heating surface, with the result of lower surface temperature for the same amount of heat input and the same room temperature.

---

* Radial component is due to centrifugal forces.

As would be expected, the effect of these two factors on heat transfer decreases as the gap increases. This was verified experimentally as shown in Fig.73. The results lead to a con - clusion that after a sufficiently wide gap the effect of rotation would completely vanish.

It was thought of interest to photograph the direction of the airstream with and without disc rotation. Fig.88 shows two photographs when the gap was 1/16". The air discharge was 62.1 pounds per hour. In Fig. 88(a) the unheated disc was at rest, while in Fig. 88(b) the speed of rotation was 400 r.p.m. Titanium tetrachloride was used to show the s tream direction.

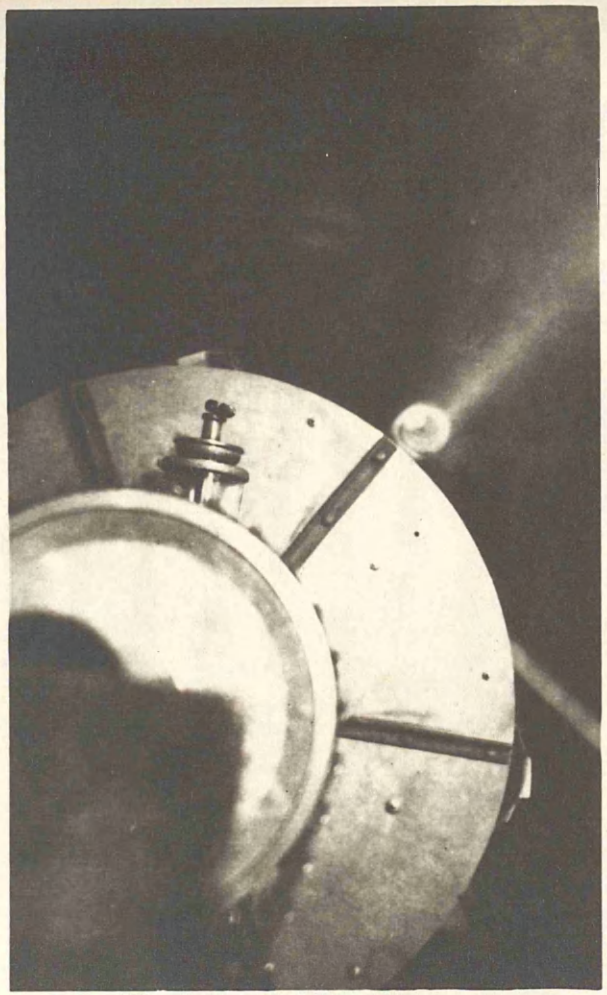

a - Disk stationary

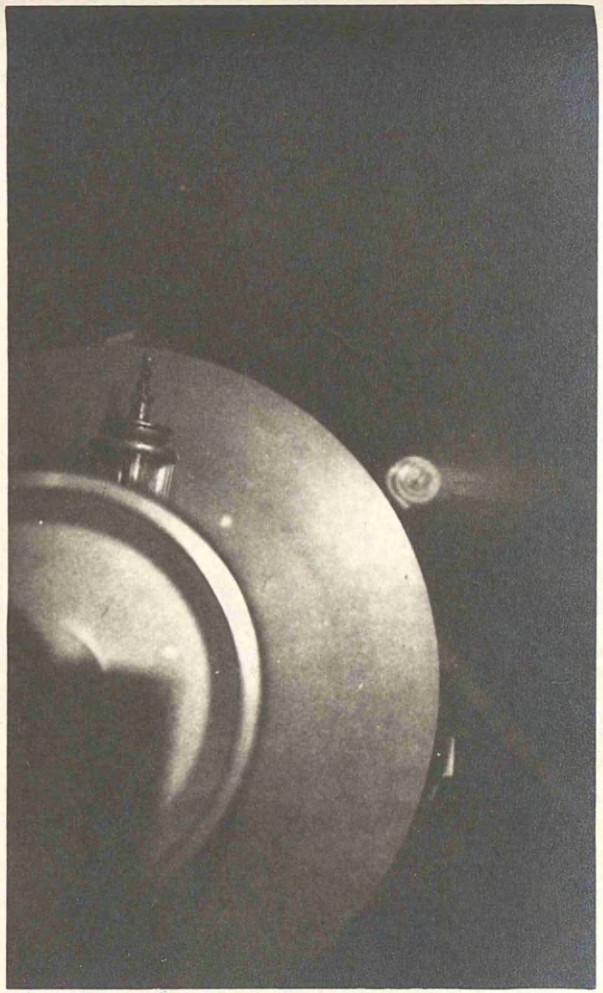

b- Speed of rotation = 400 r.p.m.

Fig. 88 : EFFECT OF ROTATION ON STREAM DIRECTION.

discharge = 62.1 lbs/hr

gap = $\frac{1}{16}$ inch

CHAPTER XIV

CONCLUSION.

In the first part of the work, when the unheated disc was stationary, the average coefficient of heat transfer by forced convection from a flat surface to air flowing in radial direction parallel to the surface was studied experimentally. The stream was bounded by the heating surface and the unheated disc. The range of air discharge included both laminar and turbulent flows.

The flow conditions were changed by changing the gap between the plates. 126 experiments were carried out on eight different gaps so as to show the effect of the gap on heat transfer. The results for each gap were represented by dimensionless groups. Correlations were given, which bring the experimental data for all the gaps together.

Theoretical comparison was made between the heat transfer for a fluid in uniform parallel flow and to a fluid in radial flow. It was predicted that when the fluid flows in an outward radial direction the heat transfer is generally less than when the fluid flows in uniform parallel flow. An approximate theoretical expression was derived, which gave results lower than the experimental ones. Introducing a factor of turbulence, which is a function of Reynolds number, the theoretical and experimental results were brought together.

Experimental results of other workers on heat transfer from flat surfaces were corrected to a plate length equal to the difference between the radii of the present heater. They were

then compared with the present results. For the small gaps the present results were lower, while for the large ones they were higher. For the middle gaps the agreement with other workers' results was good.

Heat transfer in the laminar range was compared with the theoretical values of Norris and Streid[36] for laminar flow between two parallel flat plates. The present results were a little higher than the theoretical ones in the tested range.

Measurements of the velocity distribution between the two plates were carried out. The flow pattern was determined. Laminar and turbulent regions given by the heat transfer curves were in agreement with the velocity profiles obtained from those measurements.

In the second part of the work the unheated disc was rotated The effect of rotation on both the flow pattern and heat transfer was studied.

As for the flow pattern the rotation was found to affect the ambient air in a layer of about $\frac{1}{8}$" from the disc surface. When the radial flow increased the thickness of the affected layer decreased. That decrease was reduced by the increase of the speed of rotation.

With no air discharge form the blower the effect of rotation on heat transfer was investigated for four different gaps. The heat transfer coefficient increased by increasing the disc speed, while increasing the gap weakened the effect of rotation on heat transfer.

When there was air flow from the blower the heat transfer was affected by the disc rotation only when the gap was 1/16". Yet, this effect decreased rapidly as the amount of air discharge increased.

Approximate calculations were made for the effect of the disc rotation on the path of the air particles, and the resulting change on the heat transfer. There was fair agreement with the results found experimentally.

. . . .

In spite of its importance the heat transfer from a flat surface to a fluid flowing in radial direction has not had much study ~~up~~ until the present time. The present work forms the first step in that field. There is much work to be done yet. The writer suggests that more work be done on different dimensions of apparatus. Effect of different flow conditions is to be studied, especially the difference between the two cases when the fluid is flowing outwards and inwards. This may have important results in the design of heat exchangers.

The case when the air is given tangential motion besides its initial radial motion is one of several practical applications, such as the cooling problem of turbine casings. As there is no published data it is suggested that more work is to be done in that respect. Higher disc speeds are to be tested and some kind of artificial roughness may be given to the disc.

APPENDIX I.

Calculation of the experimental laminar flow results on the basis of $Nu^+ - \Phi$ of Norris and Streid[36].

According to the definition of the equivalent diameter (b^+) of Norris and Streid, when heat is transferred from one side only we have

$$b^+ = 4\,b$$

where b is the gap between the plates.

Therefore, the value of Nu^+ will be

$$Nu^+ = \frac{h\,b^+}{k} = \frac{4\,h\,b}{k} = 4\,Nu \qquad (1)$$

Norris and Stried give

$$\Phi = \frac{b^+}{L} \cdot P_r \cdot Re^+$$

where $Re^+ = \frac{\rho U\, b^+}{\mu}$

Instead of U, U_m of the present work was taken.

This, together with $b^+ = 4\,b$, gives

$$R_e{}^+ = \frac{R_e}{2.18}$$

Putting $P_r = 0.72$, we get

$$\Phi = 0.72 \times \frac{4\,b}{L} \times \frac{R_e}{2.18} \qquad (2)$$

APPENDIX II.

TABLES

The symbols and abbreviations used in the tables are as follows

B.P. = barometric pressure, m.m. Hg.
D.B.T. = dry bulb temperature, degrees F
D.Sp. = disc speed, r.p.m.
Ex.No. = experiment number
h = average coefficient of heat transfer, Btu/(sq.ft)(hr)$^{\circ}$
H_r = heat lost by radiation, Btu/hour
H_c = heat lost by conduction, Btu/hour
H_o = net heat transferred by convection, Btu/hour
h_m = velocity head given by the small total head tube, (1 at radius $4\frac{5}{8}$", 2 at radius $7\frac{7}{8}$").
I.M.H. = input of the main heater
I.G.H. = input of the guard heater
k = thermal conductivity of air, Btu/(ft)(hr)(deg.F)
P_n = pressure difference across nozzle, inches of water
Q = amount of air discharge, pounds/hour
t_w = average temperature of the heating surface
t_d = average temperature of the unheated disc
t_i = temperature of the inner asbestos ring
t_o = temperature of the outer asbestos ring
t_a = mean temperature of the air at the working section
U_m = mean air velocity, feet/second
U_1 = mean air velocity at radius $4\frac{5}{8}$", feet/second, (mea.= measured by pitot tube, cal.= calculated from the calibration curve of the nozzle)
U_2 = mean velocity at radius $7\frac{7}{8}$", feet/second, (mea. & cal. as U_1)
z = distance from the unheated disc, inch
μ = viscosity, lbs/(ft)(hr)
Nu & R_e are Nusselt and Reynolds numbers.

Table (1): Calibration of nozzle

Velocity heads in the vertical plane at different radii, (m.m. water)

Exp. No. / Dist. from pipe axis (inch)	1	2	3	4	5	6	7	8	9	10
+ 2.66	2.62	2.21	0.87	1.81	1.48	1.11	0.63	0.52	0.35	0.26
+ 2.50	2.97	2.53	1.02	2.15	1.73	1.29	0.72	0.59	0.42	0.29
+ 2.00	3.31	2.83	1.13	2.32	1.93	1.44	0.85	0.67	0.46	0.34
+ 1.50	3.32	2.79	1.10	2.32	1.89	1.39	0.81	0.67	0.45	0.32
+ 1.00	3.56	2.97	1.16	2.40	1.99	1.48	0.86	0.71	0.49	0.36
+ 0.50	3.54	2.98	1.18	2.48	2.01	1.48	0.86	0.69	0.48	0.35
0.00	3.50	2.91	1.13	2.43	1.96	1.46	0.84	0.67	0.46	0.34
- 0.50	3.60	3.04	1.19	2.51	2.05	1.50	0.87	0.70	0.49	0.36
- 1.00	3.59	2.97	1.16	2.45	2.00	1.48	0.86	0.70	0.48	0.36
- 1.50	3.60	2.95	1.16	2.44	1.98	1.46	0.85	0.69	0.47	0.34
- 2.00	3.47	2.91	1.14	2.43	1.96	1.45	0.85	0.68	0.46	0.33
- 2.50	3.05	2.63	1.05	2.32	1.81	1.34	0.76	0.62	0.43	0.31
- 2.85	2.45	2.01	0.73	1.70	1.26	0.97	0.60	0.46	0.30	0.23

Table (2): Calibration of nozzle

Velocity heads in the horizontal plane at different radii (m.m. water)

Exp. No. / Dist. from pipe axis (inch)	1	2	3	4	5	6	7	8	9	10
+ 2.66	3.01	2.58	0.98	2.21	1.66	1.31	0.74	0.59	0.43	0.31
+ 2.50	3.25	2.72	1.05	2.35	1.87	1.34	0.78	0.63	0.45	0.34
+ 2.00	3.48	2.93	1.16	2.54	1.99	1.47	0.85	0.68	0.48	0.36
+ 1.50	3.54	2.92	1.17	2.46	1.95	1.48	0.85	0.67	0.46	0.35
+ 1.00	3.51	2.96	1.16	2.43	1.98	1.48	0.88	0.70	0.48	0.36
+ 0.50	3.59	3.02	1.18	2.50	2.01	1.49	0.87	0.70	0.48	0.35
0.00	3.49	2.92	1.13	2.41	1.96	1.45	0.84	0.67	0.46	0.34
- 0.50	3.51	3.02	1.18	2.49	1.99	1.49	0.87	0.69	0.48	0.35
- 1.00	3.49	2.95	1.15	2.40	1.96	1.47	0.87	0.69	0.48	0.34
- 1.50	3.47	2.91	1.14	2.39	1.93	1.44	0.85	0.67	0.46	0.34
- 2.00	3.42	2.94	1.14	2.42	1.92	1.44	0.85	0.67	0.47	0.34
- 2.50	3.28	2.66	1.05	2.33	1.85	1.34	0.78	0.63	0.45	0.34
- 2.85	2.63	2.23	0.88	1.92	1.50	0.99	0.64	0.51	0.36	0.26

Table (3): Calibration of nozzle. Observations

Exp.No.	1	2	3	4	5	6	7	8	9	10
Date (1954)	7-9	7-9	8-9	8-9	9-9	9-9	10-9	10-9	13-9	13-9
Bar.press. (m.m.Hg)	76.1	76.1	76.0	76.0	75.8	75.8	75.9	75.9	76.0	76.0
Dry B.T.(deg.F)	65.5	66.1	65.5	66.0	65.0	65.1	63.1	63.5	63.5	63.6
Wet B.T.(deg.F)	61.1	61.5	61.1	61.7	60.1	60.5	58.6	59.0	59.0	59.1
Pn (inches water)	4.00	3.30	1.30	2.80	2.20	1.65	0.95	0.75	0.55	0.35

Table (4): Calibration of nozzle. Results

Exp.No.	1	2	4	5	6	3	7	8	9	10
Amount of air (lbs/min)	20.73	18.85	17.35	15.45	13.34	11.76	10.24	9.10	7.61	6.50

Table (5): Calibration of small total head tube

H_s = reading of standard Pitot tube (m.m. water)

H_a = reading of small tube (m.m. water)

Position 1	H_s	0.92	1.78	3.05	3.97	5.62	7.47
	H_a	0.89	1.69	2.88	3.76	5.32	7.07
2	H_s	0.85	1.40	3.16	4.63	6.18	7.92
	H_a	0.82	1.32	2.97	4.30	5.85	7.39
3	H_s	0.66	1.57	2.88	4.15	6.82	8.60
	H_a	0.64	1.51	2.76	3.98	6.50	8.25
4	H_s	0.76	1.93	3.20	5.16	6.84	8.07
	H_a	0.75	1.86	3.02	4.88	6.47	7.64
5	H_s	0.74	1.63	2.86	4.12	6.95	8.72
	H_a	0.74	1.53	2.66	3.86	6.55	8.22
6	H_s	0.81	1.92	3.04	4.88	6.19	8.20
	H_a	0.76	1.83	2.90	4.77	5.92	7.84

Table (6). Observations of heat transfer experiments, Gap = 1/16"

Ex.No.	Date	B.P.	D.B.T.	W.B.T.	P_n	I.M.H. watts	I.M.H. Btu/hr	I.G.H. watts	t_w m.v.	t_d m.v.	t_i m.v.	t_o m.v.	t_a m.v.
1	10.2.55	76.0	63	55	0.03	282.1	963	98.2	3.177	1.096	1.94	2.105	1.055
2	10.2.55	76.0	63	55	0.35	511.0	1743	132.8	3.127	0.876	2.05	1.555	0.875
3	11.2.55	75.9	59	52	0.05	337.9	1151	110.0	3.262	1.069	1.95	2.14	0.985
4	14.2.55	75.8	62	55	0.01	230.5	786	86.6	3.239	1.426	1.96	2.24	1.315
5	15.2.55	75.9	60	53	0.005	179.7	613	70.4	3.213	1.533	1.905	2.18	1.40
6	15.2.55	75.9	60	53	0.27	481.9	1643	132.0	3.078	0.819	1.945	1.54	0.81
7	16.2.55	75.2	55	48	0.10	390.2	1331	116.8	3.194	0.811	1.895	1.84	0.76
8	16.2.55	75.2	57	49	0.15	433.4	1477	125.5	3.176	0.853	1.91	1.775	0.80
9	17.2.55	74.4	60	51	0.02	265.8	906	96.0	3.174	1.226	1.925	2.155	1.14
10	31.3.55	76.7	58	49	0.10	388.1	1324	116.8	3.286	0.904	1.98	1.905	0.845
11	31.3.55	76.7	60	50	0.40	499.6	1702	130.0	2.954	0.874	1.99	1.45	0.865
12	1.4.55	76.9	62	53	0.50	532.5	1817	132.9	2.776	0.826	1.955	1.34	0.845
13	1.4.55	76.9	63	54	0.60	589.0	2009	144.2	2.811	0.849	2.035	1.355	0.885
14	4.4.55	76.5	65	55	0.65	628.6	2140	150.3	2.909	0.901	2.135	1.44	0.93

Table (7) : Observations of heat transfer experiments, Gap = $\frac{1}{8}$".

Ex.No.	Date	B.P.	D.B.T	W.B.T	P_n	I.M.H. watts	I.M.H. Btu/hr	I.G.H. watts	t_w m.v.	t_d m.v.	t_i m.v.	t_o m.v.	t_a m.v.
1	26.1.55	75.9	61	54	0.10	232.0	792	71.2	2.95	0.824	1.75	1.75	0.815
2	26.1.55	75.9	62	55	0.20	274.0	935	76.8	2.933	0.814	1.77	1.62	0.82
3.	27.1.55	75.6	61	54	0.40	372.5	1270	96.9	2.974	0.864	1.975	1.47	0.79
4	27.1.55	75.6	62	55	0.60	444.2	1513	111.0	2.899	0.781	1.96	1.355	0.83
5	28.1.55	75.3	60	53	1.10	591.0	2018	141.4	2.823	0.734	2.075	1.27	0.765
6	31.1.55	74.7	64	57	0.05	210.0	716	71.7	3.09	0.949	1.88	1.91	0.95
7	1.2.55	74.2	63	57	0.005	130.8	446	52.2	2.954	1.216	1.90	1.94	1.195
8	1.2.55	74.2	63	57	0.01	166.9	569	63.5	3.136	1.082	1.915	1.98	1.065
9	2.2.55	74.7	65	58	0.02	179.6	613	66.6	3.081	1.04	1.915	1.945	1.045
10	2.2.55	74.7	66	59	0.03	191.4	653	71.0	3.083	1.011	1.905	1.93	1.02
11	3.2.55	73.9	67	59	0.50	390.3	1331	99.1	2.916	0.856	1.94	1.41	0.92
12	4.2.55	74.5	67	58	0.80	499.0	1700	121.1	3.011	0.874	2.105	1.43	0.915
13	23.3.55	74.9	62	55	0.15	259.2	884	75.1	3.047	0.837	1.79	1.69	0.85
14	24.3.55	75.3	63	56	0.30	317.5	1083	85.7	2.998	0.818	1.85	1.48	0.845
15	24.3.55	75.3	63	56	0.95	526.5	1797	126.2	2.797	0.786	2.02	1.31	0.815
16	25.3.55	75,7	66	58	1.40	587.0	2005	132.7	2.75	0.834	2.13	1.315	0.875
17	28.3.55	75.9	66	58	1.70	609.6	2078	137.0	2.656	0.324	2.10	1.26	0.875
18	28.3.55	75.9	67	58	2.17	651.0	2220	146.2	2.633	0.833	2.125	1.24	0.915
19	29.3.55	76.2	60	51	0.10	233.8	797	71.2	2.942	0.786	1.735	1.685	0.795
20	30.3.55	77.2	60	51	0.40	372.5	1270	96.9	2.856	0.736	1.83	1.33	0.750

Table (8) : Observations of heat transfer experiments. Gap = 3/16".

Ex.No.	Date	B.P.	D.B.T.	W.B.T	P_n	I.M.H. watts	I.M.H. Btu/hr	I.G.H. watts	t_w m.v.	t_d m.v.	t_i m.v.	t_o m.v.	t_a m.v.
1	26.4.55	76.0	61	53	0.10	238.1	812	71.0	3.287	0.876	1.885	1.80	0.825
2	26.4.55	76.0	63	55	0.30	327.8	1118	82.0	2.987	0.827	1.925	1.52	0.825
3	27.4.55	76.0	66	58	0.50	353.9	1207	82.0	2.814	0.863	1.93	1.48	0.895
4	27.4.55	76.0	67	59	1.00	456.5	1559	96.6	2.864	0.861	2.00	1.44	0.905
5	28.4.55	76.0	66	58	0.01	125.0	426	43.5	2.887	1.089	1.81	1.865	1.07
6	28.4.55	76.0	67	59	0.02	146.7	500	47.5	3.007	1.071	1.845	1.88	1.045
7	29.4.55	75.8	68	61	0.03	164.9	563	49.1	3.069	1.063	1.86	1.90	1.05
8	2.5.55	76.0	66	58	1.30	524.5	1788	113.0	2.874	0.811	2.035	1.39	0.855
9	3.5.55	75.4	67	59	2.40	607.1	2071	123.1	2.80	0.826	2.08	1.32	0.875
10	4.5.55	74.9	71	63	0.05	169.9	580	54.4	3.113	1.093	1.92	1.93	1.075
11	4.5.55	74.9	71	63	0.20	262.2	895	72.0	3.09	0.986	1.95	1.695	1.02
12	5.5.55	75.6	72	63	2.00	590.0	2012	122.6	2.929	0.92	2.155	1.43	0.98
13	5.5.55	75.6	73	64	2.80	647.0	2206	133.2	2.912	0.933	2.20	1.41	1.01
14	6.5.55	75.5	68	60	1.60	564.6	1924	118.0	2.95	0.852	2.105	1.40	0.91
15	9.5.55	75.5	69	61	0.15	234.0	799	64.8	3.12	0.956	1.91	1.72	0.965

Table (9) : Observations of heat transfer experiments, Gap = $\frac{1}{4}$".

Ex.No.	Date	B.P.	D.B.T	W.B.T.	P_n	I.M.H. watts	I.M.H. Btu/hr	I.G.H. watts	t_w m.v.	t_d m.v.	t_i m.v.	t_o m.v.	t_u m.v.
1	16.12.54	77.0	64	56	1.50	484.7	1651	112.8	2.880	0.764	1.875	1.415	0.815
2	17.12.54	77.1	67	60	0.01	125.4	426	48.5	3.150	1.118	1.875	1.945	1.11
3	20.12.54	76.8	65	58	1.90	519.1	1770	114.2	2.899	0.783	1.90	1.425	0.83
4	21.12.54	76.2	65	58	0.20	262.5	895	72.2	2.965	0.890	1.85	1.645	0.89
5	22.12.54	75.7	64	57	0.05	157.8	538	54.9	3.019	0.973	1.785	1.76	0.925
6	4.1.55	76.0	60	52	0.10	203.1	693	63.0	2.912	0.824	1.77	1.59	0.80
7	5.1.55	76.2	59	51	0.30	306.1	1045	82.8	2.922	0.75	1.83	1.51	0.735
8	6.1.55	75.7	60	53	0.03	141.3	482	51.3	2.956	0.891	1.73	1.745	0.85
9	7.1.55	75.5	60	54	0.02	126.0	430	48.5	2.866	0.911	1.685	1.71	0.86
10	10.1.55	74.6	57	52	0.50	382.6	1305	99.2	2.965	0.686	1.91	1.61	0.665
11	11.1.55	74.7	59	53	0.005	106.1	362	42.5	2.877	0.994	1.735	1.635	0.97
12	12.1.55	74.7	60	53	0.10	233.5	796	69.6	3.237	0.833	1.90	1.72	0.80
13	13.1.55	74.8	59	52	2.10	585.0	1997	129.4	2.946	0.667	1.96	1.28	0.69
14	14.1.55	74.8	62	55	1.00	479.0	1634	114.7	3.193	0.769	1.965	1.565	0.80
15	21.1.55	75.5	59	52	1.30	495.0	1689	115.0	2.922	0.691	1.915	1.37	0.695
16	15.3.55	76.4	63	55	0.02	132.8	453	48.8	3.022	1.013	1.78	1.81	0.99
17	16.3.55	76.7	63	55	1.80	530.4	1810	115.0	3.009	0.777	2.01	1.39	0.785
18	16.3.55	76.7	64	56	2.60	561.0	1914	123.8	2.867	0.794	1.955	1.405	0.83
19	17.3.55	76.5	64	54	1.40	467.0	1593	112.4	2.876	0.791	1.90	1.475	0.835
20	17.3.55	76.5	64	54	3.00	584.1	1992	124.2	2.867	0.761	2.02	1.295	0.795
21	18.3.55	76.4	64	54	0.03	139.4	475	51.3	3.022	0.994	1.785	1.795	0.965
22	18.3.55	76.4	65	55	1.00	423.1	1444	97.6	2.883	0.81	1.905	1.51	0.84
23	21.3.55	76.0	64	55	3.20	593.3	1023	126.7	2.837	0.766	1.975	1.38	0.79
24	22.3.55	75.3	64	56	4.00	630.0	2150	132.1	2.823	0.761	2.015	1.25	0.805

Table (10) : Observations of heat transfer experiments, Gap = $\frac{3}{8}$".

Ex.No.	Date	B.P.	D.B.T	W.B.T	P_n	I.M.H. watts	I.M.H. Btu/hr	I.G.H. watts	t_w m.v.	t_d m.v.	t_i m.v.	t_o m.v.	t_a m.v.
1	23.2.55	75.5	57	51	0.20	268.8	917	75.3	3.104	0.77	1.88	1.67	0.725
2	24.2.55	75.1	59	52	0.40	319.0	1089	83.0	3.122	0.767	1.88	1.62	0.745
3	24.2.55	75.1	59	52	1.00	397.7	1356	95.5	3.014	0.707	1.83	1.45	0.695
4	1.3.55	76.9	61	54	0.05	179.5	612	59.3	3.24	0.931	1.97	1.79	0.86
5	1.3.55	76.9	61	54	0.02	120.0	409	43.2	3.004	0.95	1.745	1.725	0.89
6	2.3.55	77.3	57	50	0.03	152.0	519	51.7	3.182	0.884	1.88	1.73	0.795
7	2.3.55	77.3	58	51	0.10	219.7	750	66.0	3.102	0.827	1.92	1.71	0.765
8	3.3.55	77.1	59	51	0.70	363.4	1239	90.9	3.04	0.733	1.83	1.52	0.72
9	3.3.55	77.1	59	51	2.00	514.2	1753	113.1	3.122	0.697	1.94	1.39	0.705
10	4.3.55	76.9	60	52	0.01	109.4	373	41.6	3.021	0.983	1.76	1.76	0.915
11	7.3.55	76.6	54	47	2.60	554.5	1890	122.0	3.006	0.574	1.86	1.23	0.575
12	9.3.55	76.1	59	51	1.50	445.9	1521	102.5	2.969	0.691	1.85	1.385	0.695
13	9.3.55	76.1	60	52	3.00	565.5	1930	122.8	3.102	0.71	1.98	1.345	0.725
14	10.3.55	77.1	60	51	3.70	588.0	2007	124.0	3.019	0.681	1.955	1.275	0.705
15	11.3.55	76.7	60	51	4.50	609.5	2079	127.2	2.981	0.699	1.97	1.255	0.71

Table (11) : Observations of heat transfer experiments, Gap = $\frac{1}{2}$"

Ex.No.	Date	B.P.	D.B.T.	W.B.T.	P_n	I.M.H. watts	I.M.H. Btu/hr	I.G.H. watts	t_w m.v.	t_{cd} m.v.	t_i m.v.	t_o m.v.	t_a m.v.
1	11.5.55	76.5	66	58	1.00	348.4	1189	83.4	2.973	0.857	1.905	1.55	0.855
2	12.5.55	76.4	62	54	3.60	537.0	1831	114.8	3.037	0.754	2.00	1.37	0.755
3	13.5.55	76.0	68	59	2.00	436.8	1490	97.3	3.071	0.861	2.00	1.51	0.88
4	17.5.55	74.3	62	57	0.10	193.5	660	57.7	2.949	0.899	1.89	1.685	0.845
5	17.5.55	74.3	62	58	0.40	276.0	941	72.2	2.948	0.817	1.855	1.59	0.795
6	18.5.55	75.6	62	55	0.30	233.3	796	62.7	2.959	0.853	1.86	1.625	0.82
7	18.5.55	75.6	62	55	0.70	331.9	1131	81.7	3.002	0.797	1.87	1.56	0.79
8	19.5.55	76.5	63	55	1.60	400.5	1366	89.2	2.918	0.77	1.87	1.435	0.77
9	19.5.55	76.5	64	56	4.20	565.0	1927	119.1	3.124	0.811	2.10	1.41	0.82
10	20.5.55	76.5	67	59	0.02	122.0	416	42.7	3.008	1.086	1.935	1.76	1.035
11	23.5.55	76.2	68	59	3.00	486.5	1660	108.2	3.057	0.859	2.02	1.46	0.895
12	25.5.55	76.0	66	60	0.01	98.0	334	42.5	3.08	1.119	1.925	1.78	1.04
13	25.5.55	76.0	66	60	0.05	157.0	535	52.2	2.942	0.97	1.925	1.72	0.93
14	26.5.55	75.8	65	58	4.55	566.0	1930	123.8	3.081	0.807	2.07	1.39	0.83

Table (12) : Observations of heat transfer experiments, Gap = $\frac{3}{4}$".

Ex.No.	Date	B.P.	D.B.T	W.B.T.	P_n	I.M.H. watts	I.M.H. Btu/hr.	I.G.H. watts	t_w m.v.	t_d m.v.	t_i m.v.	t_o m.v.	t_a m.v.
1	11.7.55	76.2	74	67	0.02	115.8	395	42.0	3.077	1.249	2.10	1.86	1.18
2	12.7.55	76.4	74	66	0.05	146.3	499	46.8	3.072	1.203	2.11	1.86	1.155
3	12.7.55	76.4	74	66	0.10	180.4	615	55.5	3.088	1.129	2.11	1.82	1.09
4	13.7.55	76.5	74	66	0.20	213.0	726	59.5	3.079	1.107	2.115	1.785	1.085
5	13.7.55	76.5	74	66	0.40	254.9	869	66.1	3.052	1.051	2.115	1.715	1.04
6	14.7.55	76.4	73	65	0.70	290.4	990	69.5	3.032	1.04	2.115	1.64	1.04
7	14.7.55	76.4	73	65	1.00	338.0	1152	81.8	3.09	0.983	2.14	1.59	0.98
8	15.7.55	76.8	73	66	1.50	363.1	1239	85.0	3.013	0.971	2.14	1.505	0.99
9	15.7.55	76.3	73	66	2.00	391	1333	87.1	3.006	0.98	2.17	1.475	1.00
10	18.7.55	76.4	73	66	2.50	416	1420	90.1	2.974	0.943	2.13	1.42	0.99
11	18.7.55	76.4	74	66	3.00	435	1483	96.0	2.977	0.973	2.185	1.43	1.015
12	19.7.55	76.6	74	66	3.50	464	1581	101.8	3.046	0.961	2.22	1.41	1.025
13	19.7.55	76.6	74	66	4.00	481.8	1642	103.0	3.056	0.961	2.245	1.40	1.035
14	20.7.55	76.6	74	66	4.50	503	1715	109.4	3.067	0.991	2.285	1.41	1.035

Table (13) : Observations of heat transfer experiments, Gap = 1"

Ex.No.	Date	B.P.	F.B.T	W.B.T	P_n	I M.H. watts	I M.H. Btu/hr	I.G.H. watts	t_w m.v.	t_d m.v.	t_i m.v.	t_o m.v.	t_a m.v.
1	21.7.55	76.7	72	65	0.05	141.3	482	47.3	3.067	1.114	2.08	1.75	1.055
2	21.7.55	76.7	73	66	0.10	169.0	576	54.2	3.139	1.124	2.145	1.75	1.09
3	25.7.55	76.5	72	65	0.20	200.8	685	56.5	3.118	1.042	2.115	1.655	1.02
4	25.7.55	76.5	73	66	0.40	233.0	795	65.0	3.134	1.030	2.14	1.60	1.02
5	26.7.55	76.3	71	64	0.80	274.3	936	73.4	3.083	0.966	2.125	1.47	0.97
6	26.7.55	76.3	72	65	1.40	307.1	1048	79.8	3.032	0.981	2.13	1.415	0.99
7	27.7.55	76.2	72	65	2.00	342.4	1169	81.4	3.023	0.924	2.115	1.335	0.945
8	27.7.55	76.2	73	66	2.70	361.2	1231	84.0	3.004	0.943	2.125	1.32	0.98
9	28.7.55	76.2	73	65	3.50	400.8	1367	87.8	3.053	0.943	2.16	1.30	0.98
10	28.7.55	76.2	73	66	4.50	437.8	1492	103.1	3.080	0.937	2.19	2.27	0.975

Table (14) : Results of heat transfer experiments, Gap = 1/16".

Ex.No.	Q	t_w deg.F	t_d deg.F	t_i deg.F	t_o deg.F	t_a deg.F	H_r	H_c	H_o	h	U_m	k	μ	R_e	Nu
5	43.9	180.4	106.0	122.8	135.1	93.7	103	8	502	6.07	9.58	.0154	.0456	2565	2.05
4	62.1	181.6	101.0	125.3	137.8	89.9	109	8	669	7.62	13.55	.0153	.0454	3650	2.60
9	87.8	178.3	91.6	123.7	133.9	82.5	116	8	782	8.50	19.16	.0152	.0449	5210	2.92
1	107.4	178.8	85.5	124.4	131.7	78.9	122	9	832	8.71	23.40	.0151	.0447	6400	3.01
3	139.0	182.6	84.3	124.9	133.3	75.9	129	9	1013	9.94	30.30	.0150	.0445	8340	3.45
7	196.2	179.6	72.0	122.4	120.9	66.0	136	10	1185	10.92	42.80	.0148	.0439	11860	3.85
10	196.2	183.6	76.4	126.2	122.8	69.7	139	10	1175	10.80	42.80	.0149	.0441	11880	3.78
8	240.4	178.8	74.0	123.1	117.0	67.8	131	10	1336	12.60	52.40	.0148	.0440	14600	4.45
6	322.0	174.6	72.3	124.6	106.3	68.2	127	10	1506	14.80	70.16	.0148	.0440	19700	5.20
2	367.2	176.7	75.1	129.2	107.0	71.1	129	10	1604	15.91	80.00	.0149	.0442	22150	5.57
11	393.0	169.2	75.0	126.6	102.1	70.6	117	10	1575	16.70	85.61	.0149	.0442	23700	5.85
12	439.8	161.4	72.6	125.1	97.0	69.7	107	10	1700	19.41	95.82	.0149	.0441	26500	6.84
13	480.6	162.9	73.8	128.6	97.7	71.5	108	10	1891	21.66	105.0	.0149	.0442	29000	7.60
14	501.0	167.3	76.3	133.0	101.7	73.5	113	9	2018	22.55	109.2	.0149	.0443	30200	7.90

Table (15) : Results of heat transfer experiments, Gap $\frac{1}{8}$".

Ex.No.	Q	t_w deg.F	t_d deg.F	t_i deg.F	t_o deg.F	t_a deg.F	H_r	H_c	H_o	h	U_m	k	μ	R_e	Nu
7	43.9	169.2	91.2	122.6	124.4	84.9	100	8	338	4.20	4.78	.0152	.0451	2590	2.89
8	62.1	177.1	84.9	123.3	126.2	79.3	121	8	440	4.71	6.77	.0151	.0447	3710	3.25
9	87.8	174.7	82.9	123.3	124.6	78.4	118	8	487	5.28	9.56	.0151	.0446	5240	3.65
10	107.4	174.8	81.5	122.8	124.0	77.4	120	8	525	5.65	11.70	.0150	.0446	6410	3.90
6	139.0	175.1	78.6	121.7	123.1	74.4	123	9	524	6.07	15.14	.0150	.0444	8370	4.22
1	196.2	169.0	72.6	115.9	115.9	68.4	119	9	664	6.91	21.40	.0148	.0440	11900	4.87
19	196.2	168.7	70.7	115.1	112.9	67.5	120	9	668	6.90	21.40	.0148	.0440	11900	4.87
13	240.4	173.2	73.2	117.7	113.1	70.0	125	10	749	7.59	26.20	.0149	.0441	14510	5.32
2	277.8	168.3	72.1	116.8	110.0	68.7	118	9	808	8.48	30.27	.0148	.0440	16820	5.97
14	340.2	171.1	72.3	120.4	103.5	69.7	122	10	951	9.82	37.07	.0149	.0441	20530	6.89
3	393.0	170.1	74.5	126.0	103.1	67.3	119	10	1141	11.64	42.81	.0148	.0438	23900	8.21
20	393.0	164.9	68.3	119.5	96.5	65.6	117	9	1144	12.11	42.81	.0148	.0438	23900	8.53
11	439.8	167.6	74.1	124.4	100.3	73.1	114	10	1207	13.36	47.90	.0149	.0443	26500	9.35
4	480.6	166.8	70.5	125.3	97.7	69.1	117	10	1386	14.83	52.37	.0148	.0441	29000	10.45
12	555.0	171.7	75.0	131.7	101.2	72.8	121	10	1569	16.61	60.48	.0149	.0443	33500	11.65
15	605.5	162.3	70.7	127.9	95.6	68.4	110	9	1678	18.72	66.00	.0148	.0440	36600	13.22
5	651.0	163.5	68.2	130.3	93.7	66.2	115	9	1894	20.40	70.97	.0148	.0439	39500	14.40
16	734.4	160.3	73.1	132.7	95.8	71.1	105	8	1892	22.20	80.00	.0149	.0442	44200	15.58
17	809.4	156.2	72.6	131.5	93.3	71.1	100	8	1970	24.20	88.15	.0149	.0442	48700	17.00
18	914.5	155.2	73.0	132.6	92.3	72.8	98	8	2114	26.85	99.62	.0149	.0443	55000	18.85

Table (16) : Results of heat transfer experiments, Gap 3/16".

Ex.No.	Q	t_w deg.F	t_d deg.F	t_i deg.F	t_o deg.F	t_a deg.F	H_r	H_c	H_o	h	U_m	k	μ	R_e	Nu
5	62.1	166.3	85.2	118.6	121.0	79.5	102	8	316	3.81	4.51	.0151	.0447	3700	3.96
6	87.8	171.5	84.4	120.1	121.7	78.4	111	8	381	4.29	6.38	.0151	.0446	5230	4.44
7	107.4	174.2	84.0	120.8	122.6	78.7	116	9	438	4.80	7.79	.0151	.0446	6410	4.98
10	139.0	176.1	85.4	123.5	124.0	79.7	118	9	453	4.92	10.08	.0151	.0447	8300	5.10
1	196.2	183.6	75.1	122.0	118.1	68.9	143	11	658	6.00	14.24	.0148	.0440	11880	6.35
15	240.4	176.4	78.9	123.1	114.5	75.0	124	10	665	6.87	17.45	.0150	.0444	14470	7.18
11	277.8	175.1	80.3	124.9	113.3	77.4	121	10	764	8.18	20.15	.0150	.0446	16600	8.55
2	340.2	170.6	72.7	123.7	105.4	68.9	121	10	,987	10.16	24.69	.0148	.0440	20600	10.75
3	439.8	163.1	74.5	124.0	103.5	72.0	108	9	1090	12.50	31.92	.0149	.0442	26500	13.13
4	621.0	165.3	74.4	127.1	101.7	72.4	112	9	1438	16,21	45,10	.0149	.0443	37400	17.08
8	707.5	165.7	72.0	128.5	99.3	70.2	114	9	1665	18.24	51.36	.0149	.0441	42700	19.20
14	785.0	169.0	73.9	131.7	99.8	72.6	118	7	1799	19.51	57.00	,0149	.0443	47200	20.52
12	887.8	168.1	77.2	134.0	101.2	75.7	113	9	1890	21,40	63.75	.0150	.0445	52500	22.35
9	960.3	162.5	72.7	130.6	96.0	71.1	109	9	1953	22.33	69.75	.0149	.0442	57900	23.53
13	1036.1	167.4	77.8	136.0	100.3	76.9	112	9	2085	24.16	75.16	.0150	.0446	61900	25.20

Table (17) Results of heat transfer experiments, Gap = $\frac{1}{4}$".

Exp.No	Q	t_w deg.F	t_d deg.F	t_i deg.F	t_o deg.F	t_a deg.F	H_r	H_c	H_o	h	U_m	k	μ	R_e	Nu
1															
11	43.9	165.9	80.7	115.2	110.6	75.2	106	9	247	2.84	2.39	.0150	.0444	2630	3.96
2	62.1	177.7	86.5	121.5	124.6	81.2	119	9	298	3.23	3.39	.0151	.0448	3700	4.45
9	87.8	165.4	76.8	112.9	114.0	70.4	109	9	312	3.43	4.79	.0149	.0442	5300	4.80
16	87.8	172.2	81.6	117.2	118.6	76.1	115	9	329	3.59	4.79	.0150	.0445	5250	4.97
8	107.4	169.3	75.8	114.9	115.6	70.0	116	9	357	3.76	5.86	.0149	.0441	6490	5.27
21	107.4	172.2	80.7	117.5	117.9	75.0	116	9	350	3.77	5.86	.0150	.0444	6450	5.24
5	139.0	172.0	79.7	117.5	116.3	73.3	117	9	412	4.37	7.60	.0149	.0443	8380	6.10
6	196.2	167.4	72.6	116.8	108.6	67.8	116	9	568	5.96	10.70	.0148	.0440	11880	8.41
12	196.2	181.5	73.0	122.6	114.5	67.8	139	11	646	5.95	10.70	.0148	.0440	11880	8.40
4	277.8	169.7	75.8	120.4	111.1	71.7	117	9	769	8.22	15.15	.0149	.0442	16740	11.51
7	340.2	167.8	69.0	119.5	104.9	64.9	120	10	915	9.33	18.57	.0147	.0438	20700	13.26
10	439.8	169.7	65.9	123.1	109.5	62.0	126	9	1170	11.33	24.00	.0147	.0436	26700	16.02
14	621.0	179.6	69.9	125.5	107.4	67.8	139	11	1484	13.91	33.89	.0148	.0440	37750	19.61
22	621.0	166.1	71.9	122.9	104.9	69.5	115	9	1320	14.31	33.89	.0149	.0441	37600	20.00
15	707.5	167.8	66.1	123,3	98.4	63.3	123	9	1557	15.60	38.60	.0147	.0437	43100	22.18
19	734.4	165.8	71.0	122.6	103.3	69.3	115	9	1469	15.92	40.08	.0149	.0441	44400	22.26
1	761.0	166.0	69.7	121.5	100.5	68.4	117	10	1524	16.34	41.50	.0148	.0440	46100	22.95
17	833.4	171.6	70.3	127.4	99.3	67.1	125	10	1675	16.75	45.50	,0148	,0440	50500	23.62
3	855.0	166.8	70.6	122.6	100.9	69.1	119	10	1641	17.60	46.65	.0149	.0441	51600	24.60
13	900.0	168.9	65.0	125.3	94.2	63.1	127	10	1860	18.42	49.11	.0147	.0437	54900	26.15
18	1000.0	165.4	71.1	125.1	100.0	69.1	115	9	1790	19.45	54.50	.0149	.0441	60500	27.12
20	1073.0	165.4	69.5	127.9	94.8	67.5	115	10	1867	19.95	58.50	.0148	,0440	64900	28.20
23	1110.0	164.1	69.8	126.0	98.9	67.3	114	9	1900	20.57	60.50	.0148	.0440	67200	28.90
24	1242.0	163.5	69.5	127.7	92 8	68.0	113	10	2027	22.25	67.75	.0148	.0440	75200	31.50

Table (18): Results of heat transfer experiments, Gap = $\frac{3}{8}$".

Ex. No.	Q	t_w deg.F	t_d deg.F	t_i deg.F	t_o deg.F	t_a deg.F	H_r	H_c	H_o	h	U_m	k	μ	R_e	Nu
10	62.1	172.1	80.2	116.3	116.3	72.8	117	9	247	2.61	2.26	.0149	.0443	3740	5.49
5	87.8	171.4	78.6	115.6	114.7	71.7	117	9	283	2.97	3.19	.0149	.0442	5290	6.25
6	107.4	179.1	75.5	121.7	114.9	67.6	132	10	377	3.55	3.90	.0148	.0440	6500	7.50
4	139.0	181.6	77.7	125.7	117.7	70.4	133	10	469	4.39	5.04	.0149	.0441	8400	9.20
7	196.2	175.6	72.7	123.5	114.0	66.3	129	10	611	5.85	7.12	.0148	.0439	11910	12.35
1	277.8	175.7	70.0	121.7	112.2	64.5	132	10	775	7 29	10.09	.0147	.0438	16900	15.50
2	393.0	176.3	69.3	121.7	110.0	65.3	134	10	945	8.88	14.27	.0147	.0438	23900	18.85
8	519.0	172.9	68.1	119.5	105.4	64.3	129	10	1100	10.60	18.83	.0147	.0438	31500	22.50
3	621.0	171.8	66.9	119.5	102.1	63.2	129	11	1216	11.71	22.56	.0147	.0437	37900	24.96
12	761.0	169.9	66.1	120.4	99.1	63.2	126	10	1385	13.60	27.68	.0147	.0437	46300	29.00
9	877.8	176.5	66.4	124.4	99.3	63.7	136	11	1606	14.90	31.80	.0147	.0437	53400	31.75
11	1000.0	171.5	60.4	120.8	91.9	58.0	134	12	1744	16.09	36.33	.0146	.0434	61300	34.50
13	1073.0	175.6	67.0	126.2	97.2	64.5	135	11	1784	16.80	39.00	.0147	.0438	65100	35.80
14	1192	172.0	65.6	125.1	94.0	63.7	130	11	1866	18.02	43.32	.0147	.0437	72600	38.40
15	1316.4	170.4	66.5	125.7	93.0	63.9	127	11	1941	19.08	47.83	.0147	.0437	80100	40.50

Table (19): Results of heat transfer experiments, Gap = $\frac{1}{2}$".

Ex.No	Q	t_w deg.F	t_d deg.F	t_i deg.F	t_o deg.F	t_a deg.F	H_r	H_c	H_o	h	U_m	k	μ	R_e	Nu
12	62.1	174.7	86.6	123.7	117.2	78.2	114	9	211	2.29	1.69	.0151	.0446	3710	6.34
10	87.8	171.5	85.0	124.2	116.3	78.0	111	9	296	3.31	2.39	.0151	.0446	5230	9.17
13	139.0	168.7	79.6	123.7	114.5	73.5	112	8	415	4.56	3.80	.0149	.0443	8380	12.76
4	196.2	169.0	76.2	122.2	112.9	69.7	116	9	535	5.63	5.35	.0149	.0441	11860	15.76
6	277.8	169.4	74.0	120.8	110.1	68.7	118	9	669	6.95	7.58	.0148	.0440	16850	19.56
5	393.0	168.9	72.3	120.6	108.6	67.5	119	9	813	8.38	10.71	.0148	.0440	23750	23.60
7	519.0	171.3	71.3	121.3	107.2	67.3	124	10	997	10.03	14.15	.0148	.0440	31400	28.29
1	621.0	170.1	74.2	122.9	106.7	70.2	119	10	1060	11.10	16.95	.0149	.0441	37500	31.10
8	785.0	167.7	70.0	121.3	101.4	66.5	119	10	1237	12.78	21.42	.0148	.0439	47700	36.00
3	877.8	174.3	74.4	127.1	104.9	71.3	126	10	1354	13.76	23.97	.0149	.0442	52900	38.50
11	1073.0	173.7	74.3	128.0	102.6	72.0	125	10	1525	15.72	29.23	.0149	.0442	64600	44.00
2	1176.6	172.8	69.2	127.1	98.4	65.8	128	11	1692	16.52	32.11	.0148	.0438	71400	46.60
9	1272.0	176.6	72.0	131.5	100.3	68.7	132	11	1784	17.30	34.75	.0148	.0440	77000	48.90
14	1323.0	174.7	71.7	130.1	99.3	69.1	129	11	1790	17.71	36.10	.0148	.0441	80000	50.00

Table (20): Results of heat transfer experiments, Gap = $\frac{3}{4}$".

Ex.No.	Q	t_w deg.F	t_d deg.F	t_i deg.F	t_o deg.F	t_a deg.F	H_r	H_c	H_o	h	U_m	k		R_e	Nu
1	87.8	174.5	92.7	131.5	120.8	84.2	108	8	279	3.23	1.59	.0152	.0450	5190	13.29
2	139.0	174.3	90.6	131.9	120.8	83.2	110	8	381	4.38	2.53	.0152	.0450	8240	18.04
3	196.2	175.0	87.1	131.9	119.0	80.4	114	8	493	5.45	3.56	.0151	.0448	11660	22.59
4	277.8	174.6	86.1	132.1	117.4	80.2	114	9	603	6.69	5.04	.0151	.0448	16520	27.73
5	393.0	173.5	83.4	132.1	114.3	78.2	115	9	745	8.20	7.13	.0151	.0446	23500	34.00
6	519.0	172.6	82.9	132.1	110.9	78.2	115	9	866	9.61	9.41	.0151	.0446	30900	39.90
7	621.0	175.1	80.2	133.3	108.6	75.6	121	9	1022	10.74	11.28	.0150	.0445	37200	44.72
8	761.0	171.8	79.6	133.3	104.7	76.1	116	9	1114	12.18	13.83	.0150	.0445	45500	50.70
9	877.8	171.5	80.0	134.6	103.3	76.5	116	9	1208	13.30	15.95	.0150	.0445	52400	55.50
10	981.6	170.1	78.2	132.7	100.7	76.1	115	9	1296	14.43	17.80	.0150	.0445	58900	60.13
11	1073.0	170.2	79.7	135.3	101.2	77.2	114	9	1360	15.29	19.49	.0150	.0446	64000	63.70
12	1162.8	173.2	79.2	136.9	100.3	77.6	119	10	1452	15.90	21.11	.0150	.0446	69300	66.30
13	1242.0	173.6	79.2	138.0	99.8	78.0	120	10	1512	16.54	22.56	.0151	.0446	74100	68.60
14	1316.4	174.1	80.6	139.8	100.3	78.0	119	9	1587	17.25	23.89	.0151	.0446	78500	71.60

Table (21): Results of heat transfer experiments, Gap = 1".

Ex.No.	Q	t_w deg.F	t_d deg.F	t_i deg.F	t_o deg.F	t_a deg.F	H_r	H_c	H_o	h	U_m	k	μ	R_e	Nu
1	139.0	174.1	86.4	130.3	116.0	78.9	114	9	359	3.95	1.90	.0151	.0447	8300	21.80
2	196.2	177.2	86.9	133.5	116.0	80.3	118	9	449	4.85	2.67	.0151	.0448	11680	26.78
3	277.8	176.3	83.0	132.1	111.5	77.4	120	9	556	5.89	3.78	.0150	.0446	16600	32.51
4	393.0	177.0	82.4	133.5	108.8	77.4	122	10	663	6.95	5.35	.0150	.0446	23500	38.60
5	555.0	174.3	79.4	132.6	103.3	75.2	122	10	804	8.46	7.55	.0150	.0444	33200	47.00
6	734.4	172.6	80.1	132.8	100.5	76.1	117	10	919	9.98	9.99	.0150	.0445	44000	55.50
7	877.8	172.2	77.4	132.1	96.7	74.1	119	10	1040	11.10	11.96	.0150	.0444	52700	61.85
8	1019.5	171.4	78.3	132.6	96.0	75.6	117	10	1104	12.06	13.87	.0150	.0445	61000	67.12
9	1162.8	173.5	78.3	134.2	95.1	75.6	120	11	1236	13.21	15.83	.0150	.0445	69600	73.60
10	1316.4	174.7	78.0	135.4	93.7	75.4	123	11	1358	14.30	17.90	.0150	.0445	78800	79.60

Table (22) : Velocity distribution between the plates. Observations and results.

Expt.No.	1	2	3	4	5	6	7	8	9	10	11	12	13	14
Gap (inch)	1/8	1/8	1/8	3/16	3/16	3/16	$\frac{1}{4}$	$\frac{1}{4}$	$\frac{1}{4}$	3/8	3/8	$\frac{1}{2}$	$\frac{1}{2}$	$\frac{3}{4}$
Date (1955)	25/1	25/1	23/3	18/4	18/4	18/4	21/12/54	15/12/54	17/12/54	24/2	23/2	11/5	12/5	11/7
P_n(inch H_2O)	0.05	0.40	0.80	0.15	0.60	1.50	0.20	0.90	2.10	0.40	2.00	1.00	3.60	4.00
Bar.press.(cm.Hg)	76.5	76.5	74.9	77.6	77.6	77.6	76.2	77.0	77.1	75.1	75.5	76.5	76.4	76.2
Dry B.T.(deg.F)	61	62	60	57	57	57	65	65	68	59	57	66	63	73
Wet B.T.(deg.F)	54	55	53	51	51	51	58	59	61	52	51	58	55	66
Q (lbs/hr.)	139.0	393.0	555.0	240.4	480.8	760.8	277.8	590.2	900.0	393.0	877.8	621.0	1176.6	1242.0
U_1mea.(ft/sec)	20.64	57.50	81.20	24.2	46.85	74.1	20.6	43.9	65.7	19.5	42.9	23.05	43.2	30.55
U_2mea.(ft/sec)	12.26	34.25	48.08	14.05	28.00	43.0	12.35	25.0	40.1	11.35	25.5	13.4	25.1	17.9
U_1cal.(ft/sec)	20.5	57.9	81.6	23.58	47.12	74.7	20.5	43.5	66.3	19.3	43.2	22.95	43.5	30.5
U_2cal(ft/sec)	12.05	34.0	48.0	13.87	27.7	43.9	12.0	25.6	39.0	11.3	25.3	13.4	25.45	17.9
U_1mea./U_1cal.	1.007	0.993	0.994	1.026	0.994	0.992	1.003	1.009	0.990	1.010	0.994	1.003	0.993	1.001
U_2mea./U_2cal.	1.015	1.006	1.002	1.013	1.010	0.979	1.027	0.977	1.027	1.003	1.007	1.000	0.986	1.000

Table (23): Velocity distribution between the plates

(Gap = $\frac{1}{8}$")

E.N.	Z (inch)	h_{m1} (m.m.H_2O)	Velocity (ft./sec.)	h_{m2} (m.m.H_2O)	Velocity (ft./sec.)
1	0.015	1.95	19.0	0.52	9.9
	0.020	2.40	21.1	0.69	11.4
	0.025	2.73	22.5	0.89	12.9
	0.050	3.18	24.3	1.36	15.9
	0.075	3.14	24.2	1.25	15.3
	0.100	2.66	22.2	0.82	12.3
	0.105	1.88	18.7	0.69	11.4
	0.110	1.43	16.3	0.50	9.7
2	0.015	17.86	57.6	5.38	31.6
	0.020	19.33	59.9	6.11	33.7
	0.025	19.67	60.5	6.91	35.8
	0.050	21.15	62.7	8.09	38.8
	0.075	21.63	63.4	7.50	37.3
	0.100	19.33	59.9	5.93	33.2
	0.105	16.38	55.2	5.72	32.6
	0.110	13.78	50.6	5.13	30.9
3	0.015	35.15	80.9	11.83	46.9
	0.020	36.77	82.6	12.41	48.0
	0.025	38.46	84.5	12.86	48.9
	0.050	40.14	86.4	13.95	50.9
	0.075	40.14	86.4	13.63	50.3
	0.100	38.33	84.4	13.18	49.5
	0.105	36.48	82.4	12.75	48.7
	0.110	30.90	75.3	11.68	46.6

Table (24): Velocity distribution between the plates

(Gap = $\frac{3}{16}$")

E.N.	Z (inch)	h_{m1} (m.m.H_2O)	Velocity (ft./sec.)	h_{m2} (m.m.H_2O)	Velocity (ft./sec.)
4	0.015	1.67	17.6	0.59	10.5
	0.025	3.31	24.8	0.98	13.5
	0.050	4.10	27.6	1.54	16.9
	0.075	4.18	27.9	1.73	17.9
	0.100	4.16	27.8	1.71	17.8
	0.125	3.70	26.2	1.36	15.9
	0.150	2.99	23.6	0.92	13.1
	0.165	2.36	20.9	0.66	11.0
	0.172	1.77	18.1	0.45	9.1
5	0.015	10.52	44.2	3.08	23.9
	0.025	12.24	47.7	4.04	27.4
	0.050	13.50	50.1	5.14	30.9
	0.075	14.09	51.2	5.73	32.6
	0.100	14.00	51.0	5.44	31.8
	0.125	13.60	50.3	4.75	29.7
	0.150	12.50	48.2	3.81	26.6
	0.165	9.72	42.5	2.95	23.4
	0.172	8.19	39.0	2,77	22.7
6	0.015	29.33	73.8	8.58	39.9
	0.025	31.86	77.0	10.26	43.7
	0.050	33.30	78.7	11.53	46.3
	0.075	33.82	79.4	12.38	48.0
	0.100	33.54	79.0	12.20	47.6
	0.125	32.44	77.6	11.48	46.2
	0.150	30.00	74.7	10.17	43.5
	0.165	26.63	70.4	8.09	38.8
	0.172	20.69	62.0	6.83	35.6

Table (25): Velocity distribution between the plates

(Gap = $\frac{1}{4}$")

E.N.	Z (inch)	h_{m1} (m.m.H_2O)	Velocity (ft./sec.)	h_{m2} (m.m.H_2O)	Velocity (ft./sec.)
7	0.015	0.97	13.4	0.48	9.5
	0.025	1.73	17.9	0.67	11.2
	0.050	2.78	22.7	0.97	13.4
	0.075	2.91	23.2	1.08	14.2
	0.100	2.95	23.4	1.15	14.6
	0.125	2.93	23.3	1.13	14.5
	0.150	2.91	23.2	1.07	14.1
	0.175	2.91	23.2	0.92	13.1
	0.200	2.54	21.7	0.76	11.9
	0.225	1.82	18.4	0.55	10.1
	0.235	1.25	15.2	0.47	9.3
8	0.015	7.34	36.9	2.42	21.2
	0.025	10.18	43.5	3.39	25.1
	0.050	12.08	47.4	3.78	26.5
	0.075	12.39	48.0	4.25	28.1
	0.100	12.54	48.3	4.44	28.7
	0.125	12.33	47.9	4.31	28.3
	0.150	11.99	47.2	3.90	26.9
	0.175	11.21	45.6	3.53	25.6
	0.200	9.63	42.3	3.00	23.6
	0.225	8.16	38.9	2.36	20.9
	0.235	7.22	36.6	2.16	20.0
9	0.015	17.27	56.6	6.75	35.4
	0.025	24.23	67.1	7.95	38.4
	0.050	27.75	71.8	9.55	42.1
	0.075	28.09	72.3	10.90	45.0
	0.100	28.04	72.2	11.44	46.1
	0.125	27.99	72.1	11.30	45.8
	0.150	27.21	71.1	9.99	43.1
	0.175	26.02	69.5	8.69	40.2
	0.200	22.33	64.4	7.52	37.4
	0.225	16.35	55.1	6.23	34.0
	0.235	13.94	50.9	5.80	32.8

Table (26): Velocity distribution between the plates

(Gap = $\frac{3}{8}$")

Ex.No.	Z (inch)	h_{m1} (m.m.H_2O)	Velocity (ft./sec.)	h_{m2} (m.m.H_2O)	Velocity (ft./sec.)
10	0.015	0.97	13.4	0.44	9.0
	0.025	1.27	15.4	0.51	9.8
	0.050	2.11	19.8	0.69	11.4
	0.100	2.56	21.8	0.88	12.8
	0.150	2.59	21.9	0.89	12.9
	0.200	2.56	21.8	0.88	12.8
	0.250	2.33	20.8	0.67	11.2
	0.300	1.92	18.9	0.64	10.9
	0.350	1.35	15.8	0.41	8.7
	0.360	1.16	14.7	0.39	8.5
11	0.015	8.02	38.6	2.52	21.6
	0.025	9.31	41.6	2.97	23.5
	0.050	10.73	44.7	3.75	26.4
	0.100	11.32	45.9	4.59	29.2
	0.150	11.24	45.8	4.59	29.2
	0.200	11.22	45.7	4.31	28.3
	0.250	10.62	44.4	3.72	26.3
	0.300	9.12	41.2	2.90	23.2
	0.350	7.25	36.7	1.94	19.0
	0.360	6.67	35.2	1.67	17.6

Table (27): Velocity distribution between the plates
(Gap = $\frac{1}{2}$")

Ex.No.	Z (inch)	h_{m1} (m.m.H_2O)	Velocity (ft./sec.)	h_{m2} (m.m.H_2O)	Velocity (ft./sec.)
12	0.015	1.40	16.1	0.56	10.2
	0.025	2.54	21.7	0.80	12.2
	0.050	3.78	26.5	1.12	14.4
	0.100	3.87	26.8	1.36	15.9
	0.150	3.90	26.9	1.36	15.9
	0.200	3.87	26.8	1.33	15.7
	0.250	3.80	26.6	1.24	15.2
	0.300	3.58	25.8	1.07	14.1
	0.350	3.02	23.7	0.94	13.2
	0.400	2.14	19.9	0.73	11.6
	0.450	1.27	15.4	0.47	9.4
	0.475	1.04	13.9	0.42	8.8
	0.485	0.91	12.9	0.32	7.8
13	0.015	8.09	38.8	2.51	21.6
	0.025	10.26	43.7	3.26	24.6
	0.050	11.99	47.2	3.90	26.9
	0.100	12.76	48.7	4.82	29.9
	0.150	12.84	48.9	4.96	30.4
	0.200	12.97	49.1	4.78	29.8
	0.250	12.84	48.9	4.26	28.1
	0.300	12.54	48.3	3.61	25.9
	0.350	10.72	44.6	2.99	23.6
	0.400	7.65	37.7	2.44	21.3
	0.450	4.77	29.8	1.79	18.2
	0.475	3.56	25.7	1.46	16.5
	0.485	2.93	23.3	1.22	15.0

Table (28): Velocity distribution between the plates

(Gap = $\frac{3}{4}$")

Ex.No	Z (inch)	h_{m1} (m.m.H_2O)	Velocity) (ft./sec.)	h_{m2} (m.m.H_2O)	Velocity (ft./sec.)
14	0.015	3.81	26.6	0.98	13.5
	0.025	4.31	28.3	1.13	14.5
	0.050	4.91	30.2	1.33	15.7
	0.100	5.73	32.6	1.77	18.1
	0.150	6.08	33.6	2.16	20.0
	0.225	6.11	33.7	2.40	21.1
	0.300	6.11	33.7	2.40	21.1
	0.375	6.08	33.6	2.36	20.9
	0.450	5.85	33.0	2.07	19.6
	0.525	5.17	31.0	1.79	18.2
	0.600	4.28	28.2	1.40	16.1
	0.650	3.58	25.8	1.11	14.4
	0.700	2.66	22.2	0.88	12.4
	0.725	2.22	20.3	0.73	11.6
	0.735	2.16	20.0	0.66	11.0

Table (29): Effect of disc rotation on heat transfer. Observations

E.N.	Date	Gap	D.Sp. rpm	P_n	D.B.T.	I.M.H. watts	I.G.H. watts	t_w m.v.	t_w' m.v.	t_i m.v.	t_o m.v.
2	21.11.55	1/4"	0	0.02	66.0	144.5	52.1	3.331	1.127	2.00	2.01
2a			100		66.8	144.5	52.1	3.344	1.050	2.01	2.02
2b			200		67.4	144.5	52.1	3.343	1.000	2.00	1.99
2c			300		67.7	144.5	52.1	3.340	0.977	1.98	1.97
2d			400		67.7	144.5	52.1	3.332	0.967	1.96	1.85
11	13.12	3/16"	0	0.02	63.1	165.5	56.9	3.220	1.023	1.91	1.93
11a			100		63.6	165.5	56.9	3.221	0.950	1.93	1.94
11b			200		64.0	165.5	56.9	3.222	0.923	1.92	1.93
11c			300		64.3	165.5	56.9	3.222	0.903	1.91	1.90
11d			400		64.6	165.5	56.9	3.225	0.900	1.89	1.84
12	15.12	1/8"	0	0.01	69.0	172.0	57.7	3.367	1.210	2.05	2.12
12a			100		69.4	172.0	57.7	3.366	1.127	2.05	2.10
12b			200		69.8	172.0	57.7	3.364	1.097	2.03	2.06
12c			300		69.9	172.0	57.7	3.361	1.090	2.01	2.02
12d			400		70.0	172.0	57.7	3.358	1.080	1.98	1.95

Table (30): Effect of disc rotation on heat transfer. Results

Ex.N.	Q	U_m	t_w deg.F	t_d deg.F	t_i deg.F	t_o deg.F	I.M.H. Btu/hr	H_r	H_c	H_o	h
12	62.1	6.77	187.1	90.9	129.2	132.4	587	130	9	448	3.96
12a			187.1	87.0	129.2	131.5	587	134	9	444	3.95
12b			187.0	85.6	128.3	129.7	587	135	10	442	3.95
12c			186.8	85.3	127.5	127.9	587	135	10	442	3.96
12d			186.7	84.8	126.2	124.9	587	136	10	441	3.96
11	87.8	6.38	180.7	82.1	123.1	124.0	565	128	9	428	3.81
11a			180.8	78.6	124.0	124.4	565	132	10	423	3.78
11b			180.8	77.3	123.5	124.0	565	133	10	422	3.78
11c			180.8	76.4	123.1	122.6	565	134	10	421	3.78
11d			181.0	76.2	122.2	119.9	565	135	11	419	3.77
2	87.8	4.79	185.5	87.0	127.1	127.5	493	131	10	352	3.08
2a			186.1	83.4	127.5	127.9	493	136	10	347	3.05
2b			186.1	81.0	127.1	126.6	493	139	10	344	3.04
2c			185.9	80.0	126.2	124.4	493	139	11	343	3.04
2d			185.6	79.4	125.3	120.4	493	139	11	343	3.05

Table (31): Effect of disc rotation on heat transfer

(Observations for Gap = $\frac{1}{16}$")

Ex.No	Date	P_n	D.Sp rpm	D.B.T.	I.M.H. watts	I.G.H. watts	t_w m.v.	t_d m.v.	t_i m.v.	t_o m.v.
3	23.11.55	0.01	0	66.4	231.7	64.5	3.295	1.240	2.03	2.18
3a			100	67.2	231.7	64.1	3.295	1.169	2.04	2.13
3b			200	67.6	231.7	64.1	3.284	1.140	2.02	2.09
3c			300	68.5	231.7	64.1	3.268	1.133	2.00	2.03
3d			400	68.1	231.7	64.1	3.240	1.102	1.96	1.96
4	30.11	0.05	0	63.0	312.4	80.2	3.116	0.913	1.94	1.86
4a			100	63.5	312.4	80.2	3.113	0.883	1.92	1.83
4b			200	63.7	312.4	80.2	3.103	0.877	1.91	1.81
4c			300	64.0	312.4	80.2	3.103	0.877	1.91	1.79
4d			400	64.8	312.4	80.2	3.101	0.883	1.90	1.78
5	1. 12	0.10	0	65.3	359.7	89.1	3.268	0.903	1.99	1.85
5a			100	66.0	359.7	89.1	3.279	0.903	1.98	1.82
5b			200	66.0	359.7	89.1	3.291	0.897	1.98	1.82
5c			300	66.0	359.7	89.1	3.291	0.897	1.98	1.81
5d			400	66.2	359.7	89.1	3.280	0.893	1.98	1.80
6	5. 12	005	0	63.9	175.0	56.5	3.193	1.437	1.96	2.18
6a			100	65.0	187.7	59.3	3.301	1.347	2.01	2.15
6b			200	65.4	187.7	59.5	3.258	1.283	2.01	2.09
6c			300	66.0	187.7	57.5	3.244	1.263	1.96	2.02
6d			400	66.2	187.7	57.5	3.192	1.223	1.93	1.93
7	6. 12	0.02	0	65.8	240.0	62.6	3.023	1.080	1.92	1.98
7a			100	66.4	247.3	65.0	3.098	1.043	1.94	1.99
7b			200	66.8	247.3	65.0	3.098	1.027	1.94	1.95
7c			300	67.0	247.3	65.0	3.081	1.017	1.92	1.90
7d			400	67.5	247.3	65.0	3.071	1.013	1.90	1.87
9	8. 12	0.20	0	68.2	413.5	93.3	3.068	0.950	1.99	1.64
9b			200	69.1	420.0	93.3	3.120	0.933	2.00	1.65
9d			400	69.4	420.0	93.3	3.119	0.923	2.00	1.64

Table (32): Effect of disc rotation on heat transfer

(Results for Gap = $\frac{1}{16}$")

Ex.N.	Q	U_m	t_w deg F	t_d deg F	t_i deg F	t_o deg F	I.M.H. Btu/hr	H_r	H_c	H_o	h
6	43.9	9.58	179.6	101.5	125.3	135.1	596	107	8	481	4.35
6a			184.2	97.3	127.4	133.7	640	119	9	512	4.49
6b			182.4	94.3	127.4	131.0	640	119	9	512	4.56
6c			181.8	93.4	125.3	127.9	640	120	9	511	4.62
6d			179.5	91.5	124.0	124.0	640	117	9	514	4.74
3	62.1	13.55	184.0	92.3	128.3	135.1	790	124	9	657	5.85
3a			184.0	89.0	128.8	132.7	790	128	9	653	5.85
3b			183.5	87.6	127.9	131.0	790	128	9	653	5.90
3c			182.8	87.3	127.0	128.3	790	127	9	654	5.98
3d			181.6	85.8	125.3	125.3	790	126	9	655	6.04
7	87.8	19.16	172.2	84.8	123.5	126.2	817	112	8	697	6.86
7a			175.5	83.0	124.4	126.6	843	119	8	716	6.86
7b			175.5	82.3	124.4	124.9	843	120	8	715	6.89
7c			174.7	81.8	123.5	122.6	843	119	9	715	6.95
7d			174.3	81.6	122.6	121.3	843	119	9	715	7.03
4	139.0	30.30	176.3	76.8	124.4	120.8	1066	127	9	930	8.59
4a			176.1	75.4	123.5	119.5	1066	128	9	929	8.64
4b			175.7	75.2	123.1	118.6	1066	127	9	930	8.69
4c			175.7	75.2	123.1	117.7	1066	127	9	930	8.71
4d			175.6	75.4	122.6	117.2	1066	127	9	930	8.79
5	196.2	42.80	182.8	76.3	126.6	120.4	1227	138	10	1079	9.61
5a			183.3	76.3	126.2	119.0	1227	138	10	1079	9.62
5b			183.8	76.1	126.2	119.0	1227	139	10	1078	9.59
5c			183.8	76.1	126.2	118.6	1227	139	10	1078	9.59
5d			183.3	75.9	126.2	118.1	1227	139	10	1078	9.63
9	277.8	60.60	174.2	78.6	126.6	110.9	1410	121	10	1279	12.62
9b			176.4	77.8	127.1	111.3	1431	126	10	1295	12.65
9d			176.4	77.3	127.1	110.9	1431	126	10	1295	12.68

Table (33): Observations of heat transfer experiments with stationary air blower

Ex.N.	Date	Gap	D.Sp. rpm	D.B.T.	I.M.H. watts	I.G.H. watts	t_w m.v.	t_d m.v.	t_i m.v.	t_o m.v.
1	16.11.55	$\frac{1}{4}$"	0	67.2	61.5	34.7	2.922	1.470	2.05	1.78
1a			100	68.7	72.4	38.2	3.163	1.403	2.04	1.83
1b			200	68.9	76.3	38.6	3.149	1.300	1.99	1.77
1c			300	69.2	76.3	38.2	3.022	1.203	1.90	1.61
1d			400	69.8	80.3	38.6	3.029	1.163	1.87	1.55
8	7.12	$\frac{1}{16}$"	0	66.5	71.8	38.6	3.419	2.230	2.34	2.18
8a			100	67.1	79.7	37.2	3.162	1.767	2.10	1.97
8b			200	67.9	88.0	38.6	3.100	1.641	1.98	1.92
8c			300	67.6	95.0	39.4	3.051	1.530	1.90	1.86
8d			600	67.5	106.4	41.3	2.958	1.411	1.82	1.76
10	12.12	$\frac{3}{16}$"	0	60.5	61.5	34.5	2.927	1.507	1.97	1.71
10a			100	60.8	78.5	40.0	3.080	1.311	1.88	1.68
10b			200	61.1	84.7	42.6	3.092	1.203	1.86	1.66
10c			300	61.4	93.5	44.4	3.128	1.117	1.83	1.57
10d			400	61.6	98.0	46.3	3.122	1.063	1.81	1.51
13	16.12	$\frac{1}{8}$"	0	70.0	72.2	39.0	3.628	2.143	2.45	2.22
13a			100	70.9	80.4	39.0	3.371	1.707	2.16	2.10
13b			200	71.5	88.9	39.0	3.219	1.507	2.02	1.97
13c			300	70.9	97.6	40.3	3.161	1.377	1.95	1.82
13d			400	70.9	106.9	44.5	3.174	1.303	1.91	1.75

Ta ble (34): Results of heat transfer experiments with stationary air blower

Ex.No.	t_w deg F	t_d deg F	t_i deg F	t_o deg F	I.M.H. Btu/hr	H_r	H_c	H_o	h
8	189.4	137.3	142.3	135.1	245	79	9	157	1.34
8a	178.2	116.7	131.5	125.7	272	86	8	178	1.68
8b	175.5	110.9	126.2	123.5	300	90	8	202	1.97
8c	173.4	105.8	122.6	120.8	331	92	9	230	2.27
8d	169.4	100.3	119.0	116.3	363	93	9	261	2.68
13	198.2	133.4	147.1	136.9	246	100	10	136	1.11
13a	187.3	113.9	134.2	131.5	274	106	9	159	1.43
13b	180.7	104.8	127.9	125.7	303	105	9	189	1.81
13c	178.2	98.7	124.9	119.0	324	108	9	207	2.02
13d	178.7	95.2	123.1	115.9	364	112	10	242	2.35
10	168.0	104.8	125.8	114.0	210	85	8	117	1.14
10a	174.7	95.6	121.7	112.7	268	106	10	152	1.40
10b	175.2	90.6	120.8	111.8	289	111	10	168	1.54
10c	176.8	86.5	119.5	107.7	319	118	11	190	1.72
10d	176.5	84.0	118.6	104.9	334	120	11	203	1.85
1	167.9	103.1	129.3	117.2	210	87	8	115	1.20
1a	178.3	99.1	128.8	119.5	247	107	9	131	1.25
1b	177.7	95.1	126.6	116.8	260	111	10	139	1.34
1c	172.2	90.6	122.6	109.5	260	106	10	144	1.46
1d	172.5	88.7	121.3	106.8	274	109	10	155	1.58

Table (35): Kinetic pressures at different angles with radial direction (inch of water)

(Date: 9.1.1956) Discharge = 0)

Z inch	D.Sp. rpm.	70°	80°	90°	100°
0.025	0	0	0	0	0
	100	0.005	0.006	0.007	0.007
	200	0.019	0.018	0.020	0.020
	300	0.032	0.030	0.032	0.033
	400	0.049	0.045	0.050	0.050
0.040	0	0	0	0	0
	100	0.003	0.003	0.004	0.004
	200	0.010	0.010	0.011	0.011
	300	0.019	0.018	0.019	0.019
	400	0.025	0.024	0.025	0.026
0.065	0	0	0	0	0
	100	0	0	0.001	0.001
	200	0.003	0.002	0.004	0.004
	300	0.007	0.008	0.008	0.008
	400	0.010	0.011	0.012	0.012
0.100	0	0	0	0	0
	400	0.004	0.006	0.006	0.006
0.150	0	0	0	0	0
	400 m	0.001	0.001	0.002	0.002

Table (36): Kinetic pressures at different angles with radial direction (inch of water)

(Date: 10.1.1956) Discharge = 196.2 lbs./hour)

(inch)	D.Sp. rpm	-10	0	10	20	30	40	60	70	80	90
0.025	0	0.003	0.004	0.003	0.002	0.002	0	-.001	-.001	-.001	-.002
	100	0.000	0.000	0.001	0.002	0.002	0.002	0.001	0.000	-.001	-.002
	200	-.001	0.000	0.001	0.003	0.008	0.008	0.008	0.008	0.002	0.002
	300	-.005	-.001	0.003	0.008	0.012	0.016	0.019	0.021	0.020	0.018
	400	-.011	-.004	0.003	0.011	0.018	0.025	0.030	0.031	0.031	0.030
0.040	0	0.005	0.005	0.005	0.005	0.003	0.001	-.001	-.002	-.004	
	100	0.003	0.005	0.005	0.005	0.005	0.004	0.000	0.000	-.001	
	200	0.002	0.005	0.007	0.009	0.010	0.009	0.006	0.004	0.001	
	300	0.001	0.005	0.008	0.011	0.013	0.013	0.011	0.009	0.008	
	400	0.000	0.005	0.010	0.014	0.019	0.020	0.020	0.016	0.012	
0.065	0	0.010	0.011	0.010	0.009	0.008	0.004	-.001			
	100	0.009	0.011	0.011	0.011	0.011	0.008	0.001			
	200	0.009	0.011	0.011	0.012	0.012	0.010	0.004			
	300	0.009	0.011	0.013	0.014	0.014	0.013	0.008			
	400	0.009	0.011	0.015	0.016	0.016	0.016	0.010			
0.100	0	0.013	0.014	0.013	0.012						
	400	0.012	0.016	0.017	0.015						
0.150	0	0.015	0.015	0.015	0.015						
	400	0.015	0.014	0.014	0.015						

Table (37): Kinetic pressures at different angles with radial direction (inch of water)

(Date: 12.1.1956. Discharge = 310.5 lbs./hour)

Z (inch)	D.Sp. rpm	-10	0	10	20	30	40	50	70
0.025	0	0.010	0.012	0.011	0.011	0.009	0.006	0	-.006
	100	0.008	0.010	0.011	0.012	0.010	0.008	0.004	-.004
	200	0.001	0.008	0.011	0.012	0.012	0.012	0.009	0
	300	-.002	0.005	0.012	0.019	0.019	0.020	0.020	0.010
	400	-.009	0.002	0.013	0.022	0.025	0.029	0.029	0.024
0.040	0	0.016	0.018	0.016	0.015	0.014	0.008	0.002	
	100	0.015	0.017	0.016	0.017	0.015	0.012	0.008	
	200	0.010	0.017	0.017	0.020	0.019	0.016	0.010	
	300	0.010	0.016	0.020	0.022	0.023	0.022	0.017	
	400	0.009	0.015	0.021	0.028	0.029	0.029	0.023	
0.065	0	0.023	0.024	0.023	0.022	0.020			
	100	0.023	0.024	0.024	0.023	0.020			
	200	0.020	0.026	0.027	0.028	0.024			
	300	0.020	0.026	0.030	0.031	0.029			
	400	0.020	0.026	0.030	0.033	0.030			
0.100	0	0.030	0.030	0.030	0.030	0.028			
	400	0.030	0.036	0.038	0.036	0.032			
0.150	0	0.030	0.031	0.031	0.030	0.028			
	400	0.030	0.031	0.031	0.030	0.028			

Table (38): Kinetic pressures at different angles with radial direction (inch of water)

(Date: 16.1.1956 Discharge = 440 lbs/hour)

Z (inch)	D.Sp. rpm	-10°	0	10	20	30	40	50
0.025	0	0.030	0.030	0.030	0.028	0.023	0.010	0.003
	100	0.027	0.029	0.030	0.029	0.025	0.015	0.009
	200	0.022	0.026	0.030	0.030	0.031	0.024	0.018
	300	0.019	0.025	0.030	0.032	0.033	0.031	0.024
	400	0.016	0.024	0.033	0.038	0.040	0.040	0.038
0.040	0	0.037	0.039	0.039	0.038	0.029	0.019	
	100	0.034	0.039	0.039	0.039	0.032	0.021	
	200	0.032	0.039	0.039	0.040	0.036	0.027	
	300	0.031	0.039	0.040	0.041	0.041	0.031	
	400	0.030	0.039	0.046	0.047	0.047	0.039	
0.065	0	0.052	0.055	0.055	0.047	0.039		
	300	0.049	0.055	0.056	0.054	0.050		
	400	0.048	0.055	0.059	0.057	0.054		
0.100	0	0.063	0.065	0.065	0.058	0.052		
	400	0.061	0.065	0.067	0.062	0.059		
0.150	0	0.062	0.062	0.067	0.060	0.052		
	400	0.061	0.062	0.067	0.060	0.052		

Table (39): Kinetic pressures at different angles with radial direction (inches of water)

(Date: 17.1.1956. Discharge = 621 lbs./hour)

Z (inch)	D.Sp. rpm	-10°	0°	10°	20°	30°
0.025	0	0.076	0.083	0.078	0.066	0.054
	100	0.076	0.079	0.078	0.066	0.056
	200	0.066	0.076	0.078	0.072	0.063
	300	0.061	0.076	0.079	0.078	.072
	400	0.058	0.076	0.081	0.081	.077
0.040	0	0.089	0.096	0.091	0.081	0.070
	100	0.083	0.096	0.091	0.081	0.073
	200	0.082	0.096	0.097	0.084	0.078
	300	0.081	0.096	0.099	0.090	0.081
	400	0.080	0.096	0.100	0.095	0.089
0.065	0	0.112	0.120	0.114	0.104	0.088
	400	0.104	0.119	0.121	0.116	0.110
0.100	0	0.130	0.137	0.131	0.127	0.112
	400	0.126	0.138	0.138	0.131	0.120
0.150	0	0.123	0.130	0.130	0.120	0.110
	400	0.123	0.130	0.130	0.120	0.110

APPENDIX III

BIBLIOGRAPHY

1. A.F.H. ALI : "Heat transfer from a flat surface to a moving fluid" Ph.D Thesis, University of London, 1951.

2. M.A.I.A. ARABI : "Hydraulic losses and heat transfer associated with super turbulence" Ph.D. Thesis, University of London, 1951.

3. A. BAILEY and W.F. COPE : "Heat transmission through circular, square and rectangular pipes" Aeronautical Reseach Committee, Tech.Rep. 43, 1933, pp.199-209.

4. G.K. BATCHELOR : "Notes on a class of solutions of the Navier-Stokes equations representing steady rotationally-symmetric flow" Quarterly Journal of Mechanics and Applied Mathematics, Vol.4, 1951, pp.29-41.

5. J.A.W. BYE and J SCHENK : "Heat transfer in laminar flow between parallel plates" App.Sci.Res., Vol.A3, 1952, pp.308-316.

6. W.G. COCHRAN : "The flow due to a rotating disc" Proc. Camb.Phil.Soc., Vol.30, 1934, pp.365-375.

7. W.F. COPE : "Heat transmission between surfaces and fluids flowing over them" Aer.Res.Comm.(Gt.Brit.), Tech.Rep.37, 1930, pp.384-391.

8. R.G. DEISSLER : "Turbulent heat transfer and friction in the entrance regions of smooth passages" Tr.A.S.M.E., Vol.77, Nov.1955, pp.1221-1233.

9. S.J. DAVIES and C.M.WHITE : "An experimental study of the flow of water in pipes of rectangular section" Proc.Roy. Soc.A, Vol.119, 1928, pp.92-107.

10. Th.B.DREW : "Mathematical attacks on forced convection problems; a review" Tr.A.I.C.E., Vol.26, 1931, pp.26-80.

11. E. ECKERT : "Introduction to the transfer of heat and mass" McGraw Hill, 1950.

12. F. ELIAS : The transference of heat from a hot plate to an airstream" English transalation. NACA TM.614, 1931.

13. Y.M.A.EL-SAYED : "Heat transfer coefficients of air by forced convection through annular spaces and parallel to a bank of tubes" Ph.D. Thesis, Manchester University, 1954.

14. M.FISHENDED and O.A.SAUNDERS : The caluclation of heat transmission" H.M.S.O., London, 1932.

15. M.FISHENDEN and O.A.SAUNDERS : "Errors in gas temperature measurement and their caluclation" Symposium on gas temperature and measurement, Jnl.Inst.Fuel, Vol.12, 1939, pp.S - S14.

16. M.FISHENDEN and O.A.SAUNDERS : "An introduction to heat transfer" Oxford University Press, 1950.

17. A.FRANK : "Die Warm eabgabe ebener Flächen an frei Luft" Gesundheits-Ingenieur, 52 Jahrgang, 1929, pp.541-546.

18. C.A.GENEVE : "Pressure-entropy steam tables" Government Press, Cairo, 1944.

19. S.GOLDSTEIN : Modern developments in fluid dynamics" Oxford, Clarendon Press, 1938.

20. F.H.GREEN and L.S.KING : "The influence of tube shape on heat transfer coefficients in air to air heat exchangers" Tr.A.S.M.E., Vol.68, 1946, pp.115-122.

21. E.HAUCKE : "Der Wärmeübergang an Luftzwischenzwei ebenen parallelen Platten bei Wirbelströmung" Archiv für Wärme und Dampf., Vol.116, 1930, pp.53-58.

22. C.D.HODGMAN : "Handbook of cehmistry and physics" 32 Ed. 1950-1951, Chem.Rub.Pub.Co., Cleveland, Ohio.

23. H.C.HOTTEL : "Radiant heat transmission" Mech.Engg., Vol.52, 1930, pp.699-704

24. M.JAKOB : "Measurements of the true temperature and heat exchange in a catalytic reaction" Tr.A.I.C.E., Vol.35, 1939, pp.563-586.

25. M.JAKOB : "Heat transfer" John Wiley & Sons, N.Y., 1949.

26. M.JAKOB and W.M.DOW : "Heat transfer from a cylindrical surface to air in parallel flow with and without unheated starting sections" Tr.A.S.M.E., Vol.68,1946, pp.123-134.

27. W. JÜRGES : "Der Warmeübergang an einer ebenen Wand" Beiheft zum Gesundheits-Ingenieur, Reihe I, Bieheft 19, 1924.

28. Th.von KARMAN : "On laminar and turbulent friction" English Translation NACA TM.1092, Washington, 1946.

29. G.W.C.KAYE and T.H.LABY : "Physical and chemical constants" 10th Ed., Longmans, 1948.

30. H.LATZKO : "Heat transfer in a turbulent liquid or gas stream" English translation, NACA TM.1068, 1944.

31. M.A.LÉVÊQUE : "Les lois de la transmission de chaleur par convection" Annales des Mines, series 12, Vol.13, 1928, pp.201-299, 305-362 and 381-415.

32. W.H.MACADAMS : "Heat transmission" 2nd Ed., McGraw Hill, New York, 1942.

33. K.MILLSAPS and K.POHLHAUSEN : "Heat transfer by laminar flow from a rotating plate" Jnl.Aer.Sci., Vol.19, No.2, Feb.1952, pp.120-126.

34. MOTALA : "The Motala fan-preheater" Engg. and Boiler House Review, Jan.1952, pp.13-15.

35. International Critical Tables, National Research Council, U.S.A., McGraw Hill.

36. R.N.NORRIS and D.D.STREID : "Laminar-Flow heat transfer coefficients for ducts" Tr.A.S.M.E., Vol.62, 1940, pp.525-533.

37. A.OUDANT : "Exchanges thermique pour le disque isotherme en rotation uniforme" C.R.Accad.Sci., Paris, Vol.239, 1954, pp.27-29.

38. E.OWER : "The measurement of airflow" 3rd Ed., Chapman & Hall, London, 1949.

39. J.H.PERRY : "Chemical Engineers' Handbook" 3rd Ed., McGraw Hill, 1950.

40. J.A.PRINS, J.MULDER and J.SCHENK : "Heat transfer in laminary flow between parallel plates" App.Sci.Res., Vol.A2, 1950, pp.431-438.

41. H.F.P.PURDAY : "Streamline Flow" Constable, London, 1949.

42. W.M.REHSENOW : "A graphical determination of unshielded thermocouple theraml correction" Tr.ASME, Vol.68, 1946, pp.195-198.

43. E.W.SAMS and W.F.WEILAND, Jr. : "Experimental heat transfer and friction coefficients for air flowing through stacks of parallel flat plates" NACA RM.E54F11, Washington, 1954.

44. O.A.SAUNDERS : "Notes on some radiation heat transfer formulae" Proc.Phys.Soc. of London, Vol.41,1929,pp.569-575.

45. A.SCHACK : "Industrial heat transfer" English Translation John Wiley & Sons, London & N.Y., 1933.

46. J.SCHENK and H.L.BECKERS : "Heat transfer in laminar flow between parallel plates" App.Sci.Res., Sec.A, Vol.4, 1954, pp.405-413.

47. E.SCHMIDT : "Thermodynamics" Oxford University Press, 1949.

48. L.SLEGEL and G.A.HAWKINS : "Heat transfer from a vertical plate to an airstream" Purdue University, Engg.Bulletin No.97, May 1946.

49. K.STEWARTSON : "On the flow between two rotating coaxial discs" Proc.Camb.Phil.Soc., Vol.49, 1953, pp.333-341.

50. C.WAGNER : "Heat transfer from a rotating disc to ambient air" Jnl.App.Phys., Vol.19, 1948, pp.837-839.

51. L.WASHINGTON and W.M.MARKS : "Heat transfer and pressure drop in rectangular air passages" Ind.& Engg.Chem., Vol.29, 1937, pp.337-345.

52. R.L.YOUNG : "Heat transfer from rotating plate" A.S.M.E. Paper n 54-SA-51, 1954.